Molecules of Significance in Planetary Aeronomy

Hari Mohan

JANUARY 1979

NASA

Molecules of Significance in Planetary Aeronomy

Hari Mohan
Wallops Flight Center
Wallops Island, Virginia

Dr. Hari Mohan

1930 - 1976

NOTE ADDED IN PROOF

Dr. Mohan died before he could finish the final proofreading of his manuscript. The staff of the Directorate of Applied Science at Wallops Flight Center undertook the task of ferreting out those errors that inevitably creep into any written work. Thus any errors or sins of omission found here are the responsibility of the staff and cannot be attributed to Dr. Mohan.

Page Intentionally Left Blank

The advent of the space era in modern science has been instrumental in revitalizing an active interest in a number of ancillary scientific disciplines. Spectroscopic methodology is one. Most of the diagnostic study of planetary aeronomy and atmospheric optics involves methods of spectroscopy - both qualitative and quantitative. Thus, precise and reliable information about various structural and quantitative parameters and the nature of different types of radiative and non-radiative processes in respect to relevant molecules and atoms has been significantly useful.

Optical spectroscopy is relatively a fairly established branch of scientific activity. Huge amounts of knowledge relating to a large number of atoms and molecules, both in terms of theoretical modelling and numerical data are now available. A closer perusal of the relevant literature, however, would reveal that, in many respects, this information is scattered and rather incoherent, especially in the case of molecular species. In recent years, widespread and evergrowing use of spectroscopic data in a variety of applications (including planetary aeronomy and astrophysics) such as combustion, pollution, chemical kinetics and thermodynamics, has prompted a critical review and consolidation of available information with regard to its application in diverse fields of academic and technological interest. Such data storage is particularly relevant as experiments and observations become progressively more automated.

This monograph is basically devoted to spectroscopic information of the molecules of planetary interest. Only those molecules have been dealt with which have been confirmed spectroscopically to be present in the atmosphere of major planets of our solar system and play an important role in the aeronomy of the respective planets.

The entire text is divided into three parts. Part I presents an introductory survey of the vast subject of planetary atmospheres and spectra. It also acquaints a non-specialist with the general conditions of different planets, their atmospheres and the various gaseous molecules that exist there. Some typical examples of planetary spectra are also given.

Part II is primarily concerned with the basic concepts underlying optical absorption and different quantitative molecular parameters that often have useful application in the study of planetary atmospheres. Quantities like dipole moments, transition probabilities, Einstein coefficients and line strengths, radiative life times, absorption cross sections, oscillator strengths, line widths and profiles, equivalent widths, growth curves, band

strengths, electronic transition moments, Franck-Condon factors and $\bar{r}$-centroids, etc., are discussed and their interrelationships, if any, have been established. Basics of molecular transitions in relation to the different parameters have also been presented.

Part III is devoted to the important spectroscopic information and relevant data of the 12 major molecules, viz., 6 diatomics: HF, HCl, CO, H_2, O_2, N_2 and 6 polyatomics: CO_2, N_2O, O_3, H_2O, NH_3, CH_4, so far spectroscopically identified in various planetary atmospheres. Precise descriptions are presented about electronic, vibration-rotation and pure rotational transitions and the observed spectral features. Absorption cross section data are provided only in graphic forms. An exhaustive bibliography is given for details.

CONTENTS

Physical Constants

PHYSICAL CONSTANTS

Quantity	Symbol	Value
Speed of Light in Vacuum	c	2.99793×10^{10} cm sec^{-1}
Planck Constant	h	6.62559×10^{-27} erg sec
Boltzmann Constant	k	1.3805×10^{-16} erg °K^{-1}
Universal Gas Constant	R	8.31429×10^{7} erg °K^{-1} mole^{-1}
Loschmidt Number	N_o	2.687×10^{19} cm^{-3}
Avogadro Number	N	6.0231×10^{23} mole^{-1}
Acceleration Due to Gravity	g	978.049 cm sec^{-2}
Gravitational Constant (Sea Level at Equator)	G	6.668×10^{-8} dyne cm^2 gm^2
Absolute Zero of Temperature	0°K	-273.15°C
Normal Volume of Ideal Gas (STP)	V_o	2.24136×10^{4} cm^3 mole^{-1}
Mechanical Equivalent of Heat	J	4.185×10^{8} erg cal^{-1}
Rest Mass of Electron	M_e	9.1066×10^{-28} gm
Rest Mass of Proton	M_p	1.67252×10^{-24} gm
Rest Mass of Neutron	M_n	1.67482×10^{-24} gm
Mass of an Atom of Hydrogen	M_H	1.673×10^{-24} gm
Charge of an Electron	q_e	4.803×10^{-10} esu
		1.602×10^{-20} emu
Radius of First Bohr Orbit	a_o	0.52917×10^{-8} cm
Rydberg Constant for Hydrogen	R_H	109677.576 cm^{-1}
Rydberg Constant for Infinite Mass	R_o	109737.309 cm^{-1}
Fine Structure Constant	α	7.297×10^{-3}
Wein's Constant	$\lambda_{max}T$	0.2898 cm °K

Energy Conversion Constants:

Unit	cm^{-1}	ergs/molecule	cal/mole	electron volts (eV)
1 cm^{-1}	1	1.9863×10^{-16}	2.8591	1.2398×10^{-4}
1 erg/molecule	5.0345×10^{15}	1	1.4394×10^{16}	6.2418×10^{11}
1 cal/mole	0.34976	6.9473×10^{-17}	1	4.3363×10^{-5}
1 eV	8.06573×10^{3}	1.6021×10^{-12}	2.3061×10^{4}	1
1 °K	0.69503	1.3805×10^{-16}	1.9871	8.6170×10^{-5}
1 Hz (sec^{-1})	3.3356×10^{-11}	6.6256×10^{-27}	9.5370×10^{-11}	4.1356×10^{-13}

SECTION I

SPECTROSCOPY AND MOLECULES IN PLANETARY ATMOSPHERES

Page Intentionally Left Blank

CHAPTER 1

SPECTROSCOPY AND THE ATMOSPHERES OF PLANETS

Spectroscopy basically is concerned with practically all phenomena that involve absorption and/or emission of electromagnetic radiation by matter. The spectral lines that one obtains using a spectroscopic device are, in fact, the coded messages from atoms and molecules. The spectroscopist deciphers these codes and derives valuable information about the internal constitution of these basic entities of matter. The different spectroscopic techniques simply act as different windows to enable us to peep into these structures more and more closely and thus have a better understanding of matter, energy and their interaction.

Although a considerable amount of semi-empirical work on atomic and molecular spectra was done before the advent of the quantum era in physics, almost all the later developments in the field relied heavily upon the quantum theory. Spectroscopy and quantum mechanics are now inseparable and, as a matter of fact, both go hand in hand in supporting the progress of each other. Spectrum analysis provides the bulk of useful experimental data with which the predictions of quantum mechanics are tested and the theory refined. On the other hand, theoretical deductions of quantum mechanics indicate possible directions to a spectroscopist to explore newer vistas of nature.

Spectroscopic methodology has long been of considerable interest to space physicists in their pursuit of knowledge about the universe. Perhaps the largest proportion of our present day understanding of different celestial structures; e.g., planets, stars, galaxies, nebulea, etc., is the contribution of different spectroscopic investigations undertaken from time to time. In the case of planets, spectroscopic probes ever played a very significant role. A great deal of information about the chemical composition and aeronomic diagnostics of planetary atmospheres has been obtained through judicious interpretations of planetary spectra. Both earth-based and fly-by missions have been mutually complementary in this respect.

Though the early investigations in planetary spectroscopy were made by using conventional spectrographs and big size telescopes, the state-of-the-art has undergone spectacular advances in recent years. The development of coude spectrographs, highly sensitive infrared sensors and airborne experimental facilities has enhanced the scope and efficacy of modern planetary spectroscopy tremendously. Perfection of high resolution Fourier transform spectroscopy and its application to the study of planetary radiation is another significant step forward. The resolution and purity of Fourier transform spectroscopy is so high that many new identifications of spectral features, which were hitherto hopelessly

blended with the neighboring ones, are now possible. The technique was initiated by Fellget (1958) and its first planetary application was made by Gebbie et al. (1962) to record interferograms of Venus in the near infrared out to 3μ. It is indeed a very efficient and reliable technique of exploring planetary radiation.

PLANETS

The term planet owes its genesis to the Greek word 'Planetes' which means wanderers. In ancient Ptolemaic astronomy, the word was applied to the seven heavenly bodies which were observed to change their respective locations in the sky. These bodies were the sun, the moon, Mercury, Venus, Mars, Jupiter and Saturn; all of which were supposed to revolve around the earth. In modern astronomy, the term planet is applied to all dark and opaque celestial bodies in revolution around the sun and shining by reflected sunlight.

There are nine known major planets in our solar system. In order of increasing distance from the sun, these bodies are: Mercury, Venus, Earth, Mars, Jupiter, Saturn, Uranus, Neptune and Pluto. They all revolve around the sun in certain specified orbits.

The major planets are normally classified into two groups:

(1) Terrestrial or Earth-like Planets. The planets which resemble Earth in some respects come under this category. These are: Mercury, Venus, Earth, Mars, and Pluto.

(2) Jovian or Giant Planets. Jupiter, Saturn, Uranus and Neptune come under this category. They are much larger than the terrestrial planets and their mean densities are considerably less than that of Earth. The terrestrial planets are on an average twice as dense as the giant planets.

The planets Mercury and Venus whose orbits lie inside that of Earth are also sometimes classified as Inner or Interior Planets. On the other hand, Mars, Jupiter, Saturn, Uranus, Neptune and Pluto, whose orbits fall outside the Earth's orbit, are termed as Outer or Exterior Planets.

All the major planets, with the exception of Mercury, Venus and Pluto are known to have one or more satellites or moons: Neptune (2); Uranus (5); Saturn (9); Jupiter (12); Mars (2); Earth (1). The number in parenthesis indicates the number of satellites associated with each Planet.

Besides the nine major planets, there exist a large number of minor planets in the solar system, called Asteroids. They are much smaller compared to the major planets. Among the known minor planets, Ceres is the largest. Icarus and Hermes are the other better known asteroids. The origin of these minor planets is still a mystery. They may be the remnants of a shattered planet or, alternately, matter which did not form into planets in the first place.

Tables (I and II) present the numerical values for the important physical and orbital elements of the nine major planets. Most of the values quoted here are according to Allen (1973). The values of the orbital parameters are not precise enough for use in ephemeris work.

PLANETARY ATMOSPHERES

The planets are surrounded by gaseous envelopes called atmospheres which they retain associated with themselves by their respective force of gravity. An atmosphere is a rather different concept in the case of exterior planets (Jupiter, Saturn, Uranus and Neptune) for it is believed these planets have no solid surface as such but consist of homogeneous mixtures of gases, increasing in density with depth. Only the surface layers can be studied visually or spectroscopically, and therefore the outer mantle may be regarded as the atmosphere for the purpose of comparison.

The composition of the atmosphere of a planet is a function of geological time and characteristically depends on the extent to which the gases escape from the exosphere, the degree of replenishment by exhalation from the crust (slowly or through volcanic activity), gas removal or addition by chemical reactions in the atmosphere and the capture of gaseous material from interplanetary medium or meteors. The rate at which gases escape is controlled by factors such as escape velocity, molecular weight of the gases concerned and the temperature.

The velocity of escape for a given point near the surface of a planet depends upon the mass of the planet and the distance of the point from the center of gravity of the planet. It is given by the relation:

$$v = \frac{2GE}{r}$$

where G is the universal constant of gravitation, E is the mass of the planet concerned, and r is the distance from the point to the center of gravity of the planet.

The accepted values for the symbols in the above equation when applied to the earth are:

$$G = 6.66 \times 10^{-8} \text{ dynes } cm^2/g^2$$
$$E = 5.98 \times 10^{27} g$$
$$r = 6.38 \times 10^8 cm$$

Inserting these values in the above expression as applied to earth

$$v = 11.18 \text{ Km S}^{-1}$$

Corresponding values of escape velocity for different planets are tabulated in Table (I), column 8.

TABLE I - IMPORTANT PHYSICAL CHARACTERISTICS OF THE MAJOR PLANETS

Planets	Equatorial Diameter	Ellipticity	Volume	Mass	Mean Density	Surface Gravity	Escape Velocity	Sidereal Rotation Period (Equatorial)				Equator Orbit Inclination		Visual Geometric Albedo
Units →	Km		Earth = 1	Earth = 1	$g\ cm^{-3}$	$cm\ S^{-2}$	$Km\ S^{-1}$	d	h	m	s	°	'	
Mercury	4850	0.0	0.54	0.0554	5.4	363	4.2	59	-	-	-	<28		0.10
Venus	12140	0.0	0.88	0.815	5.2	860	10.3	244.3 (retrograde)				3		0.586
Earth	12756	0.0034	1.00	1.000	5.518	982	11.2	23	56	4.1		23	27	0.39
Mars	6790	0.009	0.149	0.1075	3.95	374	5.0	- 24	37	22.6		23	59	0.15
Jupiter	142600	0.063	1316	317.83	1.34	2590	61	- 9	50	30		3	05	0.44
Saturn	120200	0.098	755	95.147	0.70	1130	37	- 10	14	-		26	44	0.46
Uranus	49000	0.06	52	14.54	1.58	1040	22	- 10	49	-		97	55	0.56
Neptune	50200	0.021	44	17.23	2.30	1400	25	- 15	48	-		28	48	0.51
Pluto	6400	-	0.1	0.17	-	-	-	6	9	-	-			0.13

Planets	Semi-Major Axis of the Orbit		Period		Mean Daily Motion	Mean Orbital Velocity	Orbital Eccentricity	Orbital Inclination to the Elliptic			Mean Longitude of Perihelion			No. of Satellites
Units	10^6 Km	A.U.	Sidereal Days	Synodic Days	°	Km S^{-1}		°	'	"	°	'	"	
Mercury	57.9	0.387	87.969	115.88	4.092339	47.89	0.206	7	0	15	75	53	54	0
Venus	108.2	0.723	224.701	583.92	1.602131	35.03	0.007	3	23	40	130	09	10	0
Earth	149.6	1.000	365.256	-	0.985609	29.79	0.017	-	-	-	101	13	11	1
Mars	227.9	1.524	686.980	779.94	0.524033	24.13	0.093	1	51	0	334	13	06	2
Jupiter	778.3	5.203	4332.589	398.88	0.083091	13.06	0.048	1	18	17	12	43	15	12
Saturn	1427.0	9.539	10759.22	378.09	0.033460	9.64	0.056	2	29	22	91	05	50	10
Uranus	2869.6	19.182	30685.4	369.66	0.011732	6.81	0.047	0	46	23	171	32		5
Neptune	4496.6	30.058	60189	367.49	0.005981	5.43	0.009	1	46	22	46	40		2
Pluto	5900	39.44	90465	366.73	0.003979	4.74	0.250	17	10		223			0

It may be presumed that originally all the planetary atmospheres comprised a mixture of elements similar to those obtained throughout the universe; i.e., hydrogen and helium in quantities far exceeding those of other elements. Subsequently, these gases slowly escaped depending on the escape velocity of the planet, the temperature and the molecular weights of the gases concerned. Ultimately a position might arise when the entire interplanetary space will be filled up by an extremely tenuous gaseous mixture; no planet having its own separate atmosphere. The rate at which a planet might lose its atmosphere will depend upon its size, mass and average temperature. The planets of our solar system are presently in the intermediate stage and almost all of them are known to possess their own characteristic atmospheres with the exception of Pluto and possibly Mercury. The giant planets have very vast atmospheres because of their relatively large force of gravity. Furthermore, their temperatures are also low because of their greater distances from the sun so that the mean velocities of atmospheric molecules are low and remain well below the respective escape velocity.

In contrast to the giant planets, the planets Mercury and Mars, which are relatively nearer to the Sun (Mercury) and on which the force of gravity is also small (Mars), have much thinner atmospheres than that of Earth. The case of Venus is intermediate. It is not very near to the sun and has a force of gravity greater than that of Earth.

In a way, for each planet, a prediction can be made as to which gases, if any, will be retained near its surface. It is found that Jupiter and Saturn will retain even the lightest gases, hydrogen and helium, for astronomically long intervals of time; while Earth and Venus will lose these light gases but will retain all heavier ones. Mars will retain CO_2, Ar and probably N_2 but may lose O_2, perhaps due to dissociative recombinations processes, (McElroy, 1976).

The observations support these predictions in a general way. The spectra of giant planets show strong absorption bands due to CH_4 and NH_3. Uranus and Neptune show weaker absorptions besides H_2. Helium causes no visible absorption of its own but modifies the absorption due to H_2. CH_4 was discovered on Saturn's satellite Titan by Kuiper (1944), but no NH_3, which would have frozen out. On Earth, hydrogen and helium are constantly being replenished in the atmosphere by the photodecomposition of water vapor in the upper atmosphere and radioactive decay in the crust, respectively. On Venus a dense atmosphere of CO_2 was discovered (Adams and Dunham, 1932). A description of the atmospheres of these planets is given in Table III.

TABLE III: GASEOUS CONSTITUENTS OF PLANETARY ATMOSPHERES

Figures in parentheses represent the abundance expressed in cm-atm.* (STP earth)

Planet	Constituents	Remarks
Mercury	CO_2 (0.12); CO (0.05)	Presence of N_2, Ar, CO and O_2 postulated.
Venus	CO_2 (10^5); CO ($\simeq$100); H_2O ($\simeq$.05%); O_2 ($\simeq$0.1); HCl (1); HF (.01)	Presence of numerous polyatomic molecules in trace amounts postulated. Mention may be made of O_3, CH_3Cl, CH_3F, C_2H_2, HCN, SO_2, COS, C_3O_2, H_2S.
Earth	N_2 (625 x 10^3); O_2 (168 x 10^3); H_2O (3000-5000, variable); Ar (74 x 10^2); CO_2 (200); Ne (15); He (4); CH_4 (1.2); Kr (0.9); N_2O (0.4); H_2 (0.4); O_3 (0.3); Xe (.07)	
Mars	CO_2 (78 x 10^2); CO (7.3); H_2O (10-15 microns) O_2 (9-10); O_3 (2 x 10^{-4})	Presence of N_2 postulated as a minor constituent.
Jupiter	H_2 (2.7 x 10^7); CH_4 (1.5 x 10^4); NH_3 (700)	Presence of He, N_2 and Ne postulated in view of the low density of the planet.
Saturn	H_2 (6.3 x 10^7); CH_4 (35 x 10^3); NH_3 (200)	Presence of He, N_2 and Ne postulated in view of the low density of the planet.
Uranus	H_2 (4.2 x 10^6); CH_4 (2.2 x 10^5)	Presence of He and N_2 postulated in view of the low density of the planet.
Neptune	H_2 (> 4.2 x 10^6); CH_4 (3.7 x 10^5)	Presence of He and N_2 postulated in view of the low density of the planet.
Pluto	No data available	

* 1 cm-atm = 1 cm-Amagat = 2.687 x 10^{19} cm^{-2}.

PLANETARY SPECTRA AND PLANETWISE REVIEW

PLANETARY SPECTRA

There is almost negligible intrinsic radiation in the optical region of a planetary spectrum. As a matter of fact, the radiation from other planets reaching the earth-based instruments is the sunlight reflected from the surface of the planets. Evidently the spectrum of this radiation is a blend of three superimposed component spectra, viz., the solar, planetary and the terrestrial. All three atmospheres leave their imprint on the spectrum so recorded. The strictures imposed by the Earth's atmospheres on the radiation reaching an earth-based instrument reduce the scope of planetary spectroscopy considerably. If the Earth's atmosphere opacity is very high in a certain wavelength range, that wavelength radiation reflected from the planet will be absorbed and will, therefore, never reach the instrument. The transparent parts of the electromagnetic spectrum that lie between these high opacity regions are called atmospheric windows and the scope of earth-based planetary spectroscopy is limited to these windows. Consequently orbiting spectroscopes are used to obtain more elaborate planetary spectra.

O_3 is a very important gas which envelopes the Earth's atmosphere about 50 km above the Earth's surface. It absorbs almost the entire ultraviolet radiation below 3000Å. This absorption shortward of 3000Å prohibits ground based observations of other planets at short ultraviolet wavelengths.

In the infrared, longward wavelength of 10,000Å, the spectrum is highly divided into a number of windows. The principal terrestrial absorbing agent in the near infrared is H_2O which is present in the troposphere. It is only through the use of balloons and high altitude sites like aircraft rockets or satellites and simply very high mountains, that one can avoid this terrestrial absorption and can obtain satisfactory observations of planets in the infrared.

PLANETWISE REVIEW

Mercury
(CO_2, CO)

Because of very low escape velocity and high order of temperatures due to close proximity of the sun, Mercury is expected to retain, if at all, only a very sparse atmos-

phere. So far there is no confirmed observational evidence of any detectable atmosphere on Mercury. The planet is considered essentially gasless.

Kozyrev (1964) reported spectroscopic observation of certain variable hydrogen emission lines in the form of small humps in the bottom of hydrogen absorption lines in the spectrum of reflected sunlight from Mercury. He suggested that perhaps atomic hydrogen might be surviving in the Mercurian atmosphere by being constantly replenished by hydrogen nuclei emitted by the sun. Gott and Potter (1970) have also given a theoretical model of a hydrogen atmosphere for Mercury originating in the solar wind. Spinrad and Hodge (1965), however, refuted Kozyrev's inferences about the presence of atomic hydrogen in the Mercurian atmosphere. These authors regard Kozyrev's emissions as simply spurious, most probably caused by the overlapping of two solar hydrogen absorptions - one in the sunlight scattered by the Earth's atmosphere and the other in the Doppler-shifted sunlight reflected by the surface of the planet.

Belton et al. (1967) and Bergstralh et al. (1967) predicted the presence of some traces of CO_2 in the Mercurian atmosphere. Moroz (1965) had earlier pointed out that carbon monoxide might be present in the atmosphere of Mercury, with an upper limit of 10 cm-atm. Lately, Fink et al. (1974) identified both these constituents spectroscopically and set an upper limit of 0.12 cm-atm for CO_2 and 0.05 cm-atm for CO.

It may, however, be pointed out that the results of the Mariner-10 flyby mission were not positive for the presence of any of these molecules in the atmosphere of Mercury.

Venus
(CO_2, H_2O, CO, O_2, HCl, HF)

The composition of the Venusian atmosphere has been a speculative matter ever since the Russian scientist, Lomonosov (1891) discovered an atmosphere in Venus during a solar transit of Venus in 1761. Besides numerous remote earth-based spectroscopic observations and radio occulation methods, the atmosphere of Venus has been quite extensively studied by a number of space entry probes such as the Russian Venera series and American Mariner series flyby missions. Venera-7 transmitted data from the Venusian surface which indicated a pressure of about 90 terrestrial atmospheres at the surface. The surface of Venus is covered by a dense layer of cloud which accounts for its high albedo. There exist varied opinions about the composition of these clouds. The latest view, however, is that they are formed of droplets of water solution of H_2SO_4. Many interesting papers on this and allied subjects can be found in J. Atmos. Sci., Vol. 32, No. 6, June 1975, which covers the recent 1974 - Goddard Conference on the Atmosphere of Venus.

Carbon dioxide (CO_2) is found to be the major constituent of the Venusian atmosphere. The quoted concentration as derived from the data obtained through Venera 5 and 6 is 97 ± 4 percent (Vinogradov et al., 1971). Spectroscopic data obtained from an aircraft

by Kuiper et al. (1969) correspond roughly to the absorption by 10-20 km of CO_2 at 0.1 bar. Work done by Belton et al. (1968); and Moroz (1968) is also quite significant with regard to Venusian spectroscopy. Connes et al. (1969) atlas provides a nice display of Venusian spectra obtained by the Fourier transform technique.

Carbon monoxide (CO) was clearly identified as a Venusian molecule by Connes et al. (1968). Spectral features corresponding to less abundant species, viz., $C^{13}O^{16}$ and $C^{12}O^{18}$, were also identified in addition to the most abundant species $C^{12}O^{16}$. The mixing ratio CO/CO_2 is estimated to be 4.6×10^{-5}.

The presence of gaseous hydrogen fluoride (HF) and hydrogen chloride (HCl) in the Venusian atmosphere was first reported by Connes et al. (1967). The halide-carbon dioxide mixing ratios were estimated as $HCl/CO_2 = 6 \times 10^{-7}$ and $HF/CO_2^2 = 5 \times 10^{-9}$. Figures (1) and (2) depict the profiles of some of the observed spectral features of these halides in the spectrum of Venus.

Belton and Hunten (1968) studied the Venusian atmosphere in greater detail with re-gard to oxygen and the upper limit of O_2/CO_2 was set at $\leq 8 \times 10^{-5}$. Lately, Traub and Carleton (1974) reported the mixing ratio O_2/CO_2 as 1×10^{-6} based on their study of the 7635Å line of O_2. Results from Venera-5 and Venera-6 implied less than 0.4% of O_2 in the atmosphere of Venus.

Study of microwave emission spectrum as well as absorption of radar signals both indicate the presence of H_2O vapor in the Venusian atmosphere and the upper limit set by these experiments is about 1% (Pollack and Morrison, 1970). Doppler-shifted spectra in the 8189Å region and balloon spectra at 1.3μ show a weak but definite planetary line and give the mixing ratio as 10^{-4} (Belton et al., 1968; Spinrad and Shawl, 1966; Botterma et al., 1965; Belton, 1968). A somewhat smaller upper limit was found in Connes spectra at longer wavelengths (Connes et al., 1967, and by Owen, 1967) at 8189Å. This disparity has been discussed by Schorn et al. (1969), who reported clear evidence for variability.

Earth
(O_2, N_2, CO_2, H_2O, O_3, CH_4, N_2O, NO_2, Ar, He, H_2, Xe, Kr, Ne, CO)

The atmosphere that surrounds the Earth, commonly called air, consists of layers of gases and mixtures of gases, as well as water vapor and solid and liquid particles. The mean pressure exerted by this atmosphere at sea level equals that of a column of mercury 760 mm in height. Higher in the atmosphere, the pressure decreases and, roughly at an altitude of six km is only one half that at sea level. The principal regions of atmos-phere, each of which is characterized by the pattern of vertical distribution of tempera-tures, are a) troposphere, b) stratosphere, c) mesosphere, d) thermosphere and e)

1 (Venus)
2 (Sun)
3 (Ratio)

(cm^{-1})
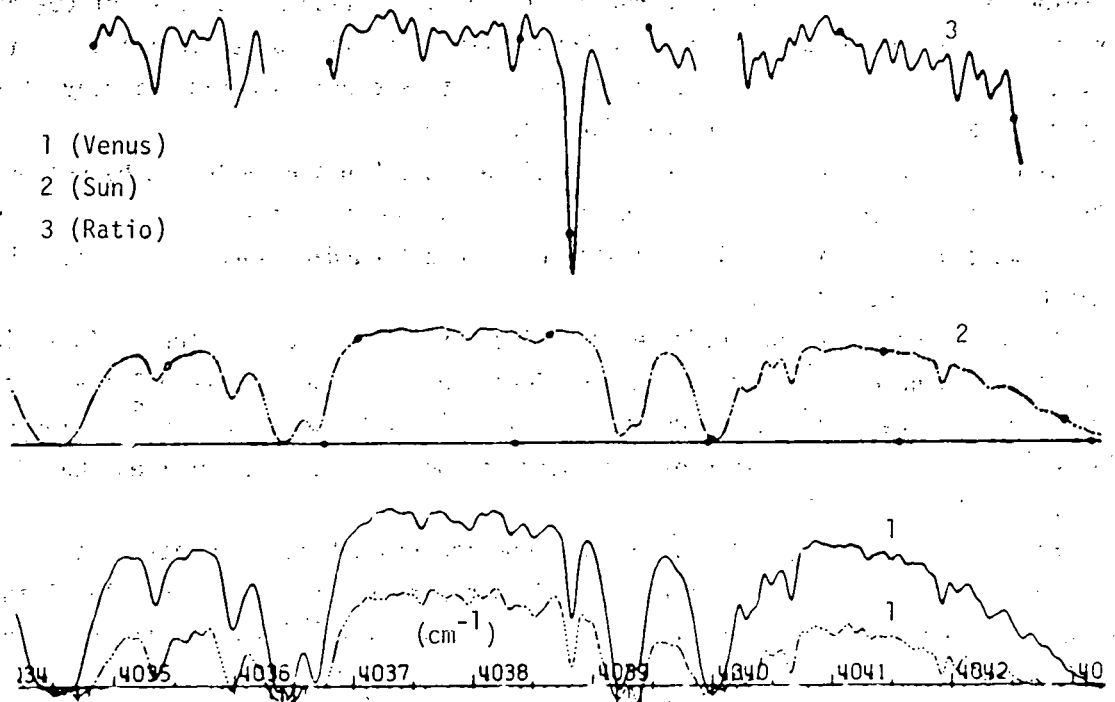
Figure 1. The R(1) line of the (1-0) band of HF in the Venusian spectrum (Connes, et al., 1969).
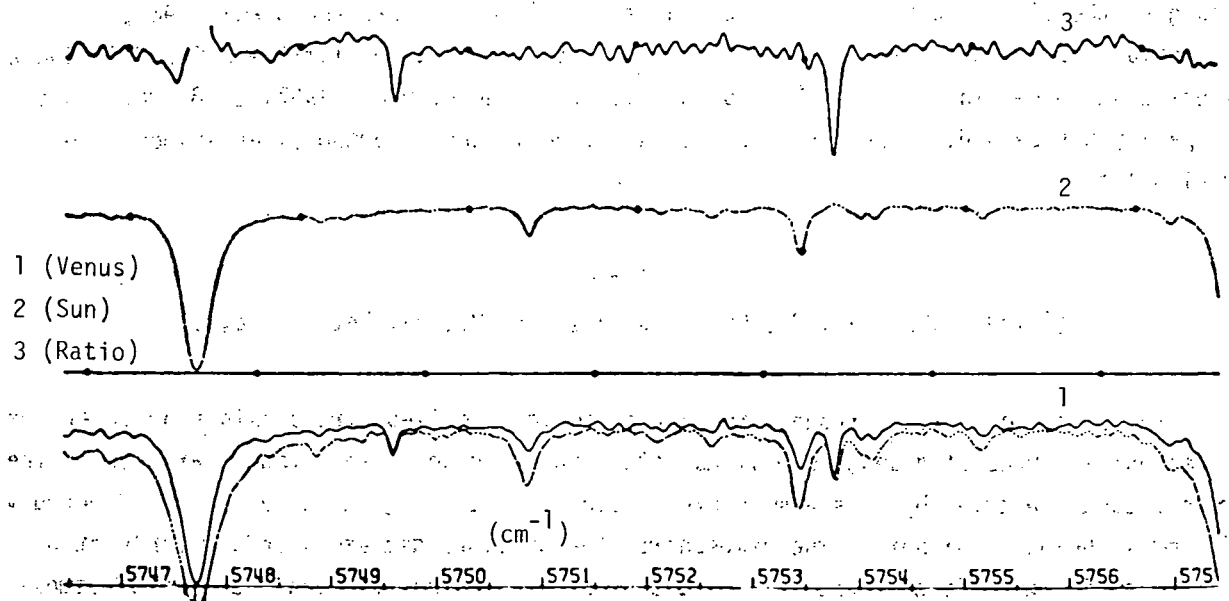

1 (Venus)
2 (Sun)
3 (Ratio)

(cm^{-1})

Figure 2. The R(4) lines of the (2-0) band of HCl^{35} and HCl^{37} isotopes in the Venusian spectrum (Connes, et al., 1969).

exosphere. The entire atmosphere extends beyond 400 km, and broadly speaking it can be divided into two regions:

(1) The lower atmosphere. This part extends roughly up to 100 km from the Earth's surface. It includes the troposphere (upper limit 17 km at the equator and about 6-8 km at the poles), the stratosphere (upper limit approximately 50 km) and the mesosphere (to a minimum up to 85 km; it is subject to strong seasonal variations).

(2) The upper atmosphere. This is the region beyond the mesopause and is entirely different in character compared to the lower atmospheric belts. The first stratum of this region is the thermosphere characterized by a continuous increase of temperature up to 500°K at night during minimum solar activity and to above 1750°K in daytime during maximum solar activity. The altitude at which this increase of temperature ceases is the thermopause, which is at the base of an isothermal region that extends into interplanetary space. As a matter of fact, the gas collisions become so rare at this level that the term temperature loses its conventional meaning.

The strongest absorption of solar radiation in the Earth's atmosphere is due to the triatomic molecules H_2O, CO_2 and O_3. Methane and nitrous oxide (CH_4 and N_2O) are present only in trace quantities and therefore contribute only a little to the total absorption although many of the spectral features of these gases show up in the solar spectrum. Some of the highlights of these absorption spectral features are given below.

Molecular Oxygen (O_2): Magnetic dipole transitions between the three lowest electronic levels lead to the red ($^3\Sigma_g^- \rightarrow {}^1\Sigma_g^+$ and infrared ($^3\Sigma_g^- - {}^1\Delta_g$) bands of O_2. These are sometimes called 'atmospheric bands'. Bands due to $O^{16}O^{18}$ and $O^{16}O^{17}$ are also detected in the solar spectrum. The main infrared bands of oxygen are the (0,0) and (0,1) band at 1.2683μ and 1.0674μ, respectively. The main bands of the red system are the (0,0) and (0,1) bands, lying at .7621μ and .6884μ, respectively. The ultraviolet absorption spectrum of $O^{16}O^{16}$ commences with weak Herzberg bands at 2600Å ($^3\Sigma_g^+ - {}^3\Sigma_g^-$). Below 2420Å, the transition becomes dissociative and the Herzberg continuum sets in. The absorption cross section of O_2 for this wavelength region lies between 10^{-23} and 10^{-24} cm^2 and is, therefore, of little importance as regards energy absorption.

The Schumann-Runge bands system of O_2 spectrum lies in the region 1950-1750Å, and has been ascribed to the electronic transition $^3\Sigma_u^- - {}^3\Sigma_g^-$. Around 1750Å, the bands merge into a continuum, which extends up to 1300Å and is the most important single feature of O_2 absorption.

Oxygen Polymers (O_2)$_2$: Dufy (1942) observed a weak band at 4774Å in the solar spectrum visible only from zenith angles greater than 85°. He ascribed this band to the oxygen polymer (O_2)$_2$. It may be pointed out here that the spectrum of the oxygen polymer (O_2)$_2$ has been recorded in the laboratory and it consists of three diffuse bands at 6290Å,

5770Å and 4774Å. Two weaker bands at 5325Å and 4470Å have also been claimed. Further, since the density of $(O_2)_2$ depends upon the square of pressure, it must form a very low lying layer. The absorption becomes significant only at large zenith angles because the low lying $(O_2)_2$ path is much longer under such circumstances.

Water Vapor (H_2O): Water vapor forms an important constituent of Earth's atmosphere, particularly in the low lying regions. In the solar spectrum, numerous vibration-rotation lines of H_2O and its isotopes have been identified from visible to the microwave region. Four isotopic forms of H_2O have identifiable lines in the solar spectrum: H_2O^{16}, H_2O^{18}, H_2O^{17}, and HDO^{16}. Each of these molecules has a different vapor pressure and their abundances depend to some extent on the evaporation-condensation cycle. The most important H_2O absorption bands in the solar spectrum center around 6.3μ, 9μ, 50μ.

Carbon Dioxide (CO_2): The ν_2 bands near 15μ are probably the most intensively studied bands in the solar spectrum. Besides the ν_2 fundamental, fourteen overtone and combination bands have also been detected in the 15μ region with a total intensity of about 10% of the fundamental.

The three ν_3 bands are responsible for the great opacity of the atmosphere near 4.3μ. There are three bands superimposed, viz.: ν_3 band ($C^{12}O_2^{16}$) - 2349.16 cm^{-1}; ν_3 band ($C^{13}O_2^{16}$) - 2283.48 cm^{-1}; and the combinational band ($\nu_1 + \nu_3 - 2\nu_2$) ($C^{12}O_2^{16}$) -2429.37 cm^{-1}.

Ozone (O_3): The solar spectrum exhibits characteristic absorption due to O_3. The Hartley bands centered at 2553Å are the most characteristic ones. They consist of a large number of weak bands, superimposed on a strong continuum. The spectral region from 3100Å to 3400Å in the spectrum of the low sun is full of another set of well-marked O_3 bands called the Huggins bands.

Between 4500Å and 7400Å lie the O_3 Chappuis bands. The overall O_3 absorption is so strong that solar radiation below 0.3μ does not penetrate the atmosphere. The infrared bands of O_3 at 710 cm^{-1}, 1043 cm^{-1} and 2105 cm^{-1} also show up in the solar spectrum.

In addition to these main atmospheric gases, there are known to exist a few minor constituent gases, viz., N_2O, CH_4, CO and also NO_2. Numerous bands due to N_2O have been reported in the solar spectrum in the region (2-17μ). Similarly, CH_4 absorption is exhibited in solar spectrum in the region (1.67 - 7.66μ). CO is known to be present in the Earth's atmosphere in such trace quantities that it is of little significance to atmospheric studies. No specific spectral features ascribed to NO_2 have been identified in the solar spectrum so far though the molecule is widely held responsible for the creation of the D-layer of the ionosphere.

Mars
(CO_2, CO, O_2, H_2O, O_3, N_2, Ar)

Mars is known to have an extensive atmosphere almost transparent to the bulk of the sun's radiation. It is very thin by terrestrial standards and is now considered to be composed of mainly CO_2 gas. Water vapor (H_2O) and carbon monoxide (CO) have also been positively identified as minor constituents. An admixture of gases, such as Ar, N_2, and O_3, is also envisaged to be present in trace amounts. Molecular description is as follows.

Carbon Dioxide (CO_2): It is the first gaseous chemical constituent ever identified positively through spectroscopic methods in the Martian atmosphere. Kuiper (1949) identified three bands at 1.96, 2.01 and 2.06μ, respectively, in the Martian spectrum, which were unequivocally ascribed to gaseous CO_2. More exhaustive investigations by numerous workers, viz., Kaplan et al. (1964); Kliore et al. (1965); Belton et al (1966); Owen (1966); Spinrad (1966); Belton et al. (1968); Giver et al. (1968); Carleton et al. (1969); Young (1969); Rasool et al. (1970); McConnel (1973) followed later. The amount of CO_2 as reported in almost all of the later reports lies within the range 50-90 m-atm. The most probable value as established by McElroy (1973) is 78 m-atm. Data obtained from Mariner space fly-by missions also support the theory that a very high abundance of gaseous CO_2 is in the Martian atmosphere.

Carbon Monoxide (CO): Kaplan et al. (1969) first detected CO molecules in the Martian atmosphere by observing the (2-0) and (3-0) bands of carbon monoxide in a high resolution Martian spectrum. These authors obtained an abundance of 5.6 cm-atm. of CO in the atmosphere.

Later on Young (1971) and Carleton et al. (1972) also determined the CO abundance in the Martian atmosphere, the value obtained by the latter being 7.3 ± 1.0 cm-atm. Most probably CO in the Martian atmosphere is the photodissociation product of CO_2 under the sun's ultraviolet radiations < 1700Å.

Oxygen (O_2): The presence of O_2 molecules has been established by detecting an absorption feature due to O_2 at 7635Å in the reflected solar spectrum (Carleton and Traub, 1972; Barker, 1972). The observations were made under certain preferential conditions so that a Doppler shift of about ± 0.3Å could be obtained. The abundance has been established as somewhere between 9-10 cm-atm. This value is consistent with the earlier lower limit of O_2 abundance proposed by Belton and Hunten (1968).

Water Vapor (H_2O): Water vapor is considered to be a very minor, variable and unevenly distributed constituent of the Martian atmosphere. Traces of water vapor were first identified spectroscopically by Kaplan, Munch and Spinrad (1963). Normally the investigation of water vapor by earth-based spectrography is rendered very difficult because of the masking of weak planetary lines by strong H_2O absorption features by the Earth's atmosphere.

Spinrad et al (1963) carried out extensive high dispersion studies of the Martian atmosphere using the 100-inch reflector at Mount Wilson. These authors identified as many as 11 rotational lines due to Martian H_2O because the Doppler shifts from their telluric counterpart were of the expected value ($0.42\overset{o}{A}$ to the red). Measurement of the average equivalent width and intensity of some of the unblended lines led them to get an abundance ratio of about 14 ± 7 microns of precipitable water. (A precipitable micron equals 3.35×10^{18} cm^{-2} or 0.125 cm-atm.) Many more earth-based spectroscopic investigations on water vapor in the Martian atmosphere followed later on (Dollfus, 1964; Barker et al., 1970; and Tull et al., 1972).

Lines attributed to H_2O absorption have also been observed in the solar reflection spectrum near $8200\overset{o}{A}$. The amount observed is variable, usually between 10 and 40μm precipitable water and frequently falls below the detection threshold (Schorn et al., 1969; Schorn, 1971).

Water vapor spectra were also obtained by the Mariner-9 flyby mission using infrared interferometry onboard. The results indicated the abundance of H_2O vapor at 10 - 20 microns of precipitable water (Hanel et al., 1972).

Atmospheric water vapor molecules can be destroyed quite rapidly on Mars through the action of ultraviolet light as a result of inefficient shielding by CO_2 and the absence of O_3. The light hydrogen atoms so released diffuse up through the atmosphere and ultimately escape into space. This produces a net gain in the O_2 content in the atmosphere. This process may explain the observed hydrogen emission in the upper Martian atmosphere as observed in Mariner-6 and 7 missions.

Ozone (O_3): The spectroscopic results obtained via the space probe Mariner-7 indicate the presence of about 10^{-3} cm-atm. of O_3 in the Martian atmosphere. Particularly the O_3 band at $2550\overset{o}{A}$ was identified in this mission near the south polar cap of Mars during its late spring season. No O_3 was detected in the rest of the planet (Barth et al., 1971). The present upper limits of the abundance of O_3 are however set on the basis of data obtained through rocketborne spectrometry (Broadfoot and Wallace, 1970) as 2×10^{-4} cm-atm. Recently, Lane et al. (1973) have identified O_3 absorption in Hartley continuum in the spectra taken on Mariner 9 orbiter.

O_3 in the Martian atmosphere is perhaps formed by the association of O_2 and 0 through a three-body process $O_2 + O + M \rightarrow O_3 + M$. In the Martian middle atmosphere, perhaps the photodissociation of CO_2 might supply sufficient atomic oxygen to promote this reaction. It may however be remarked here that the presence of O_3 appears to increase as the H_2O abundance goes down (Lane et al., 1973).

According to the theoretical study of O_3 abundance in the Martian atmosphere by Marmo and Warneck (1960, 1961), O_3 should be less than 0.0001 cm-atm.

Nitrogen (N_2): Though N_2 was once speculated to be the most abundant gaseous constituent of the Martian atmosphere, the picture is entirely different now. So far, no

spectroscopic detection of N_2 has been possible. The results of Mariner 6 and 7, however, indicate an upper limit of N_2 abundance as less than 1%.

Argon (Ar): The relative cosmological abundance of Argon, combined with its chemically inert nature and atomic weight 40, marks it as a very prospective constituent of the Martian atmosphere (Brown, 1949; Suess, 1948). The Mariner 4 results have shown that Argon may be the second most important constituent after CO_2, ranging anywhere between 0 - 20%.

Jupiter
(H_2, CH_4, NH_3, He, Ne, N_2)

The atmosphere of Jupiter is quite deep and turbulent. Hydrogen (H_2), methane (CH_4) and ammonia (NH_3) have been positively established as the constituent gases through spectroscopic evidence. Presence of inert gases like helium (He) and neon (Ne) as well as nitrogen (N_2) has also been proposed in view of the overall low density of the planet. Any water on the Jovian surface, if at all present, must be frozen out because of the low surface temperatures (-130°C).

The atmosphere is further covered by a thick envelope of clouds which are probably formed from frozen ammonia. Since methane boils at -126°C and freezes at -150°C, almost the entire quantity of methane that might be present is probably gaseous. The latest accepted view is that the Jovian atmosphere is composed of about 90% molecular hydrogen and nearly 10% helium, with very small amounts of methane and ammonia and perhaps some traces of neon and nitrogen. Molecular description is given below.

Hydrogen (H_2): Molecular hydrogen is known to be the main constituent of the Jovian atmosphere. Normally H_2 does not show any electric dipole absorption in the infrared because of molecular symmetry but a number of quadrupole transitions and pressure induced dipole transitions have been identified in the Jovian spectrum. This is most probably due to the high abundance of hydrogen in the planet.

Danielson (1966) first observed a broad, deep absorption from 2 to 2.5μ in the Jovian spectrum which was ascribed to a pressure induced dipole transition of H_2. Quadrupole transitions of H_2, particularly the 3-0 band around 8150Å and the S(1) line of the 4-0 band at 6367Å were studied by many workers in the spectrum of Jupiter (Kiess et al., 1960; Spinrad and Trafton, 1963; Beckman, 1967; Owen and Mason, 1968; Fink and Belton, 1969 and Emerson et al., 1969). Almost all of these results are in good agreement, and give the H_2 abundance in the range 2.5 - 3 x 10^7 cm-atm. Figures 3 and 4 show the profiles of 3-0 S(1) and 4-0 S(1) quadrupole lines of molecular hydrogen as reported by Fink and Belton (1969).

Methane (CH_4) and Ammonia (NH_3): First qualitative identification of a reasonable abundance of gaseous methane and ammonia through spectroscopic evidence was made by
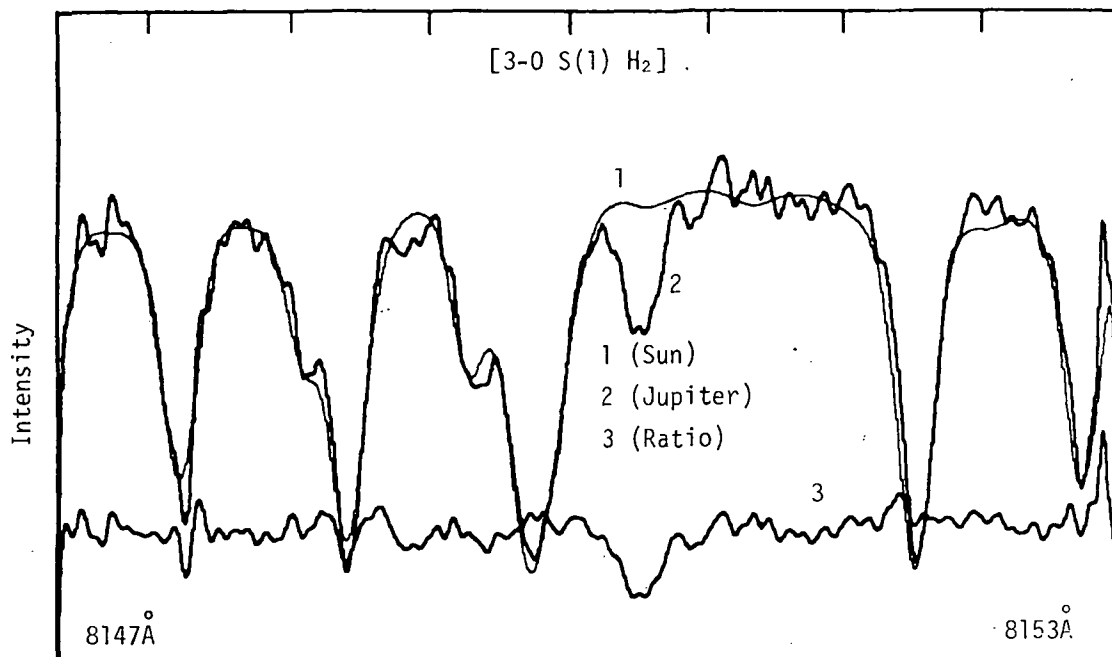
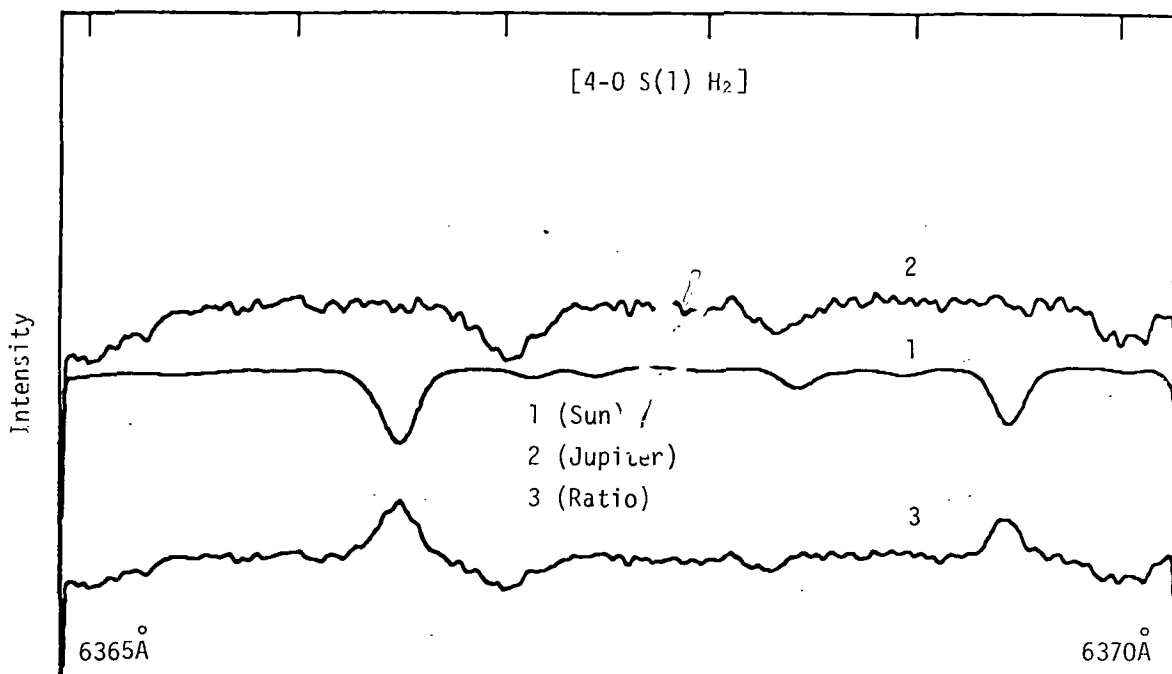Figure 3.   The 3-0 S(1) quadrupole line of H_2 in the spectrum of Jupiter (Fink and Belton, 1969).

Figure 4.   The 4-0 S(1) quadrupole line of H_2 in the spectrum of Jupiter (Fink and Belton, 1969).

Wildt (1932). Dunham (1933) later obtained high resolution spectrograms of the Jovian atmosphere using the Coudé focus at Mt. Wilson. Many rotational lines of NH_3 in the region 7900-6450Å were well resolved. Similarly, CH_4 bands at 7200Å, 8000Å and 8800Å were also well resolved.

Spectra taken with long tubes filled with NH_3 and CH_4 were compared with the Jovian planetary lines. There were considerable differences in the relative intensities of individual rotational lines in the NH_3 spectrum; this is to be expected since the laboratory data were taken at room temperature (290°K) while the temperature in Jupiter's atmosphere is near 150°K. According to Kuiper (1952) Jupiter has 700 cm-atm abundance of NH_3 and 15000 cm-atm abundance of CH_4.

Saturn
(CH_4, NH_3, H_2, He, Ne, N_2)

The planet Saturn, if taken alone without its fascinating set of rings, bears close resemblance to Jupiter. However, our knowledge about Saturn's atmosphere is much more limited as compared to that of Jupiter, mainly because Saturn is almost twice as far away.

The CH_4 absorption lines in Saturn's spectrum show up more prominently than in Jupiter's. The H_2 quadrupole lines too appear a bit more strongly in the spectrum of Saturn in comparison to their counterpart in the Jovian spectrum. The equivalent widths of these lines lead to an abundance estimate of about 10 km-atm of molecular hydrogen in Saturn's atmosphere. The estimated rotational temperature ($\sim$88°K) is also consistent with the apparent absence of ammonia (NH_3) in the Saturn atmosphere (NH_3 lines could never be identified on high dispersion spectra of Saturn). In view of the overall low density of the planet, it is speculated that in addition to the large abundance of H_2, there might also exist trace quantities of helium, neon and nitrogen.

The rings of Saturn do not exhibit any characteristic absorption features in the visible and the photographic infrared ($\lambda < 1.0\mu$).

Uranus and Neptune
(CH_4, H_2, He, N_2)

Our current knowledge of the composition of the atmospheres of Uranus and Neptune is worse than our guess for Saturn.

Both the planets show tremendous concentrations of methane in their spectra. The CH_4 absorption of Uranus corresponds to 2.2 km-atm; on Neptune the amount is about 3.7 km-atm. The methane bands on Uranus may hide weaker bands of other molecules. No NH_3 has ever been observed on Uranus or Neptune; it must be frozen out, as is CO_2 or H_2O.

21

Pressure induced dipole transitions of H_2 also show up as several faint and broad absorption lines in the red and near infrared part of the spectra of both Uranus and Neptune. A number of sharp H_2 quadrupole lines also appear in high dispersion spectra.

Pluto

The low temperature and the low mass, both suggest that Pluto may not have any atmosphere at all. Many potential molecular species, such as NH_3, CO_2 or H_2O would largely lie in the frozen state. Others such as hydrogen and helium, etc., may well have escaped. Anyway, there is no reliable evidence so far available that might indicate the presence of an atmosphere on this planet.

SECTION II

MOLECULES AND RADIATION

CHAPTER 3

BASICS OF MOLECULAR TRANSITIONS

A molecule in its simplest form may be regarded as a local assembly of two or more atoms in dynamic equilibrium. The simplest known molecule is the molecular hydrogen ion H_2^+ which is composed of only two protons and one electron. At the other extreme is the ribonuclease protein whose molecule consists of as many as 1876 nuclei and 7396 electrons. The constituent nuclei of a molecule are held together by different chemical bonds, the lengths and strengths of which normally range between 1 - 2Å and 1 - 5 eV, respectively. Such a circumstance allows a molecule to have numerous degrees of freedom, unlike atoms. It undergoes rotational motions and consequently possesses different moments of inertia depending upon the axes of rotation. It has vibratory motions and consequently involves different vibrational frequencies depending upon the number of the constituent nuclei and the bonds. Both these motions are non-existent in atoms. The total internal energy of a molecule is also characterized not only by its electronic energy but, in addition, by its vibrational and rotational energies too.

According to the Born-Oppenheimer approximation, these different energies of a molecule can be considered as separately quantized. The total internal energy, E, can, therefore, be expressed as a simple sum of the three energies; i.e.,

$$E = E_e + E_v + E_r, \qquad (3-1)$$

where E_e, E_v, and E_r represent the electronic, vibrational and rotational energy components. The electronic energy, E_e, is the energy that the molecule would possess if the nuclei were fixed in their equilibrium positions. It consists of the kinetic and potential energy of the orbital electrons and the mutual potential energy of the repulsion of the nuclei.

The vibrational energy, E_v, is the energy which the molecule would have if the nuclei were vibrating about their equilibrium positions but still did not rotate. This energy is never zero.

The rotational energy, E_r, is the additional energy that a vibrating molecule would have if the nuclei rotate as a composite unit about an axis passing through the center of mass of the molecular skeleton. It is not just the energy that the molecule would have if it rotated with its nuclei fixed in the equilibrium position but also takes care of the distortion of the molecule during rotation and electronic motions.

A molecule may also possess translational energy, E_T, by virtue of its kinetic motion, but it is not quantized.

Figure (3-1) depicts a schematic showing various vibrational and rotational levels associated with an electronic state of a typical diatomic molecule.
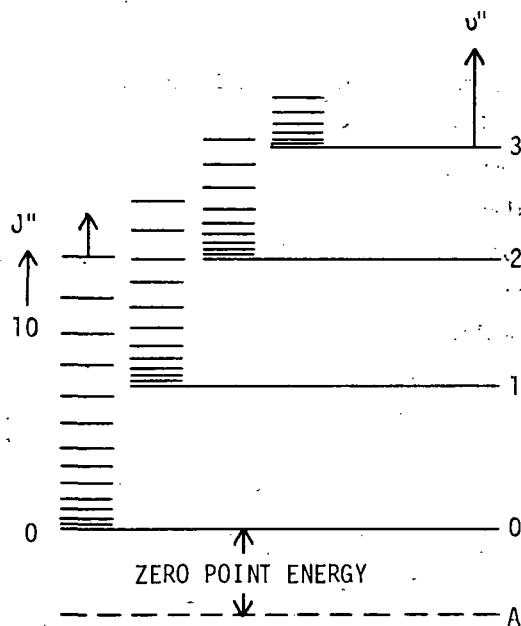
Figure (3-1). Schematic showing different rotational and vibrational levels associated with an electronic state, A.

Radiative transitions in a molecule take place between different quantized energy states subject to certain quantum selection rules. Transitions in which higher energy levels are involved are simultaneously accompanied by transitions involving lower energy levels; e.g., a transition between two vibrational states is accompanied by both rotational and vibrational transitions. Consequently, a vibrational transition does not involve quanta of single frequency but a series of quanta of different frequencies and, similarly, an electronic transition normally involves quanta of different frequencies. Figure (3-2) depicts various possible radiative transitions in a typical case.

E'(Π)

7

v=1

J
3
2
1
0

6

v=0

J
3
2
1
0

5

E"(Σ)

4

3

J
3
2
1
0

2
v=2

J
3
2
1
0

v=1

J
4
3
2
1
0

1

v=0

0

P R P Q R

ELECTRONIC
VIBRATION-ROTATION
ROTATIONAL

POTENTIAL ENERGY (eV)

1   2   3   4

INTERNUCLEAR DISTANCE (Å)
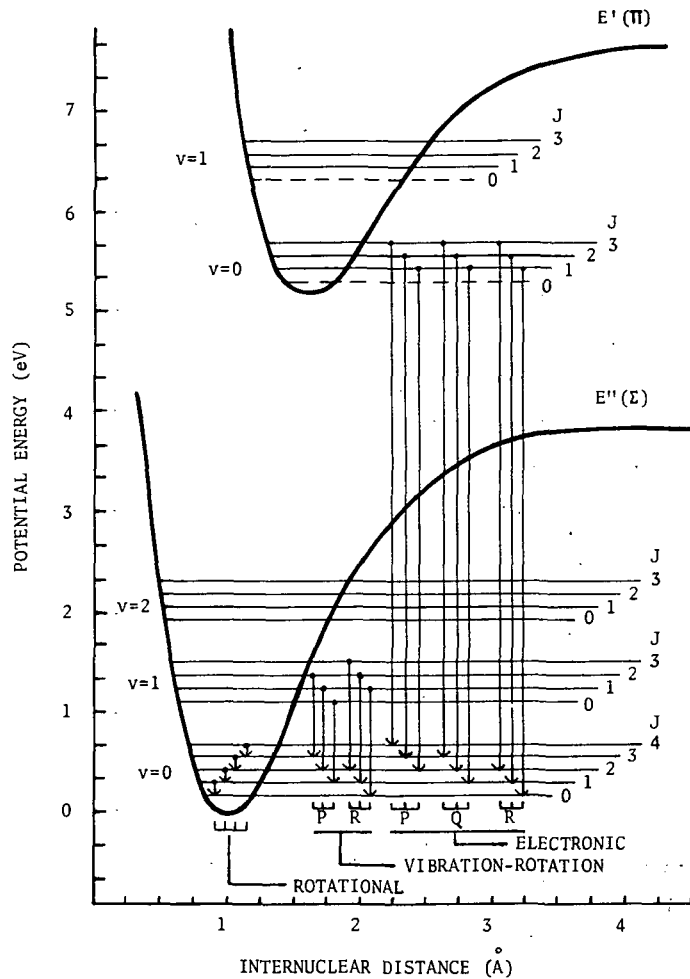
Figure (3-2).   Schematic showing various possible radiative transitions in a
                typical diatomic molecule.

DIATOMICS

Pure Rotational Spectrum

A dumb-bell with two mass-points rigidly bound to each other by a massless rod is
the simplest model of a diatomic molecule. However, a rigid dumb-bell cannot be con-
sidered a perfect model for a diatomic molecule because, as a result of the action of
the centrifugal force, the internuclear distance varies with the velocity of rotation.
A non-rigid rotator; i.e., a rotating system of two mass points joined by a massless
spring, is thus a more realistic model for a diatomic.

According to quantum theory, the rotational term value, $F(J)$, for a non-rigid
rotator can be written as

$$F(J) = \frac{E_r}{hc} = BJ(J + 1) - DJ^2(J + 1)^2 + - - - - \tag{3-2}$$

where E_r is the rotational energy of the molecule in a rotational state characterized by the rotational quantum number J.

J is related to the magnitude of angular momentum vector P by the relation $|P| = \frac{h}{2\pi} \sqrt{J(J + 1)}$ and can assume any integral value 0, 1, 2 - - -
B and D are the rotational constants, interrelated as $D = \frac{4B^3}{\omega^2}$
ω is the vibrational frequency in cm^{-1}
$B = \frac{h}{8\pi^2 Ic}$, where $I = \mu r^2$ and $\mu = \frac{m_1 m_2}{m_1 + m_2}$ m_1 and m_2 being the masses of nuclei forming the molecule.
$D \ll B$ and is a measure of the centrifugal distortion in the molecule during rotation.

The wave number of a rotation line arising from a transition, J', J", can be expressed as

$$
\begin{aligned}
\nu_{J'J"} &= F_{\nu_0}(J') - F_{\nu_0}(J") \\
&= [BJ'(J' + 1) - D(J' + 1)^2 J^2] \\
&- [BJ"(J" + 1) - D(J" + 1)^2 J"^2]
\end{aligned} \tag{3-3}
$$

or, putting J' = J + 1 and J" = J, we get the following running expression for the various rotational frequencies.

$$
\begin{aligned}
\nu_{J'J"} = \nu_{(J + 1), J} &= F(J + 1) - F(J) \\
&= 2B(J + 1) - 4D(J + 1)^3
\end{aligned} \tag{3-4}
$$

The above relation indicates that in a pure rotational spectrum, we get a number of non-equidistant lines; the interline separation decreasing, of course, slightly with increasing J. Since $D \ll B$, this effect usually is very small. For example, in the case of HCl, while $B = 10.395$ cm^{-1}, D is only 0.0004 cm^{-1} and the observed rotational lines appear to be almost equidistant, having interline separation almost equal to 2B.

Currently microwave techniques are widely utilized in the 3mm to 20 cm wavelength range, where the rotational lines of most of the diatomics normally lie. These methods provide a resolving power much higher than optical gratings and a very high order of accuracy in frequency determination.

Vibration-Rotation Spectrum

Vibration-rotation spectrum of a diatomic molecule is usually an ensemble of a few vibration rotation bands, each of which is again an ensemble of numerous rotational lines located in a certain specific order in a certain frequency range. Each line corresponds to a radiative transition from a rotational level, J', associated with a vibrational level, v', to another rotational level, J", in another vibrational level, v", in the same electronic state.

If we consider a diatomic to be a harmonic oscillator, then, according to the classical concepts, the fundamental vibration frequency of a diatomic vibrator can be written as

$$\nu_{osc.} = \frac{1}{2\pi} \sqrt{\frac{K}{\mu}} \; sec^{-1} \qquad (3-5)$$

where $\mu = \frac{m_1 m_2}{m_1 + m_2}$, the reduced mass of the molecule, and K is the force constant which is a measure of the strength of the chemical bond between the two atoms.

Now if we substitute the potential energy value, $U = 1/2 \, k \, (r - r_e)^2$, as obtained by Hooke's law for such an oscillator in the Schrodinger equation the following quantized vibrational energy expression is obtained.

$$
\begin{aligned}
E_v &= h\nu_{osc.} \; (v + 1/2) \\
&= hc\omega_e \; (v + 1/2)
\end{aligned}
\qquad (3-6)
$$

where v is the vibrational quantum number and can assume values 0, 1, 2, 3, - - -. Although the assumption that a diatomic acts as a harmonic oscillator following a quadratic potential function $V = 1/2 \, k \, (r - r_e)^2$ is satisfactory at small values of $(r - r_e)$, it is no more valid for large displacements. If we assume the vibrations of a diatomic molecule as anharmonic and for this purpose add a cubic term to the simple quadratic function as given below,

$$U = 1/2K \, (r - r_e)^2 - k' \, (r - r_e)^3 \qquad (3-7)$$

Schrodinger equation gives the following relationship for the quantized vibrational energy or in other words, the energy values of the anharmonic oscillator are given by

$$E_v = hc\omega_e \, (v + 1/2) - hc\omega_e x_e \, (v + 1/2) + hc\omega_e y_e \, (v + 1/2)^3 + - - \qquad (3-8)$$

where x_e and y_e are the anharmonicity constants; or the term value for the vibration energy can be written as

$$G(v) = \omega_e (v + 1/2) - \omega_e x_e (v + 1/2) + hc\omega_e y_e (v + 1/2)^3 + - - \cdot \qquad (3-9)$$

Here v is again the vibrational quantum number and the constant $\omega_e x_e \ll \omega_e$ and $\omega_e y_e \ll \omega_e x_e$. The zero point energy of the anharmonic oscillator is obtained from the above equation by putting v = 0;

$$G(0) = \left(\frac{1}{2}\right) \omega_e - \left(\frac{1}{4}\right) \omega_e x_e + \left(\frac{1}{8}\right) \omega_e y_e + - - \qquad (3-10)$$

If the energy levels are referred to the level v = 0, we obtain

$$G_o(v) = G(v) - G(0) = \omega_o v - \omega_o x_o v^2 + w_o y_o v^3 + - - \qquad (3-11)$$

$$\omega_o = \omega_e - \omega_e x_e + \frac{3}{4} \omega_e y_e + - -$$

where
$$\omega_o x_o = \omega_e x_e - \frac{3}{2} \omega_e y_e + - -$$

$$\omega_o y_o = \omega_e y_e + - -$$

Radiative Transitions in a Vibrating Rotator. - Vibrational transitions in a vibrating-rotating molecule are normally accompanied by almost simultaneous rotational transitions and, therefore, in considering a vibration-rotation spectrum, we have to take into account the joint effect of the two molecular motions.

The term value, $T = (E_{vr}/hc)$, of a vibrating-rotator can be written as

$$T = G(v) + F_v(J)$$

$$= [\omega_e (v + 1/2) - \omega_e x_e (v + 1/2)^2 + \omega_e y_e (v + 1/2)^3 + - -] \qquad (3-12)$$

$$= + [B_v J (J + 1) - D_v (J + 1)^2 J^2 + - - -]$$

where B_v and D_v are the rotational constants for a particular vibrational level v. These are related to the equilibrium rotational constants by the following relations:

$$B_v = B_e - \alpha_e (v + 1/2) + \qquad (3-13)$$

$$\text{and } D_v = D_e + \beta_e (v + 1/2) + \qquad (3-14)$$

Here $\alpha_e \ll B_e$ and $\beta_e \ll D_e$ and have the same units.

The various vibration-rotation frequencies (cm^{-1}) can thus be obtained using the following expression:

$$\nu_{vr} = T' - T'' = [G(v') + F_{v'}(J')] - [G(v'') + F_{v''}(J'')]$$

$$= [G(v') - G(v'')] + [F_{v'}(J') - F_{v''}(J'')] \tag{3-15}$$

The first part of the right side of this equation, viz. $[G(v')-G(v'')]$, gives the gross structure and the second part, $[F_{v'}(J')-F_{v''}(J'')]$, explains the fine structure.

The selection rules for the rotational and vibrational transitions are:

$$\Delta J = 0, \pm 1$$
$$\text{and } \Delta v = 0, \pm 1, \pm 2, \pm 3 - - -$$

Gross Structure of the VR Bands. - The frequency ν_0 of the band origin in a vibration-rotation spectrum is given by the equation:

$$\nu_0 = G(v') - G(v'')$$

$$= [\omega_e(v' + 1/2) - \omega_e x_e (v + 1/2)^2 + - - -]$$

$$- [\omega_e(v'' + 1/2) - \omega_e x_e (v'' + 1/2)^2 + - -] \tag{3-16}$$

which, in the case of a (v,o) progression, might reduce to

$$\nu_0 = v[\omega_e - (v + 1) \omega_e x_e] \tag{3-17}$$

The band origin frequencies of the fundamental and successive overtones in this progression can be expressed by the following relations:

$$1 \leftarrow 0; \quad [\nu_0]_1 = \omega_e - 2 \omega_e x_e = (1 - 2x_e)\omega_e$$

$$2 \leftarrow 0; \quad [\nu_0]_2 = 2\omega_e - 6\omega_e x_e = (1 - 3x_e)2\omega_e$$

$$3 \leftarrow 0; \quad [\nu_0]_3 = 3\omega_e - 12\omega_e x_e = (1 - 4x_e)3\omega_e \tag{3-18}$$

$$\cdot$$
$$\cdot$$

$$v \leftarrow 0; \quad [\nu_0]_v = v[\omega_e - (v + 1)\omega_e x_e]$$

<u>Fine Structure of Vibration-Rotation Bands</u>. - If we consider $G(v') - G(v'') = \nu_0$, the frequency corresponding to a particular vibrational transition $(v' - v'')$ as fixed, the rotational structure can be given by

$$\nu_{vr} = \nu_0 + [F_{v'}(J') - F_{v''}(J'')]$$

$$= \nu_0 + [B_{v'}(J' + 1)J' - D_{v'}(J' + 1)^2 J'^2]$$

$$- [B_{v''}(J'' + 1)J'' - D_{v''}(J'' + 1)^2 J''^2] \qquad (3\text{-}19)$$

Using selection rule $\Delta J = \pm 1$, ($\Delta J = 0$ has only restrictive use in vibration-rotation spectra of diatomics since, in most cases, $\Lambda = 0$ in the ground state). Therefore, we get the following relations:

$$\nu_R = R(J) = \nu_0 + (B_{v'} + B_{v''})(J + 1) + (B_{v'} - B_{v''} - D_{v'} + D_{v''})(J + 1)^2$$

$$\qquad (3\text{-}20a)$$

$$\text{for } \Delta J = +1 \text{ and where } J = 0, 1, 2, 3 - - -$$

and

$$\nu_P = P(J) = \nu_0 - (B_{v'} + B_{v''})J + (B_{v'} - B_{v''} - D_{v'} + D_{v''})J^2$$

$$\qquad (3\text{-}20b)$$

$$\text{for } \Delta J = -1 \text{ and where } J = 1, 2, 3 - - -$$

or neglecting the rotational constant D_v, since $D_v \ll B_v$, we have the simplified forms of (3-20a) and (3-20b) as

$$\nu_R = R(J) = \nu_0 + 2B_{v'} + (3B_{v'} - B_{v''})J + (B_{v'} - B_{v''})J^2$$

$$\qquad (3\text{-}21a)$$

$$\text{where } J = 0, 1, 2, 3 - - -$$

and

$$\nu_P = P(J) = \nu_0 - (B_{v'} + B_{v''})J + (B_{v'} - B_{v''})J^2$$

$$\qquad (3\text{-}21b)$$

$$\text{where } J = 1, 2, 3 - - -$$

$R(J)$ and $P(J)$ correspond to the wave numbers of the different rotational lines forming R branch and P branch, respectively.

A vibration-rotation band thus consists of normally two series of lines called R and P branches. The branch where $\Delta J = 0$ is termed as the Q-branch. It has been identified in the VR spectrum of only NO in the domain of diatomics.

Figure (3-3) depicts the various branches which constitute the fine structure of a vibration-rotation band of a simple diatomic. (Fundamental band of CO.)

A better picture of a vibrating-rotating molecule would be obtained if we take into consideration the rotation of the molecule about the internuclear axis as well. The moment of inertia resulting from the revolution of electrons about the nuclei was not involved yet. Since the mass of the electron is very small, this moment is very small too but not exactly zero. The term value for rotational energy of a symmetric top in the vibrational level, v, can be expressed as

$$F_v(J) = B_v (J + 1) J + (A - B_v) \Lambda^2 - D_v J^2 (J + 1)^2 + - - - \qquad (3-22)$$

$$\text{where } A = \frac{h}{8\pi^2 I_A c} \text{ and } B_v = \frac{h}{8\pi^2 I_B c}$$

I_A corresponds to the moment of inertia of the molecule about the internuclear axis and I_B corresponds to the axis perpendicular to it ($I_A \ll I_B$).

Λ is another quantum number, related to J by the relation

$$J = \Lambda, \Lambda + 1, \Lambda + 2, \Lambda + 3 - - -$$

The selection rules for the symmetric top are given by $\Delta J = \pm 1$, where $\Lambda = 0$ and $\Delta J = 0, \pm 1$, where $\Lambda \neq 0$. The energy levels of a symmetric top are almost the same as those of a non-rigid rotator except that there is a constant shift towards higher values by $(A - B_v) \Lambda^2$. Levels with J smaller than Λ are absent and Q branch corresponding to the rule, $\Delta J = 0$, also manifests itself in the spectrum.

Electronic Spectrum

An ensemble of various radiative transitions between different vibration-rotation levels associated with any two electronic states of a molecule is called an Electronic Band System.

An ensemble of transitions within a system corresponding to a particular pair of upper v' and lower v" vibrational quantum numbers is called an Electronic Band. A group of bands having the same v' or v" is called a v'-progression or a v"-progression as the case may be. A group of bands for which (v' - v") has a fixed value is called a "band sequence."

The lines which make up a single band come from the ensemble of all possible changes in the rotational quantum number, J, associated with the two vibrational levels involved.
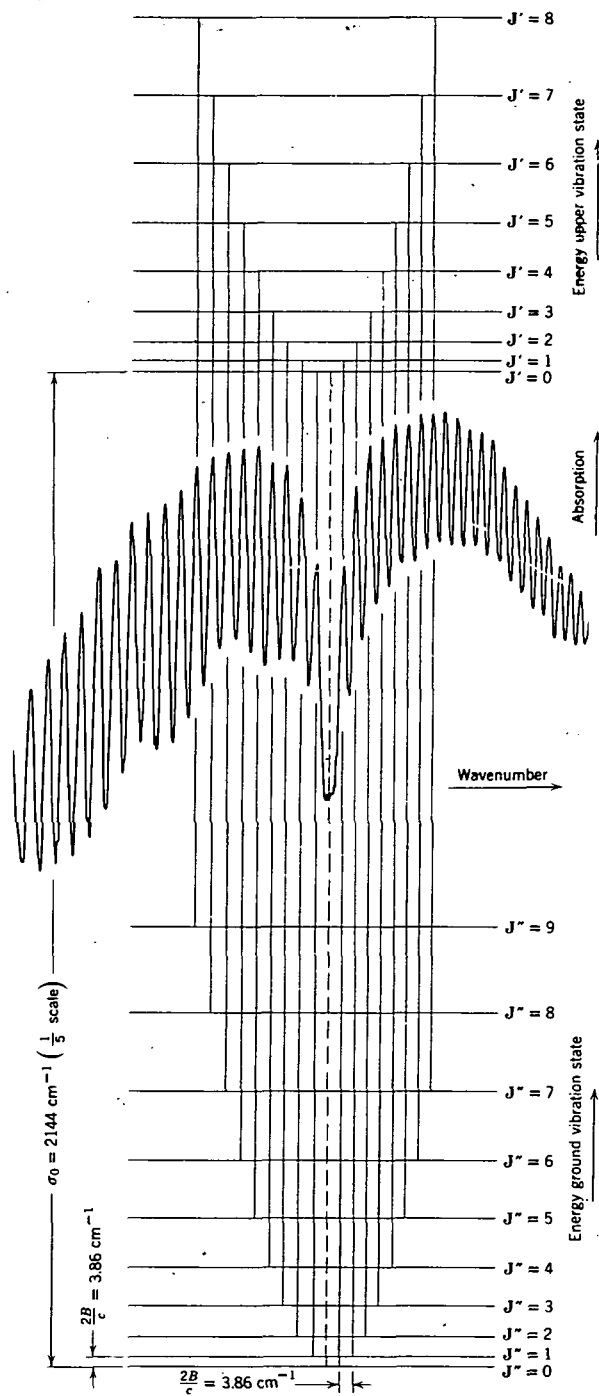
Figure (3-3).   Schematic showing rotational branches of a typical vibration-
rotation band.   (Fundamental band of CO.)

The ensemble of lines resulting from a particular change in J is called a branch of the band. As J is subject to the selection rule, $\Delta J = 0, \pm 1$, there can be three branches accordingly, commonly known as Q, R and P branches. The wave number of spectral lines in an electronic band can, therefore, be expressed as

$$\nu = T' - T'' = (T_e' - T_e'') + [G'(v') - G''(v'')] + [F_{v'}(J') - F_{v''}(J'')] \qquad (3-23)$$

where the single-primed letters refer to the upper electronic state and the double-primed letters refer to the lower electronic state.

For convenience of discussion, let us divide the spectral features of an electronic spectrum into two parts.

(1) Vibrational structure or the gross structure concerns the disposition of various band-heads (or band origins) in the entire band system.

(2) Rotational structure or the fine structure of different bands of the system concerns disposition of different rotational lines in a band.

Vibrational Structure of Electronic Transitions. - The various possible transitions between the different vibrational levels of the two participating electronic states can be expressed by the following relationships:

$$\nu = \nu_e + G'(v') - G''(v'')$$

$$= \nu_e + [\omega_e'(v' + 1/2) - \omega_e'x_e'(v' + 1/2)^2 + \omega_e'y_e'(v' + 1/2)^3 + - - -] \qquad (3-24)$$

$$- [\omega_e''(v'' + 1/2) - \omega_e''x_e''(v'' + 1/2)^2 + \omega_e''y_e''(v'' + 1/2)^3 + - - -]$$

Since $y_e' \ll x_e'$ and also $y_e'' \ll x_e''$, we can write

$$\nu = \nu_e + (v' + 1/2)\,\omega_e' - (v'' + 1/2)^2\,\omega_e'x_e' - [(v'' + 1/2)\,\omega_e'' - (v'' + 1/2)^2\,\omega_e''x_e''] \qquad (3-25)$$

In principle, in an electronic transition, Δv can have any integral value, plus or minus. That is, any vibrational state of the upper electronic state can combine with any vibrational state of the lower electronic state and thus we can expect a large number of vibrational transitions.

The above formula may also be written in a simpler way:

$$\nu = \nu_{oo} + (\omega_o'v' - \omega_o'x_o'v'^2 + \omega_o'y_o'v'^3 + - - -)$$

$$- (\omega_o''v'' - \omega_o''x_o''v''^2 + \omega_o''y_o''v''^3 + - - -) \qquad (3-26)$$

35

Here ν_{oo} corresponds to the transition $v' = 0 \to v'' \to 0$ and the ω_o's and x_o's are as defined earlier.

By comparing the two equations above, we get

$$\nu_{oo} = \nu_e + [\ \frac{\omega_e'}{2} - \frac{\omega_e' x_e'}{4} + \frac{\omega_e' y_e'}{8} + - - -]$$
$$- [\ \frac{\omega_e''}{2} - \frac{\omega_e'' x_e''}{4} + \frac{\omega_e'' y_e''}{8} + - - -]$$

(3-27)

Usually, while attempting vibrational analysis of an electronic band system, one can tabulate the wavenumbers of the different band-origins in the form of a Deslandres' scheme as shown below (Table 3-I). When the band origin data are arranged in such a scheme, it is very easy to evaluate the different vibrational constants.

TABLE 3-I. DESLANDRES' SCHEME FOR AN ELECTRONIC SYSTEM FOR A DIATOMIC MOLECULE.

	0	1	2	3	
0	ν_e+G'(0)-G"(0)	ν_e+G'(0)-G"(1)	ν_e+G'(0)-G"(2)	ν_e+G'(0)-G"(3)	....
					ΔG'(½)
1	ν_e+G'(1)-G"(0)	$_e$+G'(1)-G"(1)	$_e$+G'(1)-G"(2)	$_e$+G'(1)-G"(3)	....
					ΔG'(1½)
2	$_e$+G'(2)-G"(0)	$_e$+G'(2)-G"(1)	$_e$+G'(2)-G"(2)	$_e$+G'(2)-G"(3)	....
					ΔG'(2½)
3	$_e$+G'(3)-G"(0)	$_e$+G'(3)-G"(1)	$_e$+G'(3)-G"(2)	$_e$+G'(3)-G"(3)	....
	:	: ΔG"(½) :	: ΔG"(1½) :	: ΔG"(2½) :	: ← First Differences

On the basis of the analysis of the gross structure of an electronic band system of a molecule, we can calculate the position of the vibrational levels, the vibrational frequencies, and the harmonicities, as well as the force constants of the molecule in the two participating electronic states. Finally, knowing ν_{oo} and the various vibrational constants, one can obtain ν_e, the difference in electronic energy of the two states. This ν_e is also called the "origin of the band system."

Rotational Structure of Electronic Bands. - Various possible transitions between the different rotational levels associated with any two participating vibrational states can be expressed as

$$\nu = \nu_0 + [B_{v'} \, J'(J' + 1) - D_{v'} \, (J' + 1)^2 \, J'^2 + - - -]$$
$$- [B_{v''} \, (J'' + 1)J'' - D_{v''} \, (J'' + 1)^2 \, J''^2 + - - -]$$

(3-28)

$$\text{where } \nu_0 = [\nu_e + \nu_v]$$

If one of the participating states is other than Σ, i.e., $\Lambda = 0$ the selection rule for J is $\Delta J = 0, \pm 1$. However, if $\Lambda = 0$ in both the electronic states ($\Sigma - \Sigma$ transition), the selection rule, $\Delta J = 0$, is forbidden and only $\Delta J = \pm 1$ appears, as for most infrared bands. Thus, in general, we expect three series of lines (branches) corresponding to the three cases, viz., $\Delta J = 0$ or ± 1.

$$\Delta J = +1; \text{ R Branch}; \nu_R = \nu_0 + F_{v'}(J + 1) - F_{v''}(J) = R(J) \tag{3-29a}$$

$$\Delta J = 0; \text{ Q Branch}; \nu_Q = \nu_0 + F_{v'}(J) - F_{v''}(J) = Q(J) \tag{3-29b}$$

$$\Delta J = -1; \text{ P Branch}; \nu_P = \nu_0 + F_{v'}(J - 1) - F_{v''}(J) = P(J) \tag{3-29c}$$

If we substitute the values of F's in terms of the rotational constants, neglecting the small correction term in D_v, we get the following formulae:

$$\nu_R = \nu_0 + 2B_{v'} + (3B_{v'} - B_{v''})J + (B_{v'} - B_{v''})J^2; \; [J = 0, 1, 2, 3, - -] \tag{3-30a}$$

$$\nu_Q = \nu_0 + (B_{v'} - B_{v''})J + (B_{v'} - B_{v''})J^2; \; [J = 0, 1, 2, 3, - -] \tag{3-30b}$$

$$\nu_P = \nu_0 - (B_{v'} - B_{v''})J + (B_{v'} - B_{v''})J^2; \; [J = 1, 2, 3, 4 - - -] \tag{3-30c}$$

These equations have exactly the same form as those derived for the vibration-rotation bands.

The appearance of the three different series of rotational lines in an electronic band is depicted in Figure (3-4). A typical $'\Pi - '\Sigma$ transition is chosen for the illustration. As a result, the lowest level in the upper state has $J = 1$. The various transitions, with $J = +1, 0,$ and -1, are indicated in this figure. It can be seen that the first lines in the R, Q and P branches are those having $J = 0, 1,$ and 2, respectively. As a result, there are now two lines missing, viz., at $\nu = \nu_0$ and $\nu = \nu_0 + 2B_v$. However, the gap in the series formed by the R and P branches is not so apparent in the present case since the Q branch begins in the neighborhood of ν_0. The first Q line, $J = 1$, lies at $\nu = \nu_0 + 2(B_v' - B_v'')$. For more detailed studies of these transitions and the frequencies arising out of them, any book on diatomic spectroscopy; e.g., Herzberg's spectra of diatomic molecules, may be referred.
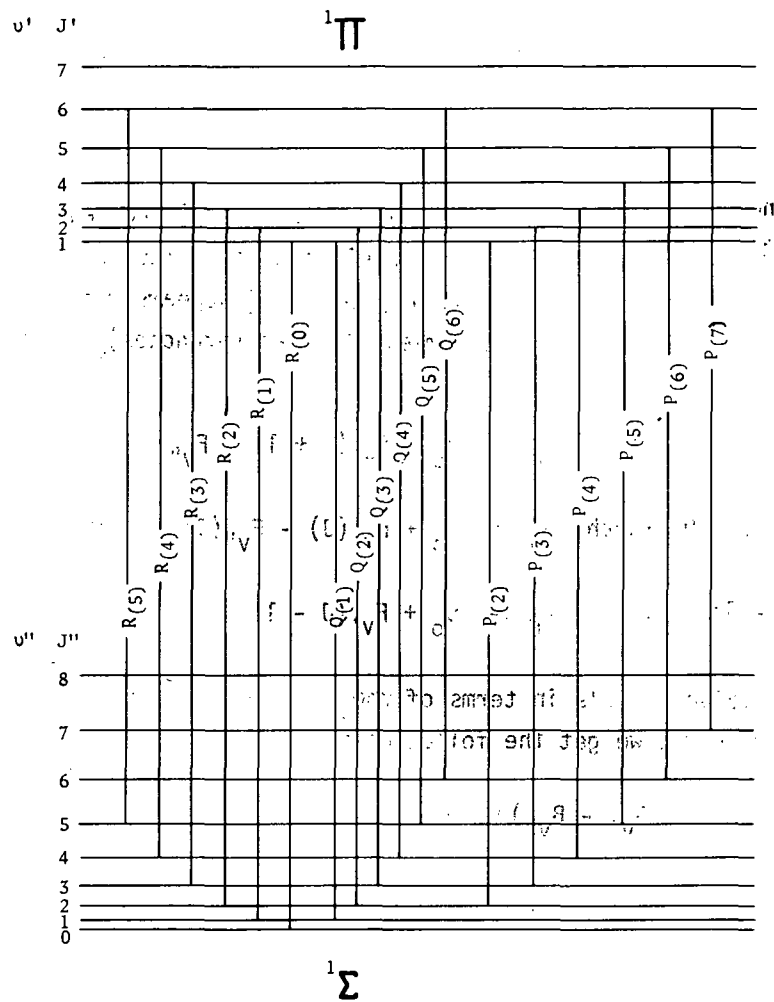
Figure (3-4). Schematic showing various rotational branches of an electronic band of a diatomic spectrum.

Interaction of Nuclear Rotation and Electronic Motion: Hund Coupling Rules

A molecule, in general, possesses four types of angular momenta which are ascribed to:

(1) orbital motion of the electrons,

(2) spin motion of the electrons,

(3) nuclear spin, and

(4) nuclear rotation.

If we neglect, for the time being, the angular momentum arising out of nuclear spin, the total angular momentum of the molecule is equivalent to the resultant angular momentum combining (1), (2) and (4).

38

In general, the angular momentum arising out of nuclear rotation and the orbital and spin angular momenta of the electrons interact magnetically, and upon the relative magnitudes of these interactions depends the resultant rotational energy of the molecule. There are five ways in which these angular momenta may be coupled and are known as Hund cases a, b, c, d and e. For each of these cases, appropriate equations can be obtained for the rotational energy in terms of the quantum numbers. All of the five cases are only the characteristic ones and many intermediate cases are found in practice. However, cases (a) and (b) are the most common.

To avoid use of lengthy phrases for the various angular momenta and their projections on the internuclear axis in our discussion for these coupling cases, let us designate them by the following symbols:

$\vec{L}$ = Total orbital angular momentum

$\vec{\Lambda}$ = Projection of $\vec{L}$ on the internuclear axis

$\vec{S}$ = Total spin angular momentum

$\vec{\Sigma}$ = Projection of $\vec{S}$ on the internuclear axis

$\vec{J}$ = Total angular momentum of the molecule

$\vec{R}$ = Angular momentum which arises from molecular rotation.

Hund Case (a). - This case arises when the spin-orbit coupling in the molecule is very strong and the coupling of nuclear rotation and electronic motion is rather weak. The $\vec{L}$ vector and the $\vec{S}$ vector, both precess about the internuclear axis and have component angular momenta, $\vec{\Lambda}$ and $\vec{\Sigma}$, respectively, along the internuclear axis. Both these momenta components are quantized separately and the total electronic angular momentum of the molecule along internuclear axis is the algebraic sum $| \Lambda + \Sigma | = \vec{\Omega}$. While Λ is constant for a particular electronic state $\vec{\Sigma}$ takes $(2S + 1)$ values from $-S$ to $+S$, and is regarded as positive or negative according as its direction is parallel or anti-parallel to that of Λ. Therefore, for a given pair of $\vec{\Lambda}$ and $\vec{S}$, $\vec{\Omega}$ takes $(2S + 1)$ values, viz., $| \Lambda - S |$ to $| \Lambda - S |$.

$\vec{\Omega}$ is compounded vectorially with the nuclear angular momentum, $\vec{R}$, to form the net angular momentum, $\vec{J}$, of the molecule. $\vec{J}$ is given by $\frac{h}{2\pi} \sqrt{J(J + 1)}$ where J is called the quantum number characterizing the resultant angular momentum and can have values $\Omega, \Omega + 1, \Omega + 2$ and so on. $\vec{R}$ is related to $\vec{\Omega}$ and $\vec{J}$ by the relation, $R = \sqrt{J(J + 1) - \Omega^2}$, and is not a good quantum number. Thus, associated with each vibrational state of case (a) electronic state, there will be a set of rotational states starting with $J_{min} = \Omega$. For example, for a state, $^2\Pi_{1 \ 2}$ or $^3\Pi_0$, none is missing but in the case of $^2\Pi_{3 \ 2}$, $J = 1/2$ will be absent. Further, since by definition Hund case (a) demands that $\Lambda > 0$ and $S > 0$, it can not arise in a Σ state where $\Lambda = 0$, of any multiplicity or in a singlet state of any type. The rotation energy in case (a), therefore, is given by the expression

$$E_r = B_v hc \{J(J + 1) - \Omega^2\} \qquad (3-31)$$

$$\text{where } J = \Omega, \Omega + 1, \Omega + 2, - - -$$

<u>Hund Case (b)</u>. - Case (b) arises when the spin-orbit coupling in the molecule is very weak in comparison to the coupling between molecular rotation and spin. $\vec{S}$ is not coupled to the internuclear axis and so Σ is no more a good quantum number. $\vec{\Lambda}$ and $\vec{R}$, which are respectively parallel and perpendicular to the internuclear axis, form the resultant angular momentum, $\vec{N} = \frac{h}{2\pi} \sqrt{N(N + 1)}$, and both $\vec{\Lambda}$ and $\vec{R}$ precess around $\vec{N}$. N here is a good quantum number whose possible values are Λ, $\Lambda + 1$, $\Lambda + 2$ and so on.

N_{min} = 0 for states having Λ = 0; i.e., for Σ states, and N_{min} = 1 for states having Λ = 1; i.e., for Π states, and so on. Here again, R is not a good quantum number and its values are obtainable from the relation

$$R = \sqrt{N(N + 1) - \Lambda^2} \qquad (3-32)$$

$\vec{N}$ and $\vec{S}$ then combine to form the resultant angular momentum, $\vec{J}$, and corresponding to (2S + 1) orientations of $\vec{S}$ with respect to $\vec{N}$, the total quantum number, J, will take (2S + 1) values; i.e., J = | N - S |, | N - S + 1 |- - - - - - | N + S |. Thus, for each value of N, there will be (2S + 1) component rotational levels differing in J values from N - S to N + S. Doublet states will have levels with J = N + 1/2 and J = N - 1/2 and triplet states will have levels with J = N + 1, N, N - 1, respectively. (See Figure 3-5.)
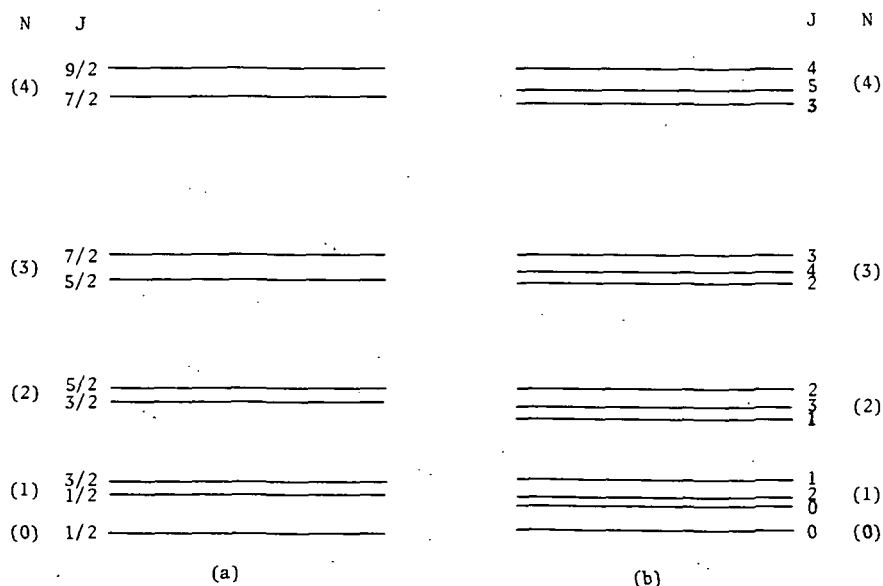

Figure (3-5). Schematic showing spin-multiplets of rotational states; (a) for a doublet state and (b) for a triplet.

The rotation energy in such a case is given approximately by

$$E_r = Bhc \{N(N + 1) - \Lambda^2\}$$

$$\text{where } N = \Lambda, \Lambda + 1, \Lambda + 2 - - -$$

(3-33)

Hund Case (c). - In the circumstance when the internuclear distance of the molecule is large the electric field along the internuclear axis is not sufficient enough to stop spin-orbit coupling. The spin and orbit angular momenta, $\vec{S}$ and $\vec{L}$, couple to give a resultant angular momentum, $\vec{J}_a$, which precesses about the internuclear axis. The vectors, $\vec{S}$ and $\vec{L}$, precess about the axis of $\vec{J}_a$. (The symbol $\vec{J}_a$ is used here to indicate its correspondence to the $\vec{J}$ used in atomic spectra which is formed from the coupling of $\vec{L}$ and $\vec{S}$.)

$\vec{J}_a$ has the axial projection $\vec{\Omega}(\Omega \frac{h}{2\pi})$, where Ω takes the values J_a, $J_a - 1$, 1/2 or 0. The vector, $\vec{\Omega}$ and $\vec{R}$, then combine to give the resultant, $\vec{J}$, the total angular momentum and precess about its axis.

It may be pointed out here that in cases where Hund case (c) is operative, Λ loses its meaning and hence the symbols signifying electronic states; viz., Σ, Π, Δ, Φ, etc., will not correspond to $\Lambda = 0, 1, 2, 3,$ etc. They are classified according to Ω values.

The rotational energy in case (c) can be given approximately by

$$E_r = Bhc [J(J + 1) - \Omega^2]$$

(3-34)

Hund Case (d). - This coupling case applies in a situation where the orbital angular momentum, $\vec{L}$, is coupled not to the internuclear axis, but to the nuclear rotation angular momentum, $\vec{R}$, which in this case is quantized. The two angular momenta give a resultant $\vec{N}$ about which both $\vec{R}$ and $\vec{L}$ precess. Finally, $\vec{N}$ and $\vec{S}$ are compounded vectorially to give the resultant $\vec{J}$ in a fixed direction about which both $\vec{N}$ and $\vec{S}$ precess.

The rotational energy expression in this case takes the form

$$F(R) = B_v (R) (R + 1)$$

(3-35)

Highly excited states of H_2 and He_2 have been found very close to this case.

Hund Case (e). - This case would occur if $\vec{L}$ and $\vec{S}$ are strongly coupled to each other to give $\vec{J}_a$ which in turn would be coupled directly to $\vec{R}$, rather than to the internuclear axis, to give the resultant angular momentum $\vec{J}$. This case has not been found to be of any practical use.

States Representing Stages Between Hund Case (a) and Hund Case (b). - When $\Lambda = 0$ and $S > 0$; i.e., in the case of higher multiplicity Σ states, it is normally the Hund case (b) which is operative but the states Π, Δ, Φ - ($\Lambda > 0$, $S > 0$) may conform to either case

(a) or case (b) according to whether the spin-orbit coupling is strong or weak in comparison with the coupling of spin vector to the rest of the molecule. If neither coupling is negligible, these states are to be represented as intermediates between Hund case (a) and (b). The condition for case (a) will be fulfilled at low speeds of rotation (R and J small) and for case (b) at high speeds (R, N and J large) and consequently the rotational levels will represent a gradual transition from case (a) to case (b) as J increases. In the case of doublet electronic states, (S = 1/2), Hill and Van Vleck (1923) derived the following general expression for the term value of the rotational energy

$$F_v(J) = B_v [J + 1/2]^2 - \Lambda^2 \pm \{(J + 1/2)^2 - \Lambda^2 \frac{A}{B_v} (1 - \frac{A}{4B_v})\}^{\frac{1}{2}} \qquad (3-36)$$

To this, the distortion term $D_v J^2 (J + 1)^2 - - -$ and a small interaction term $\frac{\gamma}{2} [J(J + 1) - N(N + 1) - S(S + 1)] - - -$ have to be added for precision. All these coupling schemes are summarized in Table (3-II). Figure (3-6) gives a schematic of their vector representations.

TABLE 3-II. RELATIONSHIPS OF ANGULAR MOMENTA IN DIFFERENT HUND CASES.

Hund Case	Relationships
(a)	$\vec{\Omega} = \mid \Lambda + \Sigma \mid$; $\vec{J} = \vec{\Omega} + \vec{R}$
(b)	$\vec{N} = \vec{\Lambda} + \vec{R}$; $\vec{J} = \vec{N} + \vec{S}$
(c)	$\Omega = (\vec{L} + \vec{S}) \cdot \vec{Z} \equiv \vec{J}_a \cdot \vec{Z}$; $\vec{J} = \vec{\Omega} + \vec{R}$
(d)	$\vec{N} = \vec{L} + \vec{R}$; $\vec{J} = \vec{N} + \vec{S}$
(e)	$\vec{J}_a = \vec{L} + \vec{S}$; $\vec{J} = \vec{J}_a + \vec{R}$

Λ-Type Doubling. - The Λ-Type splitting of rotational levels differs significantly from the spin splitting in Hund case (b), due to the effect of the magnetic field generated by molecular rotation. For illustration, let us consider a singlet electronic state. In the absence of a magnetic field the same energy results no matter whether Λ is parallel or anti-parallel to the direction of the electric field along the internuclear axis. However, when a magnetic field is set up by the rotation, the two positions of Λ give two slightly different energies for each value of J. The difference between them
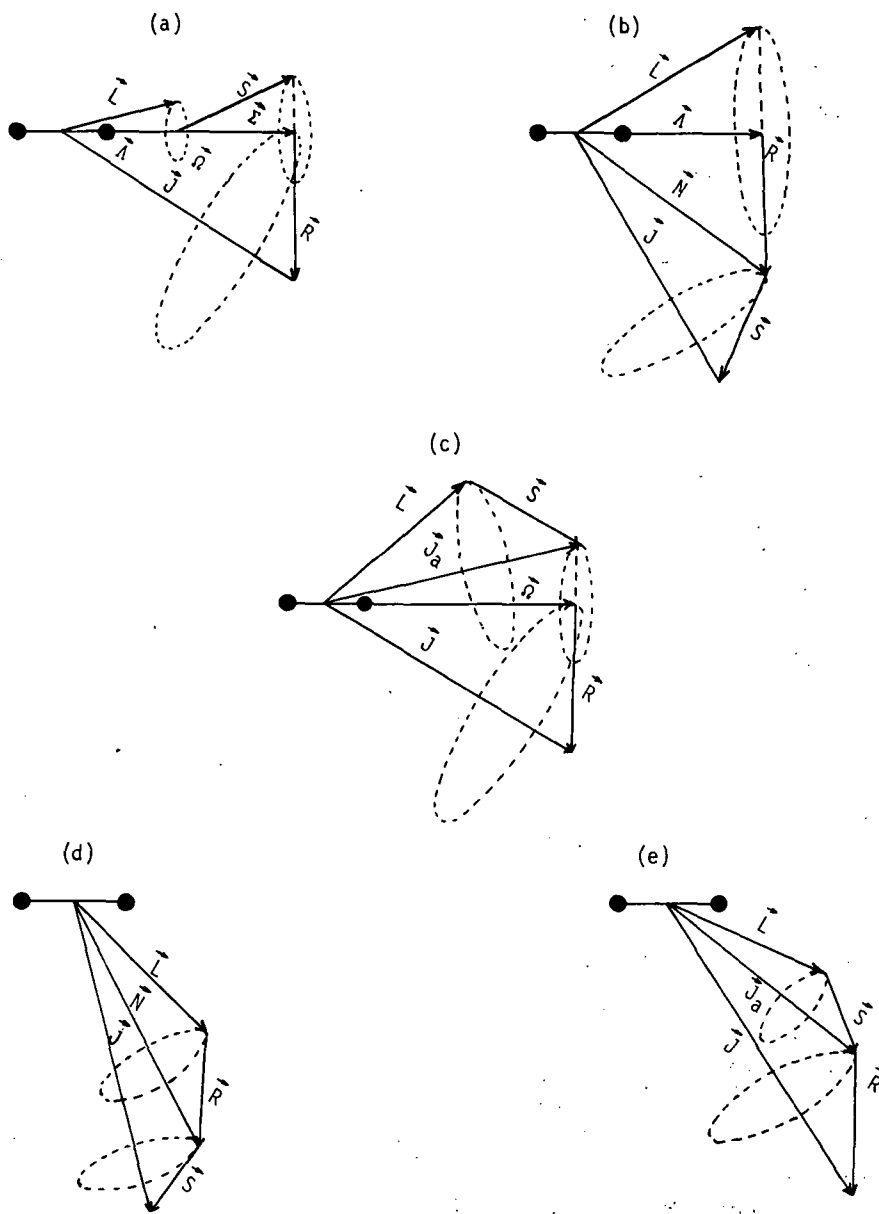
Figure (3-6). Schematic illustrating different coupling schemes of angular
momenta. [Hund cases (a) to (e).]

increases with the magnetic field, therefore with the speed of molecular rotation, i.e.,
with R and J. If $\Lambda = 0$, however, the two energies of a given J remain constant but, in
electronic states where $\Lambda > 0$, each rotational level is split up into two slightly differ-
ent sublevels, which are coincident for J = 0 and become gradually wider apart as J
increases.

This type of doubling of the rotational states is quite independent of electron spin and, therefore, occurs for all multiplicities in all electronic states except Σ states. Figure (3-7) presents a schematic showing Λ-type doubling in a $^1\Pi$ state.

$^1\Pi_u$

J
4   a+ ——————————
    s- ——————————

3   s- ——————————
    a+ ——————————

2   a+ ——————————
    s- ——————————

1   s- ——————————
    a+ ——————————
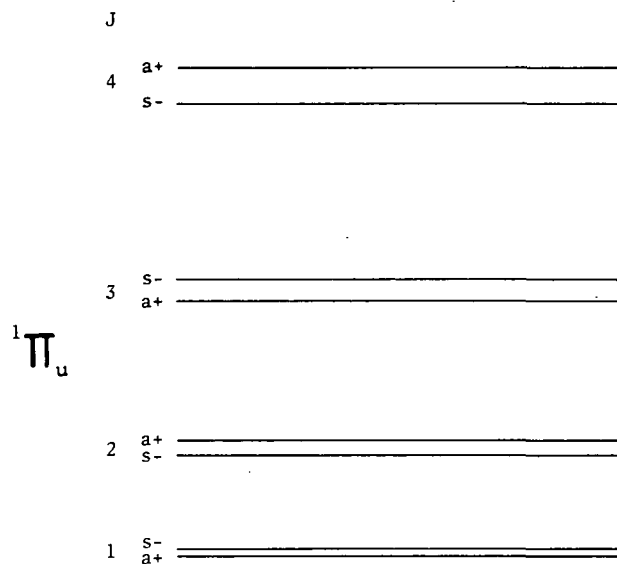
Figure (3-7).   Schematic showing Λ-type doubling of rotational levels in a typical $^1\Pi$ electronic state.

Rotational Structures of Certain Typical Electronic Bands.

(1)   [Σ - Σ] Transitions

(a) $^1\Sigma$ - $^1\Sigma'$: The simplest rotational structure of a diatomic electronic band arises in the case of a $^1\Sigma$ - $^1\Sigma$ transition. Both the involved states have (S = 1/2, Λ = 0) and, therefore, there is no distinction between Hund case (a) and (b). If we consider case (b), since $\Delta J = 0$ is forbidden and because J = N; so $\Delta N = 0$ is also forbidden. Thus only those transitions for which $\Delta J = \Delta N = \pm 1$ are permitted. We get a single P and a single R branch just like the two branches of a vibration-rotation band (Figure 3-3).

(b) $^2\Sigma$ - $^2\Sigma$: Since $^2\Sigma$ states belong strictly to Hund case (b) in such transitions, the selection rule $\Delta N = \pm 1$ holds, $\Delta N = 0$ being forbidden. We have spin-doubling in both the states, corresponding to J = N + 1/2 and J = N - 1/2 for a given value of N. These spin separations are normally small compared to the separation of successive rotational levels. Each line of the P and R branches, according to the rule $\Delta J = 0, \pm 1$ is split up into three components. In the

44

case where $\Delta J = 0$; $\Delta J \neq \Delta N$, the intensity falls off very rapidly with increasing N. In practice, however, except for very small N, one would expect each of the lines splitting into two components of about equal intensity and their separation increasing with N. Various branches in such electronic bands are schematically represented in Figure (3-8).
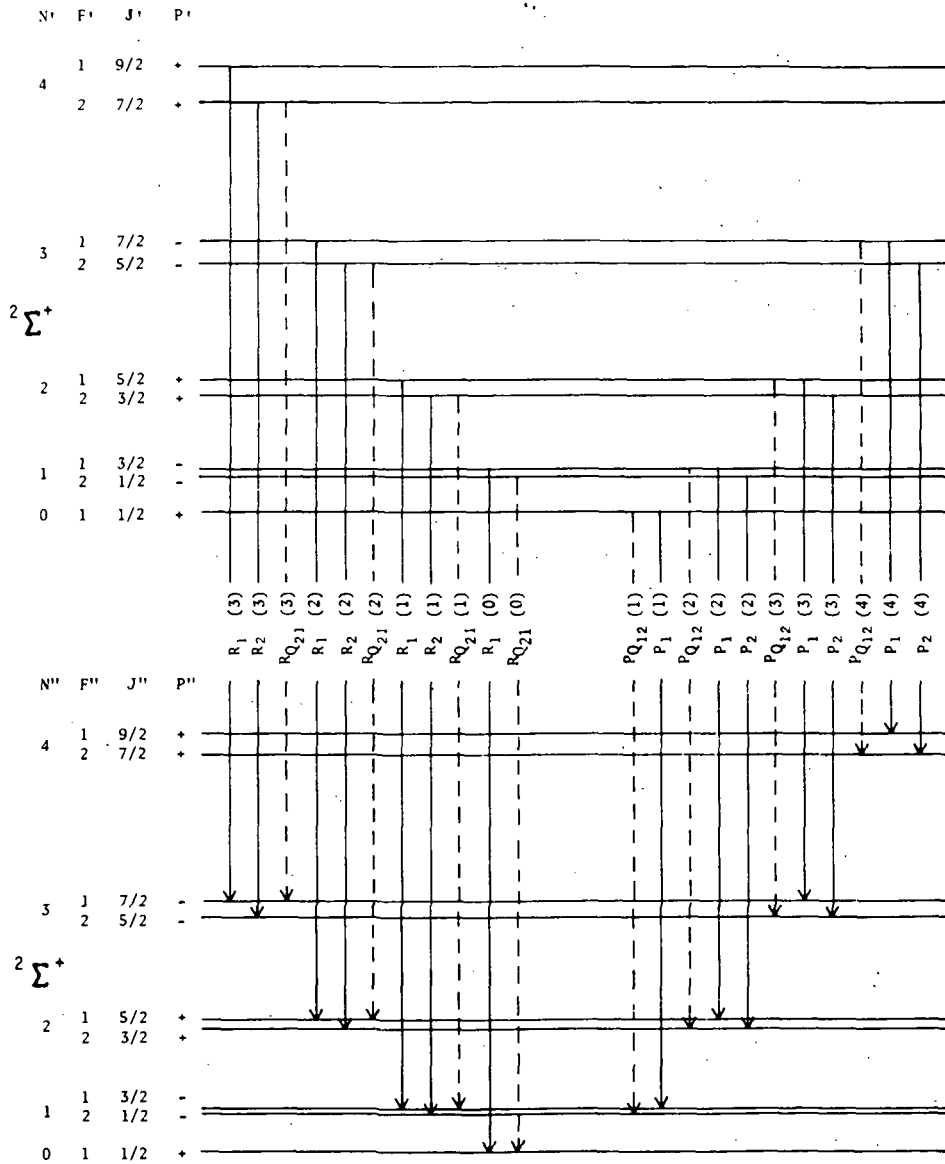

Figure (3-8). Schematic showing different rotational transitions to the formation of a $^2\Sigma$ - $^2\Sigma$ electronic band.

(2) $^2\Pi$ - $^2\Sigma$ Transitions

While (a) $^2\Sigma$ states always conform to Hund case (b), the $^2\Pi$ state may belong to either case (a) or case (b) or to a case intermediate between (a) and (b).

(a) $^2\Pi$(a) - $^2\Sigma$: When the state $^2\Pi$ belongs to case (a), there is large separation between $^2\Pi_{1\,2}$ and $^2\Pi_{3\,2}$ components. The selections rules are $\Delta J = 0, \pm 1$ and $+ \leftrightarrow -$. There will be six branches for each sub-band, making twelve in total. The branches of the first sub-band (with F_1 upper levels) are designated as P_{11}, Q_{11}, R_{11} and P_{12}, Q_{12}, R_{12} depending upon whether the lower levels are F_1 or F_2.

(b) $^2\Pi$(b) - $^2\Sigma$: When the state $^2\Pi$ belongs to case (b), the separation between the $^2\Pi_{1/2}$ and $^2\Pi_{3/2}$ components is normally very small. We get a total of six branches designated as R_1, R_2, Q_1, Q_2, P_1, and P_2. The three doublet branches correspond to the selection rules $\Delta N = + 1, 0, -1$. However, in addition to these six main branches, there exist four satellite branches for which $\Delta J \neq \Delta N$ and whose intensity decreases with increasing N. These satellite branches are designated as $^RQ_{21}$, $^QR_{12}$, $^QP_{21}$ and $^PQ_{12}$.

Schematic representation of the rotational structure in a typical band arising from the $^2\Sigma$ - $^2\Pi$(a) transition is presented in Figure (3-9). However, in a majority of actual cases, the $^2\Pi$ state belongs neither strictly to case (a) nor strictly to case (b) but usually to a transition case which approximates case (a) for small rotations and to case (b) for large rotations.

POLYATOMICS

Polyatomics, as distinguished from diatomics, possess a number of degrees of freedom; i.e., one has to consider a number of coordinates to specify the positions of all the constituent nuclei for a particular electronic state of the molecule. There are three degrees of freedom for each nucleus, making a total of 3n for a molecule of n atoms. Three of these are required to specify the position of the center of mass and three more to describe the rotation of the molecular skeleton as a whole about each of these axes. The remaining (3n - 6) specify the positions of the nuclei relative to one another and are thus concerned with the vibrational motions of the molecule.

In the case of linear molecules, such as CO_2, N_2O, etc., since rotation about the internuclear axis does not change the nuclear coordinates, only two degrees of freedom are needed for rotation, leaving (3n - 5) for vibration.

It is possible to choose these (3n - 6) or (3n - 5) coordinates in such a way that each describes a normal mode of vibration, in which all the nuclei vibrate with the same
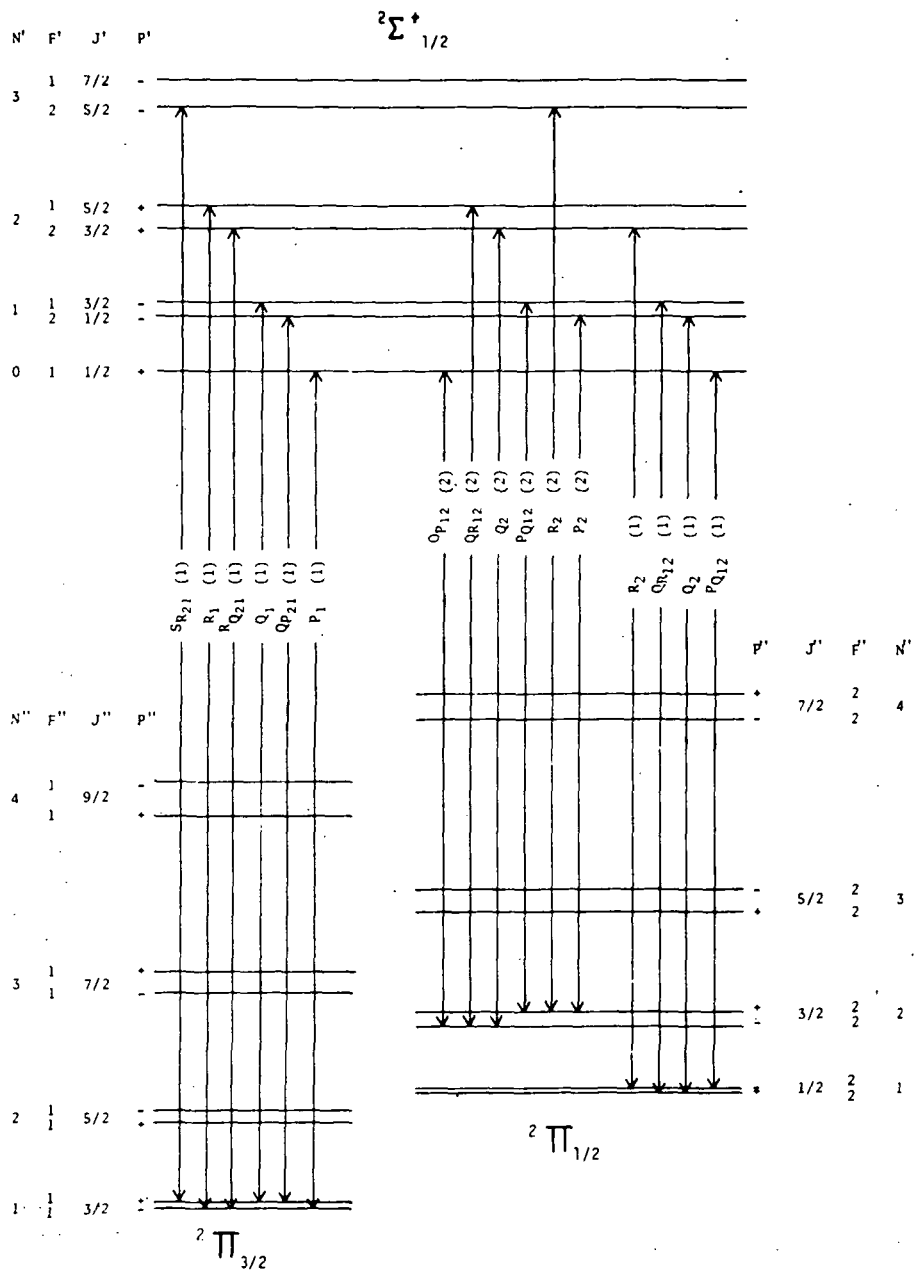
Figure (3-9). Schematic showing different rotational transitions in a $^2\Sigma$ - $^2\Pi$ band; $^2\Pi$ state belonging to Hund case (a).

frequency. In each normal mode the molecule behaves as a one-dimensional harmonic oscillator, with its energy quantized as in a diatomic. In simple molecules, it is often possible to regard each normal mode as almost equivalent to either a change in length of the bond between one pair of the atoms (stretching vibration) or change in the angle between two bonds (bending vibration). In complex molecules, the normal mode may describe

47

vibrations either of the entire molecule or of functional groups, such as OH, NH, CH_3, NO_2, etc. Vibrations of the second type are characteristic of the group concerned and are almost independent of the particular molecule to which it is attached.

Classification of Polyatomics

A non-linear polyatomic molecule may rotate about an infinite number of axes. However, for mathematical convenience, this rotation is described in terms of three orthogonal axes intersecting at the center of mass. If we neglect zero-point energy and assume a polyatomic to be a rigid body, these three principal moments of inertia of the molecule can be expressed as

$$I_{xx} = m_1 (y_1^2 + z_1^2) + m_2 (y_2^2 + z_2^2) + - - -$$

$$I_{yy} = m_1 (x_1^2 + z_1^2) + m_2 (x_2^2 + z_2^2) + - - - \tag{3-37}$$

$$I_{zz} = m_1 (x_1^2 + y_1^2) + m_2 (x_2^2 + y_2^2) + - - -$$

where the coordinates of atoms of mass m_1, m_2 . . . are (x_1, y_1, z_1); (x_2, y_2, z_2), respectively. The center of gravity of the molecule is taken as the origin of coordinates. Conventionally, these three moments of inertia about three axes $(x, y$ and $z)$ are designated as I_A, I_B and I_C. On the basis of relative values of these moments of inertia, polyatomics are generally classified in the following four groups.

Linears. - In a linear polyatomic, the moment of inertia along the axis of the molecule is zero and the other two principal moments of inertia, I_B, I_C, are equal to one another; i.e., $I_A = 0$; $I_B = I_C$. The molecules like CO_2, HCN, N_2O, C_2H_2, etc., come under this category.

Spherical Tops. - In such molecules, all three principal moments of inertia are equal to one another, none being zero; i.e., $I_A = I_B = I_C \neq 0$. The molecules like CH_4, SF_6, CCL_4, etc., come under this category.

Symmetric Tops. - In such molecules, there exist three non-zero principal moments of inertia, two of which are necessarily equal; i.e., $I_A \neq I_B = I_C \neq 0$ or $I_A = I_B \neq I_C \neq 0$. Further, if $I_A < I_B = I_C$, the molecule is classified as prolate symmetric top. The molecules like CH_3F, CH_3Cl, come under this category. If $I_A = I_B < I_C$, the molecule is classified as oblate symmetric top. The molecules such as BF_3, BCl_3, etc., come under this category.

Asymmetric Tops. - In asymmetric tops, all of the three principal moments of inertia are non-zero and they all differ; i.e., $I_A \neq I_B \neq I_C \neq 0$. Molecules like H_2O, CH_2Cl_2, C_2H_4, CH_2O come under this category. In special cases, if the molecule is planar, we

48

have $I_A + I_B = I_C$. Table 3-III presents a summary of these classifications; Figure (3-10) gives the schematic representation of the rotations.

TABLE 3-III. CLASSIFICATION OF POLYATOMICS ON THE BASIS OF PRINCIPAL MOMENT OF INERTIA.

Type	Moments of Inertia	$E_{rot.}$	Examples
Linear	$I_A = 0$; $I_B = I_C$	$J(J+1)Bhc$	CO_2, C_2H_2, OCS, etc.
Spherical Top	$I_A = I_B = I_C \neq 0$	$J(J+1)Bhc$	CH_4, CCL_4, SiH_4, SF_6, UF_6
Symmetric			
Oblate	$I_A = I_B \neq I_C$	$J(J+1)Bhc + K^2(C-B)hc$	BF_3, C_6H_6, $CHCl_3$
Prolate	$I_A \neq I_B = I_C$	$J(J+1)Bhc + K^2(A-B)hc$	C_2H_6, CH_3Cl, CH_3F
Asymmetric Top	$I_A \neq I_B \neq I_C$	No simple equation	H_2O, CH_2O, CH_3OH, etc.

LINEAR $(I_A=0$; $I_B=I_C)$

SPHERICAL TOP $(I_A=I_B=I_C\neq0)$

SYMMETRIC TOP $(I_A=I_B\neq I_C\neq0)$

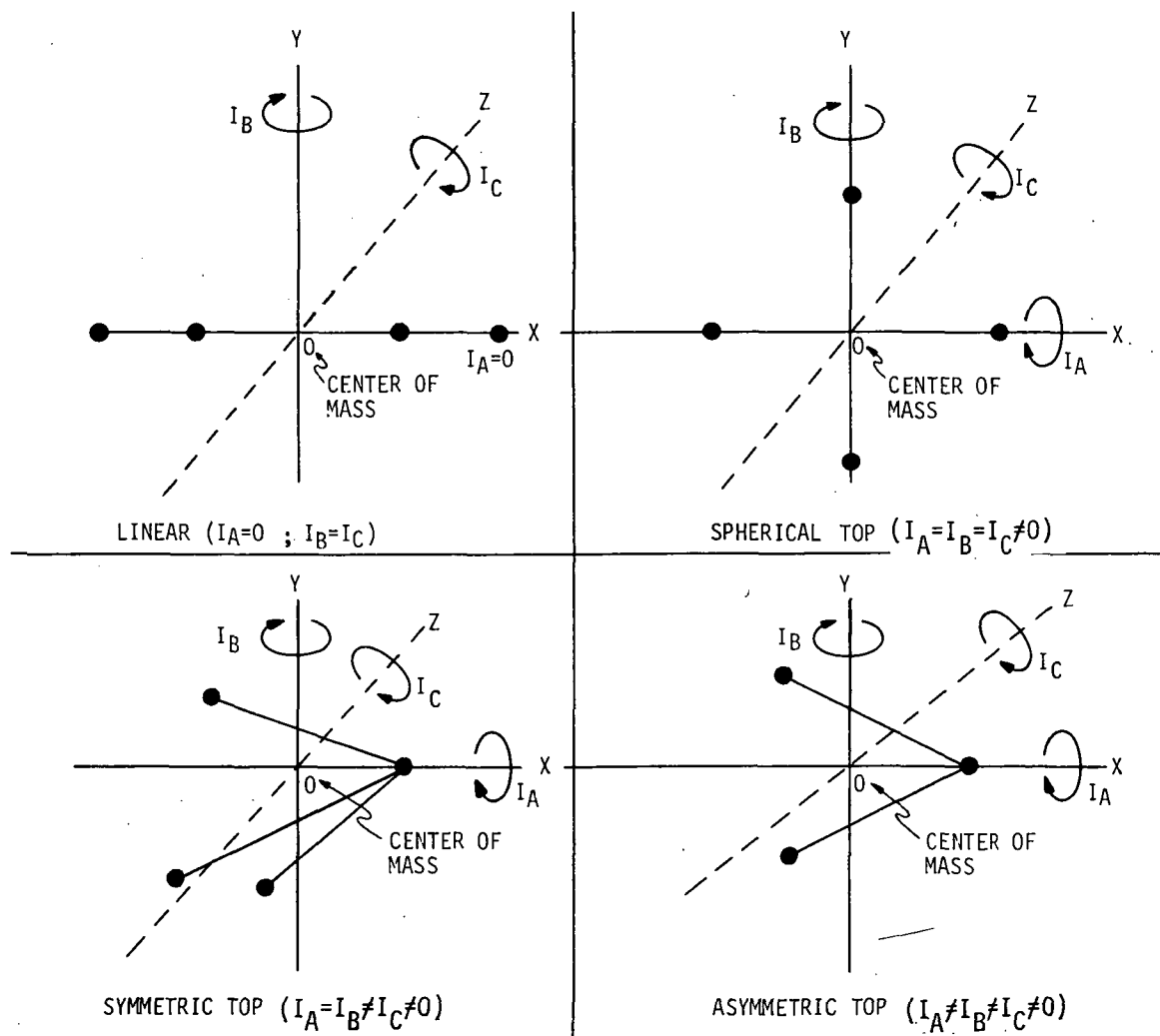ASYMMETRIC TOP $(I_A\neq I_B\neq I_C\neq0)$

Figure (3-10). Schematic representation of the rotations in different polyatomics.

Rotation of Polyatomics and Rotational Spectra

Just like diatomics, the essential factor determining the rotational spectrum of a polyatomic is the moment of inertia of the molecule about the rotation axes. In symmetric molecules, the symmetry axes are always the principal axes and planes of symmetry are perpendicular to the principal axes.

Linear. - Since, in such molecules, there is only one moment of inertia, the rotational level scheme can be obtained using the relation:

$$E_r = Bhc\ J(J + 1) - DhC\ (J + 1)^2 J^2 \qquad (3\text{-}38)$$

where B and D are rotational constants and J is the rotational quantum number. B >> D and is given by $B = \frac{h}{8\pi^2 Ic}$, where $I = \Sigma\ m_i r_i^2$ m_i is the atomic mass at a distance r_i from the axis of rotation. The selection rule is $\Delta J = \pm 1$ and obviously the corresponding absorption frequency is given by

$$\nu = 2B\ (J + 1) - 4D\ (J + 1)^3 \qquad (3\text{-}39)$$

Linear molecules may belong to the point groups $C_{\infty v}$ and $D_{\infty h}$. Molecules of the latter groups do not exhibit any rotational spectrum, since they do not possess a permanent dipole moment.

Spherical Tops. - Spherical top molecules, usually do not have any permanent dipole moment and, consequently, do not exhibit any rotational spectrum in the far infrared or microwave region. Practically all polyatomics with cubic point groups belong to this category.

Symmetric Tops. - The rotational energy scheme in the case of a symmetric top molecule, is given by

$$E_r = F(J,K)hc \qquad (3\text{-}40)$$

$$= Bhc\ J(J + 1) + hc\ (A-B)K^2 - D_J hc\ J^2(J + 1)^2 - hc\ D_{JK} - (J + 1)J\ K^2 - hc\ D_K K^4$$

where A and B are rotational constants and J and K are the rotational quantum numbers. The terms involving the constants D_K, D_J and D_{JK} take into account the centrifugal stretching and are usually very small in magnitude. The selection rules that are applicable to obtain different frequencies in the case of the symmetric top are $\Delta K = 0$; $\Delta J = \pm 1, 0$.

Asymmetric Tops. - These molecules, as already stated, have at most, one or several two-fold axes and three different moments of inertia. Consequently, the theory of rotational energy levels for such molecules involves much more complicated equations. No

simple single expression for the rotational energy can be written down in such cases. For details, refer to any treatise on the subject, such as Herzberg's Infrared and Raman Spectra of Molecules.

Vibration-Rotation Spectra of Polyatomics

The random motions of atomic nuclei in a vibrating polyatomic can be described in terms of what is called normal modes. In such a mode, all the nuclei of the molecule vibrate with the same frequency and usually in phase with each other. Exact calculation of the different normal vibration modes of a polyatomic needs a thorough understanding of group theory in which each vibrational mode is an irreducible representation.

As in diatomics, the vibration-rotation bands of polyatomics also represent the fine structure envelopes of the P Q R rotational branches. The form and intensity of these branches are determined by the selection rules based on the symmetry of vibrations and on the ratio of the moments of inertia about the three principal axes of the molecule.

Linear Polyatomics. - In contrast to diatomics, such molecules may have deformation vibrations in addition to stretching vibrations. The stretching vibrations with a transition moment in time with the symmetry axis are called parallel vibrations. These bands do not show any Q branches and are subject to the selection rules $\Delta J = \pm 1$. On the other hand, perpendicular bands (corresponding to deformation vibrations with a transition moment perpendicular to the axis of symmetry also show Q branches too ($\Delta J = 0, \pm 1$).

The vibration-rotation energy, E_{vr}, is simply given by the expression (neglecting centrifugal distortion terms):

$$E_{vr} = \Sigma_i (v + 1/2) hV_i + hc B_v J(J + 1) \tag{3-41}$$

where B_v is the rotational constant in the vth vibrational level of the ith mode.

Spherical Tops. - Spherical top molecules such as CH_4, S_iH_4, and CCl_{14}, etc., have three equal moments of inertia. All the infrared active frequencies have the same selection rules, viz., $\Delta J = 0, \pm 1$. Since the rotational energy equation is the same as that for linear molecules, the vibration-rotational bands resemble the perpendicular bands of a linear molecule with simple P, Q, and R branches.

Symmetric Tops and Asymmetric Tops. - Vibration-rotation bands of such molecules show quite a complicated rotational structure. Numerous branches with different spacings are observed.

Neglecting centrifugal distortion terms, the vibration-rotation energy may be expressed as

$$E_{vr} = \Sigma (v + 1/2)h \nu + hc [BJ(J + 1) + (A-B)K^2] \tag{3-42}$$

51

For parallel bands; the selection rules are $\Delta J = 0, \pm 1$ and $\Delta K = 0$, where $\Delta J = 0$ is forbidden when $K = 0$. For perpendicular bands; the selection rules are $\Delta J = 0, \pm 1$ and $\Delta K = \pm 1$.

It may, however, be remarked here that the real nature of the vibration-rotation structure of bands of all of these different types of molecules is significantly affected by vibration-rotation interactions. An exact solution of the problem involves due allowance for the vibrational anharmonicities, centrifugal distortion, resonance excitation and coriolis interaction. For an exhaustive account of these and allied phenomena one may be referred to any treatise on molecule vibrations, for example, Allen and Cross (1963); and Avram and Mateescu (1972).

Electronic Spectra

Almost all of the theoretical methods used to describe the electronic states and spectra of diatomics are also applicable in the case of polyatomics. These states are specified by the symmetry species or the irreducible representations of the point groups to which the particular molecule in the equilibrium conditions conforms. For example, the electronic states of a linear polyatomic, such as H-C-C-H (acetylene), conform to the point group $D_{\infty h}$ and are therefore Σ_g^+, Σ_g^-, Π_g, Δ_g, etc. Similarly, the molecule NH_3 conforms to the point group C_{3v} and the resulting electronic states are A_1, A_2 and E.

In general, a linear polyatomic molecule has a distinct value of orbital angular momentum along the internuclear axis unlike most nonlinear polyatomics where the angular momenta are usually quenched and, consequently, the symmetry species labels provides less information in the latter case.

One special feature of polyatomics is that the ground state and excited state conformations may differ, and consequently, it may be necessary to use different point groups to specify the symmetry of the possible states of ground and excited state molecules. For example, CS_2 is linear in ground state $(D_{\infty h})$ but is bent in its first and second excited states (C_{2v}).

Like diatomics, the electron spin in polyatomics is also accounted for by affixing multiplicity $2S + 1$ to the symmetry label as superscript.

Once the possible electronic states of a polyatomic are delineated, it would be easier to bring out different possible radiative transitions using group theoretical methods.

Electronic spectra of polyatomics are quite an involved subject and needs a thorough understanding of the group theoretical methods. Consequently, it does not appear expedient to examine in detail the problem of electronic molecular spectra of polyatomics in this monograph.

CHAPTER 4

DISSOCIATION AND IONIZATION OF MOLECULES

Both dissociation and ionization basically, relate to the splitting up of molecules
into two or more fragments. The fragmentation may be caused either by photon-molecule
interaction or thermal decomposition or through any other stimuli, such as high energy
particles, etc. If the break-up results in normal or excited uncharged atoms or radicals,
the process is called dissociation; if the resulting products are a molecular ion and one
or more electrons, we call it ionization.

The total energy required by a molecule in an electronic state to dissociate into two
neutral fragments is called the dissociation energy of the molecule in that particular
electronic state. However, if the molecule dissociates from its ground electronic state,
the energy necessary for this process to occur is normally called the dissociation energy
of the molecule and, in principle, should be equivalent to the heat of dissociation of the
molecule. It is usually represented by the symbol D_0^o and corresponds to the asymptotic
limit of the ground state potential curve with reference to the zero-point energy level.

The energy required to strip off one or more electrons from the molecule is called
the ionization energy of the molecule. The energy (eV) required to singly ionize the
molecule corresponds to what is called first ionization potential of the molecule. Sim-
ilarly, there are second, third, fourth. . . ionization potentials when two, three or more
electrons are removed from the molecule.

To clarify the distinction between dissociation and ionization, let us refer to the
simple case of the O_2 molecule figure (4-1). The potential curves X, A, B, C, and D
represent the ground and three electronic (excited) states. E represents the ground state
of the molecular ion. I.E. corresponds to the first ionization potential. The different
D_e values represent the different dissociation energies of the molecule in different
electronic states. D_0^o signifies the heat of dissociation.

DISSOCIATION, DISSOCIATION ENERGIES AND THEIR DETERMINATION

The term dissociation signifies a molecular process in which a molecule is split
into two fragments. One or both of these fragments may or may not be electronically
excited depending upon the nature of the electronic state of the molecule just before
splitting. A molecule may thus have different dissociation energies corresponding to its
different electronic states. However, the energy needed to dissociate a molecule in its
ground state into two fragments without losing any charge is normally defined as the
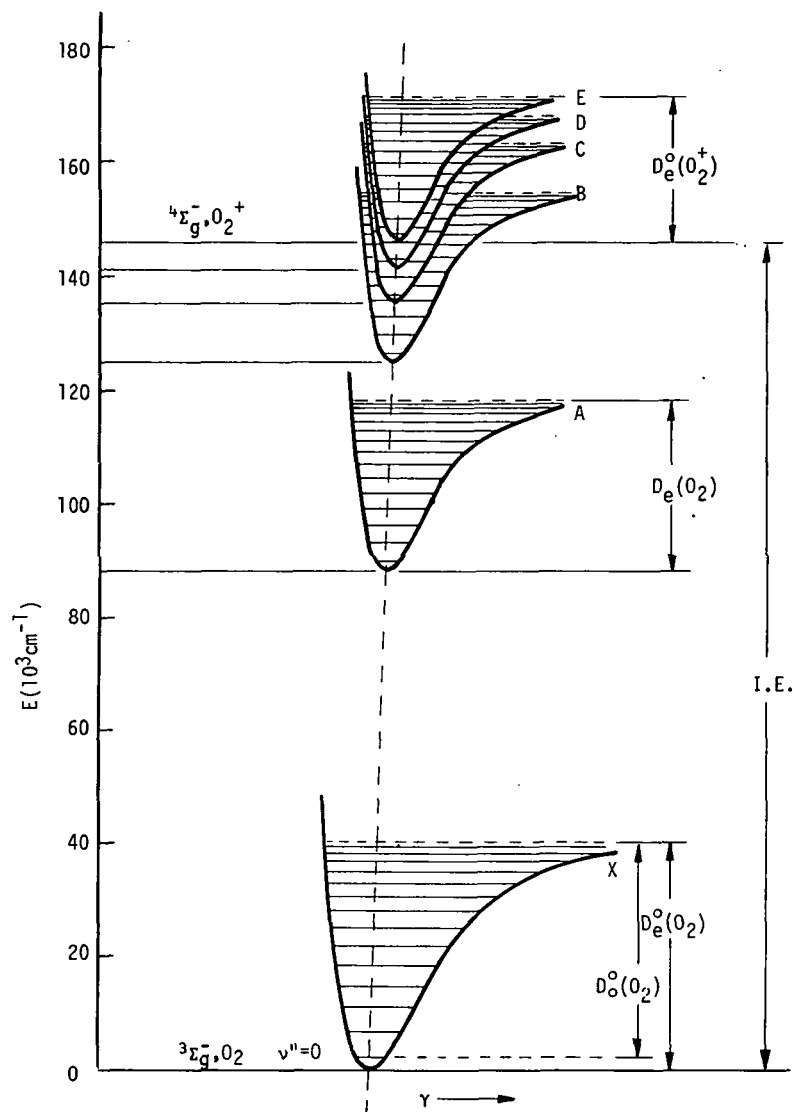
Figure (4-1).   Schematic showing various electronic states of a diatomic molecule and its corresponding ion.   A typical case of molecular oxygen is depicted.

dissociation energy (D_0^o) of the molecule.   In a potential energy diagram it is represented by the energy difference between the vibrational level $v = 0$ and the horizontal asymptotic limit of the potential curve:

$$D_0^o = V_e (\infty) - G(0) \qquad (4-1)$$

where $V_e (\infty)$ corresponds to the asymptotic limit and $G(0)$ corresponds to the zero point energy of the molecule.

54

This energy is almost equal to the thermodynamically defined heat of dissociation in the limit of low temperatures.

There exist various methods to determine dissociation energies of molecules. These can be divided into two broad categories.

Spectroscopic Methods

There are numerous spectroscopic methods which have been adopted to determine molecular dissociation energies:

(1) Band convergence limits,

(2) Birge-Sponer extrapolation,

(3) Predissociation limits,

(4) Long wavelength limits of absorption continua,

(5) Photodissociation,

(6) Chemiluminescence, and

(7) Atomic fluorescence.

Although most of the above methods have been usefully employed to determine dissociation energies under favorable circumstances, only the first two, discussed below, have been frequently used.

Method of Band Convergence Limits. - When a well-defined electronic band system appears converging to a continuum, the energy of dissociation of the molecule can be estimated by knowing the frequency at the point of convergence. If the transition probabilities are such that the absorption transitions from the $v'' = 0$ level of the ground state are observed up to the limit of vibrational structure of the upper electronic state, it is only then that one can precisely locate such a limit in an actual spectrum. Now, if one knows the wave number corresponding to the excitation energy in which the dissociation leaves the atoms, the dissociation energy of the molecule can be estimated using the following relation:

$$D_0^o = hc \, (\nu_L - \nu_A) \qquad\qquad (4-2)$$

where ν_L and ν_A correspond to the asymptotic limit of the upper state and the excitation energy of the atoms, respectively.

There are, however, two difficulties in the practical application of this method: (1) the exact point of convergence is often difficult to fix in the crowded vibrational lines, and in some cases the lines corresponding to higher vibrational quantum numbers become extremely weak before the continuum is reached; and (2) even when the frequency of the beginning of the continuum is precisely known, one or both the products of dissociation may or may not be electronically excited. Quite often, it may cause confusion; however,

if the circumstances favor this is one of the best methods of determining dissociation energy. (Dissociation energies of I_2 and O_2 have been quite precisely determined using this method.)

Method of Extrapolation to Convergence Limits. - The transition probabilities for vibrational transitions are usually such that the vibrational levels are not located all the way up to the dissociation limit. Birge and Sponer (1926) introduced the method of extrapolating the vibrational levels up to the limit at which they show vanishing interval spacing as a way of knowing the convergence limit estimating ν_L. The method is based on extrapolation of the vibrational quantum numbers according to the relation:

$$G(v) = \omega_e(v + 1/2) - \omega_e x_e (v + 1/2)^2 + \omega_e y_e (v + 1/2)^3 + \ldots \qquad (4-3)$$

The averaging spacing between successive vibrational levels can be put as

$$\Delta G(v) = \frac{d}{dv} [G(v)] = \omega_e - 2(v + 1/2) \omega_e x_e \qquad (4-4)$$

neglecting the cubic term.

As the dissociation limit approaches, $\Delta G(v)$ should gradually decrease until at a certain critical value, $\nu = \nu_c$, which represents the dissociation limit, it is almost zero.

$$\text{i.e. } \Delta G(v) = 0$$

$$\text{or } \omega_e - 2(v + 1/2) \omega_e x_e = 0$$

$$\text{or } v = \left[\frac{1}{2x_e} - 1/2 \right] = v_c. \qquad (4-5)$$

Substituting $v = v_c$ in the above equation, we get

$$G(v_c) = \frac{\omega_e}{4x_e} . \qquad (4-6)$$

As a matter of fact $G(v_c)$ is equivalent to D_e in cm^{-1} and, therefore, to get D_0°, we should subtract $G(0)$ from $G(v_c)$; i.e.

$$D_0^\circ = G(v_c) - G(0) = \frac{\omega_e}{4x_e} - \left(\frac{\omega_e}{2} - \frac{\omega_e x_e}{4} \right) \qquad (4-7)$$

Dissociation energies determined using Birge-Sponer extrapolations are normally higher than the thermochemical values. When a large number of vibrational energy levels are known, and these can be accurately represented by a formula requiring only the terms in $(v + 1/2)$ and $(v + 1/2)^2$, a more reliable result can be expected graphically. Neverthe-

less, it is the only method by which dissociation energies have been actually determined in most of the cases.

Non-Spectroscopic Methods

Non-spectroscopic methods to estimate dissociation energies of molecules can be classified into the following two broad categories:

(1) Thermal and Thermochemical Methods

(2) Electron Impact and Mass Spectrometric Methods

Although these methods are not basically spectroscopic, a closer perusal of the different steps taken till one gets dissociation energy would bear out that the thread of a spectroscopy does run practically through the whole process. In thermal and mass spectroscopic work, spectroscopic observations are normally necessary to determine the degeneracy factors of the atomic and molecular states.

In electron impact methods, we make use of the Franck-Condon principle and the concept of potential energy curves representing electronic states. The problem of determining the state of excitation of the dissociation products is always there, the solution of which is possible only through spectroscopic knowledge.

For detailed discussions on the merit and demerit of different spectroscopic and non-spectroscopic methods, one may refer to the excellent monograph, Dissociation Energies by A. G. Gaydon.

PREDISSOCIATION

Predissociation, in fact, is the molecular analog of the Auger effect observed in atomic spectra. In molecular spectroscopy, the effect was first identified by Henri (1923) in the electronic bands of diatomic sulphur. It was later observed to occur in many spectra, both diatomic and polyatomic.

In actual spectra of the molecules, predissociation manifests itself in the following forms:

(a) Abrupt termination of the banded structure or, in some cases, sudden falling off of the intensity of the band-structure beyond a certain limit in an electronic emission band system.

(b) Diffuseness in the band structure beyond a certain stage in an electronic absorption band system.

The former, however, is now regarded as the key test for the occurrence of the phenomenon.

In theoretical framework, predissociation is understood in terms of a radiationless transition from a stable excited state onto another unstable state of a molecule, having

almost the same energy. A non-radiative transition of this type leads to a spontaneous dissociation of the molecule. If this transition occurs in a lifetime that is of the order of the rotational period (approx. 10^{-11} sec.), the rotational energy that controls the rotational structure no longer remains strictly quantized and, thus, the rotational structure is no longer well defined. However, since vibrational frequencies are normally 10 to 100 times larger than the rotational frequencies, the vibrational energies which determine the gross structure of the system remain unaffected. The vibrational structure of the system thus remains intact. In borderline cases the rotational lines are simply broadened and the predissociation effect may not be clearly evident. So, for an effective display of predissociation effect, the radiationless transition should occur rapidly enough to give sufficient line broadening. However, even if this radiationless transition occurs, say 10 times the rate of spontaneous emission, most of the molecules in the first excited state will pass over to the second state and get dissociated. Although in such a case there may not be any apparent diffuseness in the absorption bands, emission bands will be drastically reduced in intensity since most of the molecules will not survive long enough in the first state to radiate spontaneously. Thus breaking-off the bands in the emission spectrum is a more sensitive test of predissociation than is diffuseness in absorption.

It may however, be pointed out that there may not be any such break-off in the bands observed in thermal emission, though predissociation may be there. In thermal equilibrium, the population of the rotational levels of the upper state is also determined by the Boltzmann factor and so the number of predissociating molecules is exactly compensated by an equal number of new molecules formed by the inverse process. There is, however; a broadening of rotational structure just as in absorption. Similar effects are observed at sufficiently high pressures. Though in such circumstances, there is no actual thermal equilibrium, the break-off in the banded structure is suppressed because of greater quenching of the non-predissociated lines by collisions. These considerations indicate that in order to detect weak predissociations, it is necessary to investigate discharge spectra at low pressures. It may, however, be pointed out that predissociation in diatomic molecules, is relatively not a frequent phenomenon. This is most probably due to the fact that the probability of a radiationless transition into the dissociating state is usually so small that long before the decomposition would have taken place, the molecule has already gone over into a lower lying discrete state with the emission of radiation.

In order for the radiationless transition probability to be so large as to make pre-dissociation feasible, there exists certain selection rules known as Kronig's selection rules, which must be fulfilled in addition to the condition of energy. These are given below:

ΔJ = 0; ΔN = 0 (For Hund Case (b) only)

+ $\leftrightarrow$ -

$S \leftrightarrow a$

and in Hund cases (a) and (b), in addition

ΔS = 0 and $\Delta\Lambda$ = 0, ± 1

If both states belong to case (a) or both to case (b), we have, respectively

$\Delta\Sigma$ = 0 or ΔN = 0

In Hund case (c), ΔS = 0 and $\Delta\Lambda$ = 0, ± 1 may be replaced by

$\Delta\Omega$ = 0, ± 1

Although Kronig's selection rules restrict the possibility of predissociation to occur considerably, they are not sufficient to exclude the theoretical possibility of its occurrence in all cases. The Franck-Condon principle plays an equally important role in this context. According to this principle, predissociation is more probable if the potential curves of the participating states intersect or at least come very close to one another. It is only in such a situation that a transition to the dissociating state is possible without an appreciable alteration of position and momentum.

It is therefore the combined effect of the three factors, viz., proximity of energy, selection rules, and the Franck-Condon principle that the occurrence of predissociation is determined.

Forms of Predissociation

Corresponding to different forms of molecular energy, three types of predissociation phenomena are normally observed: (1) Predissociation by electronic transition, (2) predissociation by vibration, and (3) predissociation by rotation. Case (1) involves a radiationless transition between discrete levels of one electronic state and the dissociation continuum of another electronic state. This type of predissociation is the most common in diatomic predissociations and applies whenever the band structure becomes diffuse or breaks off at a distance from the point of convergence of the band system (figure (4-2)).

Case (2) applies to polyatomic molecules only and has been of considerable importance in that area. Most unimolecular decompositions belong to this type. Here a radiationless transition takes place onto the continuum associated with a different vibration within the same electronic state.

Case (3) is applicable to both types of molecules but it has so far been observed in certain cases of diatomics only. It occurs for those vibrational levels of an electronic state that lie in the neighborhood of the dissociation limit, since the higher rotational levels of such vibrational levels can lie above the dissociation limit. This case is most readily observed when the dissociation energy of the state is too small.
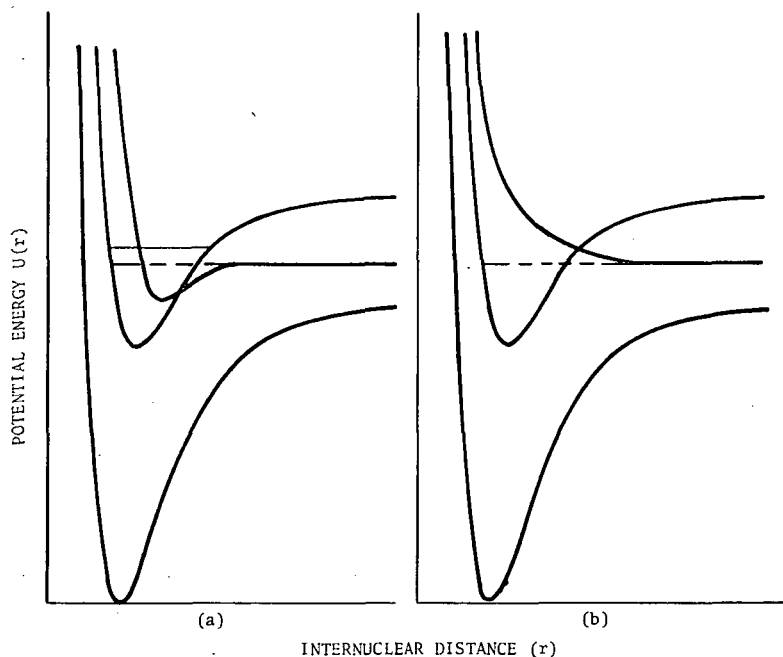
Figure (4-2). Two typical examples of predissociation (case I).

In a stable type electronic state of a diatomic molecule, the potential curve without rotation shows a pronounced minimum, which becomes less and less marked and finally disappears altogether, as we go to higher rotational levels. The electronic state will not have a minimum corresponding to such high J values and will be rotationally unstable. Excitation to such high rotational levels may thus lead to dissociation of the molecule. The onset of predissociation by rotation, therefore, does not correspond to the dissociation limit.

Miscellaneous Predissociations

Apart from the regular predissociation normally observed wherein the molecule undergoes non-radiative transition from a stable electronic state to a non-stable repulsive electronic state crossing it, a few other types of predissociation effects have been identified in certain electronic spectra:

(1) Forbidden predissociation

(2) Induced predissociation

(3) Accidental predissociation

(4) Inverse predissociation

A brief discussion follows.

Forbidden Predissociation. - For a predissociation to occur, we know that certain selection rules must be obeyed for the nonradiative transition. These are commonly known as Kronig's selection rules. Particularly, the rule $\Delta S = 0$, which applies to both Hund case (a) and case (b), holds only to the same degree as it does for radiative transitions. Since a strong predissociation has a probability $\gamma = 10^{11} \sec^{-1}$, a predissociation forbidden by the rule $\Delta S = 0$ may still have a probability $10^8 \sec^{-1}$. Such a predissociation probability may still compete with the radiative transition probability which is normally $\leq 10^8 \sec^{-1}$. It may be sufficient to cause a breaking off, or at least a drop in intensity, in emission bands even if in absorption the spectrum may remain noticeably unaffected.

The ultraviolet bands of P_2 (singlet-triplet intercombination) and Angström bands of CO, may be cited as typical examples in this context (Herzberg, 1932);(Coster and Brons, 1934). Another type of forbidden predissociation is one that is produced by magnetic fields. Quenching of I_2 fluorescence under the influence of a magnetic field is a typical example. (Turner, 1930).

Van Vleck (1932) has shown that the selection rule, $\Delta J = 0$, no longer holds strictly in a magnetic field.

Induced Predissociation. - Kronig's predissociation selection rules are, as a matter of fact, ideally derived for free molecules undergoing radiative or nonradiative processes rather independently. When the molecular assembly is at a high pressure, because of collisions, these rules no longer remain strictly operative. Therefore, a predissociation which may otherwise be forbidden, can occur under high pressure conditions. Such a pre-dissociation is termed an induced predissociation.

This phenomenon has been studied by many workers in a number of electronic spectra (I_2 [Turner (1931)]; N_2 [Kaplan (1931)]; NO [Wolf (1934)]; S_2 [Kondratjew and Olsson (1936)]; Te_2 and Se_2 [Rosen (1936)] etc.) An article by Zener (1933) provides a good theoretical perspective of the phenomenon.

Accidental Predissociation. - If a stable electronic state is perturbed by a predissociation state, one or more of the rotational levels of the perturbed state assume the properties of the corresponding predissociating levels; i.e., they also predissociate. Therefore, in emission, the corresponding lines of the bands under consideration should be missing or have abnormally small intensities. At the same time, their positions may not differ appreciably from the normal positions. In absorption, an accidental predissociation of the upper state should give rise to a broadening of a few successive lines in the band considered.

The second positive N_2 spectrum is a typical example in this context(Coster, Brons and Van der Zeil, 1933). Experimentally, accidental predissociation differs from normal predissociation, whether only a few lines, or a large number of lines, or all lines beyond a certain limit, have abnormally low intensity. Theoretically, while in normal predissociation the radiationless transition takes place from a discrete level directly into the

dissociated state; in the case of accidental predissociation this happens only through an intermediate third state. (Articles by Ittmann (1934) and Kovac's and Budo (1947) are quite exhaustive in this context.)

Inverse Predissociation. - In regular predissociation, as a result of a radiationless transition from a regular stable electronic state to an unstable repulsive state, the molecule gets dissociated. The reverse is also sometimes true. Two atoms may approach each other and, during the collision, a radiationless transition from the continuous range of energy levels to one of the discrete levels may occur if the energy coincides with that of one of these levels within their width. The molecule thus formed may pre-dissociate again unless it radiates spontaneously.

The spectrum of AlH provides a typical example in this context (Stenvinkel, 1939).

IONIZATION AND PREIONIZATION

Ionization is a process by which a net electrical charge may be imparted to an atom or molecule. In gaseous media, the atoms or molecules are stripped of one or more electrons under the action of some external stimulii. Ionization can be broadly classi-fied in the following categories:

    (a)   Photoionization (ionization produced by electromagnetic radiation).

    (b)   Thermal ionization (ionization produced by thermal energy).

    (c)   Corpuscular ionization (ionization produced by high energy particles - may be electrons, protons or cosmic particles).

Although all of these processes are significant to the study of planetary atmospheres, the first two are of immediate concern in the framework of the present monograph.

Photoionization

If the absorption of a photon raises the molecule or atom above the lowest energy level in the molecular ionic ground state, it results in the ejection of an electron from the system.

The frequency, ν, of the incident radiation should satisfy the condition $h\nu \gg V$ where V is the ionization potential. Ionization potential may thus be defined as the energy required to remove completely an electron from an atom or molecule in the ground state leaving the resulting ion in its lowest state. Quanta possessing energy less than V_i may give rise to excitation of internal states or may lead to dissociation, or both, after getting absorbed.

The process of photoionization is quite significant in the study of energy balance in various astrophysical and aeronomic problems. A precise knowledge of photoionization

cross sections with regard to various molecules and atoms of planetary interest is, therefore, no less important than that of absorption cross sections.

Photoionization cross section, σ_i, may be defined as the absorption cross section, σ, multiplied by the ionization yield, γ:

$$\sigma_i = \gamma\sigma \tag{4-8}$$

The photionization yield or efficiency, γ, represents the ratio of the number of ion-pair produced per second as a result of interaction of incident photons with the molecular or atomic assembly in the ionization chamber.

$$\gamma = \frac{\text{Number of ion-pair produced per second}}{\text{Number of photons absorbed per second}} \tag{4-9}$$

From the definition of σ, the absorption cross section we know that

$$I = I_0 \exp(-\sigma nl)$$

$$\text{or } I_{abs} = I_0 - I = I_0 [1 - \exp(-\sigma nl)] \tag{4-10}$$

The number of photons (N_A) actually absorbed per second by the molecular or atomic assembly can be expressed as

$$N_A = T I_0 [1 - \exp(-\sigma nl)] \tag{4-11}$$

where T represents the transmission coefficient of the window of the ionization chamber.

The number of primary ion-pairs produced per second or the rate of ion-pair production is thus given by

$$T I_0 \gamma [1 - \exp(-\sigma nl)] \tag{4-12}$$

For an efficient ionization chamber, this rate is equal to the average charge flow; i.e., $\left(\dfrac{i_g}{e}\right)$, where i_g is the ionization current and e is the electronic change.

We have, therefore

$$\left(\frac{i_g}{e}\right) = T I_0 \gamma [1 - \exp(-\sigma nl)] . \tag{4-13}$$

For a rare gas atom, $\gamma = \left(\dfrac{\sigma_i}{\sigma}\right)$ is taken as 1 in the region of the onset of ionization continuum and, therefore

$$\left(\frac{i_g}{e}\right) = T\, I_0\, [1 - \exp(-\sigma n l)] \tag{4-14}$$

Thus, using a rare gas ion chamber an absolute photon flux can be determined if the absorption cross section is known.

Ionization Limit and Rydberg Series

In principle, a large number of electronic states are possible for each electron in a molecule before it leaves the molecular skeleton. Molecular transitions to these states give rise to Rydberg series, as in atomic spectroscopy, represented by

$$\sigma = A - \frac{R}{(n+a)^2} \tag{4-15}$$

where A is the ionization energy expressed in cm^{-1} $\left(A = \dfrac{I \cdot E}{hc}\right)$, R is the Rydberg constant, 'a' is a correction term and 'n' is a running term.

Normally in the case of molecules, the Rydberg series is observed in the vacuum ultraviolet region. The various series limits correspond to different ionization potentials of the molecule.

For a detailed description on the molecular Rydberg series, Duncan (1971) may be referred.

Thermal Ionization

The Maxwell-Boltzmann distribution law gives a very satisfactory picture of the distribution of population in different excited states in a molecular or atomic assembly if the system is in thermodynamic equilibrium. However, at a particular temperature and density there is thermodynamic equilibrium not only among the excited states but also between the neutral and ionized atoms and electrons. The atoms will strip off electrons at a rate depending upon the temperature and ionization potentials of the atomic species. The extension of population distribution equation to ionic and neutral species in a gas assembly at a particular temperature and density under thermodynamic equilibrium was first proposed by Saha (1921). Later, the theory was extended by Menzel (1933).

According to Saha, if N^0 is the total number of atoms present in an enclosure and N^1 and N_e represent the total number of singly ionized atoms and number of electrons, respectively, then

$$\frac{N^{'}N_e}{N^o} = \frac{(2\pi mkT)^{3/2}}{h^3} \frac{2Q_1(T)}{Q_o(T)} \quad exp \left[-\frac{eV_i}{kT} \right] \qquad (4\text{-}16)$$

where $Q_o(T)$ and $Q_1(T)$ are the partition functions at temperature, T, for neutral and ionized atoms in the system and V_i is the ionization potential.

This equation may easily be generalized to any two adjacent stages of ionization to give

$$\frac{N^{q+1}N_e}{N^q} = \frac{(2\pi mkT)^{3/2}}{h^3} \frac{2Q_{q+1}(T)}{Q_q(T)} \quad exp \left[-\frac{eV_q}{kT} \right] \qquad (4\text{-}17)$$

where eV_q is the energy necessary to ionize the atoms from the qth stage of ionization to the (q+1)th stage.

Preionization

It is a phenomenon that is almost parallel to predissociation. Just as it is possible for a molecule to undergo a radiationless transition leading to spontaneous dissociation (predissociation), so it is also possible for a molecule with sufficient energy to undergo spontaneous dissociation to a molecular ion and a free electron.

For preionization to occur, the upper state involved in the transition must lie higher than an ionization limit. For molecules, usually the ionization potential lies a good deal higher than the dissociation energy and therefore preionization is not a common occurrence in diatomics. In polyatomics, particularly in molecules like CO_2, N_2O, etc., which are of great planetary interest, examples of the occurrence of preionization do exist. Diffuse absorption bands of CO in the region 785-750Å and the far ultraviolet diffuse absorption bands of H_2 have also been ascribed to preionization (Henning, 1932; Beutler and Junger, 1936).

Page Intentionally Left Blank

CHAPTER 5

QUANTITATIVE THEORY OF MOLECULAR ABSORPTION AND RELATED
SPECTROSCOPIC PARAMETERS

Whenever a beam of electromagnetic radiant energy is allowed to interact with an
assembly of molecules, there are in general, two major processes, viz., scattering and
absorption, that mainly contribute to the attenuation of energy from the traversing
radiation. The relative importance of each of these phenomena depends upon the nature of
the medium; i.e., its physical state and the structure of its constituent atoms or mole-
cules and the wavelengths present in the incoming beam.

In an absorbing medium, the process of absorption is normally associated with two
other competitive processes, viz., (a) spontaneous emission, and (b) stimulated or induced
emission. The relative significance and the role that each of these three processes
plays vis-a-vis each other depends upon the nature and lifetime of the participating mole-
cular or atomic states, energy range of the spectral features involved, and the physical
state of the medium. Let us discuss these three processes a bit elaborately.

ABSORPTION

In this process the molecule undergoes radiative transition from a lower energy state
to a higher energy state at the expense of the energy of the incident beam. The molecules
lying in the beam path interact with the traversing photons and selectively absorb only
those quanta whose energies correspond to the energy differences between their different
eigen states. The molecules are raised to higher energy states and eventually may come
back to the lower states either radiatively or through non-radiative processes.

If ν is the frequency of an incident beam of light which is isotropic and unpolarized
and $\rho(\nu)$ is the radiation density, i.e., $\rho(\nu)d\nu$ is the optical energy per unit volume in
the frequency interval ν and $\nu + d\nu$, then for an optically thin absorbing molecular layer,
we have

$$I^{nm}_{(abs)} = \rho(\nu) \, N_m \, B_{mn} \, h\nu \, \Delta x \tag{5-1}$$

where $I^{nm}_{(abs)}$ = Intensity of absorption corresponding to the transition $E_m \to E_n$.
It is the electromagnetic energy absorbed from the incident beam
of 1 cm^2 cross section per second.

N_m = Number of absorbing molecules per cm^3 present in the initial (ground) state m.

B_{mn} = Einstein coefficient of induced absorption and is a function of the electric dipole transition moment.

Δx = Thickness of the absorbing column measured in cm. The product $N_m B_{mn} \rho(\nu)$ represents the number of photons absorbed or the number of $m \rightarrow n$ transitions which take place per cm^3 per second in the system.

According to quantum mechanics, B_{mn}, when defined relative to radiation density, is given by

$$B_{mn} = \frac{8\pi^3}{3h^2} \frac{|R^{n}_{i}{}^{m}_{k}|^2}{g_m} \tag{5-2}$$

where $|R^{n}_{i}{}^{m}_{k}|$ is the matrix element of the electric dipole moment and is given by

$$|R^{n}_{i}{}^{m}_{k}| = \int \psi_n^* M \psi_m \, d\tau . \tag{5-3}$$

Here ψ_n and ψ_m represent the total wavefunctions of the molecular states n, m and M represents the electric dipole moment of the molecule. The degeneracy of the ground state m is signified by g_m, and the subscripts i and k signify the number of degenerate sublevels of the upper state n and the lower state m, respectively. The summation is carried over all possible combinations of the sublevels of the upper state with those of the lower state.

SPONTANEOUS EMISSION

The excited molecules may undergo radiative transitions from the upper energy states to the lower energy states randomly and thereby release radiant energy. This random creation of photons results in the light waves of random phase relationships and, therefore, the electromagnetic radiation so obtained is almost incoherent. For such a process to occur, the primary requisite is that the molecules should, somehow, be excited to some higher energy state and the respective transition be allowed by the selection rules.

Under conditions for which self-absorption is negligible, the intensity of spontaneous emission for the radiative transition $n \rightarrow m$ is given by the following relation.

$$I^{nm}_{(emission)} = N_n A_{nm} h\nu \tag{5-4}$$

where $I^{nm}_{(emission)}$ is the total emission intensity.

It is also a measure of the total number of photons emitted by the source per second.

N_n is the total number of molecules in the initial (upper) state n.

A_{nm} is the Einstein transition probability of spontaneous emission. It also represents the fraction of excited molecules actually undergoing radiative transition from $n \rightarrow m$ per second.

$h\nu$ represents the energy of an emitted photon.

According to quantum mechanics, A_{nm} is related to the transition moment by the following relation

$$A_{nm} = \frac{64\pi^4\nu^3}{3hc^3} \cdot \frac{\sum|R^{n_i \ m_k}|^2}{g_n} \tag{5-5}$$

where $|R^{n_i \ m_k}|$ and various other symbols convey the same meanings as spelled out earlier. g_n represents the degeneracy factor for the upper state n.

If the two states m and n are nondegenerate, $g_m = g_n = 1$ and the numerator $\sum|R^{n_i \ m_k}|^2$ can be written as $|R^{nm}|^2$.

INDUCED EMISSION

When an excited molecule undergoes radiative transition under the influence of, or by being induced by, another photon, the emission of radiation so caused is called induced or stimulated emission. The photon leaving one excited molecule strikes another excited molecule and stimulates it to give up its photon sooner than it would have been released spontaneously. This collision process between photons and excited molecules may start a chain reaction which causes more and more excited molecules to give up photons, thus releasing vast amounts of energy. This energy build-up starts a massive wave front which grows with each collision between a photon and an excited molecule. Each collision triggers the release of another photon and both the trigger photon and the newly released photon become part of the wave front. Of course, in order to let the energy build up in this way, the special condition of 'population inversion' in the system must be created.

There are two very distinctive features of induced emission. (1) The photon produced in induced emission is almost of the same energy as that of the inducing photon and, hence, the frequency spread of the light waves associated with induced photons is very small. (2) The photons emitted via induced emission are coherent and thus there exists a close phase relationship between any two photons emitted in this process.

Basically the process of induced emission can be regarded as a converse of the process of absorption. The intensity of induced emission is accordingly given by the following relation.

$$I^{nm}_{(emission, \ induced)} = \rho(\nu) \ N_n \ B_{nm} \ h\nu \tag{5-6}$$

where B_{nm} is Einstein coefficient for induced emission and various other symbols carry their usual meaning.

KINETICS OF OPTICAL ABSORPTION

Let us consider two molecular energy states m and n ($E_n > E_m$) coupled by an electric dipole allowed transition and interacting with a radiation field of energy density $\rho(\nu)$ in a system which is in thermal equilibrium.

As discussed earlier, the rate of radiative transitions from the lower level, m, to the upper level, n, (i.e., absorption) in the case of such a system can be expressed as

$$\frac{dN_m}{dt} = N_m B_{mn} \rho(\nu) \tag{5-7}$$

Similarly, the rate of radiative transitions from the upper level, n, to the lower level, m, is given by

$$\frac{dN_n}{dt} = N_n [B_{nm} \rho(\nu) + A_{nm}] \tag{5-8}$$

At equilibrium, $\frac{dN_m}{dt} = \frac{dN_n}{dt} = 0$, so the two competing rates are equal, i.e.,

$$N_m B_{mn} \rho(\nu) = N_n A_{nm} + N_n B_{nm} \rho(\nu) \tag{5-9}$$

$$\text{or } \frac{N_n}{N_m} = \frac{B_{mn} \rho(\nu)}{A_{nm} + B_{nm} \rho(\nu)} \tag{5-10}$$

According to the Maxwell-Boltzmann distribution, which is applicable in thermal equilibrium, we have

$$\frac{N_n}{N_m} = \frac{g_n}{g_m} e^{-h\nu/kT} \tag{5-11}$$

where g_i is the degeneracy factor of the ith state (i = m or n).
Now, if we combine the two relations (5-10) and (5-11), we get

$$\frac{B_{mn} \rho(\nu)}{A_{nm} + B_{nm} \rho(\nu)} = \left(\frac{g_n}{g_m}\right) e^{-h\nu/kT}$$

$$\text{or } \rho(\nu) = \frac{A_{nm} \left(g_n / g_m \right) e^{-h\nu/kT}}{B_{mn} - B_{nm} \left(g_n / g_m \right) e^{-h\nu/kT}} \tag{5-12}$$

The energy density per unit frequency interval, $\rho(\nu)$, according to Planck's black body radiation law, is given by

$$\rho(\nu) = \frac{8\pi h\nu^3}{c^3} \frac{1}{[e^{h\nu/kT} - 1]} \tag{5-13}$$

Comparing the above relations (5-12) and (5-13) we get the following

$$\text{(i) } B_{mn} = B_{nm} \left(g_n / g_m \right) \tag{5-14}$$

$$\text{and (ii) } A_{nm} = \frac{8\pi h \nu^3}{c^3} B_{nm} = \frac{8\pi h\nu^3}{c^3} g_m/g_n B_{mn} \tag{5-15}$$

Now, if we combine the relations (5-13) and (5-15), we can write

$$\frac{A_{nm}}{B_{nm} \rho(\nu)} = \left[e^{h\nu/kT} - 1 \right] = R \text{ (say)} \tag{5-16}$$

where R is the ratio of the rate of spontaneous emission to that of induced emission under thermal equilibrium conditions.

Now, for example, if ν corresponds to the frequency of green light (5 x 10^{14} Hz), the value of R comes out to be equal to e^{82}; i.e., roughly 10^{35}. Thus, the likelihood of stimulated emission taking place is almost negligible as compared to the spontaneous emission. However, if a frequency corresponding to a microwave transition is taken (10^9 Hz); R becomes approximately 0.0001. This presents a completely different situation as regards occurrence of the two processes. Radiowaves and microwaves thus arise almost entirely through stimulated effects and so are always coherent. Whatever may be the contribution of spontaneous emission to the net intensity, it manifests itself as 'noise' within the system. R becomes 1 for a wavelength, approximately 60 μm, which lies in the far infrared region; therefore, in this frequency range both emission intensities are more or less of the same order. Creation of population inversion disturbs the thermal equilibrium and then it becomes possible to obtain considerable stimulated emission even at visible and ultraviolet frequencies.

EQUATION OF ENERGY TRANSFER

If we consider a more general case of the passage of radiation through a low pressure gas in thermal equilibrium, which can emit or absorb radiation, and confine ourselves to the radiative transitions between the two states, m and n, the kinetics of the three radiative processes can be expressed by the following equations:

$$dI_\nu \, d\nu = \frac{A_{nm}}{4\pi} \, h\nu \, N_n \, dx + \frac{I_\nu}{c} \, h\nu \, dx \left[B_{nm} N_n - B_{mn} N_m \right]$$

$$\text{or} \quad \frac{dI_\nu}{dx} \, d_\nu = A - BI_\nu \tag{5-17}$$

where $A = \dfrac{A_{nm}}{4\pi} \, h\nu \, N_n$; the spontaneous emission term

and $B = \left[B_{nm} N_n - B_{mn} N_m \right] \dfrac{h\nu}{c}$; the effective absorption term

Equation (5-17) is known as the equation of radiative transfer. In this equation, if we neglect A; i.e., the spontaneous emission is assumed negligible, we have

$$\frac{dI_\nu}{dx} \, d\nu = -BI_\nu \tag{5-18}$$

which is equivalent to the differential form of the Lambert-Beer absorption law; i.e.,

$$dI_\nu \, d\nu = - \left(\int_{\Delta\nu} \alpha_\nu \, d\nu \right) I_\nu \, dx$$

$$= - \alpha'_\nu \, I_\nu \, dx \tag{5-19}$$

where α'_ν is the effective integrated absorption coefficient. Now, if we compare equations (5-17) and (5-19), we get

$$\int_{\Delta\nu} \alpha_\nu \, d\nu = \alpha'_\nu = B = \left(B_{nm} N_n - B_{mn} N_m \right) \frac{h\nu}{c}$$

$$= \frac{B_{mn} N_m h\nu}{c} \cdot \left[1 - e^{-h\nu/kT} \right] \tag{5-20}$$

which in the case of $e^{h\nu/kT} \gg 1$ becomes

$$\int_{\Delta\nu} \alpha_\nu \, d\nu = \frac{B_{mn} N_m h\nu}{c} \tag{5-21}$$

In this relation, while $\int_{\Delta\nu} \alpha_\nu \, d\nu$ is purely an experimentally measurable quantity, B_{mn} is completely a theoretical parameter and is computable from wavefunctions representing the energy states involved.

TRANSITION STRENGTH AND RELATED MOLECULAR PARAMETERS

Quantum theory of radiative transition provides that, for electric dipole radiation, the transition strength S_{nm} with respect to a molecular transition, n - m, be given by

$$S_{nm} = |R^{nm}|^2 = |<n|M|m>|^2 = \left|\int \psi_n^* M \psi_m \, d\tau\right|^2, \qquad (5\text{-}22)$$

where the sub or superscripts, n and m, signify the two quantized energy states involved in the transition ($E_n > E_m$); $|R^{nm}|$ is the matrix element of the electric dipole moment, M (also called 'transition moment'). The ψ's represent the complete wavefunctions for the upper and lower states and $d\tau$ is the configuration space element. This factor, S_{nm}, plays a very prominent role in most of the radiative transfer phenomena in molecules. The various important quantitative molecular parameters such as energy flux, molecular absorption coefficient or cross section, oscillator strength, mean life time, optical depth, photon mean free path and Einstein A & B coefficients, etc. which are frequently used in the diagnostic study of the aeronomy of planetary atmospheres and of numerous other radiative processes, are all closely linked with this factor.

Commonly used transition probability parameters defined in terms of transition strength, S_{nm}, are summarized below:

(a) Intensity of emission $(I_{nm}) \propto \nu_{nm}^4 \, S_{nm}$

(b) Molecular absorption
     Cross Section $(\sigma_{nm}) \propto \nu_{nm} \, S_{nm}$

(c) Oscillator Strength $(f_{nm}) \propto \nu_{nm} \, S_{nm}$

(d) Radiative life time $(\tau_n) \propto [\nu_{nm}^3 \, S_{nm}]^{-1}$

(e) Optical depth $(\tau_{nm}) \propto \nu_{nm} \, S_{nm}$

(f) Photon mean free path $(\Lambda_{nm}) \propto [\nu_{nm} \, S_{nm}]^{-1}$

Basic Theory

In the case of a molecule, since there exist numerous internal degrees of freedom unlike atoms and they all influence the total wavefunction corresponding to a certain energy state, ψ, in general, could be written as $\psi = \psi_{evJ\Lambda M}$ where e signifies the electronic

functional part, v the vibrational quantum number, J the total or the rotational quantum number, Λ the quantum number for the electronic angular momentum along the internuclear axis and M the magnetic quantum number, which refers to the component of J in the direction of an externally applied magnetic field.

Applying the Born-Oppenhiemer approximation, $\psi_{evJ\Lambda M}$ can be further written as

$$\psi_{evJ\Lambda M} = \psi_e(\bar{r}_s, r)\ \psi_v(r)\ \frac{1}{r}\ \psi_{J\Lambda M}(\theta,\chi,\phi), \tag{5-23}$$

where ψ_e, ψ_v and $\psi_{J\Lambda M}$ are, respectively, the electronic, vibrational and rotational (symmetric top) wave functions, $\bar{r}_s$ are the electron coordinates relative to the internuclear axis, and θ, χ and ϕ are the Euler angles of molecular coordinates relative to a fixed frame of reference.

The dipole moment, M, also can be written $M = M_e + M_n$ as the sum of contributions from electrons and nuclei. M_e can be further expressed as

$$M_e = -\sum_s e\bar{r}_s' = \left\{\sum_s - e\bar{r}_s\right\}\ \bar{D}(\theta,\chi,\phi) \tag{5-24}$$

where $\bar{r}_s'$ is the position vector of the sth electron relative to the external axes, $\bar{r}_s$ is the position vector relative to the figure axis of the molecule, and $\bar{D}(\theta,\chi,\phi)$ is the dyadic appropriate to the axes transformation. Its elements are the direction cosines of the angles between respective coordinate axes of the two systems. Also,

$$d\tau = d\tau_e dv = d\tau_e r^2 \sin\theta\ d\theta\ d\phi\ dr. \tag{5-25}$$

where dv refers to the volume element for vibration and rotation and $d\tau_e$ refers to the configuration space element for the electrons.

Now, using equations (5-23), (5-24) and (5-25), the matrix element for a component of a molecular band line can be expressed as

$$R^{e'v'J'\Lambda'M'}_{e''v''J''\Lambda''M''} = \int \psi_{e'}^*\ \frac{\psi_{v'}}{r}\ \psi_{J'\Lambda'M'}(M_e + M_n)\ \psi_{e''}\ \frac{\psi_{v''}}{r}\ \psi_{J''\Lambda''M''}\ d\tau_e dv$$

$$= \int \psi_{e'}^*\ \frac{\psi_{v'}}{r}\ \psi_{J'\Lambda'M'}\ M_e\ \psi_{e''}\ \frac{\psi_{v''}}{r}\ \psi_{J''\Lambda''M''}\ d\tau_e\ dv$$

$$+ \int \psi_{e'}^*\ \psi_{e''}\ d\tau_e \int \frac{\psi_{v'}}{r}\ \psi_{J'\Lambda'M'}\ M_n\ \frac{\psi_{v''}}{r}\ \psi_{J''\Lambda''M''}\ dv \tag{5-26}$$

and since $\int \psi_{e'}^*\ \psi_{e''}\ d\tau_e = 0$; ($\psi_{e'}$ and $\psi_{e''}$ are orthogonal)

$$R^{e'v'J'\Lambda'M'}_{e''v''J''\Lambda''M''} = \int \psi_{e'}^* \frac{\psi_{v'}}{r} \psi_{J'\Lambda'M'} M_e \psi_{e''} \frac{\psi_{v''}}{r} \psi_{J''\Lambda''M''} d\tau_e \, dv$$

$$= \int \psi_{v'} \left(\int \psi_{e'}^* \mid \Sigma e\bar{r}_s \mid \psi_{e''} \, d\tau_e \right) \psi_{v''} \, dr$$

$$\times \int \psi_{J'\Lambda'M'} \mid \bar{D} \, (\theta,\chi,\phi) \mid \psi_{J''\Lambda''M''} \sin \theta \, d\theta \, d\phi \qquad (5\text{-}27)$$

The first integral on the right hand side of equation (5-27); i.e.,

$$\int \psi_{v'} \left(\int \psi_{e'}^* \mid \Sigma e\bar{r}_s \mid \psi_{e''} \, d\tau_e \right) \psi_{v''} \, dr$$

when summed, if necessary, over degenerate electronic states and squared is called 'Band Strength' and is designated as $S^{e'v'}_{e''v''}$ or, simply, $S_{v'v''}$. It is jointly controlled by the vibrational and electronic wavefunctions of the molecular states involved in a transition and, in fact, is also responsible for the Franck-Condon principle, discussed later.

The second integral, $\int \psi_{J'\Lambda'M'} \mid \bar{D} \, (\theta,\chi,\phi) \mid \psi_{J''\Lambda''M''} \sin \theta \, d\theta \, d\phi$, is responsible for the selection rules. Dennison (1926); Kronig and Rabi (1927); Reiche and Rademacher (1926; 1927) have studied this integral for various types of molecular transitions, and Schadee (1964) has presented a review of such investigations. When this integral is summed over magnetic quantum numbers, M' and M'', and squared, it becomes the 'line intensity factor' or the 'Honl-London factor' represented by the symbol $S^{J'\Lambda'}_{J''\Lambda''}$ or simply $S_{J'J''}$. It is often a quotient of simple polynomial functions of the J's and Λ's. We thus have the relationship

$$|R|^2 = S^{e'v'J'\Lambda'}_{e''v''J''\Lambda''} = S^{e'v'}_{e''v''} \qquad S^{J'\Lambda'}_{J''\Lambda''} = S_{v'v''} \qquad S_{J'J''} \qquad (5\text{-}28)$$

__Band Strength__ - $S_{v'v''}$. - The band strength $S_{v'v''}$ is, in fact, an average of the electronic transition moment $\psi_{e'}^* \mid -\Sigma e\bar{r}_s \mid \psi_{e''} \, d\tau_e = R_e(r)$ with respect to the vibration wavefunctions $\psi_{v'}$ and $\psi_{v''}$

$$S_{v'v''} = \left| \int \psi_{v'} R_e(r) \psi_{v''} \, dr \right|^2 \qquad (5\text{-}29)$$

It may be recalled here that $R_e(r)$, the electronic transition moment, is also an average of the electric dipole moment with respect to the two electronic wave functions $\psi_{e'}$ and $\psi_{e''}$. Now if $R_e(r)$ is independent of r, equation (5-29) becomes

$$S_{v'v''} = |R_e(r)|^2 \left| \int \psi_{v'} \psi_{v''} \, dr \right|^2 \qquad (5\text{-}30)$$

but if $R_e(r)$ varies with r, in a polynomial fashion, as is more realistic, for example if $R_e(r) = \sum_n a_n r^n$, the equation (5-30) can be written as

$$S_{v'v''} = \left| \int \psi_{v'} \left(\sum_n a_n r^n \right) \psi_{v''} \, dr \right|^2 \tag{5-31}$$

Now, at this stage, if we use $\bar{r}$-centroid approximation (Fraser, 1954a, b) which is characterized by the following relations

$$\bar{r}_{v'v''} = \frac{\int \psi_{v'} \psi_{v''} r \, dr}{\int \psi_{v'} \psi_{v''} \, dr} \tag{5-32}$$

and

$$(\bar{r}_{v'v''})^n = \frac{\int \psi_{v'} \psi_{v''} r^n \, dr}{\int \psi_{v'} \psi_{v''} \, dr} \quad , \tag{5-33}$$

we can write

$$S_{v'v''} = \left| \sum_n a_n \bar{r}_{v'v''}^n \right|^2 \left| \int \psi_{v'} \psi_{v''} \, dr \right|^2$$

$$= R_e^2 (\bar{r}_{v'v''}) \quad q_{v'v''} \quad . \tag{5-34}$$

The vibration overlap integral square, $q_{v'v''}$, is called the Franck-Condon factor, and the characteristic internuclear separation, $\bar{r}_{v'v''}$, is called the $\bar{r}$-centroid associated with a (v',v'') band.

Hönl-London Factors - $S_{J'J''}$. Hönl-London factors, or line strength factors or intensity factors as they are sometimes called, are mainly responsible for determining the intensity distribution within a band; i.e., from line to line within a band. The significance of these factors was first pointed out by Hönl and London (1925), hence, the name. Subsequently these factors were investigated by various workers as applied to different types of radiative transitions under different coupling schemes. Detailed tables of these factors applicable to a large number of important transitions have been provided (Dennison, 1926; Hill and Van Vleck, 1928, Budo, 1935, 1936, 1937). For example, Hönl-London factors for the various branches applied in the case of a symmetric top molecule could be written as:

$$S_J^R = \frac{(J'' + 1 + \Lambda'')(J'' + 1 - \Lambda'')}{J'' + 1} = \frac{(J' + \Lambda')(J' - \Lambda')}{J'}$$

$$S_J^Q = \frac{(2J'' + 1)\Lambda''^2}{J''(J'' + 1)} = \frac{(2J' + 1)\Lambda'^2}{J'(J' + 1)}$$

76

$$S_J^P = \frac{(J'' + \Lambda'') (J'' - \Lambda'')}{J''} = \frac{(J' + 1 + \Lambda') (J' + 1 - \Lambda')}{J' + 1} , \qquad (5\text{-}35)$$

for $\Delta\Lambda = +1$

$$S_J^R = \frac{(J'' + 2 + \Lambda'') (J'' + 1 + \Lambda'')}{4(J'' + 1)} = \frac{(J' + \Lambda') (J' - 1 + \Lambda')}{4J'}$$

$$S_J^Q = \frac{(J'' + 1 + \Lambda'') (J'' - \Lambda'') (2J'' + 1)}{4J'' (J'' + 1)} = \frac{(J' + \Lambda') (J' + 1 - \Lambda') (2J' + 1)}{4J' (J' + 1)}$$

$$S_J^P = \frac{(J'' - 1 - \Lambda'') (J'' - \Lambda'')}{4J''} = \frac{(J' + 1 - \Lambda') (J' + 2 - \Lambda')}{4(J' + 1)} \qquad (5\text{-}36)$$

and for $\Delta\Lambda = -1$

$$S_J^R = \frac{(J'' + 2 - \Lambda'') (J'' + 1 - \Lambda'')}{4(J'' + 1)} = \frac{(J' - \Lambda') (J' - 1 - \Lambda')}{4J'}$$

$$S_J^Q = \frac{(J'' + 1 - \Lambda'') (J'' + \Lambda'') (2J'' + 1)}{4J'' (J'' + 1)} = \frac{(J' - \Lambda') (J' + 1 + \Lambda') (2J' + 1)}{4J' (J' + 1)}$$

$$S_J^P = \frac{(J'' - 1 + \Lambda'') (J'' + \Lambda'')}{4J''} = \frac{(J' + 1 + \Lambda') (J' + 2 + \Lambda')}{4(J' + 1)} \qquad (5\text{-}37)$$

Here the superscript, R, Q or P, indicates the branch for which the particular expression holds. Further, of the two alternative forms given, the first is more useful for absorption and the second for emission. For further details on calculating Hönl-London factors in respect to different transitions, one may refer to Kovacs (1969). The sum rules for Hönl-London factors are:

$$\sum_{J'} S_{J'J''} = (2J'' + 1); \sum_{J''} S_{J'J''} = (2J' + 1) \qquad (5\text{-}38)$$

Franck-Condon Principle. Since nuclear motions in molecules are much slower compared to electronic motions, one can reasonably expect that, while the electron architecture of a molecule changes instantaneously from one potential $U(r)$ to another in a radiative transition, it will leave the nuclear motion--both internuclear separation and momentum-- unaffected. This is called the Franck-Condon principle.

A molecular oscillator (v' or v'') spends most of its time in the neighborhood of the classical turning points at the extreme ends of its motion. Thus, a transition is most likely to originate at a turning point of oscillation. By the Franck-Condon principle,

it must terminate at the same internuclear separation and possess the same momentum of nuclear oscillation. Thus a 'vertical' transition, i.e. a transition with no change in internuclear separation will occur. The transition starts at a turning point of vibratory motion in another potential to conserve momentum, which is zero at each turning point.

The Franck-Condon principle thus asserts that the most probable transitions occur between those v' and v" levels which have one pair of classical turning points in common. The quantum statement of the principle is embodied in the expression for the Franck-Condon factors; i.e., $q_{v'v"} = |\psi_{v'} \psi_{v"} dr|^2$, $q_{v'v"}$ is the square of an overlap integral of vibrational wavefunctions. The relatively large, terminal antinodes of $\psi_{v'}$ and $\psi_{v"}$ in the region of $r'_{1,2}$ and $r"_{1,2}$ respectively imply in quantum terms, a large probability of finding the molecule in regions near the turning points of the classical oscillator. This overlap integral will have a large value when there is strong overlap between pairs of terminals antinodes which are located in the region of classical turning points. Thus, vertical transitions will be necessary.

Franck-Condon factors ($q_{v'v"}$). Squares of the vibrational overlap integrals $|\psi_{v'} \psi_{v"} dr|^2$ in respect to different vibrational transitions in an electronic band system are called Franck-Condon factors. The nomenclature for this derived physical parameter was given by Bates (1949) in view of the close correspondence of these factors with the Franck-Condon principle in molecular spectroscopy. Normally, in literature, Franck-Condon factors have been expressed as $q_{v'v"}$ arrays and represent basic molecular data which are very useful in interpreting intensity distribution in an electronic band system.

The first requirement for the calculation of q arrays is a knowledge of the vibrational wavefunctions appropriate to the molecule in the upper and lower states of the transitions. Once these are known, a number of derived quantities of the wavefunctions, including q-values, can be calculated.

No completely realistic analytic potential is, in fact, available for the diatomics. All analytic potentials are empirical and constitute representations of what has been thought to be a reasonable approximation to the molecular behavior. The parabolic or simple harmonic potentials were the first to be used. Many other empirical functions have been suggested. (These have been reviewed by Varshni, 1957, and Steele, Lippincott and Vanderslice, 1962.) However, the Morse (1929) potential function* was freely used in molecular calculations. Rydberg (1931, 1933), Klein (1932), and Dunham (1932) developed methods of constructing molecular potentials numerically from the location of the classical turning points of the oscillator at each value. Rees (1946) placed this method on a

---

*$U(r) = D_e \left[1 - \exp \left\{ - \beta (r - r_e) \right\} \right]^2$

where $\beta = 2 \left[\frac{2\pi^2 c}{h} \mu \omega_e x_e \right]^{1/2}$

sound analytic basis. The starting point of such calculations was a set of measured molecular constants, particularly the B_v values derived from band analysis. These potentials are named RKDR potentials after the authors. A number of realistic RKDR potentials for many molecular electronic states have been computed. The resulting wavefunctions have then been used to compute Franck-Condon factors by straightforward numerical integration of their products. For more details about computing methods for Franck-Condon factors, one may refer to a recent article by Chakraborty and Pan (1973).

A comparison between arrays of Franck-Condon factors computed from realistic molecular potentials and from Morse potentials indicates that, in general, there is very good agreement between the two arrays at low quantum numbers and limited agreement at high quantum numbers. However, in some cases, the divergence is much smaller than might have been expected a priori.

$\bar{r}$-centroids. - The $\bar{r}$-centroid ($\bar{r}_{v'v''}$) given by $\bar{r}_{(v'v'')} = \dfrac{\int \psi_{v'} \; \psi_{v''} \; dr}{\int \psi_{v'} \; \psi_{v''} \; dr}$ is an

important derived quantity of vibrational wavefunctions and is frequently used in the theoretical calculations of intensities in molecular spectra.

It is a characteristic internuclear separation to be associated with each (v'v'') transition. Based on numerical computations on a number of diatomic transition, Fraser (1954) showed that the relations

$$\int \psi_{v'} \; r^n \; \psi_{v''} \; dr \;=\; \left[\bar{r}_{v'v''}\right]^n \int \psi_{v'} \; \psi_{v''} \; dr \qquad (5\text{-}39)$$

$$\text{or} \; \int \psi_{v'} \; f(r) \; \psi_{v''} \; dr \;=\; f(\bar{r}_{v'v''}) \int \psi_{v'} \; \psi_{v''} \; dr \qquad (5\text{-}40)$$

hold good provided: (1) $\mu\omega_e \sim 10^4$ for the molecule under consideration, where μ is the reduced mass of the molecule in atomic mass units, and ω_e is the vibrational frequency in cm^{-1}. (2) $0.01\overset{\circ}{A} < |r_{e1} - r_{e2}| < 0.25\overset{\circ}{A}$, r_{e1} and r_{e2} being the two internuclear separations related the transition. (3) v' and v" do not exceed about 10. (4) if $f(r)$ is a polynomial in r, the highest power of r should not exceed about 10.

Recent studies by Drake and Nicholls (1969) have, however, shown that these limits are probably conservative. Nevertheless, this approximate property allows us to resolve the integral of the product of $\psi_{v'}$ and $\psi_{v''}$ and a function of r taken at an argument $\bar{r}_{(v'v'')}$. The validity of this approximation has been tested for a wide variety of transitions for which $q_{v'v''}$ was not extremely small.

In relation to physical meaning attached to $\bar{r}_{(v'v'')}$, we can say the following:

(a) From the relation $\bar{r}_{(v'v'')} = \dfrac{\int \psi_{v'} \; r \; \psi_{v''} \; dr}{\int \psi_{v'} \; \psi_{v''} \; dr}$, it is seen to be a weighted average

with respect to $\psi_{v'}$, $\psi_{v''}$ in the range of r values experienced by the molecule in both the states v' and v". (b) From the same relation, $\bar{r}_{(v'v'')}$ represents the r-coordinate of the centroid of the 'area represented by the overlap integral.

A simple relationship between r-centroids and the average of r experienced by a molecule in a certain vibrational level, v' or v", may also be written as below:

$$\bar{r}_{v'} = \sum_{v''} q_{v'v''} \; \bar{r}_{v'v''} \tag{5-41}$$

$$\text{and} \quad \bar{r}_{v''} = \sum_{v''} q_{v'v''} \; \bar{r}_{v'v''} \tag{5-42}$$

These equations clearly indicate that the average internuclear separation, $\bar{r}_v$, experienced by a molecule in the vibrational level, v' or v", may be considered as a weighted average, with respect to $q_{(v'v'')}$, of the $\bar{r}_{(v'v'')}$ values taken over all transitions which involve that level. Thus, $q_{(v'v'')} \; \bar{r}_{(v'v'')}$ is the appropriate contribution from the v' - v" transition to each of $\bar{r}_{v'}$ and $\bar{r}_{v''}$.

An array of $\bar{r}$-centroids for a band system is a set of discrete values of r over the range experienced by the molecule in all the vibrational levels of both potential energy curves. It has been found that the $\bar{r}$-centroids vary slowly from band to band. Various methods of evaluating $\bar{r}$-centroids have been discussed by Nicholls and Jarmain (1955).

Electronic Transition Moment $R_e(r)$. - The electronic transition moment, $R_e(r)$, is an average of the electric dipole moment, $M_e = (-\Sigma\; e\bar{r})$, with respect to the two electronic wave functions, ψ_e' and ψ_e'', involved in a radiative transition.

$$R_e(r) = \int \psi_e' \; M_e \; \psi_e'' \; d\, T_e \tag{5-43}$$

$R_e(r)$ can be determined experimentally in two main ways: (1) intensity measurement of emission or absorption bands, and (2) measurement of life time of the upper state. Intensity measurements and $R_e(r)$:for the integrated intensity of a (v',v") band, we know that

$$I^{(v'\;v'')}_{\text{emission}} = K\; N_{v'} \; \nu^4_{v'v''} \; S_{v'v''}$$
$$= K\; N_{v'} \; \nu^4_{v'\;v''} \; R_e^2(\bar{r}_{v'v''})\; q_{v'v''} \tag{5-44}$$

where K is a constant which allows for the units and the geometry of the apparatus. $I^{(v'v'')}$ is measured band by band either by photographic or photoelectric methods and $S_{v'v''}$ values are compared band by band.

$$S_{v'\;v''} = I^{v'\;v''} / K\; N_{v'} \; \nu^4_{v'\;v''} \tag{5-45}$$

This approach requires either a knowledge of $N_{v'}$ or the determination of $S_{v'v''}$ along progressions of bands for which $N_{v'}$ is constant. The method, though straightforward in application, has the disadvantage of the relative error varying from band to band. Strong bands have large area profiles and are therefore more accurately measured than weak bands.

Another method is to plot $\left[I_{(v'v'')}/q_{(v'v'')}v^4_{(v'v'')} \right]^{1/2}$ vs. $\bar{r}_{(v'v'')}$ for progressions of bands for which v' is common in each. This plot is equivalent to $N_{v'}^{1/2} \cdot R_e(\bar{r}_{v'v''})$ vs. $\bar{r}_{(v'v'')}$. It has been applied to many band systems. The result is a set of segments which delineate the relative variation of $R_e(r)$ with r. These segments are displaced in ordinate from each other by an amount controlled by $N_v^{1/2}$. Rescaling procedures allow all of the segments to be placed on the same ordinate scale and provide a knowledge of N_v. All the measured intensities have then played a role in the delineation of $R_e(r)$ and a smooth empirical curve can be fitted by least square methods to the final set of points.

Relationship of S_{nm} with Other Molecular Intensity Parameters

Intensity of Emission. - The intensity of a spectrum line* in emission $I_{emission}^{(nm)}$ is defined as the total electromagnetic energy of wave number ν_{nm} that is emitted by the light source per second in all directions of space.

According to quantum mechanics, $I_{emission}^{(nm)}$ in respect to radiative transition $(n \rightarrow m)$ is given by

$$
\begin{aligned}
I_{emission}^{(nm)} &= N_n \, hc \, \nu_{nm} \, A_{nm} \\
&= N_n \, hc \, \nu_{nm} \left[\frac{64\pi^4}{3h} \quad \nu_{nm}^3 \quad \frac{|R^{nm}|^2}{g_n} \right] \\
&= \left(\frac{64\pi^4 c}{3} \right) \left(\frac{N_n}{g_n} \right) \left(\nu_{nm} \right)^4 \left(S_{nm} \right) .
\end{aligned}
\tag{5-46}
$$

where $|R^{nm}|^2$ is represented by S_{nm}, called the transition strength.

---

*The phase 'intensity of a spectrum line' in emission is used frequently in spectroscopy but is often confused with the 'brightness of a line', which is conceptually different from the former. Brightness or radiance is not the rate at which the electromagnetic energy is received (in the wavelength region covered by the line) per unit area of the receiver from unit solid angle of an extended source. It is measured in watt $m^{-2} strad^{-1}$.

In the case of a molecular rotational line $(e'v'J' \to e''v''J'')$ equation (5-46) takes the following form after substituting the value of S_{nm} from equations (5-28) and (5-34),

$$I_{e''v''J''}^{e'v'J'}(\text{emission}) = \left(\frac{64\pi^4 c}{3}\right)\left(\frac{N_{e'v'J'}}{g_{e'v'J'}}\right)\left(\nu_{e''v''J''}^{e'v'J'}\right)^4 R_e^2(\bar{r}_{v'v''})\, q_{v'v''}\, S_{J''\Lambda''}^{J'\Lambda'}$$
(5-47)

where $N_{e'v'J'}$ is the molecular population in the Jth level of the vth vibrational level, in the upper electronic state, e'. $g_{e'v'J'}$ is the net 'statistical weight' of the Jth level, which is equal to $(2 - \delta_{o\Lambda})(2S + 1)(2J' + 1)$ where $\delta_{o,\Lambda}$ is the Kronecker delta symbol.

$$\delta_{o,\Lambda} = 1 \text{ when } \Lambda \neq 0, \text{ i.e., for states other than } \Sigma \text{ states}$$

and $\quad \delta_{o,\Lambda} = 0 \text{ when } \Lambda = 0, \text{ i.e., for } \Sigma \text{ states.}$

(The vibrational statistical weight is always unity.) $R_e(\bar{r}_{v'v''})$ is the electronic transition moment, $(\bar{r}_{v'v''})$ is the $\bar{r}$-centroid; $q_{v'v''}$ is the Franck-Condon factor and $S_{J''\Lambda''}^{J'\Lambda'}$ is the Hönl-London factor; all relevant to the $J' \to J''$ transition.

$(2S + 1)$ is the spin multiplicity of the electronic state concerned

$(2J' + 1)$ is the statistical weight of the J' level.

Similarly, the integrated intensity of a complete $(v'v'')$ vibration band $I_{e''v''}^{e'v'}$ or simple $I^{(v'v'')}$, which is often a measured quantity, can be obtained through proper summations of the relevant terms:

$$I_{\text{emission}}^{(v'v'')} = \sum_{J'J''} I_{e''v''J''}^{e'v'J'}\text{emission}$$

$$= \left(\frac{64\pi^4 c}{3}\right)\frac{R_e^2(\bar{r}_{v'v''})}{g_{e'}}\left(\nu_{e''v''}^{e'v'}\right)^4 q_{v'v''} \sum_{J'}\frac{N_{e'v'J'}}{2(J'+1)} \sum_{J''} S^{J'J''}$$
(5-48)

According to sum rule, we have

$$\sum_{J''} S^{J'J''} = (2J' + 1)$$
(5-49)

where $N_{v'}$ is the molecular population of all the rotational levels of the vibrational level v' and also,

$$\sum_{J'} N_{e'v'J'} = N_{v'}$$
(5-50)

Substituting these values of $\sum_{J''} S^{J'J''}$, $\sum_{J'} N_{e'v'J'}$ and also of $g_{e'}$; $\left[g_e = (2 - \delta_{0,\Lambda}) \right]$ (2S + 1) in equation (5-48) we have, for the integrated intensity of a (v',v") band, the following expression:

$$I_{emission}^{(v'\ v")} = \left(\frac{64\pi^4 c}{3} \right) \frac{R_e^2(\bar{r}_{v'v"})}{(2-\delta_{0\Lambda})(2S+1)} \left(\bar{\nu}^{v'\ v"} \right)^4 q_{v'v"} N_{v'} \tag{5-51}$$

Absorption: Intensity of Absorption. - Because of the effects of natural line width, the definition of the intensity of an absorption line is relatively complicated. However, these effects could be ignored if the absorbing layers are thin. If $I_0^{(nm)} = c\rho_{nm}$ is the intensity of incident radiation; i.e., the energy falling on unit area (1 cm^2) of the absorbing layer per second, the intensity of absorption; i.e., energy absorbed from the incident beam of 1 cm^2 cross section per second, is given by

$$\begin{aligned} I_{absorption}^{(nm)} &= \rho_{nm} N_m' B_{mn} \Delta x \, hc\nu_{nm} \\ &= I_0^{(nm)} N_m' B_{mn} h\nu_{nm} \Delta x \end{aligned} \tag{5-52}$$

where Δx is the thickness of the absorbing layer, ρ_{nm} is density of radiation of incident beam of wave number ν_{nm}, N_m' is molecular number density in the initial lower state m, and B_{mn} is the Einstein transition probability of absorption. Naturally, $[\rho_{nm} N_m' B_{mn} \Delta x]$ denotes the total number of radiative transitions taking place per second in the layer of thickness Δx. $N_m' \Delta x = N_m$, the total number of molecules in the lower state m.

It is, however, assumed here that the incident radiation has a constant intensity for a wave number interval about ν_{nm} sufficient to cover the whole line width.

According to wave mechanics, for a dipole radiation,

$$B_{mn} = \frac{8\pi^3}{3h^2} \frac{|R^{nm}|^2}{g_m} \tag{5-53}$$

where g_m is the degeneracy factor for the state m, and R^{nm} is, as usual, equal to $< n \mid M \mid m >$ the matrix element of the electric dipole moment M. If we now substitute the above value of B_{mn} in equation (5-52)

$$\begin{aligned} I_{absorption}^{(nm)} &= I_0^{(nm)} \frac{N_m}{g_m} h\nu_{nm} \left[\frac{8\pi^3}{3h^2} \mid < n \mid M \mid m > \mid^2 \right] \\ &= \frac{8\pi^3}{3h} I_0^{(nm)} \left(\frac{N_m}{g_m} \right) \nu_{nm} S_{nm}. \end{aligned} \tag{5-54}$$

If we define $\dfrac{I^{nm}_{absorption}}{I^{nm}_o} = k_{nm}$ as 'absorption coefficient',

we have

$$k_{nm} = \frac{8\pi^3}{3h} \; \frac{N_m}{g_m} \; \nu_{nm} \, S_{nm} \tag{5-55}$$

In the case of a molecular rotational line (J' ← J"), equation (5-55) takes the following form

$$k^{e'v'J'}_{e"v"J"} = \left(\frac{8\pi^3}{3h}\right) \left(\frac{N_{e"v"J"}}{g_{e"v"J"}}\right) \left(\nu^{e'v'J'}_{e"v"J"}\right) R^2_e(\bar{r}_{v'v"}) \; q_{v'v"} \; S^{J'\Lambda'}_{J"\Lambda"} \tag{5-56}$$

where $g_{e'v'J'}$ is the net statistical weight of the J" level associated with the v" level in the lower electronic state e".

Equation (5-56) may be modified to take account of the normalized line profile factor, $F(\nu)$, which obeys the relation $\;\;F(\nu)\; d\nu = 1$ and, therefore, it can be written in the form

$$k^{e'v'J'}_{e"v"J"} \approx \left(\frac{8\pi^3}{3h}\right) \left(\frac{N_{e"v"J"}}{g_{e"v"J"}}\right) \left(\nu^{e'v'J'}_{e"v"J"}\right) R^2_e(\bar{r}_{v'v"}) \; q_{v'v"} \; S^{J'\Lambda'}_{J"\Lambda"} \; F(\nu) \tag{5-57}$$

It may be remarked here that various instrumental, thermal and environmental influences control $F(\nu)$ and therefore its value should be determined pertinent to the circumstances of the experiment.

In the case of a vibration band, $k^{e'v'}_{e"v"}$, or simply $k_{(v'v")}$, can be given as follows:

$$k_{(v'v")} = \sum_{J'J"} k^{e'v'J'}_{e"v"J"} = \left(\frac{8\pi^3}{3h}\right) \frac{R^2_e(\bar{r}_{v'v"})}{g_{e"}} \; \bar{\nu}_{v'v"} \; q_{v'v"} \sum_{J"} \frac{N_{e"v"J"}}{(2J"+1)} \sum_{J"} S^{J'J"} \tag{5-58}$$

Further since $\;\;\displaystyle\sum_{J'} S^{J'J"} = (2J"+1)$ and $\;\;\displaystyle\sum_{J"} N_{e"v"J"} = N_{v"}$

Equation (5-58) reduces to the form

$$k_{(v'v")} = \left(\frac{8\pi^3}{3h}\right) \frac{R^2_e(\bar{r}_{v'v"})}{(2-\delta_{o,\Lambda})(2S+1)} \; \nu_{v'v"} \; q_{v'v"} \; N_{v"} \tag{5-59}$$

Oscillator Strength 'f_{mn}'. - The oscillator strength of a radiative transition is a dimensionless parameter and is defined through the relation

$$\left[k_\nu\right]_{mn} = \left[\frac{\pi e^2}{m_e C}\right] N_m \, f_{mn} \tag{5-60}$$

84

where $[k_\nu]_{mn}$ is the 'absorption coefficient' for the transition $m \rightarrow n$ and e and m_e are electronic charge (in esu) and mass (in g_m/electron), respectively. According to the preceding discussion, the 'absorption coefficient', $[k_\nu]_{mn}$, for a transition, $m \rightarrow n$, is related to the transition strength, S_{nm}, through the following relation

$$\left[k_\nu \right]_{mn} = \frac{8\pi^3}{3hc} \frac{N_m}{g_m} \nu_{nm} S_{nm} \tag{5-61}$$

Now, comparing equations (5-60) and (5-61), we get

$$f_{mn} = \left(\frac{8\pi^2 m_e}{3he^2} \right) \left(\frac{\nu_{nm}}{g_m} \right) S_{nm} \tag{5-62}$$

In the case of a molecular rotational line $m(e''v''J'') \rightarrow n(e'v'J')$, $f_{J'J''}$ can be expressed as

$$f_{J'J''} = \left[\frac{m_e c}{\pi e^2 N_m} \right] \left[k_\nu \right]_{mn} \tag{5-63}$$

where $(k_\nu)_{mn}$ corresponds to a rotational line $(J'J'')$ and $N_m = N_{e'v'J'}$. Substituting $(k_\nu)_{J'J''}$ value for $(k_\nu)_{mn}$ from equation (5-61), we get

$$f_{J'J''} = \left[\frac{8\pi^2 m_e}{3he^2} \right] \left[\frac{\nu^{J'J''}}{g_{J''}} \right] \left[R_e^2(\bar{r}_{v'v''}) q_{v'v''} S_{J''\Lambda''}^{J'\Lambda'} \right] \tag{5-64}$$

Similarly for a (v',v'') band, f_{mn} or $f_{v'v''}$ can be expressed as

$$f_{v'v''} = \left[\frac{m_e c}{\pi e^2 N_{v''}} \right] \left[k_\nu \right]_{v'v''} \tag{5-65}$$

Substituting for $[k_\nu]_{v'v''}$ from equation (5-61) in equation (5-65), we have

$$f_{v'v''} = \left[\frac{8\pi^2 m_e}{3he^2} \right] \left[\frac{R_e^2(\bar{r}_{v'v''})}{(2-\delta_{o,\Lambda})(2S+1)} \right] \nu_{v'v''} q_{v'v''} \tag{5-66}$$

The electronic oscillator strength, $f_{e'e''}$, for the entire band system can also be formally defined likewise, though it would not be a uniquely defined parameter.

$$f_{e'e''} = \sum_{v''} f_{v'v''} = \frac{8\pi^2 m_e}{3he^2} \sum \nu_{v'v''} R_e^2(\bar{r}_{v'v''}) q_{v'v''} \frac{1}{g_{e''}} \tag{5-67}$$

$$\text{where } g_{e''} = (2 - \delta_{o,\Lambda})(2S + 1)$$

If we could average $\nu_{v'v''}$ for the whole band system at a characteristic frequency $\bar{\nu}$ and similarly $R_e(\bar{r})_{v'v''}$ could be averaged across the complete system as $\bar{R}_e$ then

$$f_{e'e''} = \frac{8\pi^2 m_e}{3he^2} \quad \frac{1}{g_{e''}} \quad \bar{R}_e^{\,2} \quad \bar{\nu}. \tag{5-68}$$

$$\text{since} \sum_{v'} q_{v'v''} = 1$$

$$\text{or} \quad \frac{f_{e'e''}}{f_{v'v''}} = \frac{\bar{R}_e^{\,2} \, \bar{\nu}}{R_e^{\,2} \, (\bar{r}_{v'v''})} \quad \frac{1}{\nu_{v'v''} \, q_{v'v''}} \tag{5-69}$$

$$\text{and if} \quad R_e(\bar{r}_{v'v''}) \sim \bar{R}_e$$

$$\text{we have} \quad f_{e'e''} = \frac{f_{v'v''} \, \bar{\nu}}{q_{v'v''} \, \nu_{v'v''}} \tag{5-70}$$

These parameters are found quite useful in discussions on the emissivity and opacity of thick molecular vapors.

Radiative Lifetime 'τ'. - Radiative lifetime, τ, of a molecule is directly linked with A_{nm}, the Einstein A-coefficient for spontaneous emission which, in turn, is controlled by S_{nm}.

$$\text{We have,} \quad \tau = \frac{1}{A_{nm}} \tag{5-71}$$

$$\text{where} \quad A_{nm} = \frac{64\pi^4}{3h \, c^3} \quad \frac{\nu_{nm}^{\,3}}{g_n} \quad S_{nm}$$

However, if there is a possibility of radiative transitions to more than one low lying state, it would be necessary to sum A_{nm} over all the possible lower states and, therefore, equation (5-71) will take the form

$$\tau = \frac{1}{\sum_m A_{nm}} \tag{5-72}$$

In the case of a simple two-level radiative transition, $n \rightarrow m$, Einstein A-coefficient, A_{nm}, actually signifies the fraction of total number of molecules in the upper state, n, that undergo radiative transitions per second. The total number of photons thus emitted per second would be $A_{nm} N_n$, where N_n represents the total number of molecules in the upper state n. This means that, on an average, after every $\frac{1}{A_{nm} N_n}$ sec. one photon would be emitted by the system if there are N_n molecules in the upper state. Had there been only one molecule in the upper state, it would have shed off its photon after the time $\frac{1}{A_{nm}}$ sec.

τ is therefore defined as follows:

If a molecule is in an excited state and is completely free to emit spontaneously, then, on an average, after the time $\tau = \frac{1}{A_{nm}}$ it will emit a photon. This is why τ is also called 'mean lifetime of the excited state'.

The law controlling spontaneous emission is, in fact, the usual exponential law, very similar to that of radioactive decay, or first order reaction, in chemical kinetics or molecular absorption.

$$- \frac{dN_N}{dt} = A_{nm} N_n \quad \text{where } N_n \text{ is the number of excited} \qquad (5\text{-}73)$$
$$\text{molecules at any instant t.}$$

$$\text{or} \quad - \frac{dN_n}{N_n} = A_{nm} \, dt$$

$$\text{or} \quad - \log N_n = A_{nm} \, t + C$$

Now, when $t = 0$, $N_n = N_n^0$ and consequently $C = - \log N_n^0$

we can thus write, $\log \frac{N_n^0}{N_n} = A_{nm} \, t$

$$\text{or} \quad N_n = N_n^0 \, e^{-A_{nm} t} \qquad (5\text{-}74)$$

Further, if $t = \frac{1}{A_{nm}}$, we have

$$N_n = \frac{N_n^0}{e} \qquad (5\text{-}75)$$

Equation (5-75) suggests that after time $\tau = \frac{1}{A_{nm}}$, the original number of excited molecules will be reduced to $\frac{1}{e}$ times.

In the case of a rotational level, $\tau_{J'}$ may thus be written as

$$\frac{1}{\tau_{J'}} = \frac{64\pi^4}{3hc^3} \quad \frac{\sum R_e^2 \, (\bar{r}_{v'v''}) \, q_{v'v''} \left(\nu_{e''v''J''}^{e'v'J'} \right)^3 \cdot S_{J'J''}}{(2 - \delta_{o,\Lambda}) \, (2S + 1) \, (2J' + 1)} \qquad (5\text{-}76)$$

and for the vibrational level v', we can write

$$\frac{1}{\tau_{v'}} = \frac{64\pi^4}{3hc^3} \frac{\sum_{v''} R_e^2 (\bar{r}_{v'v''}) \, q_{v'v''} \, \nu_{v'v''}^3}{(2 - \delta_{0,\Lambda}) \, (2S + 1)} \tag{5-77}$$

where $\tau_{v'}$ is the mean life time of the upper level v'.

CHAPTER 6

LINE PROFILES AND THEIR SIGNIFICANCE IN ABSORPTION

Integrated absorption due to a molecular band system is, in fact, a cumulative effect of the integrated absorption caused by the constituent bands in the system. Similarly, the total absorption due to a band is the resultant of the absorption by numerous rotational lines that form the band. When the spectral lines in a band do not overlap appreciably, the integrated absorption by the entire band can be computed by just summing the individual contributions from the constituent lines. However, in most cases, the rotational lines in a band do overlap appreciably and this fact must be taken into account while calculating the integrated absorption by a band. Moreover, the intensities and relative spacings of these lines and also the absorption cross sections quite often differ widely. Therefore, the computation of integrated absorption due to a band needs great care. •

INTEGRATED ABSORPTION DUE TO A SINGLE LINE

A spectral line is not a geometrical line but it exhibits a certain intensity profile, which, apart from being dependent on certain intrinsic properties of the absorbing or emitting atoms or molecules, depends upon certain external physical parameters such as pressure and temperature. Every spectral line is associated with a finite spread of energy and hence of frequency. Even if we record the spectrum on a spectrograph of infinite resolving power, the spectral line emitted by a real source will have a certain width.

There are three different processes which normally contribute to the finite width of spectrum lines.

Natural Broadening

The natural width of a spectrum line is directly associated with the natural lifetimes of the two participating energy states involved in the radiative transition. According to the Heisenberg uncertainty principle, if an energy state, n, has a finite lifetime, Δt, then the energy uncertainty, ΔE_n, for that state is given by

$$\Delta E_n \cdot \Delta t \simeq \frac{h}{2\pi} , \qquad (6\text{-}1)$$

or the corresponding frequency spread, $\Delta\nu_n$, for that state is given by

$$\Delta\nu_n \simeq \frac{h}{2\pi\Delta t} \tag{6-2}$$

Now, whereas $\Delta\nu_n$ is negligible for the ground state, the upper states of allowed electric dipole transitions have lifetimes of the order of 10^{-6} to 10^{-9} sec. Any spectral line involving this level and the ground level must therefore have a frequency spread of the order of 10^{-5} to 10^{-2} cm^{-1}. However, if both the levels have frequency spreads $\Delta\nu_n$ and $\Delta\nu_m$, the width of the resulting line will be given by

$$\Delta\nu_{nm} \doteq \Delta\nu_n + \Delta\nu_m = \frac{h}{2\pi}\left[\frac{1}{\tau_n} + \frac{1}{\tau_m}\right] = \frac{h}{2\pi}\left[\frac{1}{\tau_{nm}}\right] \tag{6-3}$$

The radiative lifetime of an excited state, n, in the absence of collisions, is related to the transition probability for spontaneous emission, A_{nm}, by the relation

$$\tau_{nm} = \frac{1}{A_{nm}}$$

or

$$\tau_{nm} = \frac{1}{\sum_i A_{nm}} \tag{6-4}$$

if i represents the number of transitions that occur from the level n. Since A_{nm} is proportional to ν^3, the natural width of a spectrum line decreases rapidly in the infrared and microwave regions, but may become appreciable in the far ultraviolet.

The shape of the broadened line depends on the profile of the energy distribution of the two levels involved in the transition. According to quantum theory of radiation, the shape factor, $f(\nu-\nu_o)$, of a naturally broadened spectrum line is given by the relation,

$$f(\nu-\nu_o) = \frac{1}{2\pi}\left[\frac{\alpha_n}{(\nu-\nu_o) + (\alpha_{n/2})}\right] d\nu \tag{6-5}$$

where α_n is called line width and ν_o, the central frequency. It represents a Lorentzian profile. In the case of an absorption line, the shape factor is related to the absorption coefficient, k_ν, by the relation $k_\nu = S \cdot f(\nu-\nu_o)$ where S represents the line intensity.

Thermal Doppler Broadening

Doppler broadening of spectrum lines is a result of the well known Doppler effect which is the apparent shift in wavelength of a radiation from a certain source moving towards or away from the receiver.

90

According to kinetic theory, atoms or molecules in a gas at a certain temperature are in perpetual random thermal motion; any movement of these particles, along the line of sight, according to Doppler effect, is likely to create some modification in the frequency of the radiation actually absorbed or emitted by the moving particle. In an actual source, therefore, a large number of atoms having different velocities emit a spread of wavelengths, i.e., a broadened line. In the case of an emitter approaching the observer with velocity u, the Doppler shift in a line of wavelength λ_0 is given by

$$\lambda = \lambda_0 \left(1 + \frac{u}{c}\right) \tag{6-7}$$

$$\text{or} \quad -\frac{d\lambda}{\lambda_0} = \frac{\Delta\nu}{\nu_0} = \frac{u}{c} \tag{6-8}$$

Now, if we know the proportion of atoms that possess velocities in a given range, we can calculate their contribution to a particular spectral line and hence build up the profile.

If the gas under consideration is in thermal equilibrium, then according to Maxwell-Boltzmann distribution law, the fraction of atoms having velocity lying between u and u + du along any one axis (the line of sight in the present case), i.e. $\frac{dn_u}{n}$ is given by

$$\frac{dn_u}{n} = \frac{e^{-u^2/\alpha^2}}{\alpha\pi^{\frac{1}{2}}} \quad du \tag{6-9}$$

$$\text{where} \quad \alpha = \left(\frac{2KT}{m}\right)^{\frac{1}{2}} = \left(\frac{2RT}{M}\right)^{\frac{1}{2}}$$

Here m is the atomic mass, M the mass number, K the Boltzmann constant and R the universal gas constant.

Substituting the value of u from equation (6-8) in equation (6-9), we have for the fraction of atoms emitting in the frequency interval, ν, and $\nu + d\nu$, the following relation

$$\frac{dn_\nu}{n} = \frac{1}{\alpha\pi^{\frac{1}{2}}} \quad e^{-c^2(\Delta\nu)^2/\nu_0^2\,\alpha^2} \quad \frac{c}{\nu_0} \quad d\nu \tag{6-10}$$

Since the intensity at ν is proportional to dn_ν, the line profile can be expressed in terms of the central intensity I_0 as

$$I_\nu = I_0\, e^{-c^2(\nu-\nu_0)^2/\nu_0^2\,\alpha^2} \tag{6-11}$$

Equation (6-11) represents a Gaussian distribution about the central frequency ν_0 with a width determined by α. The half-intensity points ($\nu^{\frac{1}{2}}$) in this profile would be for which

$$I_\nu = 1/2 \, I_o \tag{6-12}$$

$$\text{that is,} \quad \frac{c^2}{\nu_o^2 \alpha^2} (\nu - \nu_{\frac{1}{2}})^2 = \ln 2 \tag{6-13}$$

The Doppler width $\delta\nu_D$ is therefore given by

$$\delta\nu_D = \frac{2\nu_o \alpha}{c} \left(\ln 2\right)^{\frac{1}{2}} \tag{6-14}$$

$$\text{or} \quad \delta\nu_D = \frac{2\nu_o}{c} \left(\frac{2RT \ln 2}{M}\right)^{\frac{1}{2}}$$

$$= 7.16 \times 10^{-7} \, \nu_o \left(\frac{T}{M}\right)^{\frac{1}{2}} \tag{6-15}$$

Equation (6-15) can conveniently be expressed in the dimensionless form as

$$\frac{\delta\nu_D}{\nu_o} = \frac{\delta\lambda_D}{\lambda_o} = 7.16 \times 10^{-7} \left(\frac{T}{M}\right)^{\frac{1}{2}} \tag{6-16}$$

It may, however, be pointed out here that the observed Doppler widths are not necessarily attributable to the gas kinetic motion at some temperature. In many astrophysical and some laboratory sources, there may be strong turbulence or bulk motion of the gas. Usually this also results in a Gaussian profile but in certain circumstances departures from the Gaussian shape have been observed. For a detailed discussion on this subject, one may refer to Gill (1965).

Pressure Broadening

If the pressure of an emitting or absorbing gas is increased, it is observed that the spectral lines, in general, get broadened and in many cases also exhibit peak-shift and asymmetry in their profiles. All these phenomena arise due to the interactions with other particles in the system. We may classify pressure broadening into two categories.

Collision Broadening. - This type of broadening of a spectral line is caused due to premature foreshortening of the oscillator lifetime by a collision between the light emitting center and another atom, the perturber.

If the rate, $\gamma = \frac{1}{\tau}$, at which an excited state actually decays with the emission of light, exceeds the natural decay rate, $\frac{1}{\tau_{nm}} = A_{nm} = \gamma_{nm}$, by the collision rate $\gamma_{(co)} = \frac{1}{\tau_{(co)}}$, i.e.,

$$\gamma = \gamma_{nm} + \gamma_{co} \tag{6-17}$$

$$\text{or} \quad \frac{1}{\tau} = \frac{1}{\tau_{nm}} + \frac{1}{\tau_{co}} , \tag{6-18}$$

the spectral line shape in such a situation can be simply given by the relation similar to natural broadening except that now γ_{nm} should be replaced by γ. The resulting profile is thus given by the following relation

$$I(\omega) = I_o \left(\frac{\gamma}{2\pi}\right) \frac{1}{(\omega-\omega_o)^2 + \left(\frac{\gamma}{2}\right)^2} \tag{6-19}$$

According to Kinetic theory, τ_{co} is equal to half of the mean free time, i.e., $\frac{1}{v}$, where $1 = \frac{KT}{4(2\pi\rho^2 P)^{\frac{1}{2}}}$, the mean free path for a cross section $\pi\rho^2$, pressure P and $v = (8KT/\pi M)^{\frac{1}{2}}$, the mean velocity.

The line widths due to collision broadening can thus be easily computed if the collision cross sections and the velocities of the interacting particles are precisely known.

Stark Broadening. - An emitting particle at a distance r from an ion or electron is perturbed by the electric field, $F = \frac{e}{4\pi E_o r^2}$. In general, such a perturbation is proportional to F^2 except in the case of hydrogen where it is found proportional to F.

The linear Stark effect results in a symmetric line pattern. The statistical averaging process effectively smears out this line pattern to give a symmetrically broadened unshifted line.

The quadratic effect splits the levels asymmetrically and also shifts their center of gravity. Since the shift is usually greater for the higher states, the frequency of the transitions is usually reduced. A line broadened by the quadratic effect therefore tends to be asymmetric and shifted to longer wavelengths.

Pressure dependence of line profiles is quite an involved phenomenon; a full discussion on the various facets of the problem is not intended here. Apart from the various early articles, e.g., Lorentz (1906); Weisskopf (1932); Kuhn and Margenau (1935); Lindhom (1942); Anderson (1949), etc., recent reviews by Hindmarsh and Farr (1972) and Burgess (1972) deal with the subject quite elaborately.

LINE PROFILES AND ABSORPTION COEFFICIENTS

According to the Lambert-Beer law, the fractional absorptance, A, over a wavenumber interval $\Delta\nu$ at ν can be expressed as

$$A\Delta\nu = \int_{\Delta\nu} \frac{I_o - I}{I_0} \, d\nu = \int_{\Delta\nu} (1 - e^{-k_\nu L}) \, d\nu \qquad (6\text{-}20)$$

where k_ν is the absorption coefficient for the gas at the wavenumber ν and L is the length of the absorbing gas in a column of unit cross section.

In the case of a spectrum line having Lorentzian profile, k_ν is given by the relation

$$k_\nu = \frac{S}{2\pi} \left[\frac{\alpha_n}{(\nu - \nu_o)^2 + (\frac{\alpha_n}{2})^2} \right] \qquad (6\text{-}21)$$

where S is the integral coefficient of absorption for the line and $S = \int_o^\infty k_\nu d\nu$; ν_o is the frequency of the line center and α_n is the line width.

According to kinetic theory, the line width α_n depends on both pressure P and the absolute temperature, T, as

$$\alpha_n = (\alpha_n)_o \left(\frac{P}{P_o} \right) \left(\frac{T_o}{T} \right)^{\frac{1}{2}} \qquad (6\text{-}22)$$

where the subscript o refers to the value of the quantity corresponding to STP.

In the case of a Doppler-broadened line, k_ν is expressed as

$$k_\nu = \frac{2S}{\Delta\nu_D} \left(\frac{\ln 2}{\pi} \right)^{\frac{1}{2}} \exp \left[-\frac{4 \ln 2}{(\Delta\nu_D)^2} (\nu - \nu_o)^2 \right] \qquad (6\text{-}23)$$

where $\Delta\nu_D$ is the line width of the Doppler broadened line and is given by the relation

$$\Delta\nu_D = \frac{2\nu_o}{c} \left(\frac{2RT \ln 2}{M} \right)^{\frac{1}{2}} \qquad (6\text{-}24)$$

The equation (6-22) shows that the Doppler line shape is concentrated more near the line center and falls off exponentially in the wings of the line.

However, in most cases spectral lines subjected to both pressure broadening as well as Doppler broadening, i.e., the resultant profile is a blend of both Lorentzian and Gaussian (Voigt profile). In such cases, the k_ν value is given by

$$K_\nu = \frac{(\ln 2)^{\frac{1}{2}}}{\pi^{3/2}} \cdot \frac{Sa}{\Delta\nu_D} \int_{-\infty}^{+\infty} \frac{e^{-x^2}}{a^2 + (w-x)^2} \, dx \qquad (6\text{-}25)$$

where $a = (\ln 2)^{\frac{1}{2}} \frac{\alpha_n}{\Delta\nu_D}$; $w = (\ln 2)^{\frac{1}{2}} \frac{2(\nu - \nu_o)}{\Delta\nu_D}$ and $x = \left(\frac{Su}{\pi\alpha_n} \right)$.

Substituting appropriate k_ν values depending upon the circumstances, in equation (6-25), the integrated absorptance due to a spectrum line can be determined. For details in the subject, one may refer to Wolfe (1965); Hottel and Sarofim (1967); or Penner (1967).

Integrated Absorption Due to a Band

When the constituent rotational lines in a band do not overlap appreciably, the integrated band absorptions can be computed by summing up the contributions from the individual lines. The absorptance of a band of overlapping lines, as is usually the case, depend upon the details of the relative spacing between the lines and their intensity distributions. The absorption coefficient quite often varies rather rapidly in a band and hence it is very difficult to integrate the equation

$$A\Delta\nu = \int_{\Delta\nu} (1 - e^{k_\nu L}) \, d\nu \qquad (6-26)$$

even with a large computer. In order to compute effective integrated absorptance due to a band, there are currently four models that represent the absorption from an actual band with reasonable accuracy in a number of cases. These models are discussed below.

Elsasser Model. - This model assumes that the constituent rotational lines of a molecular band are evenly spaced and that they all have the same intensity and linewidth. This model represents a typically ideal case but is far from reality in the majority of cases. However, some portions of the CO_2 spectrum can be represented with fair accuracy by this model. Actually, a band is normally a blend of numerous weak and strong lines with varying intensities not evenly spaced. The weak lines absorb an increasing share of radiation as the path length becomes longer. The Elsasser model, therefore, is not of much practical value in computing integrated band absorption.

Mayer-Goody or Statistical Model. - The rotational lines within a band quite often show a random distribution of intensities and position. A very simple expression for the average transmittance of such a band model may be derived in terms of equivalent width A_L of a single line, evaluated at a mean line intensity, S, and the mean spacing d between the lines. The contribution, K_ν^i, of one line to the net absorption coefficient is a function of the line intensity S, the half line width b_i and the displacement $(\nu - \nu_i)$ of the line center from the wavenumber of interest, i.e.,

$$K_\nu^i = f(S_i, b_i, \nu_i) \qquad (6-27)$$

Typically, for a Lorentzian line shape

$$K_\nu^i = \frac{S_i}{\pi} \left[\frac{b_i}{(\nu-\nu_i)^2 + b_i^2} \right] \qquad (6-28)$$

Since there is no correlation between the different line intensities and line positions, the total transmissivity is the product of the transmissivity of the individual lines.

Random Elsasser Model. - This model assumes the random superposition of several different Elsasser bands forming one single band. Each of these superimposed bands may have a different line intensity and spacing. As many different Elsasser bands as desired may be superimposed in this model. Thus all of the weak spectral lines that contribute to the absorption for longer path lengths can be included in the absorption calculations.

This model is particularly suited to the computation of absorption for such gases whose vibrational-rotational bands show an almost regular line spacing and which as a result of the excitation of higher vibrational levels have several such bands superimposed over one another. For a critical study of this model, one may refer to Plass (1958).

Quasirandom Model. - This model is the most accurate and by far the most complicated of the band models. The absorptance is calculated first for a frequency interval that is much smaller than the interval size of interest. This localizes the stronger lines to a narrow interval around their actual positions and prevents the introduction of over-lapping effects. The absorptance of each of the N spectral lines in the frequency interval is calculated separately and the results combined by assuming a random placing of the spectral lines within the small interval. The absorption from the wings of the lines in neighboring intervals is also included in the calculation. Finally the absorp-tance values for all of the small intervals that fill the larger interval of interest are averaged to obtain the final value. An electronic computer is commonly used to calculate absorptance according to this model. For a detailed review on the various theoretical and applicational aspects of these band models, one may refer to Penner (1967) or Hottel and Sarofim (1965).

96

CHAPTER 7

PRINCIPLES OF THE MEASUREMENT OF ABSORPTION
AND
DETERMINATION OF ABSORPTION CROSS SECTIONS

The quantitative measurement of absorption of electromagnetic radiant energy by different absorbing media has long been of great scientific interest. These measurements, in most part, have been based on the well-known exponential absorption law; i.e., Beer's law, which works quite satisfactorily in many cases. It is, however, subject to certain intrinsic limitations and boundary conditions in its application, which must be taken into consideration while making actual measurements and drawing inferences therefrom.

LAWS OF ABSORPTION

It was Bouguer (1729) who probably was the first to propose a precise formulation of the exponential law of optical absorption. The law, basically, was applicable to optically thin layers of absorbing media and truly monochromatic radiations. Lambert (1760) reformulated Bouguer's principle into an analytic form and later Beer (1852) introduced the concept of concentration into the Bouguer-Lambert formulation.

Bouguer-Lambert Law

According to Bouguer-Lambert law, the loss of radiant intensity ($-dI$) after traversing an optically thin absorbing layer of thickness (dl) is proportional to the incident radiant intensity (I_0) and the thickness of the layer, dl; i.e.,

$$-dI = b \, I_0 \, dl. \qquad (7-1)$$

On integration between limits, $l = 0$ (where the intensity is I_0) and $l = L$ (where the intensity is I), equation (7-1) takes the form

$$I = I_0 \, e^{-bL} \qquad (7-2)$$

or

$$I = I_0 \, 10^{-aL} \qquad (7-3)$$

where a and b are commonly called the Naperian absorption coefficient and Decadic absorption coefficient, respectively, and a = 0.4374b.

The relation (7-3) sometimes is also expressed in its logarithmic form

$$\log_{10}\left(\frac{I_o}{I}\right) = aL \tag{7-4}$$

where the product aL is called optical density (O.D.). In the equation (7-4), if we put $I = \frac{I_o}{10}$, we get aL = 1 or a $= \frac{1}{L}$ which means that the coefficient, a, is numerically equal to the reciprocal of the path length when the intensity is reduced to $\frac{1}{10}$ of its initial value.

Beer Law

According to Beer law, the coefficients a or b in equations (7-2) or (7-3) are taken as linearly proportional to the concentration of the absorbing entities interacting with the traversing radiation beam; i.e.;

$$b = \bar{k}C \tag{7-5}$$

and

$$a = \varepsilon C \tag{7-6}$$

where C represents the concentration of the absorbing particles (mole/litre) and k and ε are called Molar Naperian absorption coefficient and Molar Decadic absorption coefficient, respectively.

If, however, the absorbing medium is composed of different absorbing constituents with $\bar{k}$ or ε values as $\bar{k}_1 \ \bar{k}_2 \ \bar{k}_3$ - - - - and $\varepsilon_1 \ \varepsilon_2 \ \varepsilon_3$ - - - -, then according to Beer law one can also write

$$\bar{k}C = \bar{k}_1C_1 + \bar{k}_2C_2 + \bar{k}_3C_3 \ - - - \tag{7-7}$$

and

$$\varepsilon C = \varepsilon_1C_1 + \varepsilon_2C_2 + \varepsilon_3C_3 \ - - - \tag{7-8}$$

These relations, under favorable circumstances, are found quite useful in quantitative analysis of mixtures of absorbing species.

Combining the Bouguer-Lambert Law and Beer Law, a single expression can be written which incorporates the underlying concepts of both.

$$I = I_o e^{-\bar{k}CL} \tag{7-9}$$

or

$$I = I_o \cdot 10^{-\epsilon CL} \tag{7-10}$$

Now, if we choose to express concentration in terms of number density, n; and L in cm units, we have

$$I = I_o e^{-\sigma_\lambda nL} \tag{7-11}$$

or

$$I = I_o 10^{-(0.434)\sigma_\lambda nL} \tag{7-12}$$

where σ_λ is a constant, commonly known as absorption cross section.

Comparing relations (7-11) and (7-12) and using the relation $n = \dfrac{CN_A}{1000}$; where N_A represents the Avagadro number, we can establish a relation between ϵ and σ_λ as

$$\epsilon = (2.6 \times 10^{20}) \sigma_\lambda \tag{7-13}$$

σ_λ is related to another constant k by the relation $\sigma_\lambda = \dfrac{k}{n_o}$ where n_o is the Loschmidt's number (2.7×10^{19} molecules per cm^3 at STP). k is called the absorption coefficient at STP.

We can also express the Lambert-Beer Law as:

$$I = I_o e^{-k\left(\frac{n}{n_o}\right)L}$$

$$\text{or} \quad I = I_o e^{-kL_o} \tag{7-14}$$

$$\text{or} \quad I = I_o e^{-\sigma_\lambda n_o L_o}$$

where $L_o = \left(\dfrac{n}{n_o}\right) L = \left(\dfrac{P}{P_o}\right)\left(\dfrac{T_o}{T}\right) L$, according to kinetic theory of gases; L and L_o are called geometrical length and reduced length, respectively. P and T represent the ambient pressure and temperature of the gas and P_o and T_o are the standard values; $P_o = 760$ mm Hg and $T_o = 273.2°C$. However, if σ_λ varies appreciably over the wavelength range of the incident radiation and varies smoothly, the law as stated in (7-14) will not hold and its modified form (7-16) should be used:

$$I = I_o e^{-n_o L_o \int_{\Delta\lambda} \sigma_\lambda d_\lambda} . \tag{7-15}$$

ABSORPTION CROSS SECTION (σ) AND ITS DETERMINATION

Absorption cross section is an important observable that one often looks for while computing various physical parameters in atmospheric optics. It is closely related to the transition strength of the molecular transition involved in the process of absorption. It has dimensions of area and, in fact, represents the effective absorbing area of the molecule, assuming that it is completely opaque to the given radiation. It is usually expressed in units of megabarn where 1 Mbn = 10^{-18} cm^2.

The measurement of absorption cross section of a molecular gas for a particular wavelength is based on the Lambert-Beer Law as expressed in equation (7-14); i.e.,

$$I = I_0 \exp\left[-\sigma_\lambda n_0 \left(\frac{P}{P_0}\right) \left(\frac{T_0}{T}\right) L\right]$$

or

$$\log_e\left(\frac{I_0}{I}\right) = \sigma_\lambda n_0 \frac{P}{P_0} \left(\frac{T_0}{T}\right) L. \tag{7-16}$$

Keeping L and T constant, we obtain different values of $\log_e\left(\frac{I_0}{I}\right)$ for the wavelength in question and at different pressures, preferably in the low pressure range. If a plot of $\log_e\left(\frac{I_0}{I}\right)$ versus P gives a straight line passing through the origin, σ_λ can be determined from the slope of this line.

At times it so happens that in a certain pressure range, we may get a linear plot for $\log_e\left(\frac{I_0}{I}\right)$ versus P but the straight line, on extrapolation, does not pass through the origin. In such circumstances, the slope of the line will not give the characteristic absorption cross section.

It is usual in absorption spectroscopy to limit the values of I_0/I to a maximum of 2.80 (65% absorption) and to a minimum of 1.1 (10% absorption).

Applicability of the Lambert-Beer Law and its Limitations

On many occasions, it is observed that certain measurements in optical absorption do not obey the Lambert-Beer Law. As a matter of fact, Beer Law in its simplest form, is subject to certain basic assumptions and if these conditions are not maintained, the law is to be regarded as not applicable rather than not valid.

Monochromaticity and Intensity of the Incident Radiation. Lambert-Beer Law is valid only for truly monochromatic radiation of an infinitely narrow band pass. Departure from this prerequisite is likely to involve deviation from the applicability of the law.

No apparent deviations from the Beer Law have been observed with regard to the variation of incident radiation intensity. However, according to Vavilov (1950), absorption cross section does vary with incident intensity when the optical absorption in question involves electronic transition with long life times.

This aspect of dependence of σ_λ on incident intensity can be well explored where powerful lasers are used as the radiation source. Here the dependence of σ_λ on $I_o(\lambda)$ should manifest itself differently for different lines (Zuev, 1974).

Absorbing Medium. - The absorbing gas should be homogeneous, isotropic, chemically or otherwise non-interacting and optically thin. There should exist no simultaneous processes of attenuation of radiant flux; e.g., induced emission, fluorescence, scattering, ionization, dissociation, etc., by which the transmitted energy flux can get modified.

The absorbing gas should be free from effective molecular interactions; i.e., each molecule should absorb independently of other molecules in the system. It has been shown by numerous experiments that this assumption is, in general, truly valid only in a very low pressure range. Increasing the concentration of the absorbing gas and the addition of some foreign non-absorbing gas in the system very often ends up in the amplification of intermolecular collisions. Temperature is another factor which influences the intermolecular interaction because of increased thermal motion. The nature of the absorbing entities may also change with pressure due to hydrolysis, polymerization, ionization, hydrogen bonding, etc. Beer Law is no longer applicable in such circumstances.

Instrumental Conditions. - We know that Beer Law is ideally suited for truly monochromatic radiation of an inifinitely narrow band pass. However, if the absorption cross section does not vary, or is a slowly varying function of wavelength over a given band pass, an effective absorption cross section can be determined for the band pass range. This method usually gives satisfactory results in the case of smooth absorption continua.

The situation becomes more involved in the case of discrete structures, unless the instrumental band width is less than the line width. True absorption cross sections are difficult to determine in such cases. Previously, the criterion to measure true absorption cross sections was based on the observations of the pressure dependence. Beer's Law was assumed to be applicable if a plot of $\log\left(\frac{I}{I_o}\right)$ versus n was linear. The true absorption cross section was then equal to the slope of the curve. If the instrumental band width was greater than the line width of discrete structure, the linearity relation did not hold good and a pressure effect was observed. In such a case, the common practice has been to extrapolate these pressure-dependence curves to zero pressure to obtain true absorption cross section. However, both these criteria could be misleading.

Hudson and Carter (1968) have shown that the absorption cross section can decrease rapidly by a fraction of 1 to 0.4 of its peak value as the ratio of the band width to line width varies from 0 to 2, even though a straight line plot of log (I/I_o) versus n could be obtained over this range.

If A_o $(\lambda',\Delta\lambda)$ denotes the integrated flux reaching the photomultiplier when there is no absorbing gas in the path, A $(\lambda',\Delta\lambda)$ represents the corresponding quantity when the absorbing gas is in the path and λ' is the wavelength of the center of the band width $\Delta\lambda$, then we have:

$$\frac{A_o(\lambda',\Delta\lambda)}{A(\lambda',\Delta\lambda)} = \frac{\int_{\lambda'-\Delta\lambda}^{\lambda'+\Delta\lambda} S(\lambda)G(\lambda)d\lambda}{\int_{\lambda'-\Delta\lambda}^{\lambda'+\Delta\lambda} S(\lambda)G(\lambda) e^{-N\sigma_\lambda} d\lambda} \tag{7-17}$$

where $S(\lambda)$ is the flux from the light source at the wavelength λ, which is incident on the entrance slit; $G(\lambda)$ is the slit function of the spectrograph, N is the total number of atoms or molecules in the light path, σ_λ is the absorption cross section at wavelength λ.

In the case of the continuum source, $S(\lambda)$ is a constant across the band width of the spectrograph and, hence, will cancel from equation (7-17), the shape of $G(\lambda)$ versus λ can be calculated from the known grating parameters.

Further, if σ_λ is a constant across the band width of the spectrograph, then equation (7-17) reduces to

$$\frac{A_o(\lambda',\Delta\lambda)}{A(\lambda',\Delta\lambda)} = \exp(N\sigma_\lambda') \tag{7-18}$$

It has been recognized that the above equation will not hold at the peak of a line which is narrow compared to the instrumental band width and that a pressure dependent absorption cross section results. But another assumption that often seems to be made is that, if at a peak a plot of log $\left(\frac{A_o}{A}\right)$ versus N is a straight line passing through the origin; i.e., if Beer Law is obeyed, then the slope of that line is assumed to be the peak absorption cross section.

It is well known that the absorption cross section in the vicinity of the peak is a rapidly varying function of λ and thus the slope of the line should represent an average cross section across the band width of the instrument. Hudson and Carter (1968) calculated, using equation (7-17), the values of the ratio A_o/A versus N for different functional forms of σ_λ in order to determine the relationship between σ_λ the absorp-

102

tion cross section at the center of the band width and $\sigma_{\lambda+\Delta\lambda}$ the slope of the line obtained by plotting log $\left(\dfrac{A_o}{A}\right)$ values against N.

Figure (7-1) represents a semi-log plot of the ratio (A_o/A) versus N for different values of $\dfrac{\Delta\lambda}{\Delta L}$ where ΔL is the line width and $\Delta\lambda$ is the band width. The functional form of σ_λ here has been assumed as Lorentzian.
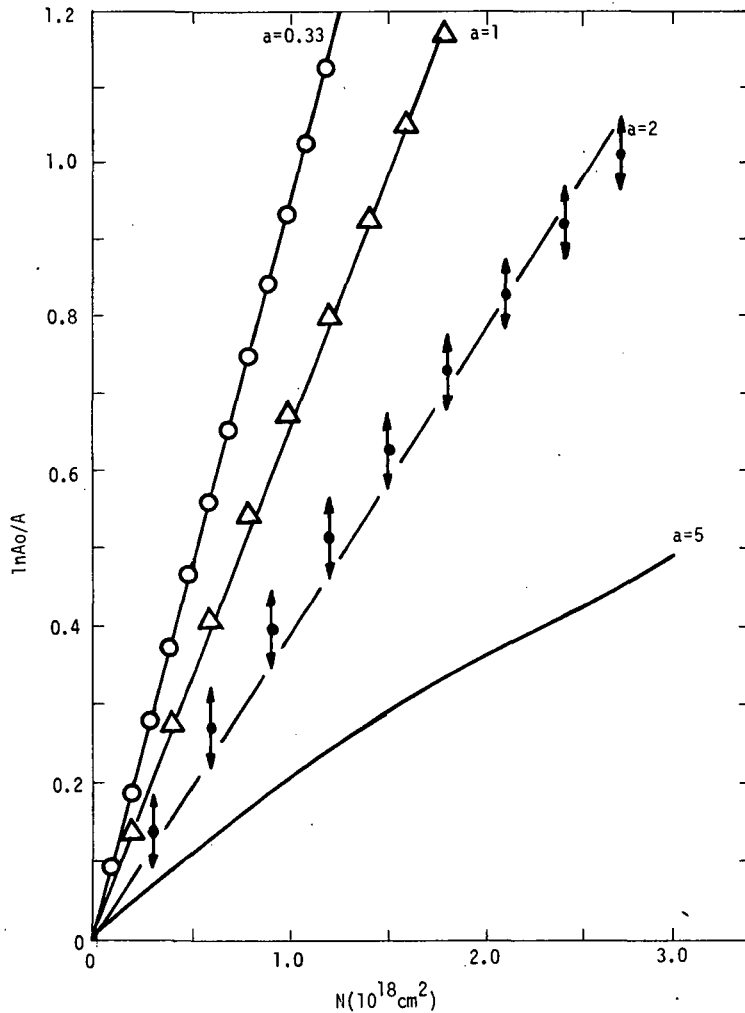
Figure (7-1). Semi-log plot of the ratio (A_o/A) versus N for different values of $a = \Delta\lambda/\Delta L$.

It is evident from this figure that as $\frac{\Delta\lambda}{\Delta L}$ = a gets larger, the shape of the curve diverges from that of a straight line. However, for a $\leq$ 1, we get straight line plots but with different slopes. Hudson and Carter (1968) made a detailed analysis of the band pass dependence of absorption cross sections, taking different functional forms of σ_λ, and their analysis has shown that:

(1) All measured cross sections are necessarily the cross sections averaged over the bandwidth of the spectrograph. Resolving power of the spectrograph thus plays a very vital role in these determinations.

(2) The Beer law criterion is not a sufficient indication that the true peak or minimum absorption cross section has been measured.

(3) In general, the σ_λ value obtained from a Beer Law plot will always be less than the true peak absorption cross section and more than the true minimum absorption cross section.

(4) The relationship between the average absorption cross section and the true absorption cross section at the center of the bandwidth is a function of the instrumental band width and the functional form of the absorption cross section across the band width.

PRESSURE-INDUCED EFFECTS IN MOLECULAR ABSORPTION

Absorption of electromagnetic radiation by a molecular gas, either composed of one single species or a mixture of species, is quite often found to be intrinsically influenced by the pressure, particularly in the high pressure range. Significant deviations from the applicability of the Lambert-Beer Law are observed as regards absorption under such conditions. The phenomenon is generally ascribed to the involvement of intermolecular interaction which become appreciable at high pressures and play a significant role in modifying the effective absorption cross section of the gas.

Two types of pressure-induced effects are generally observed in the case of radiative transitions in molecules.

Distortion of Spectrum Line Profiles

The perturbation of a spectral transition by pressure significantly modifies the energy distribution of radiation emitted or absorbed by an atom or a molecule.

The effect of the modification of integrated molecular absorption resulting from the line profile distortions induced by pressure was first observed experimentally in the infrared region by Angström (1889; 1890; 1892; 1901) in the study of integral absorption by CO_2. Schaefer (1905) investigated spectral absorption of CO_2 bands at 2.7μ and 4.3μ and also found that the absorption coefficient was a function of partial pressure.

Von Bahr (1909, 1910, 1911) investigated the absorption of infrared radiation by mixtures of various absorbing and non-absorbing foreign gases and observed departures from the applicability of the Beer Law. For all of these changes in the absorption coefficient values, broadening of spectral lines due to intermolecular collisions was held to be the responsible factor.

Induced Spectral Features

Pressure-induced spectral features can be broadly classified into two categories:
(1) A radiative transition, which is forbidden by normal selection rules for electric dipole radiation in the case of isolated molecules and which may become effective as a result of strong intermolecular forces. Appearance of forbidden transitions, combination frequencies and satellite bands are a few of the examples of this nature.
(2) A transition, which is normally allowed by the selection rules, and which may get modified under the induction effect of the intermolecular forces.

In compressed gases, the distortion of the electron distribution due to binary and higher order collisions induces a dipole moment in the collision system. Dipole absorption can thus occur, though in the case of a free molecule it does not. The induced dipole moments which are responsible for the induced absorption depend strongly on the separations between interacting molecules; whereas, the permanent dipole moments responsible for the allowed spectra are, to a good approximation, independent of the intermolecular separations. As a result, the dependence of the absorption on the density and the temperature of the absorbing medium is quite different in the two cases.

These induced dipole moments are modulated by the vibration and rotation of the collision partners and also by their respective translational motion. A variety of induced spectra are, therefore, known, ranging from pure translational spectrum in the far infrared to the fundamental and overtone rotation-vibration spectra in the near infrared and electronic spectra in the visible and ultraviolet regions.

General Characteristics of Pressure-Induced Spectral Features. - The salient features of different types of pressure induced spectra which have been borne out on the basis of experimental observations can be summarized as follows.

In the case of a mixture of gas (1) of density (ρ_1) and another gas (2) of density (ρ_2), the integrated absorption coefficient, $\int \alpha d\nu$, for an induced transition in gas (1) can be expressed as a power series of densities of the two constituent gases.

$$\int \alpha d\nu = [\int \alpha_{11}(\rho_1)^2 + \int \alpha_{11}'(\rho_1)^3 + - - -]$$
$$+ [\int \alpha_{12}(\rho_1\rho_2) + \int \alpha_{12}'\rho_1(\rho_2)^2 + \int \alpha_{12}''(\rho_1)^2\rho^2] \qquad (7\text{-}19)$$
$$+ - - - - - - - - -$$

105

In the above equation, while the first set of terms arises from (1) - (1) collisions, the second set arises due to (1) - (2) collisions. In such regions of pressures where binary collisions predominate, only the quadratic terms in this expression need to be retained as first approximation; i.e.,

$$\int \alpha d\nu = \int \alpha_{11}(\rho_1)^2 + \int \alpha_{12}(\rho_1\rho_2) \tag{7-20}$$

For example, in the case of pure H_2 gas at room temperature and a pressure of 100 atmospheres, the cubic term, $\int \alpha'_{HH}(\rho_{H_2})^3$, contributes only about 7% to the total integrated absorption (Chisholm and Welsh, 1954).

The rotational selection rules operative for induced transitions are $\Delta J = 0, \pm 2$, which are the same as for Raman effect. The normal dipole transition rules, $\Delta J = 0, \pm 1$, do not hold good here.

Double or simultaneous transitions are also of common occurrence. Both molecules of the collision-pair simultaneously undergo the same or different transitions with the absorption of a single photon. Welsh, et al. (1951) were the first to postulate the occurrence of such simultaneous transitions while studying the induced vibrational spectra of H_2.

This hypothesis of double or simultaneous transitions was confirmed later on by the study of induced spectra in a number of cases (Fahrenfort and Ketelaar, 1954; Fahrenfort, 1955; Coulon, et a., 1955, 1956; Vodar, 1958; Colpa and Ketelaar, 1958; Rettsschnick, 1962; Farmer and Houghton, 1966; Dianov-Klokov and Malkov, 1973.

Induced transitions are greatly broadened as a result of high collision frequency, which can be construed as a consequence of the Heisenberg uncertainty principle. As the temperature of the absorbing gas is lowered, the duration of a collision increases and the breadth of the transition decreases.

The broad induced transition is, in effect, a continuum of summation and difference tones of the molecular frequency with the continuous distribution of relative kinetic energies of the colliding pairs. The intensities in the low and high frequency wings at frequencies displaced by $\Delta \nu$ (cm^{-1}) from the molecular frequency ν_o are, therefore, related by the Boltzmann distribution. This imparts a characteristic asymmetry to the intensity profile of the spectrum line.

The intensity distribution of the high frequency wing has, to a good approximation, a dispersion line shape (Kiss and Welsh, 1955). Detailed theory of pressure induced molecular absorption has been developed by Van Kranendonk, 1957, 1958. According to his proposed model, the induced dipole moment, μ, is regarded as the sum of two contributions; viz., the quadrupole interaction and the electron overlap forces and can be expressed as

$$\mu = (A/r^4) + \xi e^{-\frac{r}{\rho}} \tag{7-21}$$

where r is the intermolecular separation and A, ξ and ρ are different constants. The first term is due to quadrupole interaction and has a relatively long range. The second term $[\xi\, e^{-(\frac{r}{\rho})}]$ arises from the electron overlap forces and has a shorter range. The induced moment is strongly dependent on the relative orientation of the molecules in the collision pair. Numerous examples of different types of induced spectral transitions have been reviewed by Colpa (1965) and Vodar (1965) in the book "Physics of High Pressures and the Condensed Phase" edited by A. Van Itterbeek.

OPTICAL DEPTH, EQUIVALENT WIDTH AND THE CURVE OF GROWTH

Optical Depth

The optical depth of a medium is usually defined as equivalent to $\int_0^L k_\nu\, d\nu$, which for a homogeneous medium becomes $k_\nu L$; where k_ν represents the absorption coefficient and L the optical path length. In this definition, k_ν is assumed to be independent of depth. In many astrophysical conditions, this assumption is, however, not valid.

A layer of gas is defined as optically thin if $k_\nu L \ll 1$ and optically thick if $k_\nu L \gg 1$. Because of large variations of k_ν with ν, the medium may be optically thick for one line and thin for another or thick at the center of a single line but thin in the wings. In absorption, an optically thin path is that in which the absorption shows no signs of saturation; i.e., doubling the path length halves the transmitted intensity. In emission, it is one in which there is no self absorption.

When the medium is optically thin over the entire profile of an absorption line the effect of increasing the optical depth either by increasing the absorption length or the number density can be investigated using Beer Law. According to the Lambert-Beer Law,

$$I = I_0\, e^{-\sigma_\nu n L} = I_0\, e^{-N\sigma_\nu} = I_0\, e^{-\tau} \tag{7-22}$$

where τ represents the optical depth; n is number density; L is the length of the absorption column, N is the total number of absorbing molecules in the line of sight and σ_ν represents the absorption cross section. Optical depth is thus the product of absorption cross section and the total number of absorbing particles in the line of sight.

Equivalent Width

As optical depth increases, while the curve $k_\nu L$ versus ν stays the same shape throughout, the shape of the curve I_ν versus ν changes significantly. Since the dip in the latter cannot go down below the baseline, i.e., the line corresponding to the zero transmitted intensity, the absorption must saturate first at the center of the line and

then outwards toward the wings. The area of this dip, as a matter of fact, is equal to the rate at which the energy is absorbed from the incident beam in a particular spectral line. The fractional radiant absorptance over a finite wavenumber interval $d\nu$ is called equivalent width W_ν of the spectral line.

$$W_\nu = \int_{Line} \frac{I_o - I_\nu(L)}{I_o} \, d\nu \tag{7-23}$$

The equivalent width is so called because it is the width of the rectangle that has the same area covered by the actual dip in the I_ν versus ν curve, Figure (7-2). Now, if we express equations (7-23) in terms of absorption coefficient k_ν, we get

$$W_\nu = \int_{Line} (1 - e^{-k_\nu L}) \, d\nu \tag{7-24}$$

and, since k_ν is proportional to $N_m f_{mn}$, for an optically thin absorber we can write

$$W_\nu = \int k_\nu L \, d\nu$$

$$= L \int k_\nu d\nu = \frac{e^2}{4\varepsilon_o mc} N_m f_{mn} L. \tag{7-25}$$

where f_{mn} denotes the oscillator strength for the transition $m \rightarrow n$.
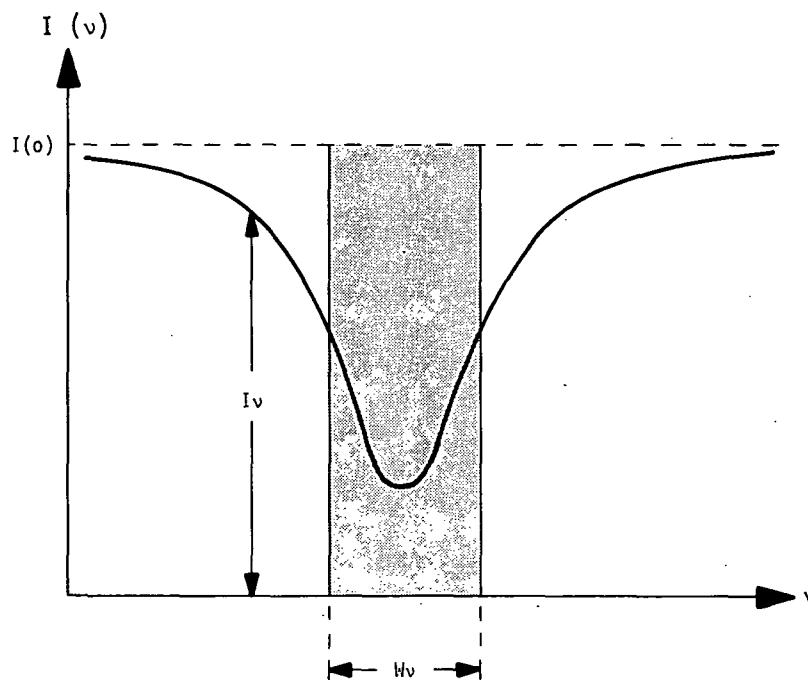

Figure (7-2). Schematic illustrating the concept of equivalent width of a spectral line.

Curve of Growth

The curve of growth for a given spectral line describes the behavior of its equivalent width as the number of absorbing species in the line of sight is increased. It usually takes the form of a plot of $\log W_\nu$ against $\log NfL$. The exact form of the curve depends on the width and the shape of the line, but the width dependence can be taken care of by plotting as ordinate the dimensionless quantity $W_\nu/\delta\nu_D$.

$$\frac{W_\nu}{\delta\nu_D} = \frac{e^2}{4\varepsilon_o mc} \cdot \frac{NfL}{\delta\nu_D}$$

$$= 2.65 \times 10^{-6} \frac{NfL}{\delta\nu_D} \quad (N \text{ is in } m^{-3}, L \text{ is in } m \text{ and } \delta\nu_D \text{ is in } sec^{-1})$$

or

$$\log \frac{W_\nu}{\delta\nu_D} = -5.58 + \log \left(\frac{NfL}{\delta\nu_D}\right) \tag{7-26}$$

The curve of growth must therefore start as a straight line of unit gradient. When the medium is no longer optically thin for the center of the line, W_ν increases less rapidly than NfL and the curve starts flattening out. The linear limit and the behavior of the curve thereafter depends on the profile of the spectral line. In a Lorentzian profile, the wings are more prominent than in a Doppler profile and consequently there is a lower peak height for the same total area. However, in many cases of practical interest, the net line shape is a blend of both Lorentzian and Doppler (Voigt profile); therefore, the relative importance of the two components - - i.e., the Lorentzian and Doppler - - is measured by the ratio of their half widths.

$$a = \frac{\delta\nu_L}{\delta\nu_D} \tag{7-27}$$

For relatively small values of a, the central part of a Voigt profile is almost Doppler type, while the wings are Lorentzian. As a result, all of the curves in this region remain fairly flat and the absorption is mainly confined to the Doppler core.

If NfL is increased still further, i.e., in the optically thick region, the absorption in the Lorentzian wings becomes significant and W_ν increases much faster. In such a case, it is shown that

$$W_\nu = \left(\frac{e^2}{4\varepsilon_o mc} \delta\nu_L\right)^{\frac{1}{2}} \left(NfL\right)^{\frac{1}{2}}$$

$$\log \left(\frac{W_\nu}{\delta\nu_D}\right) = \text{const.} + 1/2 \log a + 1/2 \log \left(\frac{NfL}{\delta\nu_D}\right) \tag{7-28}$$

which means, the curve of growth finishes up as a straight line of gradiant one half, but lines having different values of, a, are separated according to the value of 1/2 log (a). A typical growth curve is depicted in Figure (7-3). Details on the various aspects of the use of growth curves particularly in the context of astrophysical problems can be found in Aller (1963) or Cowley (1970).
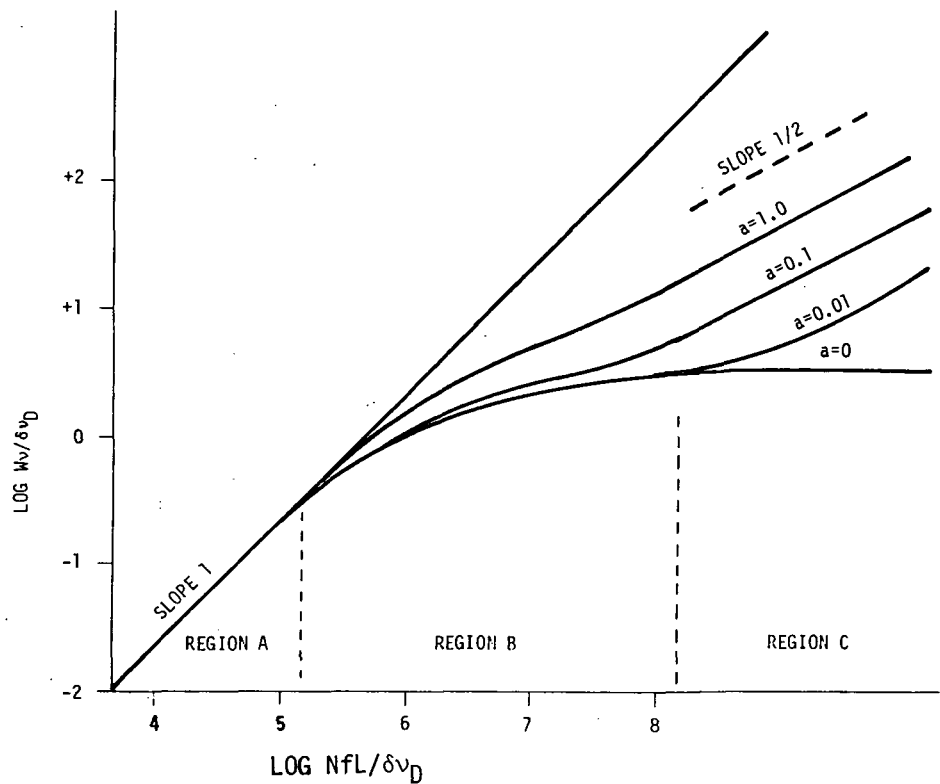
Figure (7-3). Growth curve in the case of a typical spectrum line.

CHAPTER 8

BAND SPECTROSCOPIC METHODS OF TEMPERATURE DETERMINATION

Spectroscopic methods under favorable circumstances, are often quite useful in determining temperature of the source of emission or absorption. Effective temperatures corresponding to the degree of rotational, vibrational or electronic excitation can be computed using intensity measurements on different spectral features. These 'spectroscopic' temperatures are sometimes called 'rotational', 'vibrational' and 'electronic' temperatures and are normally different from the true thermodynamic temperature of gas. However, if the gas under consideration is in thermal equilibrium, all of these spectroscopic temperatures should be identical and equal to the true kinetic or thermodynamic temperature.

From the theoretical standpoint, if the gas under consideration is in thermodynamic thermal equilibrium, the particles conform to Maxwellian velocity distribution and gas temperature is equivalent to the kinetic temperature defined by the relationship

$$\overline{v} = \left(\frac{8KT}{\pi m} \right) \qquad (8-1)$$

where $\overline{v}$ is the average particle velocity, K is Boltzmann constant, T is absolute temperature and m is mass of the gas particle.

Most methods of measuring spectroscopic temperatures are subject to the condition that energies of all the particles in the gas assembly conform to the Maxwell-Boltzmann law. Making intensity measurements on individual rotational lines in a band, or integrated intensity measurements on the different bands in a system, relative populations of the relevant energy levels are determined and subsequently corresponding spectroscopic temperatures are evaluated using the Maxwell-Boltzmann distribution law.

ROTATIONAL TEMPERATURES

Rotational temperatures may be determined from the observed intensities of the rotational lines, using the general intensity relations as applied to rotational transitions.

The intensity of a rotational emission line in a (v',v'') band can be given by

$$I_{em}^{J'J''} = DN_{v'} \, E_{v'v''}^4 \, P(v'',v'') \left(\frac{S_{J'J''}}{Q_r} \right) \exp\left(-E_{J'}/KT\right) \qquad (8-2)$$

where D = a constant depending upon the geometry of the instrument and the units employed.

$N_{v'}$ = molecular population of the upper vibrational level

$E_{v'v''}$ = energy corresponding to the (v',v") band

$p(v',v'')$ = vibrational transition probability given by the relation

$$p(v',v'') = | \psi_{v'} R_e(r) \psi_{v''} dr |^2$$

$S_{J'J''}$ = line strength factor

Q_r = rotational partition function

$E_{J'}$ = rotational energy of the upper level J', given by $E_{J'} = B_{v'}(J'+1)J'hc$.

Now, since the integrated intensity $I_{v'v''}$ of the band (v',v") is expressed as

$$I^{v'v''} = DN_{v'} E^4_{v'v''} p(v',v'') . \tag{8-3}$$

Equation (8-2) can be rewritten as

$$I^{J'J''} = I^{v'v''} \left(\frac{S_{J'J''}}{Q_r} \right) \exp[-B_{v'} J'(J' + 1) hc/KT] \tag{8-4}$$

or taking log of each side of the above, we have

$$\log \left(\frac{I^{J'J''}}{S^{J'J''}} \right) = \log \left(\frac{I^{v'v''}}{Q_r} \right) - B_{v'} J'(J' + 1)hc/KT. \tag{8-5}$$

Now, when $\log \frac{I_{J'}}{S_{J'J''}}$ is plotted versus $J'(J' + 1)$, the curve is a straight line with slope equal to $(-B_v/KT)$.

Although the determination of a rotational temperature is the most precise when the rotational lines are completely resolved, it is possible to obtain an average value of the rotational temperature even when lesser resolution is available. If a group of rotational lines in a single branch is not resolved, the transition probabilities and frequencies of the blend can be averaged and treated as a single rotational line. If only the band envelope with some of the gross fine structure is resolved, it may be possible to obtain the approximate temperature by comparing the observed band envelope with envelopes calculated for several temperatures. The method is obviously not very sensitive and the error may be significant.

Determining temperatures by means of rotational intensity distribution is often the most accurate of the spectroscopic methods, the advantage being that relative rotational transition probabilities can be explicitly calculated from theory for most diatomic molecules. There are some disadvantages too. The first one is the requirement of quite high resolutions. The second one is that sometimes, there is non-negligible coupling between the rotational and vibrational modes which introduces appreciable error.

112

VIBRATIONAL TEMPERATURES

Vibrational temperatures may be obtained from the measurements of integrated intensities of two or more vibrational bands by using the intensity relations as applied to vibrational transitions. There are, however, a number of difficulties in these determinations which do not come across in the determination of rotational temperatures. One of the most serious of these is the lack of precise information on the transition probabilities for various vibrational transitions. Further, if the vibrational bands overlap, it may not be possible to measure correctly the total band intensity.

The basic equation for the intensity of a (v',v") emission band is expressed as

$$I_{v'v''} = DN_{v'} E^4_{v'v''} P(v',v'') \tag{8-6}$$

where D = a constant depending upon the geometry of the recording instrument and the units.

$N_{v'}$ = population of the upper vibrational state v'.

$E_{v'v''}$ = energy difference in the transition (v' - v")

$p(v',v'')$ = $| \psi_{v'} R_e(r) \psi_{v''} dr|^2$, relative transition probability whose dependence on rotational angular momentum is often extremely small; $\psi_{v'}$, $\psi_{v''}$ are the wavefunctions of the states v' and v", respectively, and $R_e(r)$ represents the electronic transition moment.

If the system is in thermodynamic equilibrium, the relative molecular population $N_{v'}$ of the upper vibrational level, v', can be expressed as

$$N_{v'} = (N/Q) \exp [-G(v') hc/KT] \tag{8-7}$$

where N is the molecular concentration in the system, Q is the partition function which is constant for a given temperature and electronic state, and $G_{v'}$ is the term value for the upper vibrational level v' and is given by the following expression:

$$G_{v'} = \omega_e(v + 1/2) - \omega_e x_e (v - 1/2)^2 + \omega_e y_e (v + 1/2)^3 \tag{8-8}$$

Here, ω_e, $\omega_e x_e$ and $\omega_e y_e$ are the vibrational constants for the chosen state and are obtainable from the analysis of the spectra.

Substituting for $N_{v'}$ in equation (8-6) we now have:

$$I_{v'v''} = DNQ^{-1} E^4_{v'v''} P(v',v'') \exp [-G(v') hc/KT] \tag{8-9}$$

or $\log \left[I_{v'v''}/E^4_{v'v''} P(v',v'') \right]$ = $G(v')/0.6925T$ + Constant $\tag{8-10}$

In a plot of log $I_{v'v''}/E_{v'v''}^4 \, P(v',v'')$ as a function of $G(v')/0.6925$, the slope of the curve gives the reciprocal of the vibrational temperature $\frac{1}{T}$. If the curve is not a straight line, it is inferred that the vibrational thermodynamical equilibrium is not approached or there is non-negligible self-absorption and the above method is unsatisfactory under such conditions.

It may however be remarked that measurement of temperatures via intensity measurements on rotational and vibrational features must be ruled out for temperatures beyond 5000°K because the molecular species are essentially all dissociated at such elevated temperatures. The molecule CN is perhaps the only exception but its spectrum also disappears at temperatures in the neighborhood of 8000°K.

ELECTRONIC TEMPERATURES

Electronic temperatures of gases are normally determined from the intensity of atomic transitions, though in principle the same approach is applicable to molecular electronic transitions. In general spectroscopic determination of temperatures from the degree of electronic excitation has had rather limited application except in arcs and in a few flames. The method is particularly susceptible to errors caused by abnormal excitation and self absorption. It is also quite difficult to obtain a reliable detector calibration over the wide wavelength range necessary for any reliable results.

KINETIC OR TRAN .ATIONAL TEMPERATURES

A direct measure of kinetic temperature of a gas can be obtained spectroscopically utilizing Doppler effect in the frequency of the emitted radiation. If the line broadening arises solely from the thermal motion of the emitting atom, the intensity distribution within the line is given by

$$I(\nu) \; d\nu \; = \; I_0 \; \exp \left\{ -(Mc^2/2RT) \left[(\nu_0 - \nu)^2/\nu_0^2 \right] \right\} \tag{8-11}$$

where M, R and T are molecular weight, universal gas constant and absolute temperature, respectively, and the intensity $I(\nu) \; d\nu$ emitted in the interval $d\nu$ is assumed to be proportional to the number of atoms dN having values of v_x in the appropriate range. Accordingly, the half width $\Delta\lambda$ of the line can be expressed as

$$\Delta\nu \; = \; \frac{2\bar{\nu}_0}{c} \left(\frac{2RT \ln 2}{M} \right)^{1/2} = \; 7.16 \times 10^{-7} \; \bar{\nu}_0 \left(\frac{T}{M} \right)^{1/2} \tag{8-12}$$

where T is the temperature in degrees Kelvin. It may be remarked here that this method of temperature determination is not very precise even when interferometric methods are employed. Its use, therefore, is very limited.

114

In plasmas, there is however another temperature called ion temperature. The electron and ion temperatures are not generally the same. The only established technique for measuring the ion temperature is the Doppler broadening of a spectral line. However, the Doppler broadening is often small compared to the stark broadening, and some independent check must be made to determine which broadening mechanism is predominant before reliable measurement may be obtained.

The rotational temperature obtained from molecular band spectra may also be used as a measure of ion temperatures, but the technique is limited by molecular dissociation to temperatures below about 10^4°K.

Page Intentionally Left Blank

SECTION III

SALIENT SPECTROSCOPIC FEATURES
AND
DATA ON PLANETARY MOLECULES

Page Intentionally Left Blank

SALIENT FEATURES OF THE SPECTRA

AND

SPECTROSCOPIC CONSTANTS OF PLANETARY MOLECULES

Spectroscopic investigations have so far confirmed the presence of twelve gaseous molecules in the planetary atmosphere: six polyatomics, viz., Methane (CH_4), Carbon dioxide (CO_2), Ammonia (NH_3), Water vapor (H_2O), Ozone (O_3), Nitrous oxide (N_2O); and six diatomics, viz., Hydrogen (H_2), Nitrogen (N_2), Oxygen (O_2), Carbon monoxide (CO), Hydrogen chloride (HCl), Hydrogen fluoride (HF). The presence of numerous other molecular constituents, such as C_2H_2, C_2H_4, C_2H_6, C_2N_2, CH_3NH_2, SO_2, HCN, CH_3Cl, CH_3F, CH_2O, COS, - - - etc., has been either postulated or is subject to further confirmation.

Salient features of the observed spectra and important spectroscopic constants for the above mentioned well-established 12 molecules are presented in this chapter. Polyatomics are discussed first, since as a class they are known to have an overall higher abundance in the complex of planetary atmospheres. All the molecules, in their own groups, are also arranged in the order of their relative planetary abundance. Spectroscopic constants of frequent use in aeronomical studies, such as dipole moment, ionization potential, dissociation energy, ground state electron configuration, fundamental vibration frequencies, and rotational constants in respect to each molecule are presented in the beginning of each molecular discussion for ready reference. This is followed by a brief account of the observed spectral features of the individual molecule. The diatomics N_2, O_2 and CO are discussed only very briefly since there already exist reasonably extensive reviews covering these molecules individually. An adequate bibliography is provided in each case.

POLYATOMICS

Methane (CH_4)

Dipole Moment, M: Zero, (.02 Debye in the ν_3 vibrational state)

Ionization Potential, I.P.: 12.99 eV

Dissociation Energy, $D(CH_3-H)$: 4.40 eV

Ground Electronic State Configuration: $(1a_1)^2 (2a_1)^2 (1f_2)^6 - {}^1A_1$

Fundamental Vibration Frequencies:

	ν_1	ν_2	ν_3	ν_4
	2916.7	1533.6	3018.9	1306.2

Rotational Constants:

B_0	$r_e(H-H)$	$r_e(C-H)$
5.2412 cm^{-1}	1.81Å	1.11Å

Methane is perhaps the simplest and the most abundant stable aliphatic hydrocarbon in nature. It is a colorless, odorless gas often resulting from the decomposition of organic matter under water in marshes and stagnant pools. It burns with a faintly luminous flame; forms an explosive mixture with air; and can be liquefied at -164°C and solidified at -186°C. It happens to be a major constituent of natural gas too.

Methane molecule (CH_4) is a non-polar tetrahedral type spherical top five-atomic molecule characterized by the T_d point group symmetry. The four hydrogen atoms are known to occupy the corners of a regular tetrahedron at whose center lies the carbon atom. The bond lengths r_e(C-H) and r_e(H-H) are 1.11Å and 1.81Å, respectively (Figure 9-1).
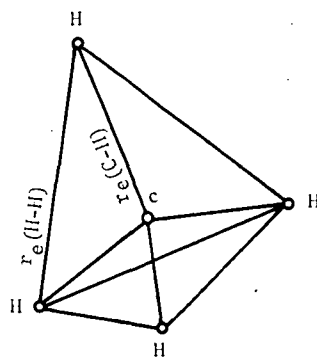

Figure (9-1). Geometrical configuration of methane molecule.

Molecular Spectrum

The observed spectra of methane can be well classified into three broad categories: (1) Electronic Spectrum, (2) Vibration-Rotation Spectrum, and (3) Rotational Spectrum.

Electronic Spectrum. - Methane exhibits a fairly widespread electronic spectrum that has an onset around 1600Å and extends through 20Å in the extreme vacuum ultraviolet. The early spectrographic work on the ultraviolet absorption of methane is due to Leifson (1926); Rose (1933); Duncan and Howe (1934), etc. Photoelectric measurements on the absorption cross sections were made later by different workers in different frequency segments, notably, Wilkinson and Johnston, 1950; Moe and Duncan, 1952; Watanabe, et al., 1953; Ditchburn, 1955; Sun and Weissler, 1955; Wainfan et al., 1955; Schoen, 1962; Thompson et al., 1963; Metzger and Cook, 1964; Rustgi, 1964; Lukirskii et al., 1964; Laufer and McNesby, 1965.

120

The observed spectra can be put in two broad spectral subdivisions:

(1) 1650-1000Å

For the most part the optical absorption in this region of the spectrum is characterized by almost a continuous band with superimposed banded structure appearing in certain narrow regions. According to Watanabe et al., (1953) there definitely exist at least two flat maximum ($\lambda_{max} \sim$ 1260Å and 1190Å) and a possible third maximum with λ_{max} around 1075Å. The continuum with $\lambda_{max} \sim$ 1260Å is only a broad one with apparently no superimposed banded structure. Mulliken attributes this absorption to the electronic transition $^1A_1 \rightarrow {}^1T_2$ (P) $\rightarrow$ 3S. The 1190Å continuum is found to have several superimposed weak and diffuse bands with approximate wavelengths as 1178; 1190; 1201; 1207; 1218; 1230 (Å). No proper analysis seems to have been proposed so far for these bands. Regarding the third reported continuum with probable $\lambda_{max} \sim$ 1075Å there exists no verification yet. In the region 1642-1606Å, Watanabe et al., 1953, reported about 11 bands, which are again weak and diffuse. The wavenumbers for these bands are reported as 62260; 62970; 63530; 64180; 64810; 65360; 66010; 66620; 67200; 67800; 68400 (cm^{-1}). The frequency interval of these bands is about 600 cm^{-1}, and their intensity decreases as the region of continuous absorption is approached. Watanabe's results are presented in Figure (9-2).

(2) 1000-20Å

Absorption by CH_4 molecules in this region is almost a smooth continuum with $\lambda_{max} \sim$ 9300Å. Absorption cross sections in these spectral limits have been studied by different workers in different wavelength segments:

Ditchburn (1955)	[1500 - 400Å]
Sun and Weissler (1955)	[1300 - 400Å]
Wainfan et al. (1955)	[960 - 470Å]
Schoen (1962)	[1000 - 600Å]
Metzger and Cook (1964)	[1000 - 600Å]
Rustgi (1964)	[1000 - 170Å]
Lukirskii et al. (1964)	[250 - 20Å]

An overall picture of the absorption cross section profile in the region (1000-200Å) is presented in Figure (9-3) which is according to Rustgi (1964), whose results agree fairly well with those of others. Rustgi's data for the region (500-170Å) and the data of Lukirskii et al. for the region (200-20Å) - all data unconfirmed - is all that is available to date.
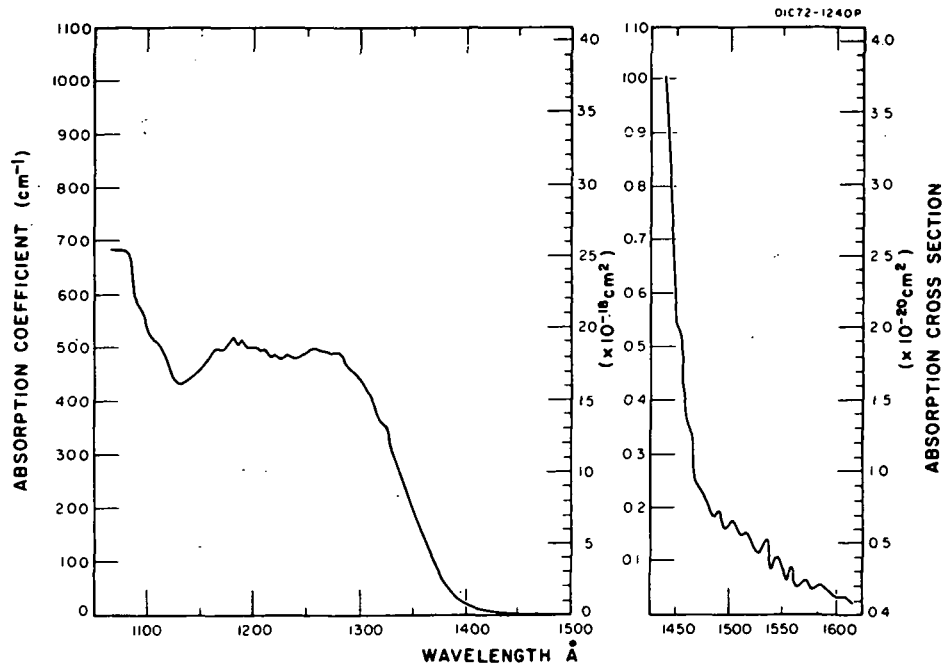
121

Figure (9-2).   Absorption cross section profiles of methane (1600-1050Å).
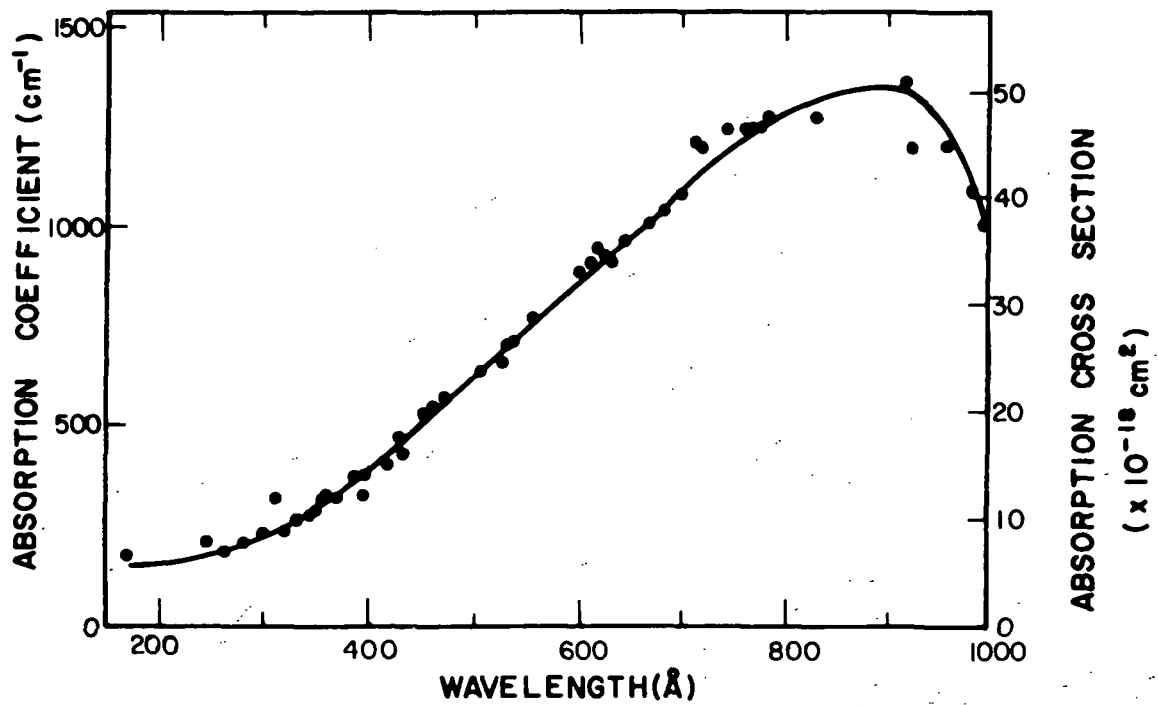[Watanabe (1953)]

Figure (9-3).   Absorption cross section profile of methane for the wavelength
region 1000-170Å. [Rustgi (1964)]

<u>Vibration-Rotation Spectrum.</u> - Being a spherical top, the molecule of methane possesses a high degree of molecular symmetry, which in turn creates a high degeneracy in its vibration frequencies. Out of the $(3 \times 5 - 6) = 9$ possible fundamentals, one is two-fold degenerate and two are three-fold degenerate and consequently the molecule is effectively left with only four fundamental frequencies, viz., $\nu_1 = 2916.7$ cm^{-1}; $\nu_2 = 1533.6$; $\nu_3 = 3018.9$ cm^{-1} and $\nu_4 = 1306.2$ cm^{-1}. ν_1 is fully symmetric; ν_2 is two-fold degenerate and the others, ν_3 and ν_4, are each three-fold degenerate. Further, the frequencies ν_1 and ν_2 are infrared inactive; thus, as regards the fundamentals, only ν_3 and ν_4 show up in the absorption spectrum. All of the four frequencies are, however, Raman active. It may, however, be noted that, since $2\nu_2 \simeq \nu_1 \simeq \nu_3$, there exist numerous possibilities for mutual interaction both by Fermi resonance and Coriolis effect.

(1) Overtones and Combination Frequencies

A large number of overtone and combination bands of methane have been identified in the visible and infrared region and, from the viewpoint of planetary spectra, these are quite important. A number of bands in the spectra of giant planets, viz., Jupiter, Saturn, Uranus and Neptune have been positively identified as CH_4 bands. In the laboratory, these have been observed using thick absorbing layers of methane gas (Wildt, 1932; Mecke, 1933; Dunham, 1933; Adel and Slipher, 1939). Data on numerous harmonics and combination bands that have been identified in the laboratory spectra are given in Table (9-I). Quite a few of these bands have also been observed in the solar spectra (see Table 9-II). Photographic records and numerical data on the rotational structures of many of the CH_4 bands that lie in the region 2.8 to 8.9μ are given in the atlas of Migeotte, Neven and Swensson (1958). High resolution studies of many of the vibration-rotation bands of CH_4 have been reported by Boyd, Thompson and Williams (1952); Margolis and Fox (1968); Bregier and Hilice (1970); Henry, Husson, Andin and Valentin (1970); Husson and Dang Nhy (1971), Hunson and Poissique (1971); Botineau (1972). It may, however, be remarked that correct assignments of the higher overtone and combination bands are rather uncertain for several reasons (Herzberg, 1945):

(a) Because of the anharmonicity, the overtones of the triply degenerate infrared vibration split into a number of subbands.

(b) Since $\nu_1 \simeq \nu_2 \simeq \nu_3$, the combinations $(n\nu_1 + m\nu_3)$, $(2k\nu_2 + m\nu_3)$ are close to $(n + m) \nu_3$ and $(k + m) \nu_3$, respectively. They too are split into subbands.

(c) Perturbations between the sublevels of (a) and (b) bring about further deviations from the simple quadratic formula.

(d) Band centers are often very ill-defined because of overlappings.

TABLE 9-I FREQUENCIES OF THE INFRARED-VIBRATION-ROTATION BANDS OF METHANE

$\nu(cm^{-1})$	Assignment	Intensity	$\nu(cm^{-1})$	Assignment	Intensity
1720	$\nu_2 - \nu_3$		8807	$2\nu_1 + \nu_3$	vs
2600	$2\nu_4$		8900	$\nu_1 + 2\nu_3$	s
2823	$\nu_2 + \nu_4$		9047	$3\nu_3$	s
4123	$\nu_2 + 2\nu_4$		10114	$\left\{\begin{array}{l}2\nu_1 + \nu_2 + \nu_3\end{array}\right.$	s
4216.3	$\nu_1 + \nu_4$		10300	$\left\{\begin{array}{l}\nu_1 + \nu_2 + 2\nu_3 \\ \nu_2 + 2\nu_3\end{array}\right.$	s
4313.2	$\nu_3 + \nu_4$				
4546	$\nu_2 + \nu_3$		11270	$\left\{\begin{array}{l}3\nu_1 + \nu_3\end{array}\right.$	s
5585	$\nu_3 + \nu_4$		11620	$2\nu_1 + 2\nu_3$	m
5775	$\nu_1 + \nu_2 + \nu_4$		11885	$\left\{\begin{array}{l}\nu_1 + 3\nu_3 \\ 4\nu_3\end{array}\right.$	w
5861	$\nu_2 + \nu_3 + \nu_4$				
6006	$2\nu_3$		12755	$\left\{\begin{array}{l}3\nu_1 + \nu_3 + \nu_4 \\ 2\nu_1 + \nu_2 + 2\nu_3\end{array}\right.$	vw
7514	$\nu_2 + 2\nu_3$				
8421	$2\nu_1 + 2\nu_4$		13790	$\left\{\begin{array}{l}4\nu_1 + \nu_3 \\ 3\nu_1 + 2\nu_3\end{array}\right.$	m
8604	$2\nu_3 + 2\nu_4$	vs			

REMARKS

s = strong
w = weak
m = medium
vs = very strong
vw = very weak

TABLE 9-II METHANE BANDS IN THE SOLAR SPECTRUM

Band Center		Transition	Molecular Strength of Band under Standard Conditions, cm	
cm^{-1}	μ			
6005	1.67	0000-0020	$3.6.10^{-20}$	(1)
5861	1.71	0000-1101	--	
5775	1.73	0000-0111	--	
4420	2.20	0000-0110	--	
4313	2.32	0000-0011	--	
4216	2.37	0000-1001	--	
4123	2.43	0000-0102	--	
3019	3.31	0000-0010	$1.26.10^{-17}$	(2)
3823	3.55	0000-0101	--	
2660	3.85	0000-0002	$1.04.10^{-17}$	(3)
1306	7.66	0000-0001	$6.9.10^{-13}$	(2)

(1) Goldberg, L.; Mohler, O. C.; and Donovan, R. E. (1952).

(2) Burch, D. E. and Williams, D. (1960).

(3) Thorndike, A. M. (1947).

Clements and Stoicheff (1970) investigated the Q-branch of ν_1 Raman band at 2917 cm^{-1} using a pressure scanned Fabry-Perot interferometer and a 400 mW He - Ne laser. The relative positions and intensities of the Q-branch lines were computed and the calculated band profile was shown to fit fairly well with the observed frequencies.

Rotational Spectrum. - Although CH_4 is a nonpolar molecule, it has been found that the molecule possesses a very small permanent dipole moment in the degenerate vibrational state, ν_3, which is of the order of 0.02 Debye (Mizushima and Venkateswarlu, 1953; Uchara, Sakurai and Shimoda, 1969; Luntz and Brewer, 1971).

Curl and Oka (1973) observed a rotational transition of CH_4 in the ν_3 state caused by the small vibrational induced dipole moment. The rotational transition which corresponds to a frequency 6900 MHz, occurs between two components of the 6_7 levels which are split by vibration-rotation interaction. This is a very weak transition (calculated absorption coefficient being of the order of 6×10^{-15} cm^{-1}) and conventional microwave absorption spectroscopy is unable to cope with it. Curl and Oka (1973) detected this transition in their microwave-infrared double resonance experiment using a 3.39μm He Ne laser cavity.

Curl (1973) also observed the $F_2(2) \leftarrow F_1(2)$ and $F_2(2) \leftarrow F_1(1)$ transitions of the J = 7 level of the ground state of methane using the above technique. For details, original papers by these authors may be referred.

Carbon Dioxide (CO_2)
Dipole Moment, M: Zero
Ionization Potential, I. P.: 13.769 eV
Dissociation Energy, D(CO-O): 5.453 eV
Ground Electronic State Configuration: $(3\sigma_g)^2 (2\sigma_u)^2 (4\sigma_g)^2 (3\sigma_u)^2 (1\pi_u)^4 (1\pi_g)^4 - - - {}^1\Sigma_g^+$

Fundamental Vibration Frequencies:	ν_1	ν_2	ν_3
	1388.2	667.4	2349.2 (cm^{-1})
	1285.5*		

Rotational Constants:	B_o	r_e(C-O)
	0.3902 cm^{-1}	1.162Å

Carbon dioxide is a colorless gas with a pungent odor and acid taste. It may be liquefied at any temperature between its triple point (-70°F) and critical point (87.8°F) by appropriate compression. CO_2 does not support combustion but it plays a very vital role in plant growth through photosynthesis.

---

*Fermi resonance between ν_1 and $2\nu_2$

Carbon dioxide (CO_2) is a symmetrical, linear, triatomic molecule belonging to the $D_{\infty h}$ point group symmetry. The geometrical configuration of the molecule is illustrated in Figure 9-4.
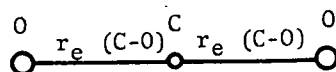

Figure (9-4). Geometrical configuration of the carbon dioxide molecule.

Out of the $(3 \times 3 - 5) = 4$ expected fundamental frequencies, spectroscopically we get only three. The deformation frequency (ν_2) is two-fold degenerate. Further, of the three frequencies, viz., ν_1, ν_2 and ν_3, it is only the latter two which are infrared active. On account of symmetry considerations, the mode ν_1 involves no change in dipole moment and hence under normal conditions, this frequency does not show up in the infrared spectrum. Carbon dioxide is known to exist in the following principal isotopic forms: $C^{12}O_2^{16}$, $C^{13}O_2^{16}$, $C^{12}O^{16}O^{17}$, $C^{12}O^{16}O^{18}$. The species $C^{12}O_2^{16}$ is the most abundant in Earth's atmosphere. The other three isotopic forms, viz., $C^{13}O_2^{16}$, $C^{12}O^{16}O^{17}$, $C^{12}O^{16}O^{18}$ constitute only 1.108, 0.0646 and 0.4078 per cent of the total CO_2 concentration..

Molecular Spectrum

The observed spectra of carbon dioxide can be described in the following two categories: (1) Electronic Spectrum, and (2) Vibration-Rotation Spectrum. On account of symmetry considerations, CO_2 does not normally exhibit any pure rotational spectrum.

Electronic Spectrum. - Carbon dioxide gas is known to possess a widespread absorption spectrum, ranging from about 2000Å in the extreme vacuum ultraviolet. It does not show any significant optical absorption in the visible or near ultraviolet and is therefore almost transparent to these wavelengths. Electronic absorption spectrum of CO_2 has been extensively studied both through spectrographic methods as well as absorption cross section measurements (Lyman, 1908; Leifson, 1926; Henning, 1932; Rathenau, 1932; Price and Simpson, 1938; Preston, 1940; Wilkinson and Johnston, 1950; Inn, Watanabe and Zelikoff, 1953; Sun and Weissler, Samson, Ogawa and Cook, 1959; Tanaka and Ogawa, 1962; Schoen, Judge and Weissler, 1962; Dixon, 1963; Judge, Morse and Weissler, 1964; Nakata, Watanabe and Matsunaga, 1965; Cairns and Samson, 1965 and 1966; Cook, Metzger and Ogawa, 1966; Belozerova, 1967; McCulloh, 1973). For the convenience of discussion, the observed spectra can be divided in the following wavelength segments, according to Herzberg, 1966.

(1) $\tilde{A} \leftarrow \tilde{X}$ (1750-1400Å) Absorption; (3800-3100Å) Emission

These bands are fairly well studied (Price and Simpson, 1939; Inn, Watanabe and Zelikoff, 1953; Dixon, 1963; and Nakata, Watanabe and Matsunaga, 1965). The spectrum consists of a number of weak and diffuse bands overlapping a broad continuum with $\lambda_{max} \sim 1450$Å. The intensities and the spacings between the bands are quite irregular. The upper state A of this electronic transition most probably conforms to the electron configuration $1\pi_u^4\, a_2^2\, b_2\, a_1 - - (^1B_2)$ which represents a bent molecule with an apical angle equal to $122° \pm 2°$ and $r_o \simeq 1.246$Å.

(2) $\tilde{B} - \tilde{X}$ (1390-1220Å)

This part of the spectrum has also been investigated by Price and Simpson (1939); Inn, Watanabe and Zelikoff (1953); Dixon (1963); and Nakata et al. (1965). It consists of numerous fairly sharp bands superimposed upon a continuum with $\lambda_{max} \sim 1332$Å. This continuum is somewhat more intense than the one at 1450Å and the bands are also more intense, less diffuse, and more regularly spaced than the 1450Å band. There exist perhaps two progressions in the frequency 1228 cm^{-1}. The state, B, may be a two-state ensemble represented by the electron configurations:

$$^1B_1\ (\Sigma_g^-) - b_1 a_1^2 a_2^2 b_2^2 a_1$$

$$^1A_1\ (\Delta_g) - b_1^2 a_1 a_2^2 b_2^2 a_1$$

These bands therefore might be the outcome of two different electronic transitions and thus possibly represent band systems with T_o values as 73100 cm^{-1} and 72480 cm^{-1} respectively.

(3) $\tilde{C} - \tilde{X}$ (1170-1130Å)

Besides the early studies of Rathenau (1934), these bands have been quite thoroughly investigated by Tanaka, Jursa and LeBlanc (1960). The bands are grouped together in two progressions - one weak and another strong. The strong progression corresponds to the frequency difference 1270 cm^{-1} and the weaker one to the frequency difference 1165 cm^{-1}. The corresponding T_o values are reported as 85160 cm^{-1} and 85840 cm^{-1} respectively.

(4) $\tilde{D} \leftarrow \tilde{X}$ (1129-1122Å)

(5) $\tilde{E} \leftarrow \tilde{X}$ (1070-1010Å)

(6) $\tilde{F} \leftarrow \tilde{X}$ (1035-969Å)

(7) $\tilde{G} \leftarrow \tilde{X}$ ($\sim$1007Å)

(8) $\tilde{H} \leftarrow \tilde{X}$ ($\sim$994Å)

(9) $\tilde{I} \leftarrow \tilde{X}$ ($\sim$991Å)

Rathenau (1934) and later Tanaka, Jursa and LeBlanc (1960) studied this absorption in detail. It consists of a host of strong bands which have

been classified into a number of Rydberg series leading to the first ionization limit of CO_2. Tanaka et al. grouped these bands in five Rydberg series, viz., (a) two main series (I, II), (b) two minor series (III, IV), (c) one vibration series (V), and (d) three independent transitions.

(a) Main Series I and II; $\widetilde{D} \leftarrow \widetilde{X}$ (1129-1122Å)

Bands of these series are quite strong and degraded to the violet. The formulae representing these bands are as follows (Herzberg, 1966).

$$\nu(I) = 111240 - R/(n-0.65)^2; \; n = 3, 4, 5, - - - 15$$

$$\nu(II) = 111060 - R/(n-0.65)^2; \; n = 3, 4, 5, - - - 15$$

According to Tanaka, et al. (1960) these two series are represented by

$$\nu(I) = 111240 - R/(n + 0.35)^2; \; n = 2, 3, 4 - - -$$

$$\nu(II) = 111060 - R/(n + 0.35)^2; \; n = 2, 3 - - - - - 11$$

The separation of about 180 cm^{-1} in the T_o values of these series is ascribed to the doublet separation of about 160 cm^{-1} in the case of the ground state of CO_2^+ ($^2\Pi_g$).

(b) Minor Series III and IV; $\widetilde{E} \leftarrow \widetilde{X}$ (1070-1010Å)

The bands that fit into these series are not so strong and according to Herzberg (1966), the representative formulae are

$$\nu(III) = 111250 - [R/(n - 0.57)^2]; \; n = 3, 4, - - - 11$$

$$\nu(IV) = 111250 - [R/(n - 0.97)^2]; \; n = 4, 5, - - - 11$$

Tanaka et al (1960) gave the following formulae for these series

$$\nu(III) = 111250 - [R/(n + 0.43)^2]; \; n = 2, 4, 5 - - - 10$$

$$\nu(IV) = 111250 - [R/(n + 0.43)^2]; \; n = 3, - - - - - -10$$

(c) Vibration Series; $\widetilde{F} \leftarrow \widetilde{X}$ (1035-969Å)

There exists another series of bands representable by the following formula

$$\nu(V) = 112510 - [R/(n + 0.30)^2]; \; n = 4, 5, 6 - - -$$

Tanaka et al. (1960) called it a "Vibration Series" as it corresponds to the first ΔG in the ground state of CO_2^+.

(d) Independent Transitions; $\widetilde{G} \leftarrow \widetilde{X}$ ($\sim$1007Å); $\widetilde{H} \leftarrow \widetilde{X}$ ($\sim$994Å); $\widetilde{I} \leftarrow \widetilde{X}$ ($\sim$991Å)

Tanaka et al. (1960) have mentioned three more transitions, $G \leftarrow X$, $H \leftarrow X$, and $I \leftarrow X$, with centers approximately at 1007, 994 and 991Å, respectively. No more details are available on these transitions.

(10) $\tilde{L} \leftarrow \tilde{X}$ (787-712Å)

(11) $\tilde{M} \leftarrow \tilde{X}$ (787-758Å)

(12) $\tilde{S} \leftarrow \tilde{X}$ (752Å)

(13) $\tilde{R} \leftarrow \tilde{X}$ (765Å)

(14) $\tilde{P}_1 \leftarrow \tilde{X}$ (146490 cm^{-1})

(15) $\tilde{P}_2 \leftarrow \tilde{X}$ (147280 cm^{-1})

(16) $\tilde{P}_3 \leftarrow \tilde{X}$ (149500 cm^{-1})

Absorption in this wavelength region has been investigated by Henning, 1932; Tanaka, Jursa and LeBlanc, 1960; Tanaka and Ogawa, 1962; Nakata et al., 1965; and Cook, Metzger and Ogawa, 1966. Two Rydberg series converging to the $^2\Sigma_u^+$ state of CO_2^+ and three Rydberg series converging to the $^2\Sigma_g^+$ state of CO_2^+ have been identified. The five series are classified as series I to V. The formulae representing these are given below (Ogawa et al., 1962).

[R - X]; $\nu(I)$ = $145800 - [R/(n + 0.068 + 3.25/n^3)^2]$; n = 3 - - 18

[S - X]; $\nu(II)$ = $145800 - [R/(n - 0.305)^2]$; n = 3 - - - 18

[P$_1$ - X]; $\nu(III)$ = $156390 - [R/(n - 0.29)^2]$; n = 3 - - - 8

[P$_2$ - X]; $\nu(IV)$ = $156390 - [R/(n + 0.44)^2]$; n = 2 - - - 8

[P$_3$ - X]; $\nu(V)$ = $156390 = [R/(n - 0.05)^2]$; n = 4 - - - 8

The first two series correspond to the second ionization potential of CO_2 and the last three series, most probably, correspond to the third ionization stage. In addition to these five series, Ogawa et al. (1962) identified two more Rydberg series which are represented by the following formulae.

[L - X]; ν = $139726 - [R/(n - .063 - 0069/n)^2]$; n = 3 - - - 10

[M - X]; ν = $139634 - [R/(n - .044 - 0.34/n)^2]$; n = 4 - - - 9

While the first series is composed of six members lying in the region (787-712Å), the second series lies in the region (784-758Å) and only five members of it are known so far. Both of the series converge to the $^2\Pi_u$ state of CO_2^+; L - X to the $^2\Pi_{1/2}$ component, and M - X to the $^2\Pi_{3/2}$ component.

(17) 600-200Å

CO_2 absorption in this region has been investigated by Astoin, Sanson and Bonnelle (1960). Three distinct continua having λ_{max} at about 570, 350 and 280Å have been identified. These have been ascribed to the different dissociative ionization processes. For want of reliable data, nothing specific can be said about the nature of these transitions.

Figure (9-5) presents a schematic showing various electronic states which are involved in the various known transitions. Figure (9-6) presents the energy level diagram of CO_2^+

including the Rydberg levels of CO_2. Absorption cross section measurements on gaseous carbon dioxide as made by Inn et al., 1953; and Nakata et al.; are also presented in Figures (9-7a, b, c), (9-8a, b), (9-9a, b) and (9-10a, b), respectively.
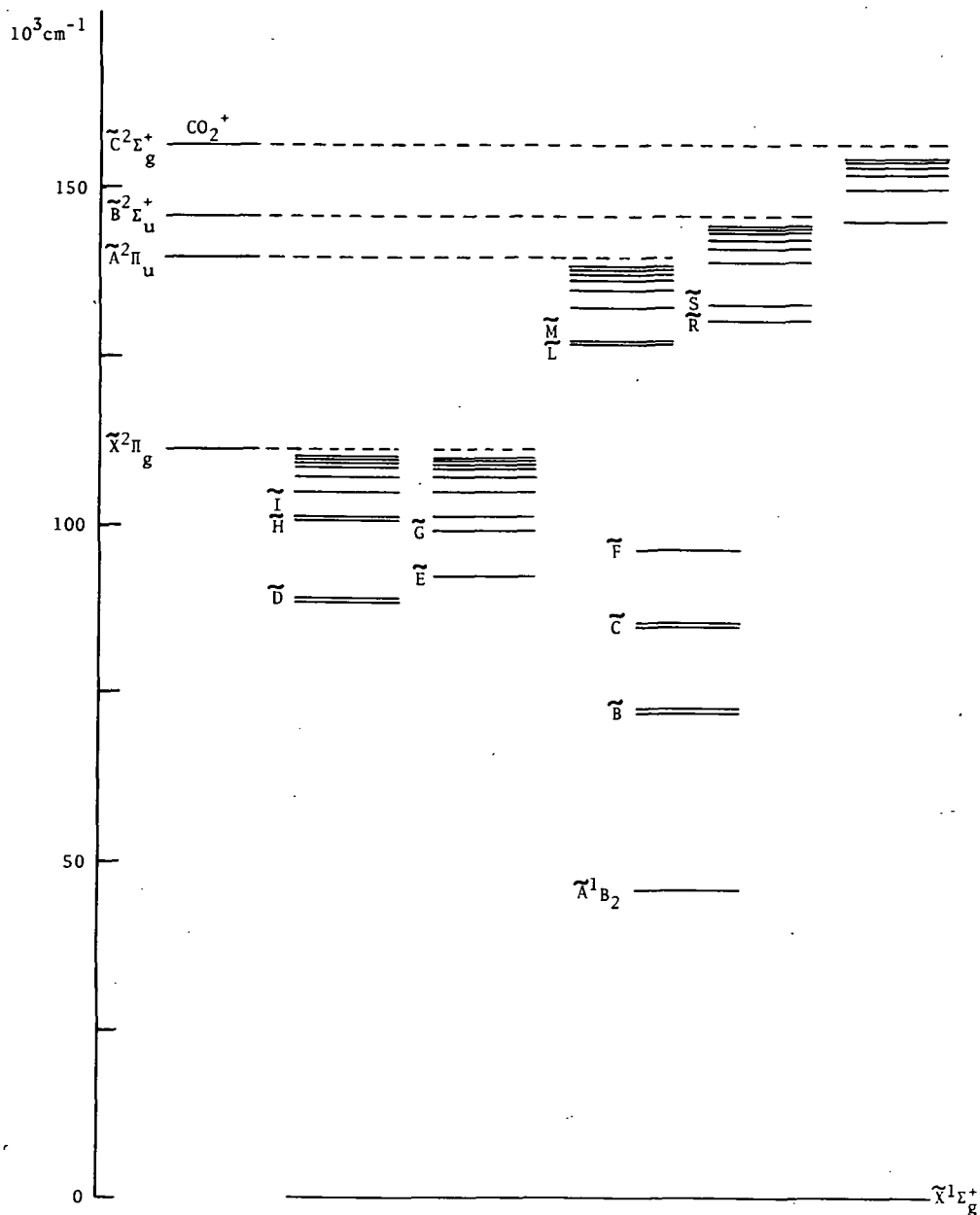
Figure (9-5). Schematic showing relative disposition of the various electronic states of CO_2. [According to Herzberg (1966)]
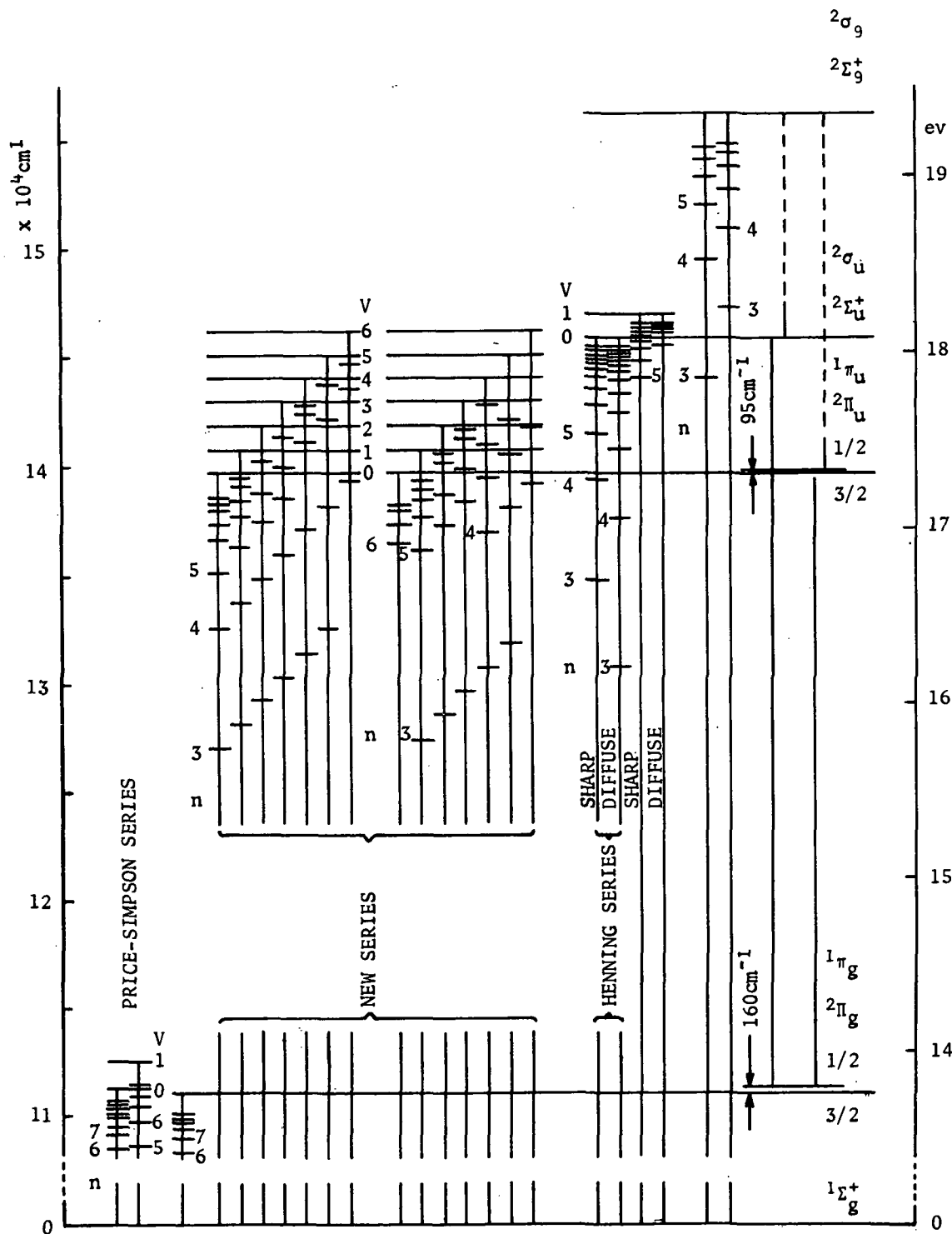
Figure (9-6). Schematic showing energy levels of CO_2^+ along with the Rydberg levels of CO_2. [Tanaka and Ogawa (1962)]
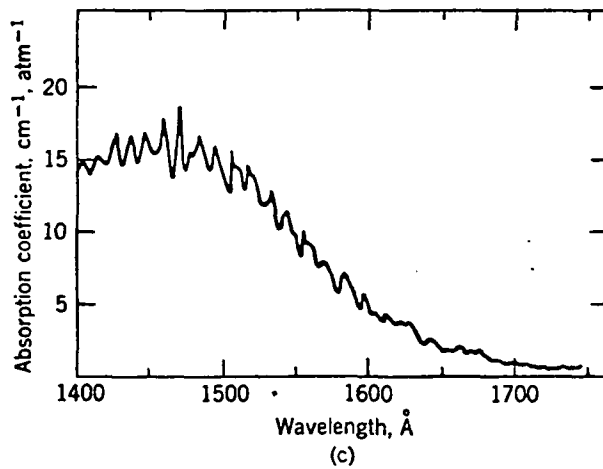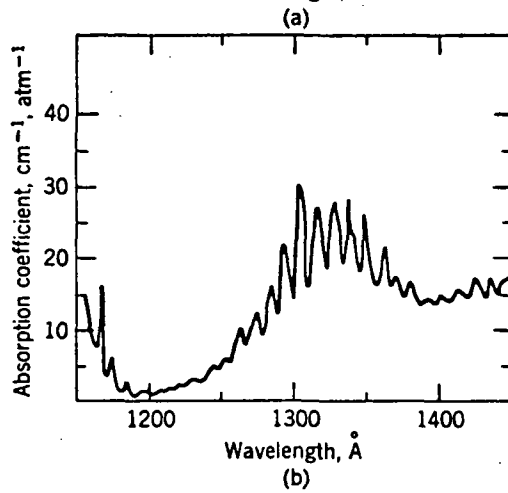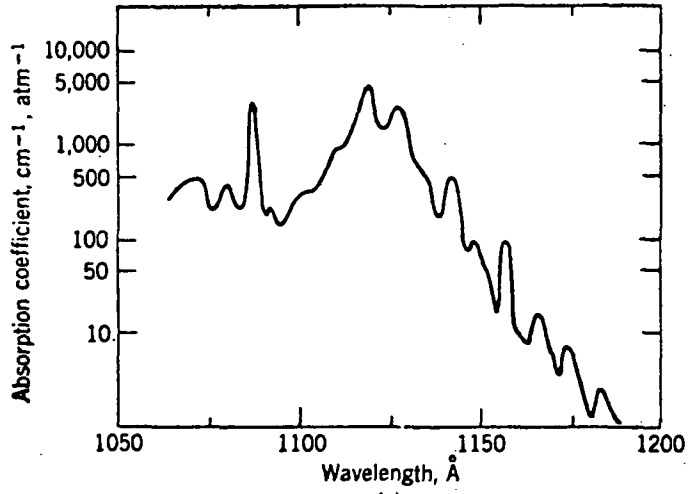
Figure (9-7).   Absorption coefficient profiles of CO_2 for the wavelength region 1750-1050Å.   [Watanabe et al. (1953)]
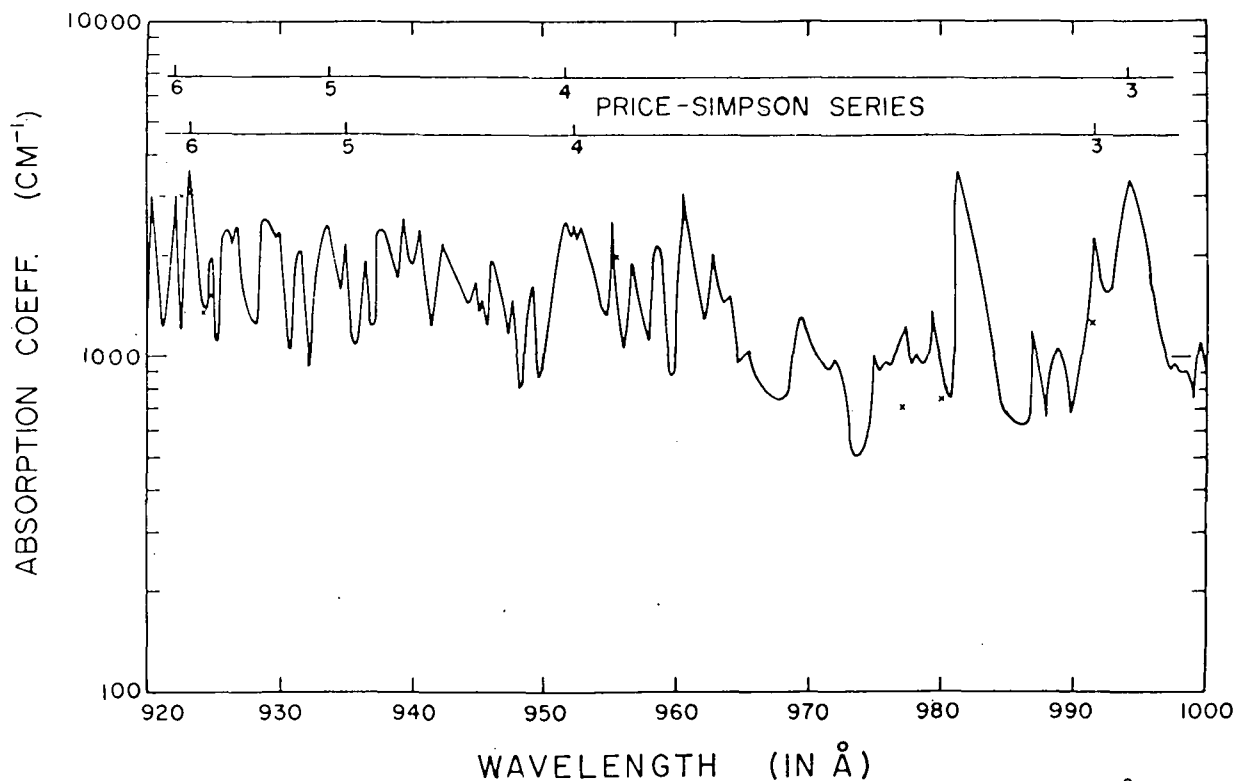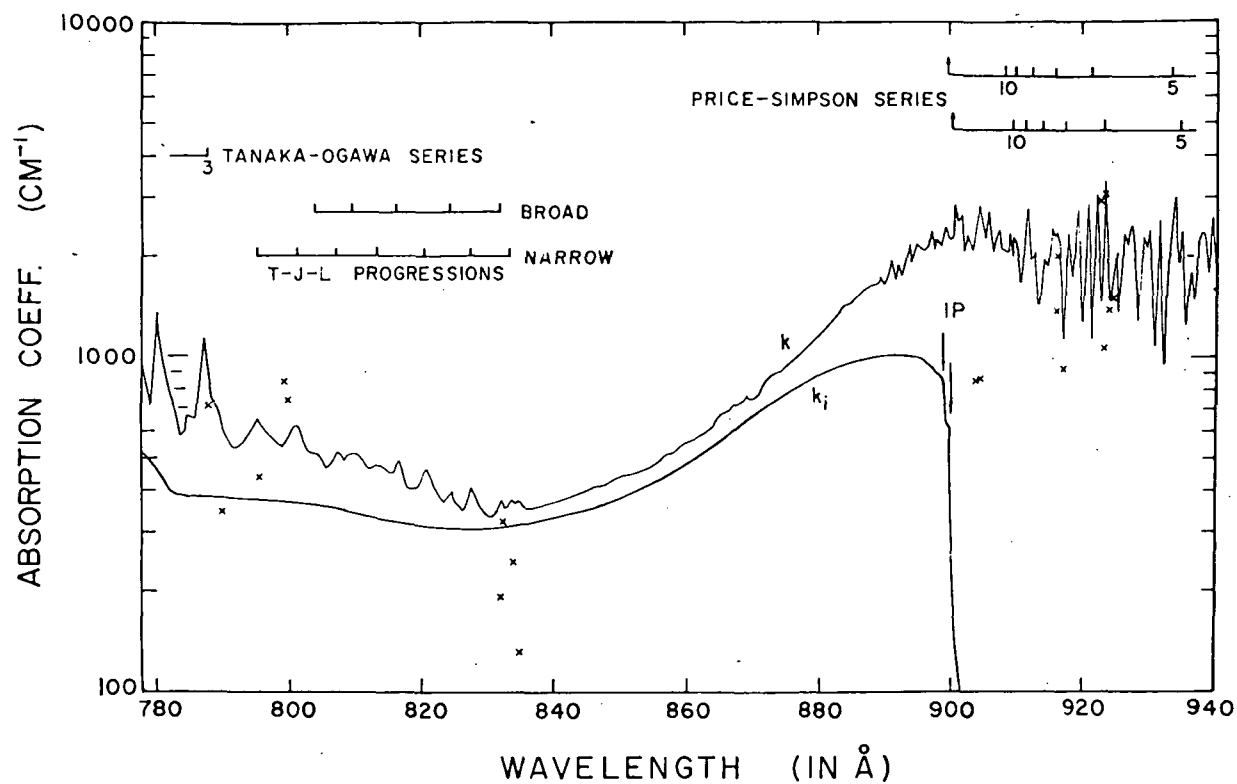
Figure (9-8). Absorption coefficient profiles of CO_2 for the region 940-780Å and 1000-920Å. [Nakata, Watanabe and Matsunaga (1965)]
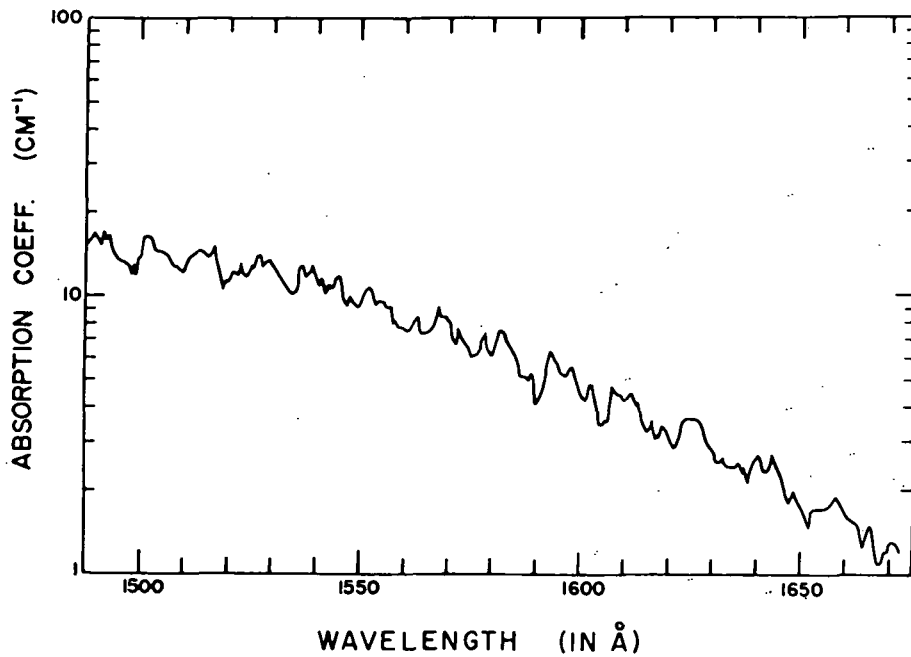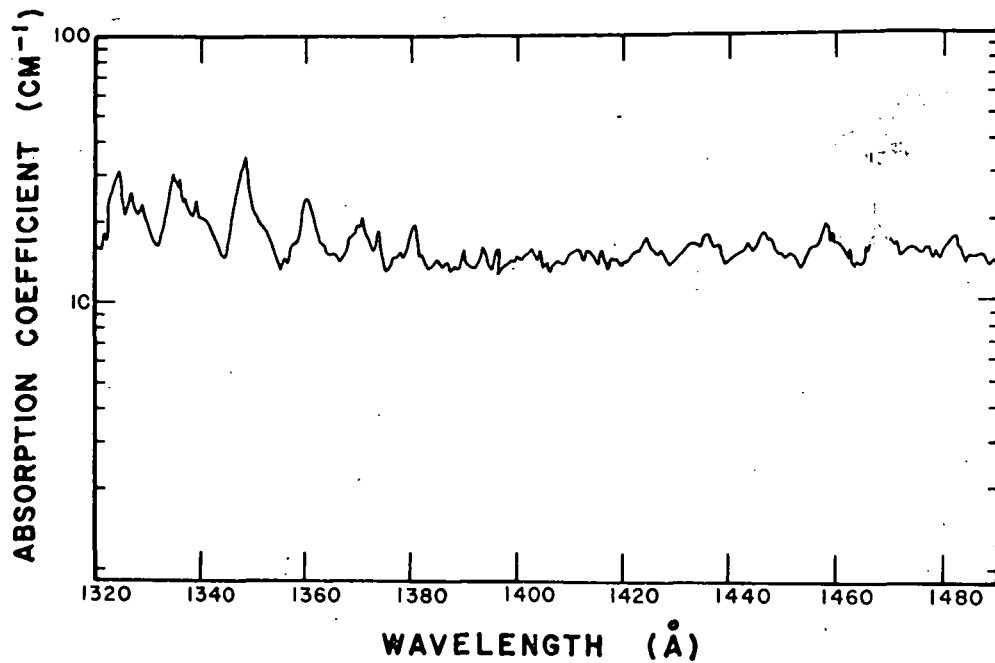
Figure (9-9). Absorption coefficient profiles of CO_2 for the wavelength regions 1490-1320Å and 1670-1490Å.
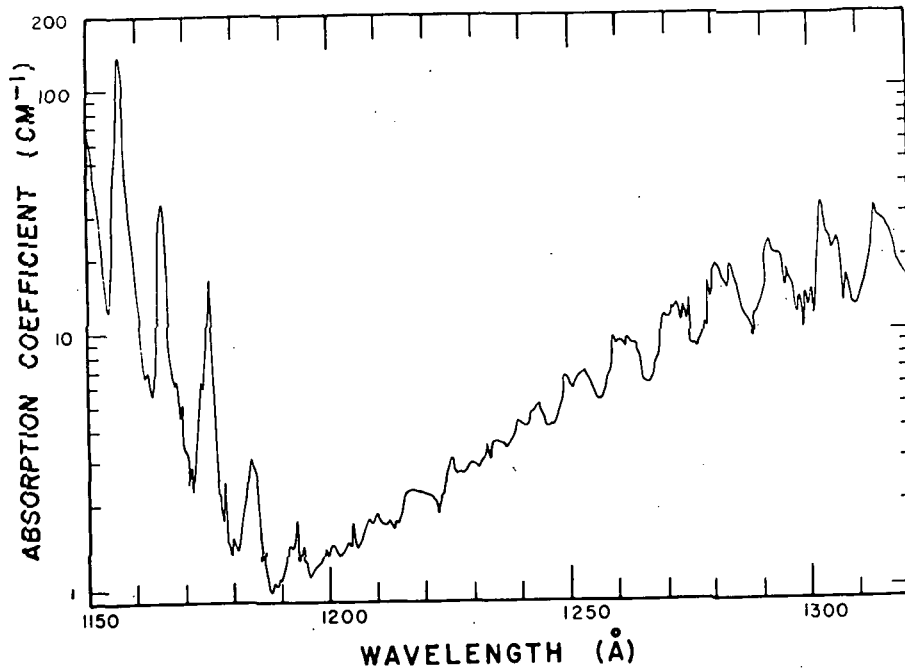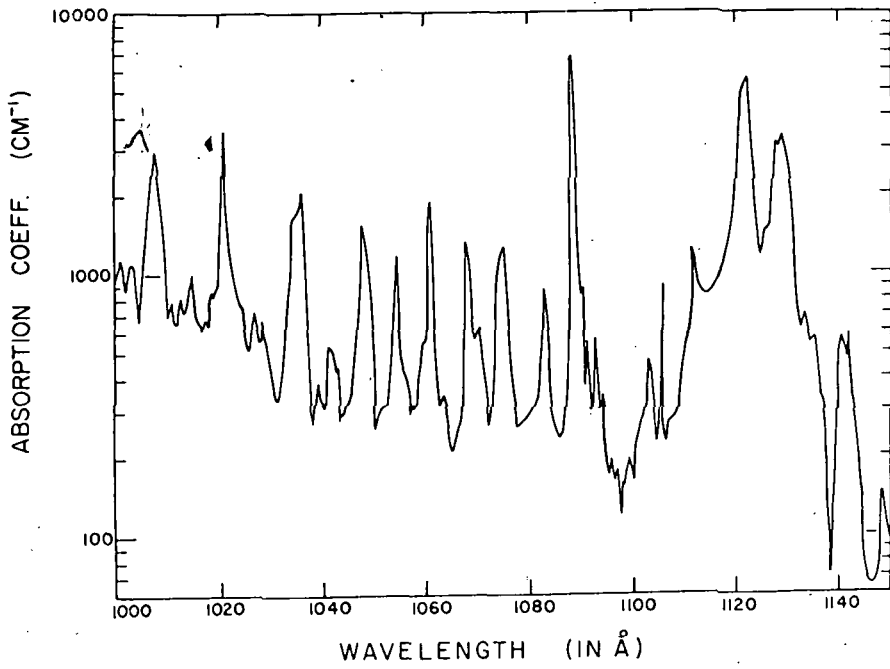
Figure (9-10). Absorption coefficient profiles of CO_2 for the wavelength regions 1150-1000Å and 1320-1150Å.

135

<u>Vibration-Rotation Spectrum.</u> - The vibration-rotation spectrum of carbon dioxide has been the subject of numerous investigations since the beginning of infrared spectroscopy. The early work up to 1945 is reviewed by Herzberg (1945). Important references that cover the later work on the subject are: Kaplan, 1947; Kaplan, 1950; Jones and Bell, 1950; Benedict and Silverman, 1952; Goldberg, 1954; Mohler, 1955; France and Dickey, 1955; Rossman, Rao and Nielson, 1956; Migeotte et al., 1956; France, Rao and Nielson, 1956; Kaplan and Eggers, 1956; Madden, 1957; Courtoy, 1957; Kostkowsky and Kaplan, 1957; Yamamoto and Sasamori, 1958; Burch et al., 1960; Edwards, 1960; Madden, 1961; Plyler, Tidwell and Benedict, 1962; Maki, Plyler and Thibault, 1963; Gordon and McCubbin, 1965 and 1966; Burch, Gryvnak and Patty, 1968; Yamamoto, Tanaka and Aoki, 1969; Gordon and McCubbin, 1971; Korb, Stafwik, Hunt and Plyler, 1971; Val, 1971; Burch and Gryvnak, 1971; McCubbin et al., 1974, besides many others.

Of the three fundamentals (ν_1, ν_2, ν_3) for the CO_2 molecule, only the latter two, i.e., ν_2 and ν_3, are infrared active. The infrared spectrum of carbon dioxide is thus composed of two main strong bands. The band corresponding to ν_2 (667 cm^{-1}) is located around 15μ and the other that corresponds to ν_3 (2349 cm^{-1}) lies at 4.3μ ($C^{12}O_2^{16}$). The 15μ band shows a strong Q-branch while the band at 4.3μ does not.

The fundamental frequency ν_1 is Raman active and shows up strongly in the vibrational Raman spectrum. However, when we examine the Raman spectrum of CO_2 for the ν_1 Raman displacements 1285.8 cm^{-1} and 1388.4 cm^{-1}. The mean of these frequencies ($\sim$1337 cm^{-1}) is almost equal to $2\nu_2$. This doubling was first explained by Fermi (1931) as due to resonance phenomenon occurring between ν_1 and $2\nu_2$. This results in a mutual sharing of the wave functions of the two states and hence in the appearance of two bands instead of one. The resonance interaction between vibrational levels corresponding to different fundamentals in polyatomics is known as Fermi Resonance, which also manifests as displacement of many combinational bands in CO_2 from their normal positions.

(1) The 15μ Band

   The ν_2 fundamental is located at 15μ. It is accompanied by about 15 over-
   tone and combinational bands occupying a wide spectral range from 12 to 20μ
   approximately. The total intensity of these additional bands has been
   estimated at about 10% of the intensity of the fundamental. This whole set
   of bands around 15μ is frequently called the CO_2 - 15μ band. In the
   vicinity of the central part of this band (13.5 - 16.5μ), atmospheric CO_2
   absorbs the entire solar radiation of these wavelengths and that is why
   the 15μ CO_2 band is of significant importance in atmospheric physics.
   These bands are listed in Table (9-III).

(2) The 4.3μ Band

   The ν_3 fundamental centers around 4.3μ. It is almost overlapped by two
   other bands, viz., the ν_3 fundamental of $C^{13}O_2^{16}$ (2483.48 cm^{-1}) and the

TABLE 9-III CO_2 BANDS IN THE 15μ REGION

Isotope	Transition	Band Center cm^{-1}	μ	E" cm^{-1}	Molecular Strength of Band at cm
$C^{12}O^{16}O^{16}$	00^00-01^10	667.40	15.0	0.0	$7.89.10^{-18}$
$C^{13}O^{16}O^{16}$	00^00-01^10	648.52	15.4	0.0	$7.9.10^{-20}$
$C^{12}O^{18}O^{16}$	00^00-01^10	662.39	15.1	0.0	$3.7.10^{-20}$
$C^{12}O^{16}O^{16}$	01^10-02^00	618.03	16.2	667.4	$1.75.10^{-19}$
-	01^10-10^00	720.83	13.9	667.4	$2.3.10^{-19}$
-	01^10-02^20	667.76	15.0	667.4	$6.2.10^{-19}$
-	10^00-03^10	647.02	15.5	1285.43	$4.2.10^{-19}$
-	10^00-11^10	791.48	12.6	1285.43	$8.2.10^{-20}$
-	02^20-03^10	597.29	16.7	1335.16	$5.83.10^{-22}$
-	02^20-11^10	741.75	13.5	1335.16	$5.2.10^{-21}$
-	02^20-03^30	668.3	15.0	1335.16	$3.2.10^{-21}$
-	02^00-03^10	544.26	18.4	1388.19	$1.64.10^{-20}$
-	03^30-04^20	581.2	17.2	2003.28	$1.56.10^{-22}$
-	03^30-12^20	756.75	13.2	2003.28	$2.2.10^{-22}$
-	03^10-12^20	828.18	12.1	1932.45	$1.8.10^{-22}$
-	03^10-12^00	740.5	13.5	1932.45	$5.2.10^{-22}$
-	04^40-13^30	769.5	13.0	2674.76	$1.5.10^{-23}$

combinational band $\nu_1 + \nu_3 - 2\nu_2$ of $C^{12}O_2^{16}$ (2429.37 cm^{-1}). All the three bands are parallel and consequently exhibit no Q branch. The cumulative strength of this 4.3μ band is so high that up to 20 km altitudes, the solar radiation in the range 4.2 - 4.4μ is totally absorbed by the vertical layer of the atmosphere.

(3) Weaker Bands

Besides the two strong bands at 15μ and 4.3μ, the infrared absorption of CO_2 shows quite a few relatively weak bands whose centers lie at 104μ, 9.4μ, 5.2μ, 4.8μ, 2.7μ, 2.0μ, 1.6μ, and 1.4μ. A number of still weaker bands also appear in the region (1.24 and .78μ) particularly in long path infrared absorption of CO_2 (Herzberg and Herzberg, 1953). Recently, McCubbin, Pliva, Pulfrey, Telfain and Todd (1974) obtained extensive data on the emission spectrum of $^{12}CO_2^{16}$ from 4.2 to 4.7μ. Electrical excitation of the CO_2 emission spectrum in a CO_2 - N_2 - He mixture made possible the observation of the bands in the $00\nu_3 \rightarrow 00$ ($\nu_3 - 1$) sequence to $\nu_3 = 4$ as well as some other bands. The two parallel bands in the 10μ region (10.4μ and 9.4μ) have frequencies 1063.8 cm^{-1} (020 - 001 transition) and 961.0 cm^{-1} (100 - 001 transition) respectively. Absorption in the regions 1.4, 1.6, 2.0, 2.7, 5.2 and 4.8μ region is due to the bands as detailed in table (9-IV, 9-V, and 9-VI). Herzberg's photographic infrared bands are listed in table (9-VII).

TABLE 9-IV CO_2 ABSORPTION BAND NEAR 2.0, 1.6 AND 1.4μ

Band μ	Isotope	Transition	Band Center cm⁻¹	μ	E" cm⁻¹	Molecular Strength of Band at 259°K, cm
2.0	$C^{12}O_2^{16}$	00^00-04^01	5100	1.96	0	$1.6.10^{-20}$
	$C^{12}O_2^{16}$	00^00-12^01	4978	2.00	0	$3.7.10^{-20}$
	$C^{12}O_2^{16}$	00^00-20^01	4853	2.06	0	$1.0.10^{-20}$
	$C^{12}O_2^{16}$	01^10-05^10	5132	1.94	667.40	-
	$C^{12}O_2^{16}$	00^10-13^11	4965	2.01	667.40	-
	$C^{12}O_2^{16}$	00^10-21^11	4808	2.07	667.40	-
	$C^{13}O_2^{16}$	00^00-04^01	5046	1.98	0	$1.8.10^{-22}$
	$C^{13}O_2^{16}$	00^00-12^01	4887	2.04	0	$4.1.10^{-22}$
	$C^{13}O_2^{16}$	00^00-20^01	4748	2.10	0	$1.1.10^{-22}$
	$C^{12}O16O18$	00^00-04^01	5042	1.98	0	7.10^{-23}
	$C^{12}O16O18$	00^00-12^01	4905	2.03	0	$1.5.10^{-23}$
	$C^{12}O16O18$	00^00-20^01	4791	2.08	0	4.10^{-23}
1.6	$C^{12}O_2^{16}$	00^00-06^01	6503	1.53	0	-
	$C^{12}O_2^{16}$	00^00-14^01	6350	1.57	0	-
	$C^{12}O_2^{16}$	00^00-22^01	6228	1.60	0	$2.9.10^{-22}$
	$C^{12}O_2^{16}$	00^00-20^01	6076	1.64	0	-
1.4	$C^{12}O_2^{16}$	00^00-00^03	6973	1.43	0	$8.6.10^{-22}$

TABLE 9-V CO_2 ABSORPTION BAND NEAR 2.7μ

Band μ	Isotope	Transition	Band Center cm⁻¹	μ	E" cm⁻¹	Molecular Strength of Band at 259°K, cm
2.7	$C^{12}O_2^{16}$	$000-02\ 1$	3613.03	2.76	0	$1.0.10^{-18}$ (1.4×10^{-18})
	-	$000-101$	3714.56	2.69	0	$1.3.10^{-18}$ (2.10^{-18})
	-	01^10-03^10	3580.81	2.79	667.40	-
	-	01^10-11^11	3723.05	2.68	667.40	-
	$C^{13}O_2^{16}$	$000-02^01$	3527.70	2.83	0	$1.1.10^{-20}$
	-	$000-101$	3632.92	2.75	0	$1.4.10^{-20}$
	-	01^10-03^11	3498.72	2.85	667.40	-

TABLE 9-VI 5.2 AND 4.8μ ABSORPTION BANDS OF CO_2

Band μ	Isotope	Transition	Band Center cm^{-1}	μ	E" cm^{-1}	Molecular Strength of Band at 259°K, cm
5.2	$C^{12}O_2^{16}$	$000-03^10$	1932.45	5.17	0	$2.4.10^{-21}$
4.8	$C^{13}O_2^{16}$	$000-11^10$	2037.08	4.90	0	$4.0.10^{-22}$
	$C^{12}O_2^{16}$	$000-11^10$	2076.86	4.81	0	$3.2.10^{-20}$
	$C^{12}O_2^{16}$	01^10-12^20	2093.35	4.77	667.40	$2.0.10^{-21}$
	$C^{12}O_2^{16}$	01^10-200	2129.79	4.69	667.40	$8.0.10^{-22}$

TABLE 9-VII PHOTOGRAPHIC INFRARED BANDS OF CO_2

λ	cm^{-1}	Intensity	Band Heads Assignments
12334.2	8105.3	2	$2\nu_2 + 3\nu_3$
12262.5	8152.7	8	$3\nu_2 + 3\nu_3 - \nu_2$
12177.3	8209.7	100	$2\nu_2 + 3\nu_3$
12054.9	8293.0	8	$\nu_1 + \nu_2 + 3\nu_1 - \nu_2$
12030.4	8309.9	100	$\nu_1 + 3\nu_2$
10626.7	9407.6	4	$4\nu_2 + 3\nu_3$
10487.6	9532.3	20	$\nu_1 + 2\nu_2 + 3\nu_3$
10361.7	9648.2	8	$2\nu_1 + 3\nu_3$
8688.7	11505.9	1	$5\nu_3$
8735.9	11443.8	0.05	$\nu_2 + 5\nu_3 - \nu_1$
7882.8	12682.3	.1	$2\nu_2 + 5\nu_3$
7820.1	12784.0	.3	$\nu_1 + 5\nu_3$
7158.2	13966	.02	$\nu_1 + 2\nu_2 \quad 5\nu_3$

Ammonia (NH_3)

Dipole Moment, M: 1.44 Debye

Ionization Potential, I.P.: 10.166 eV

Dissociation Energy, $D(NH_2-H)$: 4.3 eV

Ground Electronic State Configuration: $(1a_1)^2(2a_1)^2(1e)^4(3a_1)^2 - {}^1A_1$

Fundamental Vibration Frequencies:*

	ν_1	ν_2	ν_3	ν_4	
	3337.2	968.3	3443.9	1627.4	(cm^{-1})
	3336.2	932.5	3443.6	1626.1	

Rotational Constants:

B_0	$C_0 (=A_0)$	$r_0(N-H)$	$r_0(H-H)$	$\alpha(HNH)$
9.9443 cm^{-1}	6.196 cm^{-1}	1.0173Å	1.631Å	107.8°

Ammonia is a colorless gas at ordinary pressures. It is lighter than air and possesses a pungent odor. It is fairly stable at ordinary temperatures and decomposes into nitrogen and hydrogen at 450°C under atmospheric pressure. On compressing and cooling, it condenses to a liquid about 60% as heavy as water.

The molecule of ammonia (NH_3) is a symmetric top type tetratomic molecule. It is characterized by the symmetry group C_{3v} in its ground electronic state but in excited states, the symmetry configuration of the molecule changes and conforms to the point group D_{3h}.

The geometric configuration of the ammonia molecule is pyramidal, in which the nitrogen atom lies at the apex and each of the three remaining corners of the pyramid is occupied by an atom of hydrogen. It is illustrated in the figure (9-11) given below.
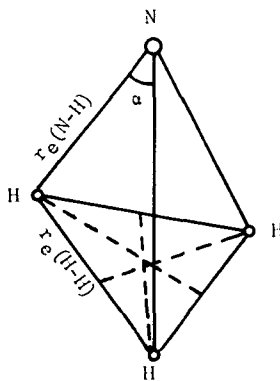

Figure (9-11). Geometrical configuration of the ammonia molecule.

---

*Double values correspond to the inversion components.

The apical angle α is known to be about 107° and the bond lengths N-H and H-H as nearly 1Å and 1.6Å, respectively. The vertical height of the pyramid is about 0.38Å. Ammonia occurs mainly in two isotopic forms, NH_3 and ND_3.

Molecular Spectrum

The observed spectra of gaseous ammonia can be described under the following three categories: (1) Electronic Spectrum, (2) Vibration-rotation Spectrum, and (3) Microwave Spectrum.

<u>Electronic Spectrum</u>. - Ammonia is almost transparent to the visible and near ultra-violet radiation. The characteristic optical absorption has been observed with an onset around 2400Å down through 370Å in the vacuum ultraviolet. The spectral region (2400-1000Å) is full of band structure and the region below 1000Å, i.e., 1000-370Å is occupied by almost a continuum. All these features have been extensively studied by many workers in the past. (Leifson, 1926; Dixon, 1933; Duncan, 1935; Duncan, 1936; Duncan and Harrison, 1936; Thompson and Duncan, 1953; Watanabe, Zelikoff and Inn, 1953; Tennenbaum, Coffin and Harrison, 1953; Thompson and Duncan, 1946 and 1953; Watanabe, 1954; Sun and Weissler, 1955; Walker and Weissler, 1955; Sun and Weissler, 1955; Watanabe and Mottl, 1957; Walsh and Warsop, 1961; Douglas and Hollas, 1961; Thompson, Harteck and Reeves, 1963; Metzger and Cook, 1964; Douglas, 1963; Watanabe and Sood, 1965; DeReilhac and Damany, 1970.)

A summary of various known electronic band systems is presented below.

(1) $\widetilde{A}$ - $\widetilde{X}$ Bands (2170-1700Å) [$^1A_2''$ - $^1A_1$]

These bands of ammonia were first observed by Leifson (1926) who obtained a long progression of diffuse bands in the spectral region 2168-1700Å. Dixon (1933) reported a few additional bands of this group up to 2431Å. Later, Duncan (1935) and recently Walsh and Warsop (1961) obtained detailed vibrational analysis of these bands based on high resolution spectra. Corresponding bands for the isotopic molecule ND_3 were studied by Benedict (1935), Duncan (1935), Walsh and Warsop (1961) and Douglas (1963). According to Walsh and Warsop (1961), frequencies of the Q-heads of the main progression of these bands in the case of NH_3 can be represented by the following relation:

$$\nu_{A-X} = 46136 + 874\, v_2' + 4.0\,(v_2')^2$$

The frequency 874 cm^{-1} is interpreted as that of bending vibration ν_2 in the upper state and the progression of the bands arises from excitation of the out-of-plane vibration ν_2. A similar conclusion has been drawn on the basis of the rotational analysis of some of the bands in the corresponding system of ND_3 (Benedict, 1935; Douglas, 1963). In the case of NH_3, the bands are too

diffuse to show any measurable rotational structure. Table (9-VIII) provides band data on this system (Walsh and Warsop, 1961).

(2) $\widetilde{B}$ - $\widetilde{X}$ Bands (1690-1400Å) [$^1E''$ - $^1A_1$]

This is a weak system, consisting of a long progression of fairly sharp bands occupying the spectral region 1690-1400Å. Besides the early work on this part of the spectrum by Duncan (1935) and Duncan and Harrison (1936), lately, Walsh and Warsop (1961), Douglas and Hollas (1961) and Douglas (1963) investigated this system under high resolution conditions. According to Douglas, who obtained a complete rotational analysis of a number of these bands, these are the perpendicular bands and the upper electronic state in the transition is a $^1E''$ state of the planar molecule NH_3. The band origins in this progression can be represented by the following relation:

$$\nu_{B-X} = 59225.5 + 880.60 \, v_2' + 18.437 \, (v_2')^2 - .71863 \, (v_2')^3$$

Vibrational analysis of these bands further shows that the vibronic levels of the upper state are degenerate and this degeneracy, most probably, is electronic as is supported by the observation of a Zeeman effect with a g-value of 0.6. Table (9-IX) provides data on these bands.

(3) $\widetilde{C}$ - $\widetilde{X}$ Bands (1570-1480Å) [$^1A_1'$ - $^1A_1$]

This is a progression of relatively weak bands which lie in almost the same spectral region as the stronger bands belonging to the system $\widetilde{B}$ - $\widetilde{X}$. Some of these bands, particularly on the long wavelength end, are almost coincident with the $\widetilde{B}$ - $\widetilde{X}$ bands. These bands exhibit a fairly well-resolved rotational structure and the rotational analysis of quite a few of them has shown that they are parallel bands. It may be pointed out that though the line width in these bands is considerably greater than that of the $\widetilde{B}$ - $\widetilde{X}$ bands, the analysis has been quite satisfactory. The corresponding bands in the case of ND_3 have been reported by Douglas (1963). The assignment of the state, C as $^1A'$, having an electron configuration $(1e')^4 \, (1a_2'') \, (3pa_2'')$ as discussed by Douglas (1963) is however not certain. It is possible that these bands represent a forbidden component of the $\widetilde{B}$ - $\widetilde{X}$ system made possible by vibronic interaction.

(4) $\widetilde{D}$ - $\widetilde{X}$, $\widetilde{E}$ - $\widetilde{X}$, $\widetilde{F}$ - $\widetilde{X}$ Bands (1435-1220Å)

It was Duncan (1935) who first observed strong characteristic bands of NH_3 in the region (1433-1248Å). Later, Walsh and Warsop (1961) studied these bands extensively and grouped the observed bands into three distinct, though partially overlapping, progressions in the region 1450-1220Å. The three

142

TABLE (9-VIII) · FREQUENCIES OF THE BANDS IN THE 2168Å ELECTRONIC TRANSITION

Walsh and Warsop (1961)

v	Duncan heads cm^{-1}	Duncan band centre cm^{-1}	Walsh and Warsop heads cm^{-1}	Walsh and Warsop band centre cm^{-1}	Calc. Frequencies cm^{-1}
0	46,126 46,202	46,164*	46,130 46,231	46,181*	46,180
1	47,010 47,069	47,040*	47,002 47,104	47,053*	47,059
2	47,914 47,962	47,939*	47,903 47,988	47,946*	47,946
3	48,803 48,868	48,836*		48,842	48,841
4		49,712		49,735	49,744
5		50,663		50,659	50,655
6		51,555		51,550	51,574
7		52,501		52,504	52,501
8		53,444		53,430	53,436
9		54,411		44,388	54,379
10		55,341		55,324	55,330
11		56,287		56,297	56,289
12		57,272		57,244	57,256
13		58,225		58,170	58,231
14		59,209		59,196	59,214

*mean of heads.

143

TABLE (9-IX)   FREQUENCIES OF THE Q HEADS OF THE BANDS IN THE 1665Å ELECTRONIC TRANSITION

(Walsh and Warsop, 1961)

Observed Frequencies

v	(Duncan) cm^{-1}	(Douglas) cm^{-1}	calc. Frequency cm^{-1}	$\nu_{obs} - \nu_{calc.}$ cm^{-1}
1	60,136	60,066	60,064	2
2	61,069	61,019	61,021	-2
3	62,026	61,991	61,991	0
4	63,024	62,971	62,974	-3
5	64,017	63,972	63,970	2
6	65,025	64,981	64,980	1
7	66,042	66,001	66,001	0
8	67,091	67,045	67,039	6
9	68,140	68,083	68,088	-5
10	69,192	69,145	69,150	-5
11	70,248	70,230	70,226	4
12	71,316			

progressions correspond to three different electronic states $\widetilde{D}$, $\widetilde{E}$ and $\widetilde{F}$, each coupled to the ground state X. These are discussed below.

(a) $\widetilde{D}$ - $\widetilde{X}$ (1435-1270Å) [$^1A_2'' - {}^1A_1$]; or 1440Å Progression

The Q heads for $\widetilde{D}$ - $\widetilde{X}$ bands can be represented by the relation:

$$\nu_{D-X} = 69731 + 901.6 \, (v')^2 + 10.04 \, (v')^2$$

(b) $\widetilde{E}$ - $\widetilde{X}$ (1330-1270Å) [$^1A_2'' - {}^1A_1$]; or 1330Å Progression

At 1330Å there begins a progression of bands which overlaps some of the bands in the 1440Å progression. These bands are quite sharp and their intensity increases as one moves towards shorter wavelengths as distinguished from the R-branches of the 1440Å bands which are diffuse and decrease in intensity towards shorter wavelengths. The observed frequencies of this progression can be expressed by the relation:

$$\nu_{E-X} = 75205 + 917 \, v' + 10.0 \, (v')^2$$

(c) $\tilde{F} - \tilde{X}$ (1290-1220Å); or 1286Å Progression

The bands of this progression overlap the Q branches of some of the bands of the 1440Å progression. The two progressions can be distinguished by their intensities and their slightly different vibrational frequencies. The first observed band is at 1286Å. The bands observed are the strongest bands of the progression, the weaker ones being obscured.

The Q heads of the 0000 ← 0000 bands of the 1286Å, 1434Å and 1330Å progressions can be arranged in a Rydberg series, as follows:

$$\nu = 82150 - \frac{R}{(n - 1.02)^2} , \; n = 3, 4, 5$$

The ionization potential obtained using this formula agrees very well with the photoionization value 10.15 eV. Table (9-X) provides data on these transitions.(Walsh and Warsop, 1961).

(5) G - X Bands (1210-1150Å)

Duncan (1935) observed a progression of bands running from 1207Å to 1164Å, i.e., at wavelengths below 1220Å that correspond to the first ionization potential. Walsh and Warsop (1961) could not identify these bands but Watanabe (1954), Watanabe and Mottl (1957) did find banded structure in the continuum beyond the first ionization potential. Absorption cross sections of gaseous ammonia have been measured by Watanabe (1954) in the region (2200-1050Å). Sun and Weissler (1955) and later Metzger and Cook (1964) measured the absorption coefficients in the region 1300-374Å. Recently, DeReilhac and Damany (1970) made measurements in the region 500-100Å. These results are presented in figures (9-12), (9-13), (9-14) and (9-15). Figure (9-16) presents a schematic showing a few known potential energy curves of ammonia molecule and figure (9-17) depicts the known transitions.

<u>Vibration-Rotation Spectrum.</u> - Vibration-rotation spectra of NH_3 and its various isotopic forms have been the subject of numerous detailed investigations in the past. (Benedict, 1935; McCubbin, 1952; Hansler and Oetjen, 1953; Benedict and Plyler, 1956; Benedict, Plyler and Tidwell, 1958; Guring, Nielsen and Rao, 1959; Benedict, Plyler and Tidwell, 1960; Rao, Brim, Hoffman, Jones and Mellowell, 1961; Jones, Brim and Rao, 1963; Rao, 1964; Walsh, 1969; Shimizu and Shimizu, 1970; McBridge and Nicholls, 1963.)

In addition to the four fundamental frequencies, which are all infrared active, the vibration-rotation spectrum of NH_3 exhibits quite a large number of overtone and combinational bands. The series of bands with frequencies ν_1, $2\nu_1$, $3\nu_1$, $4\nu_1$, $5\nu_1$, and $6\nu_1$ is very prominent. Further, since ν_3 is very close to ν_1, the bands ($\nu_1 + \nu_3$) and $2\nu_3$ overlap $2\nu_1$; $2\nu_1 + \nu_3$, $\nu_1 + 2\nu_3$; $3\nu_3$ overlap $2\nu_1$ and so on. While the overtones ν_1, $2\nu_1$, $2\nu_2$, etc., are parallel in character, the bands overlapping them are usually perpendicular or

TABLE (9-X) WAVENUMBERS OF THE BAND PROGRESSIONS 1440Å, 1330Å, 1286Å AND 1266Å

1440Å Transition

n'	Walsh	Watanabe and Sood	
0	69758	69579	
			878
1	70644	70637	
			925
2	71569	71562	
			954
3	72516	72516	
			970
4	73498	73486	
			1002
5	74497	74488	
			1012
6	75508	75500	
			1040
7	76545	76540	
			1034
8	77590	77574	
			1066
9	78649	78640	
			1073
10		79713	
			1056
11		80769	

1330Å Transition

n'	Walsh	Watanabe and Sood	
0	75212	75216	
			922
1	76133	76138	
			945
2	77064	77083	
			951
3	78045	78034	
			974
4	79031	79008	
			1031
5	80042	80039	
			1025
6	81072	81061	
			1058
7	82098	82122	
			1066
8		83188	
			1051
9		84239	
			1063
10		85302	

1286Å Transition

n'	Duncan	Watanabe and Sood	
0		(77715)	
			930
1		(78645)	
			955
2		(79600)	
			980
3	80618	80580	
			999
4	81597	81579	
			1018
5	82606	82597	
			1036
6	83600	83633	
			1055
7	84749	84688	
			1068
8	85769	85756	
			1065
9	86839	86821	

1266Å Transition

n'	Duncan	Watanabe and Sood	
0	78931	(78940)	
			940
1		(79880)	
			960
2	80832	(80840)	
			980
3	81884	81820	
			996
4	82857	82816	
			1020
5	83843	83836	
			1039
6	84872	84875	
			1050
7	85928	85925	

146

Figure (9-12). Absorption coefficient profiles of NH_3 for the wavelength regions 1000-600Å and 1190-1000Å. [Watanabe and Sood (1965)]
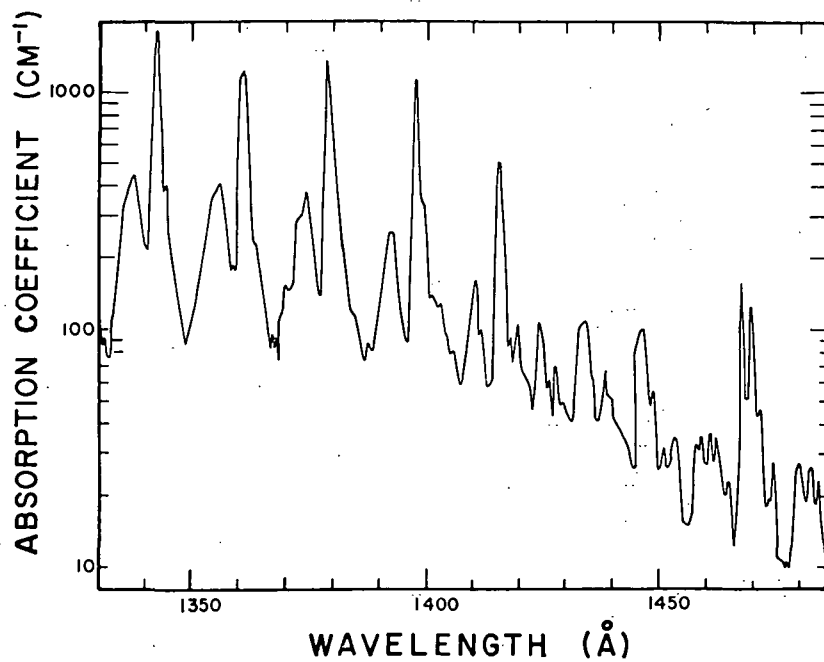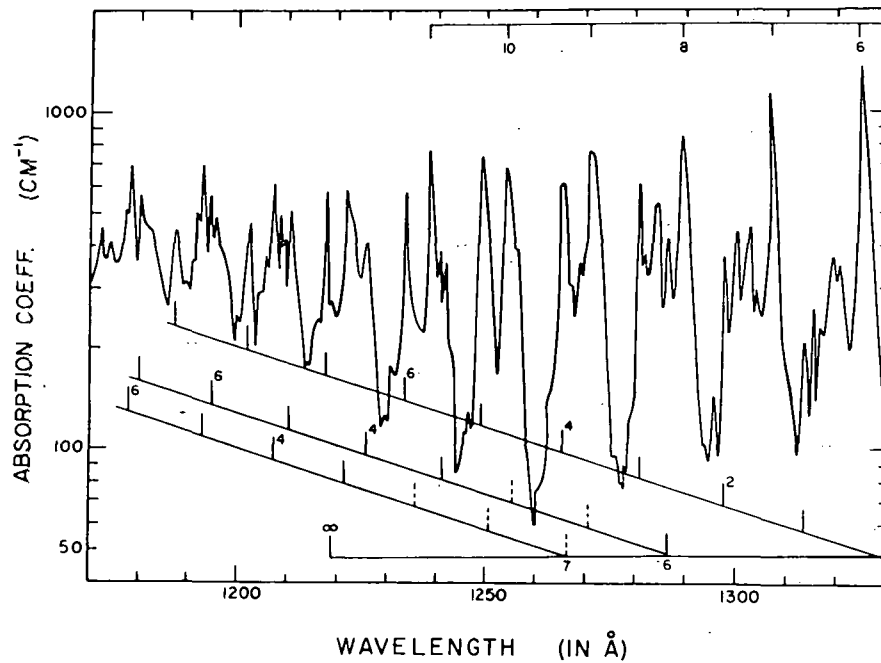
Figure (9-13). Absorption coefficient profiles of NH_3 for the wavelength regions 1330-1170Å and 1490-1330Å.
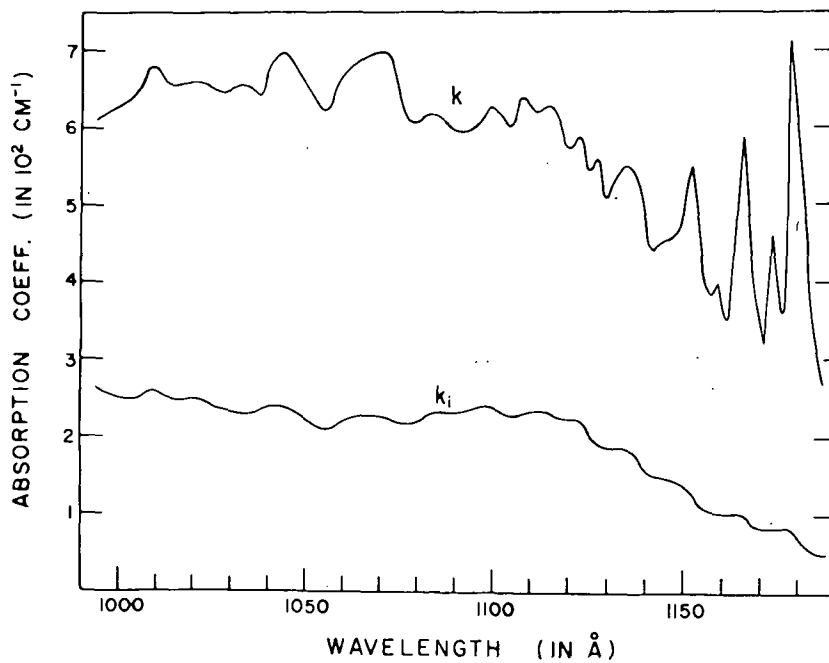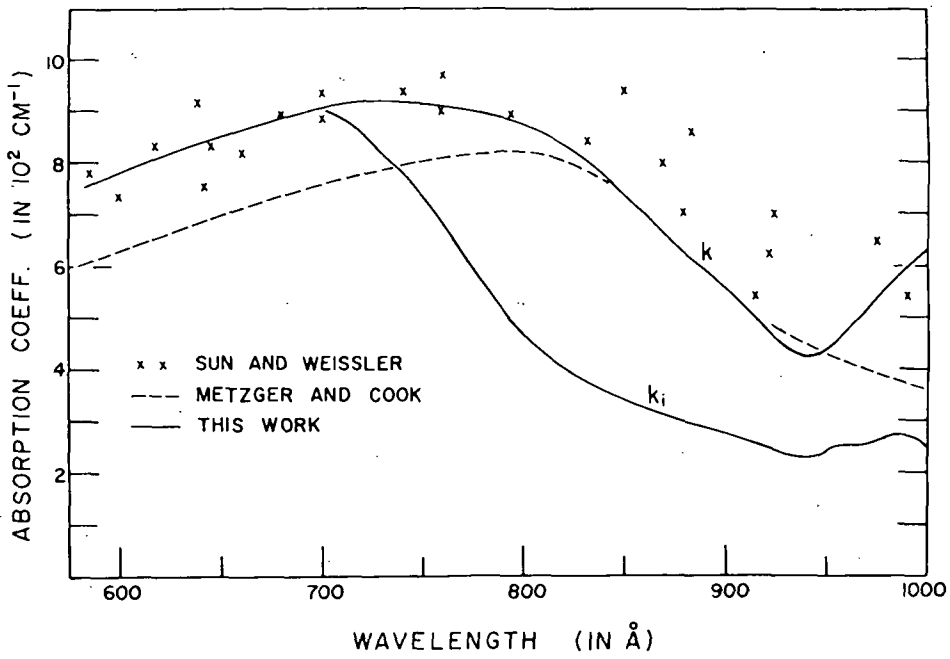
Figure (9-14). Absorption coefficient profiles of NH$_3$ for the wavelength region 1650-1480Å. [Watanabe and Sood (1965)]
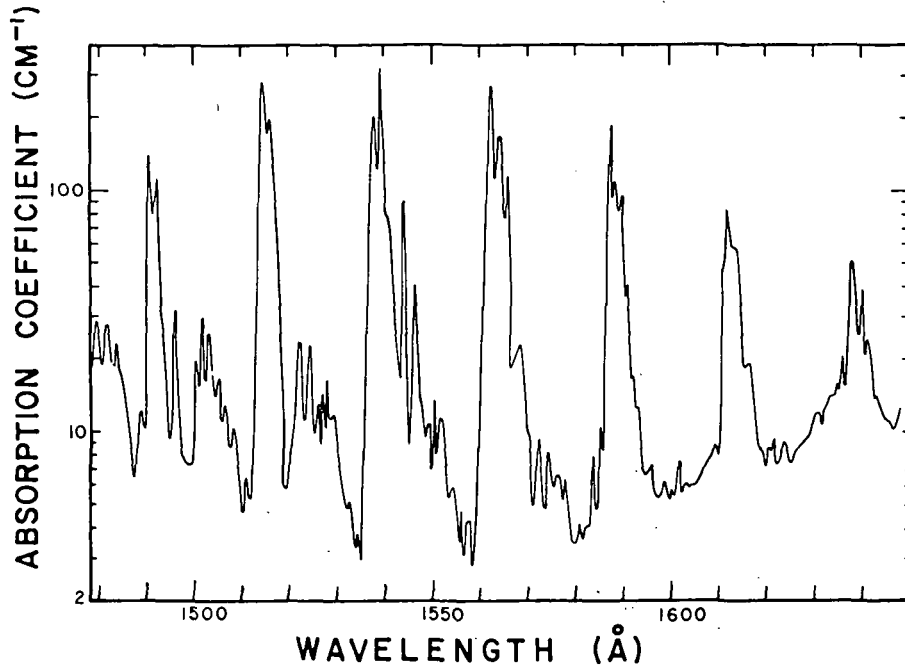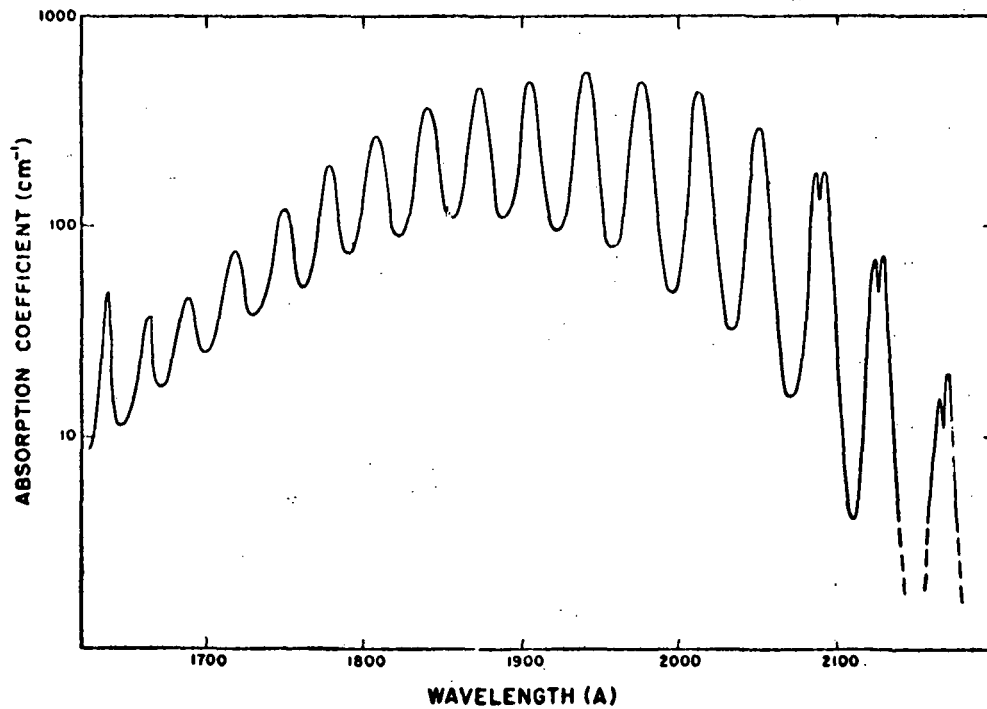

Figure (9-15a). Absorption coefficient profiles of NH$_3$ for the wavelength region 2200-1640Å. [Watanabe, et al (1953)]
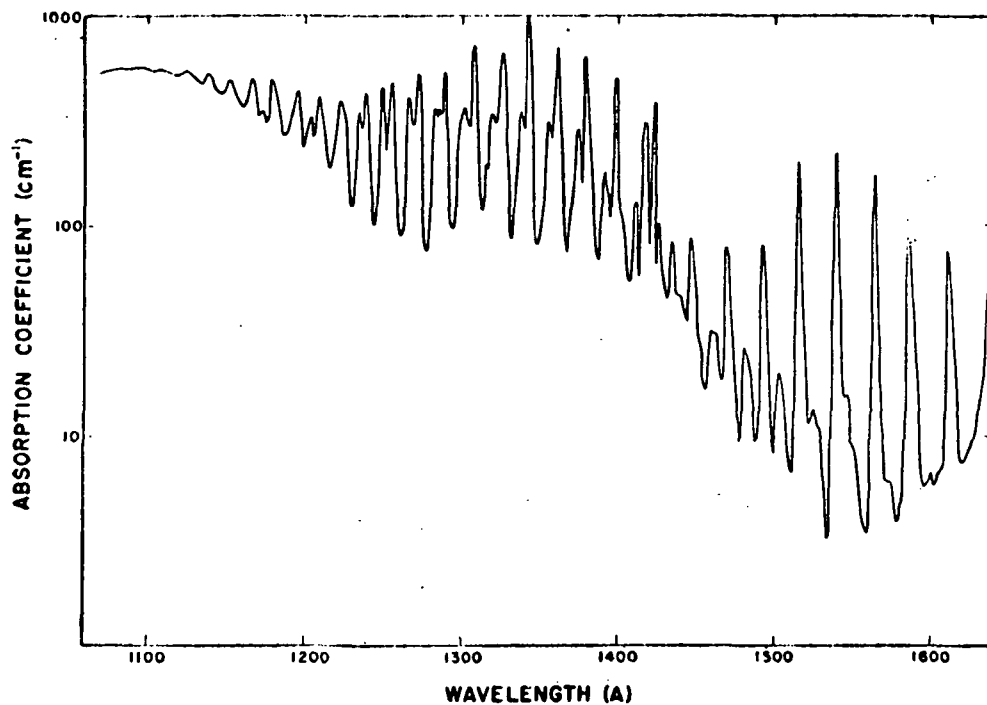
Figure (9-15b). Absorption coefficient profiles of NH_3 for the wavelength region 1650~1050Å. [Watanabe et al (1953)]
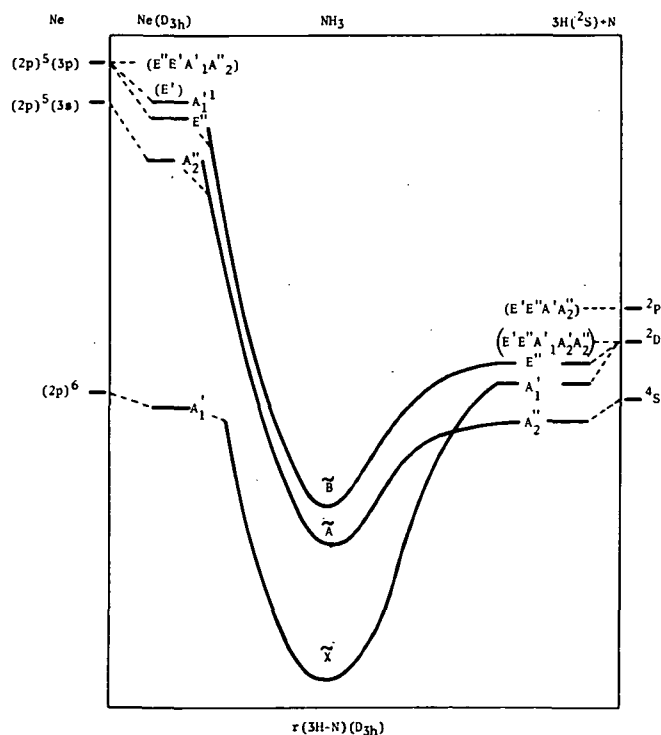

Figure (9-16). Schematic showing potential energy curves for a few important electronic states of NH_3. [Douglas (1963)]
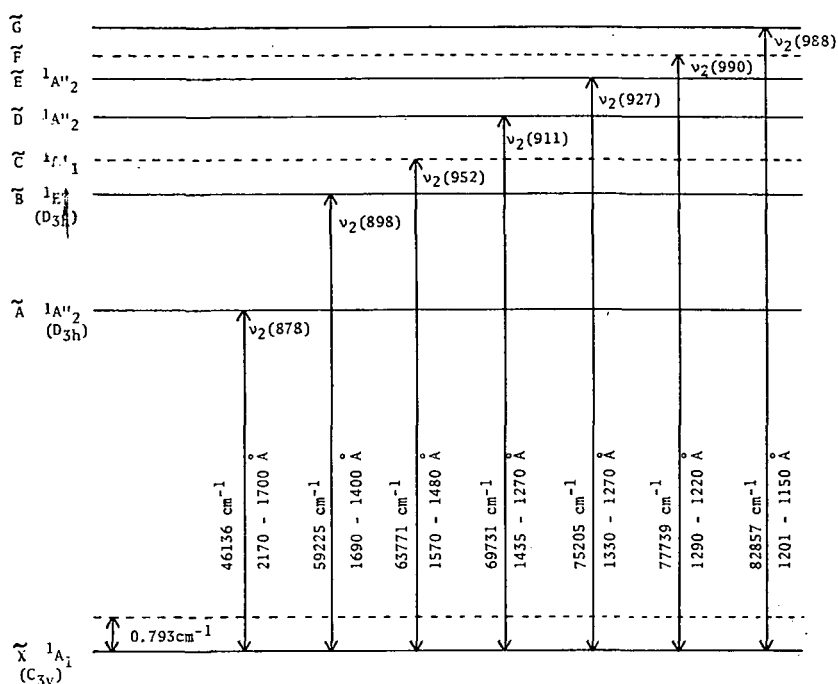
G̃

F̃

Ẽ $^1A''_2$

D̃ $^1A''_2$

C̃ $^1A'_1$

B̃ $^1E''$ (D$_{3h}$)

Ã $^1A''_2$ (D$_{3h}$)

ν$_2$(988)
ν$_2$(990)
ν$_2$(927)
ν$_2$(911)
ν$_2$(952)
ν$_2$(898)
ν$_2$(878)

46136 cm^{-1} | 2170 - 1700 Å | 59225 cm^{-1} | 1690 - 1400 Å | 63771 cm^{-1} | 1570 - 1480 Å | 69731 cm^{-1} | 1435 - 1270 Å | 75205 cm^{-1} | 1330 - 1270 Å | 77759 cm^{-1} | 1290 - 1220 Å | 82857 cm^{-1} | 1201 - 1150 Å

0.793 cm^{-1}

X̃ $^1A_1$ (C$_{3v}$)

Figure (9-17). Schematic showing various observed electronic transitions of NH$_3$.

consisting of parallel and perpendicular sub-bands. All these circumstances give rise to different types of resonance interactions in the vibrational and rotational states. High resolution studies of many of the infrared bands of NH$_3$ and those of its isotopic forms have been reported in a series of papers specially by Benedict et al., and by Rao et al. Reference may be made to these articles for details.

Table (9-XI) gives the prominent overtone and combination bands of NH$_3$. Some data on the known vibrational states is presented in Table (9-XII). Table (9-XIII) gives the rotation-vibration inversion interaction constants.

Microwave Spectrum. - The most widely studied microwave spectrum of ammonia is its inversion spectrum. NH$_3$ is pyramidal in its equilibrium configuration with a relatively low potential barrier separating the two equivalent potential minima. A plot of the potential energy curve shows two minima with a hump in between (figure 9-18). The eigenfunctions are alternately symmetric and antisymmetric with respect to a reflection through the plane defined when all the four atoms are coplaner. The first two levels are almost coincident and the inversion doubling becomes larger as the levels approach the barrier-top. Above this point, the levels approach a harmonic spacing which corresponds to an out-of-plane bending vibration.

The separation of the symmetric and antisymmetric sublevels of the 0th vibration level is about 23700 MHz. Since the selection rule is S → a, the pure rotational transitions J, K → J + 1, K appear as doublets. These fall in the far infrared. In addition,

$\Delta J = 0$ transitions between the 0^S and 0^a levels are also allowed and these give rise to a very intense microwave spectrum.

In the zeroth approximation, all the $\Delta J = 0$ lines are coincident. Actually, the vibration-rotation interactions are quite large in NH_3, and the transitions extend over a wide range. The strong lines which involve low rotational states fall near 24000 MHz.

It may, however, be mentioned that inversion splitting is a very sensitive function of both the barrier height and the geometry. No such spectra have been so far observed outside of NH_3 and its isotopic species.

Detailed discussion on the inversion spectrum of NH_3 may be found in Townes and Schawlow (1955).

TABLE (9-XI)   INFRARED VIBRATION ROTATION BANDS OF NH_3

ν(cm^{-1})	Assignment	Intensity	ν(cm^{-1})	Assignment	Intensity
629.3	$2\nu_2-\nu_2$	w	5953	$\nu_3+\nu_4$	s
932.58	ν_2	vs	6016	$\nu_2+\nu_3+\nu_4$	m
968.08			6595	$2\nu_1$, $(2\nu_3,\nu_1+\nu_3)$	m
1627.5	ν_4	vs	6624		
1922.	$2\nu_2$	vw	7665.	$2\nu_1+\nu_2$	w
2440.1	$\nu_3-\nu_2$; $\nu_2+\nu_4$	w	7899		
2472.6			8177	$2\nu_1+\nu_4$	w
2861	$3\nu_2$	vw	8202		
3219.1	$2\nu_4$	m	8460	$2\nu_3+\nu_4$	w
3335.9	ν_1	vs	9760.4	$3\nu_1$	w
3337.5			10099.7	$\nu_1+2\nu_3$	w
3413.	ν_3	s	10104.9		
4176	$\nu_2+2\nu_4$	m	11364	$3\nu_1+\nu_4$	w
4216			12609.2	$6\nu_1,2\nu_1+2\nu_3$	w
4269	$\nu_1+\nu_2$	s	12619.8		
4302			15440	$5\nu_1,4\nu_1+\nu_3$	w
4433	$\nu_2+\nu_3$	s	18150	$6\nu_1,5\nu_1+\nu_3$	w
4595					

w = weak   s = strong

vs = very strong   m = medium

vw = very weak

TABLE (9-XII)   VIBRATIONAL LEVELS OF AMMONIA (cm^{-1})

ν_1	$\nu_3^{l_3}$	$\nu_4^{l_4}$	ν_2 $\nu=0$	0	1	1	2	2	3	3	
0	0^0	0^0	0.00	0.793	932.51	968.32	1597.6	1910	2383.46	2895.48	
0	0^0	1^1	1626.1	1627.4	2539.6?	2585.0?					x_{24}= -14.5?
0	0^0	2^0	(3216.4)	(3218.6)							
1	0^0	0^0	3336.18	3337.18	4294.51	4320.06					x_{12}= +20.58
0	1^1	0^0	3443.59	3443.94	4416.91	4435.40					x_{23}= +32.36
1	0^0	1^1	4955.94	4956.8							x_{14}= -6.7
0	1^1	1^1	5052.61	5053.18	6012.72	6036.40					x_{34}= -17.25
											x_{24}= -10.73
1	1^1	0^0	6608.71								
0	1^1	2^0	(6700.?)								x_{13}= -92??
0	2^2	0^0	6849.96	6850.39							x_{33}= -18.50

ND_3

ν_1	$\nu_3^{l_3}$	$\nu_4^{l_4}$	ν_2 $\nu=0$	0	1	1	2	2	3	3	
0	0^0	0^0	0.00	0.053	745.7	749.4	1359	1429	1830	2106.60	
0	0^0	1^1	1191								
0	0^0	2^0	(2359)		3093.01	3099.46					x_{24}= -5??
1	0^0	0^0	2420.05	2420.64	3171.89	3175.87					x_{12}= +5.9
0	1^1	0^0	2563.96		3327.94	3329.56					x_{23}= +17.1
0	1^1	2^0	4887.29	4887.67							x_{34}= -18??
1	1^1	0^0	4938.44								x_{13}= -45.84?
0	2^1	0^0	5100.66								x_{33}= -13.63

TABLE (9-XIII) ROTATION-VIBRATION-INVERSION INTERACTIONS IN AMMONIA

ν_1	ν_2	ν_3	ν_4	Rotation-Vibration Interactions				Rotation-Inversion Splittings		
				B_r-B_0	C_v-C_0	C_0-C_v	$\Delta G°$	ΔB	ΔC	Δ
						NH_3				
0	1	0	0	00.032	-0.105		35.81	-0.179	0.053	
0	0	0	1	0.235	-0.066	7.756	1.3			
1	0	0	0*	-0.085	-0.083		1.0-	-0.012	0.003	
1	1	0	0*	-0.1280	-0.1360		25.55	-0.1265	0.0470	
0	0	1	0	-0.176	0.009	5.934	0.35	-0.003	0.001	
0	1	1	0	-0.1975	-0.0863	5.9958	18.49	-0.0984	0.0429	0.0037
0	1	0	1	0.26	-0.14	7.82	44.8	-0.21	0.06	
1	0	0	1*	0.12	-0.105	7.739	0.86			
0	0	1	1	0.035	-0.0535	4.830	0.57			
0	1	1	1	0.012	-0.152	4.882	23.68	-0.130	0.054	0.016
1	0	1	0†	0.03	-0.12	5.98				
0	0	2^2	0	-0.33	0.00	6.72	0.73			
0	2	0	0	0.31	-0.35					
0	3	0	0	-0.45	-0.09					
0	3^a	0	0	-0.76	0.09					
						ND_3				
1	0	0	0†	-0.004	-0.02		0.59			
0	1	0	2^0	0.0935	-0.11		6.45	-0.011	0.03	
1	1	0	0	-0.0535	-0.051		3.98	-0.005	0.00	
0	0	1	0	-0.0650	0.0002	2.702				
0	1	1	0	-0.119	-0.0286	2.709	1.62	-0.002	0.0005	
0	0	1	2^0	-0.03	-0.058	2.844				
1	0	1	0	0.00	-0.040	2.704				
0	0	2^2	0	-0.126	0.0026	3.946				
0	3^a	0	0	-0.133	-0.03					

* Levels are in partial Fermi resonance; constants for resonating level not available.

† Levels are in close Fermi resonance; constants for resonating level not available.

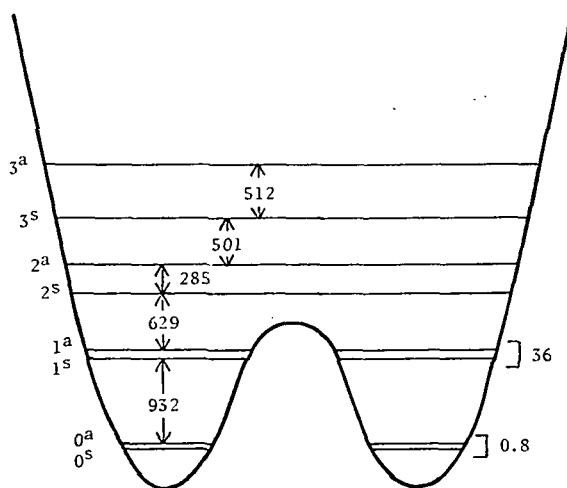a Levels are in close Fermi resonance; constants for both levels as listed.

Figure (9-18). Potential function and observed energy levels for the ν_2 mode of NH_3.

Water Vapor (H_2O)

Dipole Moment, M: 1.854 Debye

Ionization Potential, I.P.: 12.61 eV

Dissociation Energy, D(OH-H): 5.113 eV

Ground Electronic State Configuration: $(1a_1)^2 (2a_1)^2 (1b_2)^2 (3a_1)^2 (1b_1)^2 - - {}^1A_1$

Fundamental Vibration Frequencies:

ν_1	ν_2	ν_3
3656.7	1594.8	3755.8 (cm^{-1})

Rotational Constants:

A_o	B_o	C_o	r_e(O-H)	α(H-O-H)
27.8778 cm^{-1}	14.5092 cm^{-1}	9.2869 cm^{-1}	0.9572Å	104.52°

Pure water is a colorless liquid at ordinary temperatures and has a vapor pressure of about 6 millibar at 0°C. The water molecule (H_2O) is a nonlinear, asymmetric top tri-atomic molecule characterized by the C_{2v} point group symmetry. The three principal moments of inertia are known to be as $I_A = 1.004 \times 10^{-40}$; $I_B = 1.929 \times 10^{-40}$ and $I_C = 3.104 \times 10^{-40}$ (g x cm^2).

The two hydrogen atoms and one oxygen atom lie at the three vertices of an obtuse isoceles triangular framework (figure 9-19). The apical angle α(H-O-H) is 104.52 and the bond length r_e(O-H) is about 0.957Å which is slightly less than the bond length in OH radical.
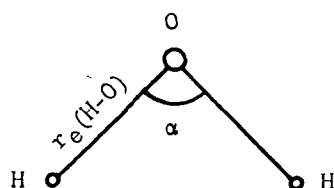
155

Figure (9-19). Geometrical configuration of the water molecule.

The principal isotopic species of the water molecule that usually occur in nature are: $H_2^1O^{16}$, $D_2^2O^{16}$, $H^1D^2O^{16}$, $H_2^1O^{17}$, $H_2^1O^{18}$.

Molecular Spectrum

The observed spectra of H_2O can be classified into three broad categories: (1) Electronic Spectrum, (2) Vibration-rotation Spectrum, and (3) Rotational Spectrum.

Electronic Spectrum. - Water vapor exhibits quite a rich electronic spectrum lying in the vacuum ultraviolet. It has an onset of around 1860Å and is known to extend to 500Å. The different features of this absorption have been quite extensively studied by various workers in the past (Leifson, 1926; Henning, 1932; Rathenau, 1933; Preston, 1940; Price, 1936; Wilkinson and Johnston, 1950; Harrison, Cederholm and Terwilliger, 1959; Johannin-Giles, 1956; Watanabe and Zelikoff, 1953; Watanabe and Jursa, 1964; Astoin, Johannin-Giles and Vodar, 1953; Wainfan, Walker and Weissler, 1955; Watanabe, Zelikoff and Inn, 1953; Thompson, Harteck and Reeves, 1963; Bell, 1965; Metzer and Cook, 1964; Johns, 1963; Hopfield, 1938; Hopfield, 1950; Astoin, 1956; Laufer and McNesby, 1955; DeReilhac and Damany, 1970). For the convenience of discussion the observed spectra can be divided into the following wavelength segments.

(1) 1860-1430Å

This spectral region is occupied by a continuum with λ_{max} ~1650Å at which the absorption cross section is about 120 cm^{-1}. Results of various authors on the absorption in this continuum are in fairly good agreement. However, Wilkinson, and Johnston (1950) reported three diffuse bands with λ_{max} ~1608, 1648 and 1718Å superimposed on this continuum. Johannin-Gilles et al. (1956) identified as many as six bands superimposed on this continuum. Watanabe et al. (1953) and Laufer and McNesby (1955) could not observe any banded structure.

(2) 1450-1250Å

An absorption continuum with λ_{max} ~1290Å (absorption cross section 200 cm^{-1}) mainly occupies the 1450-1250Å region. There also exist several strong but

156

diffuse bands superimposed on the short wave side of this continuum. This banded structure was earlier reported by Rathenau (1933) and Price (1936). Their rotational structure also was studied by Price (1936). Most of these bands fit into a Rydberg series. Watanabe et al. (1953) scanned this band structure using photoelectric recording. Table (9-XIV) presents λ_{max} data for the various bands identified by them and figure (9-20) represents the absorption profile for this entire region.

(3) 1250-1050Å

Early studies on the absorption of H_2O in this region are those of Rathenau (1933) and Price (1936). There exist numerous strong bands, some of which are diffuse and others which possess discrete rotational structure. A number of these bands have been identified as members of two Rydberg series, which have a common limit of 12.62 eV. The band of 1204Å is the (0-0) band of the first member of the npa_1, B series. It shows discrete rotational structure which has been extensively investigated recently by Johns (1963). Bell (1965) has carried out an exhaustive vibrational analysis of the band systems having origins at 1240Å and 1219Å with a common convergence limit at 982Å. He also reported discrete bands at 1185Å, 1166Å, 1144Å and a diffuse band at 1156Å. Watanabe, Zelikoff and Inn (1953) measured absorption cross section of water vapor using photoelectric techniques and identified quite a few of the reported bands. Higher members of the Rydberg series could not be scanned because of experimental limitations. Figure (9-21) presents the results obtained by Watanabe et al. (1953).

TABLE (9-XIV) WAVELENGTHS (Å) OF THE DIFFUSE BANDS OF H_2O
VAPOR IN THE REGION FROM 1250 to 1450Å

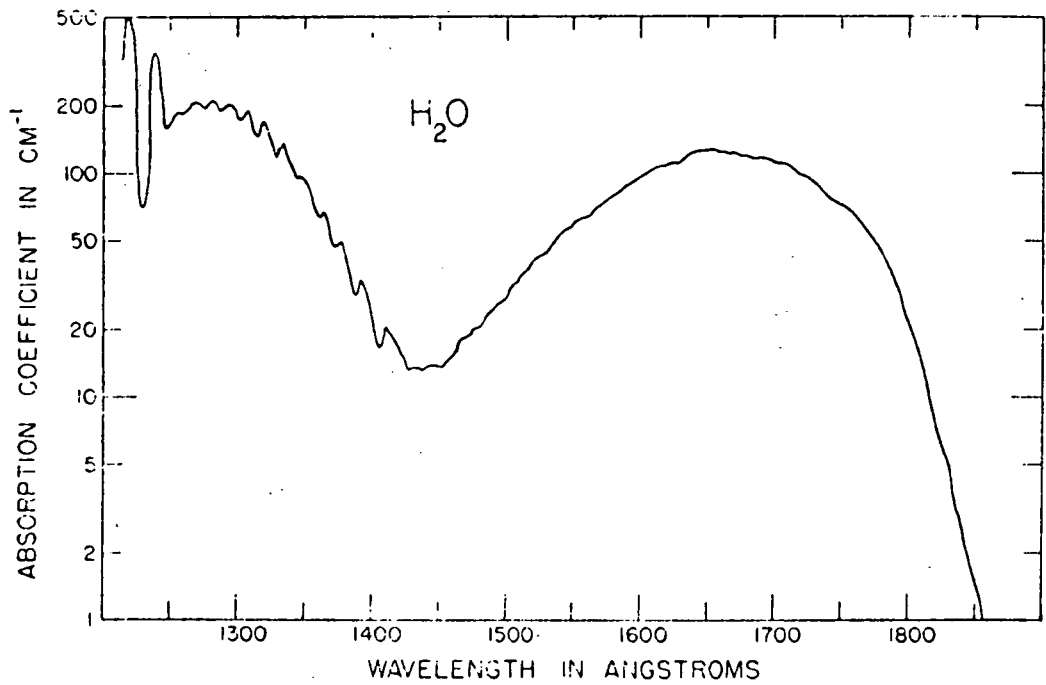| Rathenau	Watanabe et al
	1411
	1392
	1378
1361-1372	1364
1346-1357	1348
1332-1341	1335
1318-1324	1321
1306-1309	1308
1291-1297	1295
1279-1284	1281
1267-1271	1269
1253-1257	1257

Figure (9-20). Absorption coefficient profile of H_2O vapor for the wavelength region 1850-1250Å. [Watanabe et al. (1953)]
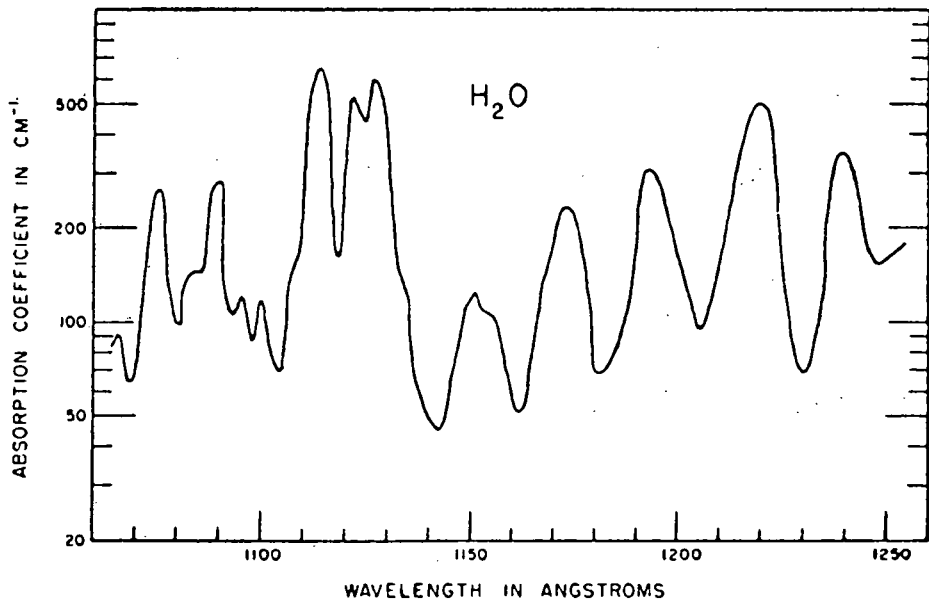

Figure (9-21). Absorption coefficient profile of H_2O for the wavelength 1250-1050Å. [Watanabe et al. (1953)]

(4) 1000-200Å

Earlier studies of H_2O absorption in this region are of Henning (1932)
and Hopfield (1938) who observed a banded structure superimposed over a
broad continuum in the region 1000-850Å. Absorption cross sections in
this region were measured by Watanabe and Jursa (1964) and Metzger and Cook
(1964) using photoelectric measurements. While Watanabe et al. reported
banded structure throughout the region 1110-850Å, Metzger et al. reported
a smooth curve. However, in view of the support from spectrographic obser-
vations, Watanabe and Jursa's results are preferred. The results of Watanabe
and Jursa (1964) are depicted in figure (9-22). The data on absorption
cross sections in the region 850-600Å are quite conflicting. The region
is covered by a continuum whose absorption is estimated differently by
different workers. While Metzger and Cook (1964) reported only a continuous
absorption band, Dibeler et al. (1966) found a banded structure between
860-690Å and around 687Å they observed the onset of dissociative ionization
of H_2O. Lately, Katayama, Huffman and O'Bryan (1973) reported absorption
and photoionization cross sections for H_2O and D_2O over the wavelength
range 1050-580Å. Besides identifying a number of new members of the already
known Rydberg series that converges to the (000) level of the ionic state,
a host of unreported bands superimposed on broad continua peaking at
approximately 720Å and 925Å were also observed. These bands are most likely
due to progressions belonging to Rydberg states converging to the first and
the second excited states of H_2O^+ (figures 9-23 and 9-24). At shorter wave-
lengths (500-100Å) absorption coefficients were measured by DeReilhac and
Damany (1970). Earlier, Astoin (1956) had reported several intense absorp-
tion bands and an underlying continuum in the region 500-200Å. The absorp-
tion is found to be pressure dependent. Astoin's results are presented in
figure (9-25). The dashed curve shows the continuum shape, and the curve A
is from Wainfan, Walker and Weissler (1955). There appears to be good
agreement between the two in the region of comparison. Absorption dis-
continuities were also observed from 12.4, 16.7, 24.2 and 33.5 eV. The
33.5 eV discontinuity (270,000 cm^{-1}) is probably due to the fourth ioniza-
tion potential of the H_2O molecule. Smyth and Mueller's (1933) experiments
on ionization by electron impact show the appearance of H_2^+ ions at 33.5 eV.
Figure (9-26) presents a schematic showing various observed electronic
states of the molecule H_2O.
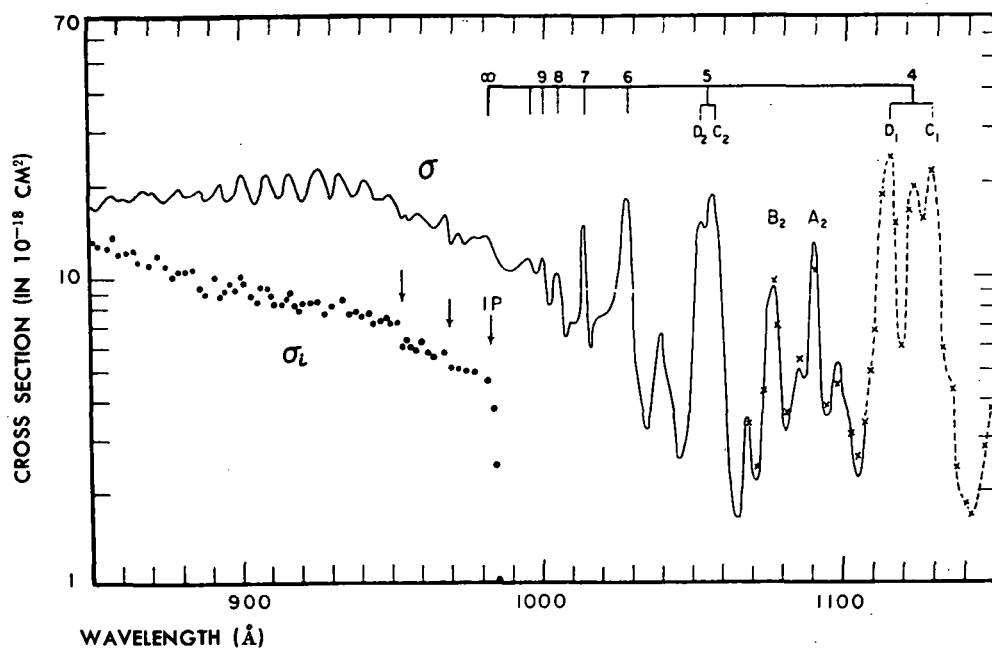
Figure (9-22). Absorption cross section profile of H_2O vapor in the region 1100-850Å. [Watanabe and Jursa (1964)]
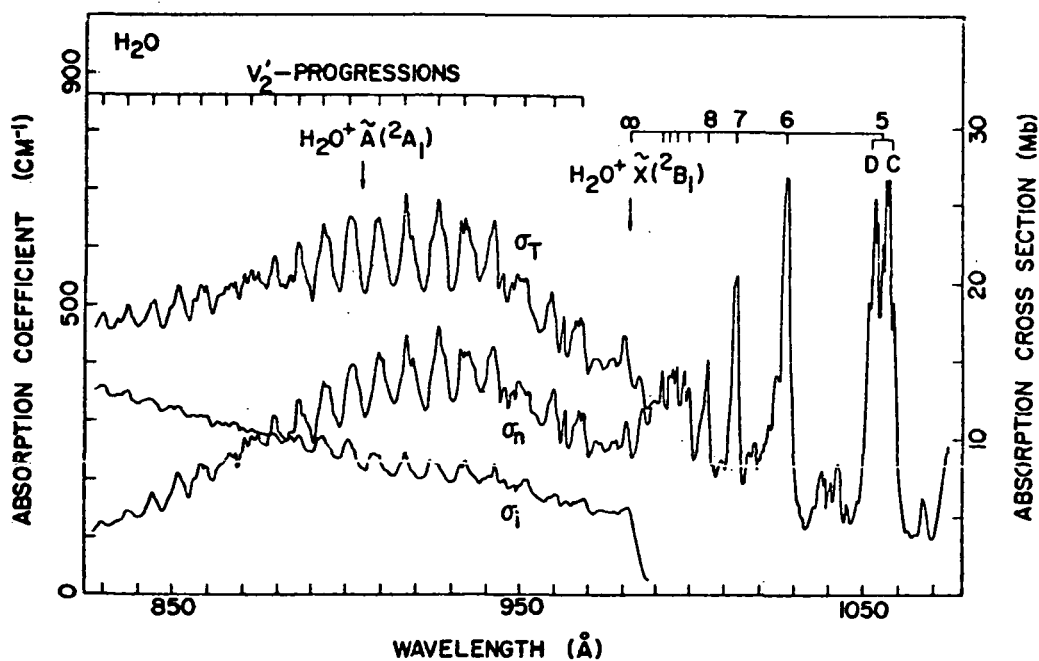
Figure (9-23). Total absorption (σ_T), photoionization (σ_i) and neutral product (σ_n) cross sections for H_2O in the region 1070-825Å. [Katayama et al(1973)]
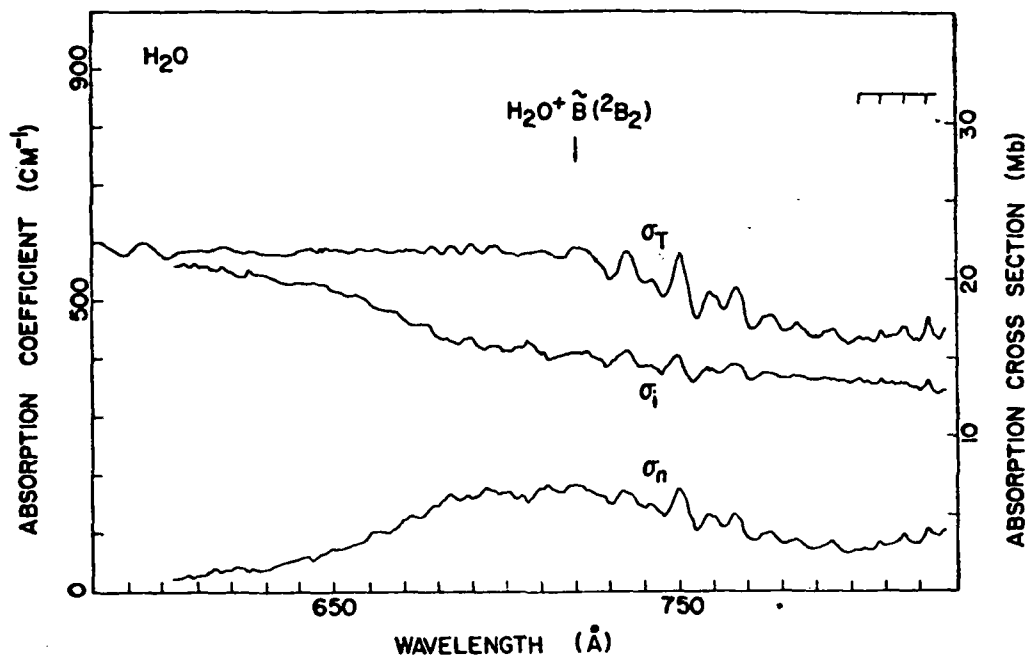
Figure (9-24). Total absorption (σ_T), photoionization (σ_i) and neutral product (σ_n) cross sections for H_2O in the region 825-580Å. [Katayama et al (1973)]
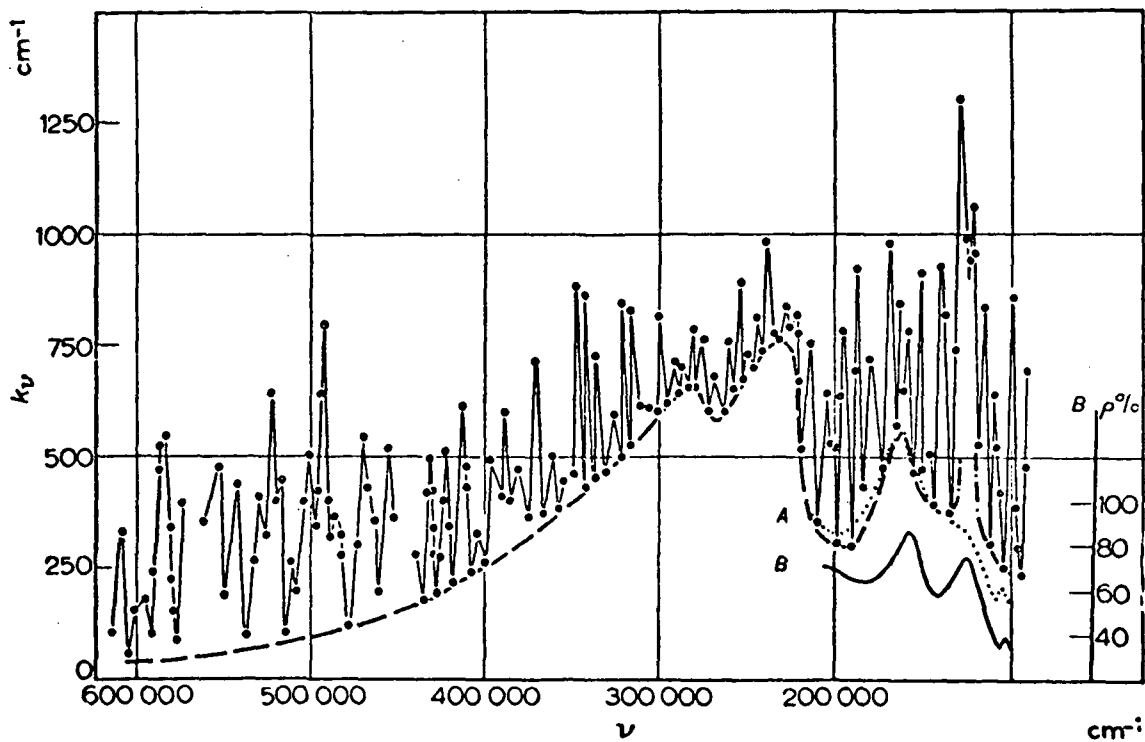
Figure (9-25). Absorption profile of gaseous H_2O in the region 1000-150Å. [Astoin (1956)]
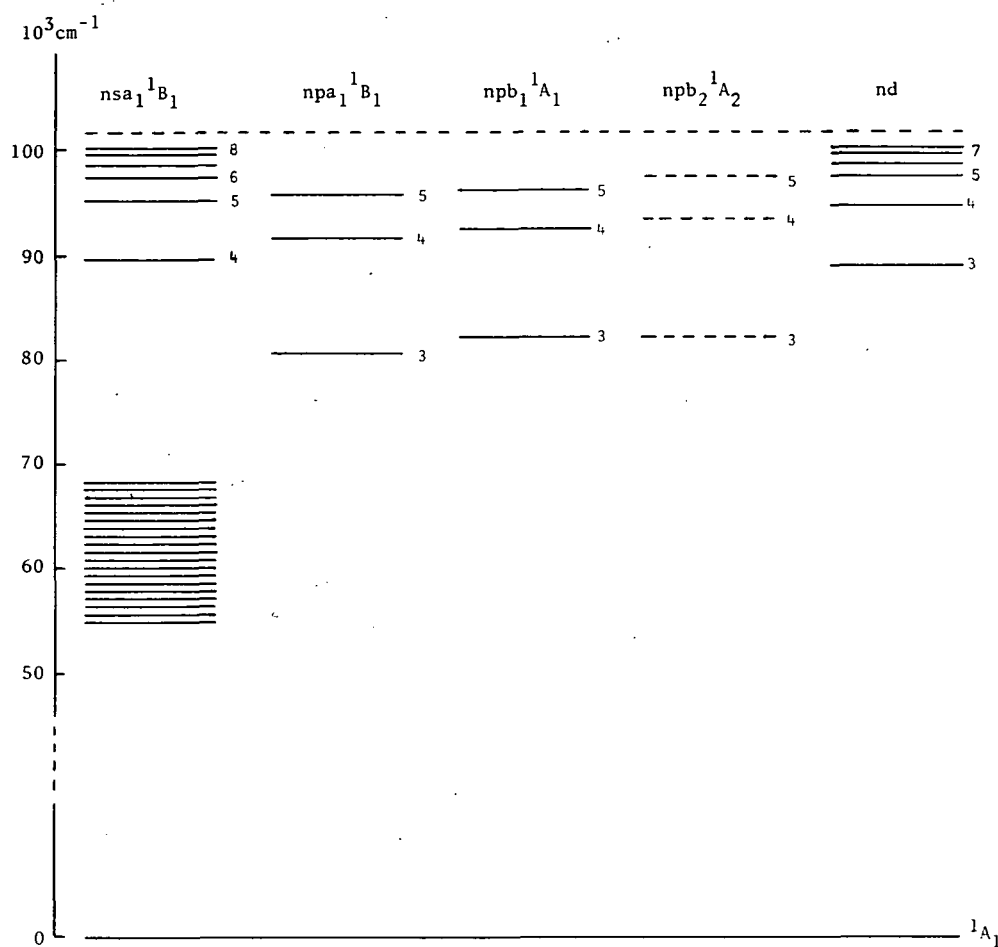
Figure (9-26). Observed electronic states of H$_2$O molecule. [Herzberg (1966)]

Vibration Rotation Spectrum. - Since the three principal moments of inertia of a free H$_2$O molecule differ appreciably (roughly in the ratio 1:2:3), the vibration-rotation spectrum of water vapor appears quite complex. Besides the three fundamental frequencies, the infrared spectrum consists of numerous overtones, combinational frequencies and higher state bands. Out of all of these, it is the ν_2 fundamental (called the 6.3μ water band) which is most intense; ν_3 comes next and then the ν_1 which is considerably weaker than the ν_3. Another prominent band of H$_2$O is the $2\nu_2$ harmonic at 3.7μ. Tables (9-XV, 9-XVI, and 9-XVII) give lists of the various vibration-rotation bands that have been identified and studied in the laboratory spectra. For more details, papers by Plyler and Tidwell, 1957; Eldridge, 1967; Zuev et al., 1968; Fraley et al., 1969; Williamson et al., 1971; may be referred.

162

TABLE (9-XV) H₂O BANDS IN THE VISIBLE SPECTRAL REGION

Transition	Band Center		Strength (S_n)
	(cm^{-1})	(μ)	(cm)
000-411	18 394	0.54	2.10^{-23}
000-203	17 495	0.57	1.10^{-22}
000-401	16 899	0.59	3.10^{-22}
000-302	16 898	0.59	3.10^{-23}
000-321	16 822	0.59	2.10^{-22}
000-113	15 832	0.63	2.10^{-23}
000-311	15 348	0.66	2.10^{-22}
000-103	14 319	0.69	1.10^{-21}
000-400	14 221	0.70	1.10^{-22}
000-301	13 831	0.72	3.10^{-21}
000-202	13 828	0.72	2.10^{-23}
000-221	13.653	0.73	6.10^{-21}
000-013	12 565	0.79	1.10^{-22}
000-112	12 408	0.81	6.10^{-21}
000-211	12 151	0.82	6.10^{-23}
000-210	12 140	0.82	1.10^{-22}
000-131	11 813	0.85	2.10^{-21}

TABLE (9-XVI) H₂O BANDS IN THE NEAR INFRARED SPECTRAL REGION

Bandname	Transition	Band Center		Strength (S_n)
		(cm^{-1})	(μ)	(cm)
ρ	000-003	11 032	091	2.10^{-21}
	000-102	10 869	092	4.10^{-22}
σ	000-201	10 613	094	1.10^{-20}
	000-300	10 600	094	6.10^{-22}
τ	000-121	10 329	097	2.10^{-21}
	000-220	10 284	097	$< 4.10^{-23}$
	000-041	9 834	101	6.10^{-23}
φ	000-012	9 000	111	3.10^{-22}
	000-121	8 807	113	8.10^{-21}
	000-210	8 762	114	1.10^{-23}
	000-130	8 274	120	7.10^{-24}
	000-131	8 374	119	3.10^{-23}
ψ	000-002	7 445	134	1.10^{-21}
	000-101	7 250	137	$1.5.10^{-19}$
	000-200	7 201	138	$1.5.10^{-20}$
	000-021	6 871	145	1.10^{-20}
	000-120	6 775	147	2.10^{-22}
Ω	000-011	5 331	187	$2.2.10^{-19}$
	000-110	5 235	191	7.10^{-21}
	000-030	4 667	214	3.10^{-22}

TABLE (9-XVII)   BANDS OF HIGHER STATES OF H_2O

| Transition | Frequency | | Strength (S_n) |
	(cm^{-1})	(μ)	(cm)
010-001	2161.64	4.62	2.10^{-22}
010-100	2062.27	4.84	8.10^{-23}
010-020	1556.82	6.42	9.10^{-22}
010-010	0-500	$\infty - 20$	$4.6.10^{-20}$

Rotational Spectrum. - Since H_2O has a relatively high value of dipole moment, it exhibits an intense and extensive rotational spectrum running from about 8μ to several cms of wavelength.   Recent laboratory work of Lichtenstein, Derr and Gallagher (1966); Hall and Dowling (1967); Izatt, Sakai and Benedict (1969); Fraley, Rao and Jones (1969); Fraley and Rao (1969); Hall and Dowling (1970); Steenbeckeliers and Bellet (1971); Lucia, Cook, Helminger and Gordy (1972a); Lucia, Helminger, Cook and Gordy (1972b) is worth mentioning in this context. Moller and Rothschild (1971) calculated and tabulated the frequencies of some 278 rotational lines in the range 12-305 cm^{-1}.

Lately Lucia, Helminger and Kirchhoff (1974) have presented a critical review on the microwave spectrum of water which, besides providing the wavelength data on different observed rotational transitions, presents data on rotational constants, centrifugal distortion constants, hyperfine coupling parameters and dipole moments for the water molecule and its deuterated forms. Table (9-XVIII) presents the observed data on the microwave spectra of two principal isotopic forms of H_2O ($H_2^{16}O$ and $H_2^{18}O$).

TABLE (9-XVIII) MICROWAVE SPECTRA OF $H_2^{16}O$ AND $H_2^{18}O$

Upper State	Lower State	$H_2^{16}O$ Observed Frequency (MHz) (Est. Uncertainty)	Lower State Energy Level (cm^{-1})	Line Strength	$H_2^{18}O$ Observed Frequency (MHz) (Est. Uncertainty)	Lower State Energy Level (cm^{-1})	Line Strength
1(1,0)	1(0,1)	556 936.002(0.089)	23.794	1.500	547 676.44(0.06)	23.754	1.500
2(1,1)	2(0,2)	752 033.227(0.489)	70.091	2.073	745 320.20(0.48)	69.925	2.061
3(1,3)	2(2,0)	183 310.0906(0.0015)	136.164	0.102	203 407.52(0.02)	134.780	0.100
4(1,4)	3(2,1)	380 197.372(0.025)	212.157	0.123	390 607.76(0.04)	210.795	0.119
4(2,3)	3(3,0)	448 001.075(0.022)	285.419	0.132	489 054.26(0.08)	282.302	0.132
5(1,5)	4(2,2)	325 152.919(0.027)	315.780	0.091	322 465.17(0.05)	314.455	0.086
5(3,3)	4(4,0)	474 689.127(0.072)	488.135	0.118	537 337.57(0.47)	482.671	0.119
5(3,2)	4(4,1)	620 700.807(0.387)	488.108	0.122	692 079.14(0.60)	482.642	0.123
6(1,5)	5(2,3)	22 235.07985(0.00005)	446.511	0.057	5 625.147(0.015)	445.155	0.053
6(4,3)	5(5,0)	439 150.812(0.053)	742.078	0.101	520 137.32(0.47)	733.696	0.103
6(4,2)	5(5,1)	470 888.947(0.192)	742.074	0.102	554 859.87(0.47)	733.692	0.103
7(1,7)	6(2,4)	488 491.133(0.375)	586.480	0.036	517 181.96(0.21)	583.987	0.033
7(5,3)	6(6,0)	437 346.667(0.201)	1045.063	0.088			
7(5,2)	6(6,1)	443 018.295(0.210)	1045.062	0.088			
10(2,9)	9(3,6)	321 225.644(0.244)	1282.924	0.089			

For $H_2^{16}O$ and $H_2^{18}O$ all transitions below 800 GHz and between levels with total rotational energy below 1000 cm^{-1} have been observed in the laboratory and are listed in this table.

Ozone (O_3)

Dipole Moment, M: 0.58 Debye

Ionization Potential, I.P.:   12.8 eV

Dissociation Energy, $D(O_2 - O)$:   1.04 eV

Ground Electronic State Configuration: $(5a_1)^2 (4b_2)^2 (6a_1)^2 (1a_2)^2$ - $^1A_1$

Fundamental Vibration Frequencies:

	ν_1	ν_2	ν_3
	1110	705	1042.2 (cm^{-1})

Rotational Constants:

A_0	B_0	C_0	r_e(0-0')	α ($> $00'0)
3.55345 cm^{-1}	0.445276 cm^{-1}	0.394749 cm^{-1}	1.2717Å	116.8°

Ozone, at ordinary temperature, is a blue unstable gas with a characteristic pungent odor. It transforms to a deep blue liquid at critical values of temperature and pressure equal to -12.1°C and 54.6 atm., respectively.

The ozone molecule (O_3) is a nonlinear, asymmetric top triatomic having a C_{2v} point group symmetry. The three oxygen atoms form three vertices of an obtuse isoceles triangular framework with apical angle, α(>00'0) = 116.8°, and the bond length r_e (0-0') = 1.2717Å, as illustrated in figure (9-27).

Figure (9-27). Geometrical disposition of the molecule O_3.

The bond length 0-0' (1.2717Å) is shorter than the single 0-0 bond (1.48Å in H_2O_2) and longer than the double 0 = 0 bond (1.21Å in O_2), which indicates that the 0-0 bond in ozone should have a considerable double bond character. The binding may be considered as consisting of two σ bonds between the central and the outer oxygen atoms and a delocalized π orbital spread over the entire molecular skeleton. According to the valence bond approach, O_3 is described as a hybrid resonance structure, as shown in figure (9-28).

Figure (9-28). Resonance structure of molecule O_3.

Now, if such a hybrid structure is taken to be true, it gives a higher dipole moment than determined experimentally. In order to explain this discrepancy, Shand and Spurr (1943) proposed the involvement of two additional resonance structures (figure 9-29), which also contribute to the main resonance hybrid. They tend to neutralize each other's polarity and decrease the resultant dipole moment of the hybrid.
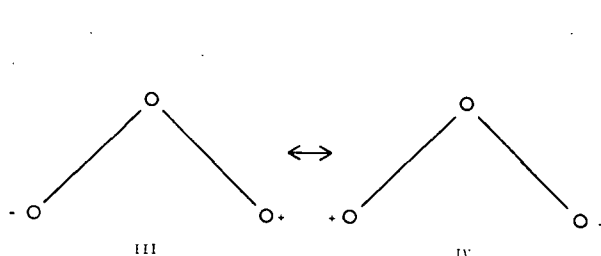

Figure (9-29). Proposed resonance structure of molecule O_3.

The smaller than expected dipole moment can be accounted for by assuming the σ bonds to be formed by sp^2 hybridization of the central oxygen atom, leaving two electrons in the third sp^2 atomic orbital, directed upwards, and producing a negative center, opposing the dipole of structure a and b.

Ozone is known to exist in nature in three principal isotopic forms, viz., $O^{16}O^{16}O^{16}$; $O^{16}O^{18}O^{16}$; $O^{16}O^{16}O^{18}$. The first two species are symmetrical while the third one is asymmetrical and, hence, behaves differently as regards spectra.

Molecular Spectrum

Ozone exhibits a fairly rich electronic spectrum that extends from the microwave through the visible to the shortwave ultraviolet. The observed spectral features can be divided into three main categories: (1) Electronic Spectrum; (2) Vibration-Rotation Spectrum; and (3) Rotational Spectrum.

Electronic Spectrum. - The electronic spectrum of ozone has been studied very extensively in absorption. The observed features can be grouped in the following sub-heads. (1) Vacuum Ultraviolet System (2000-500Å); (2) Hartley System (3000-2000Å); (3) Huggins System (3500-3000Å); (4) Chappuis System (8500-4400Å); and (5) Near Infrared System (10,000-7000Å).

(1) Vacuum Ultraviolet System (2000-500Å)

The vacuum ultraviolet absorption spectrum of ozone is almost continuous with a few diffuse and rather indistinct overlapping continuous bands (Price and Simpson, 1941; Tanaka, Inn and Watanabe, 1953; Ogawa and Cook, 1958). There exist at least six distinct continua whose maxima occur at: (a) 1725Å; (b) 1450Å; (c) 1330Å; (d) 1215Å; (e) 1120Å; and (f) 750Å. The

continuum which has its peak at 1725Å merges around 2000Å with the Hartley continuum (discussed later). Two subsidiary weak continua with peaks around 1165Å and 1170Å were also reported by Tanaka et al. (1953). These authors found that the diffuse bands overlapping the continua at 1330, 1215 and 1120Å form progressions with spacings of about 600 and 800 cm^{-1}. Ogawa and Cook (1958) reported yet another continuum with a peak at 750Å. The band starts at 950Å, a wavelength that corresponds to the first ionization potential of O_3 (12.8 eV). A few weak bands overlapping this continuum were also reported by Ogawa and Cook (1958) in the spectral region 520-750Å. The figures (9-30), (9-31), and (9-32) present profiles of ozone absorption in this region.
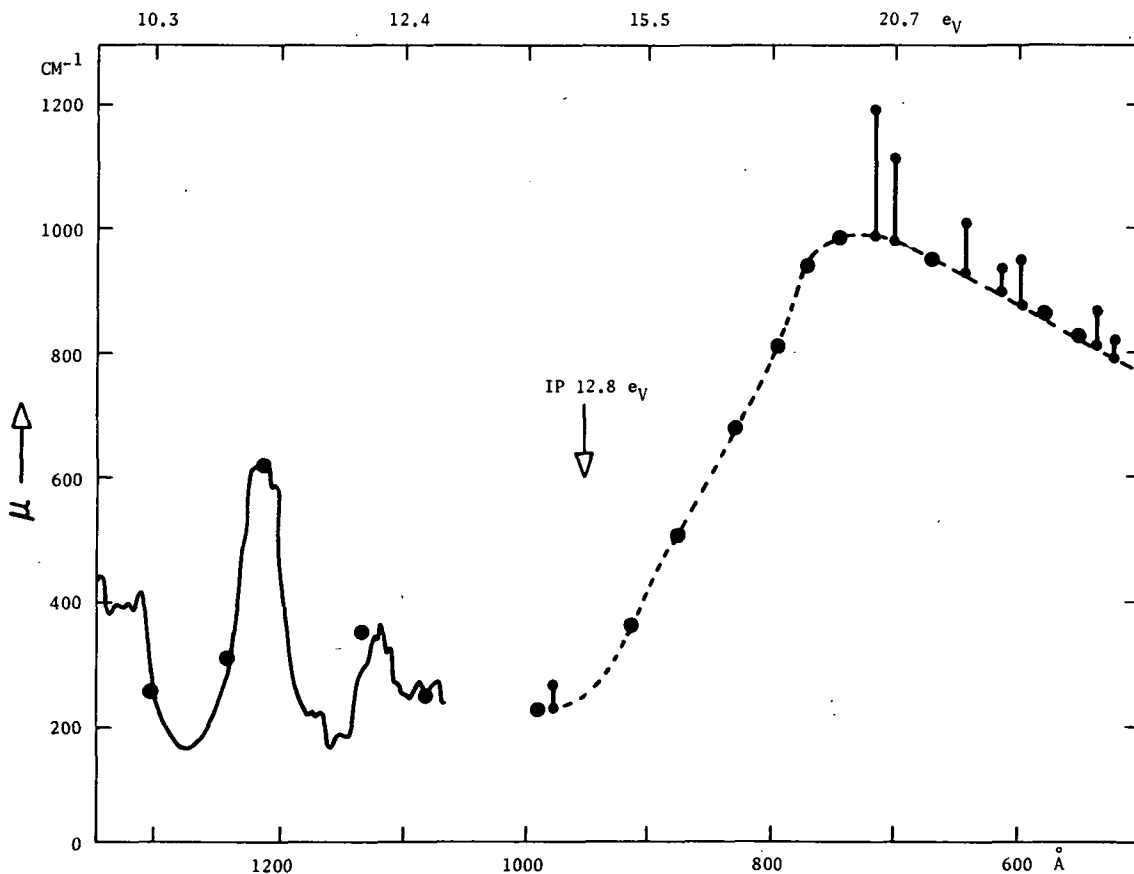

Figure (9-30). Absorption coefficient profile of O_3 for the wavelength region 1000-500Å. [Ogawa and Cook (1958)]
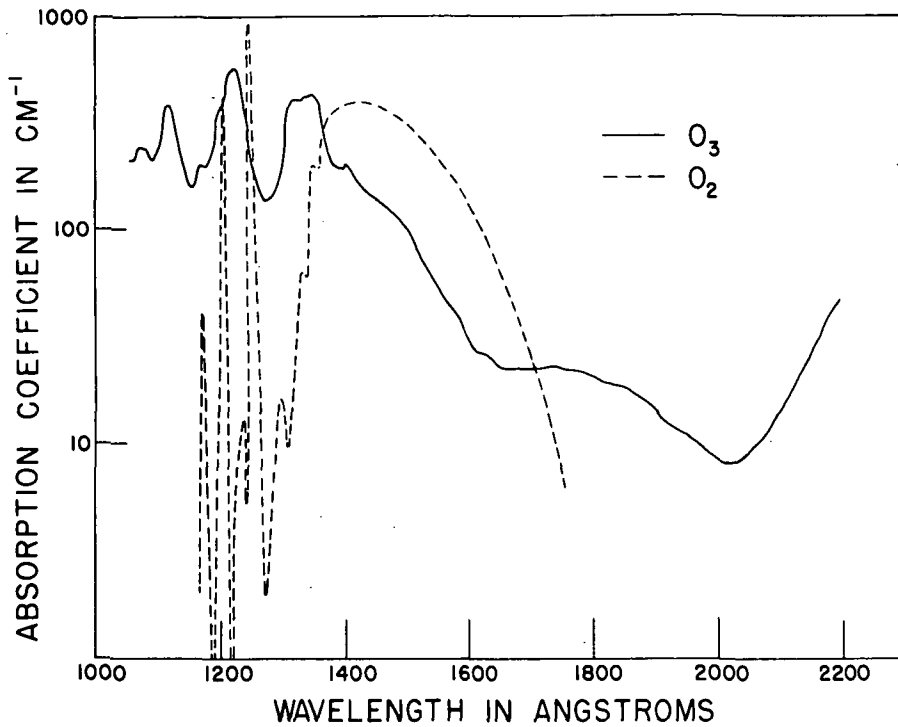
Figure (9-31). Absorption coefficient profile of O_3 for the wavelength region 2200-1050Å. [Watanabe et al. (1953)]
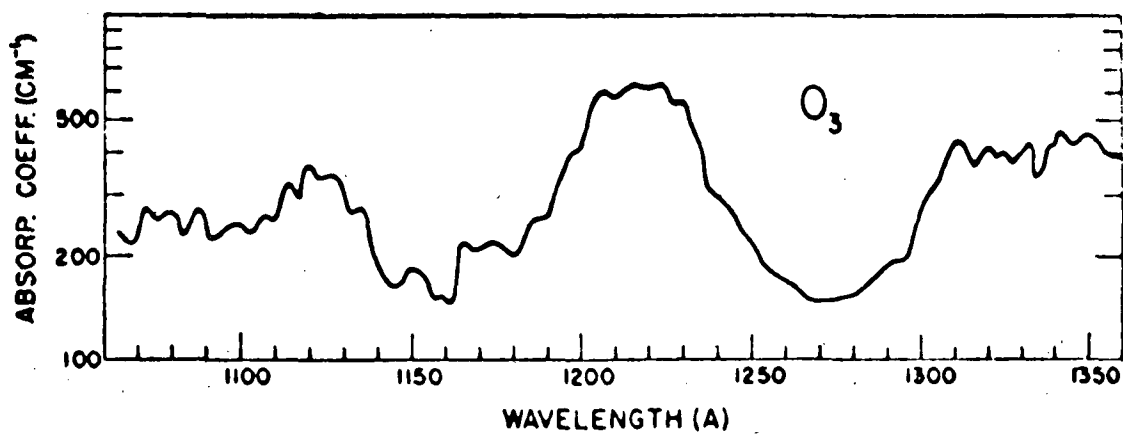

Figure (9-32). Absorption coefficient profile of O_3 for the region 1350-1000Å. [Watanabe et al. (1953)]

(2) Hartley System (3000-2000$\overset{\circ}{\text{A}}$)

   Hartley absorption represents the strongest of the absorptions by ozone. Most of
   the total heat budget of the upper atmosphere is due to absorption of the sun's
   energy by the ozone layer in the Hartley region. This spectrum consists of a
   broad absorption continuum lying between wavelength limits 3000-2000$\overset{\circ}{\text{A}}$, with a
   high and almost symmetrical peak near 2550$\overset{\circ}{\text{A}}$. A number of weak diffuse bands from
   2340$\overset{\circ}{\text{A}}$ to about 2850$\overset{\circ}{\text{A}}$ overlap the continuum. It is not yet certain whether these
   diffuse bands belong to the same electronic transition as the Huggins System (to
   be discussed next) or whether the Huggins System and the Hartley System arise from
   two entirely different transitions. However, there is an enormous difference in
   the intensity budget of the two systems. The peak of the Hartley band at 2550$\overset{\circ}{\text{A}}$
   has an absorption coefficient around 160 cm^{-1} while the absorption coefficients
   for Huggins bands range from 5 cm^{-1} at 3000$\overset{\circ}{\text{A}}$ to 0.01 cm^{-1} at 3430$\overset{\circ}{\text{A}}$ and 0.0003 cm^{-1}
   at 3650$\overset{\circ}{\text{A}}$. Figure (9-33) depicts the data of Inn and Tanaka (1953) which are con-
   sidered the most reliable so far. Recent laboratory studies made by Griggs (1968)
   using pure O_3 and a much higher resolution, (Beckman DK-1A dual beam spectrometer)
   have also yielded results concurrent with those of Inn and Tanaka. It may be remarked
   here that absorption in the Hartley bands is somewhat temperature sensitive. The
   ratio K(θ) (18°C) for θ between -72°C and -46°C varies from about 0.88 at 3100$\overset{\circ}{\text{A}}$
   to 0.97 near 2500$\overset{\circ}{\text{A}}$. At θ = -30°C this ratio is 0.92 at 3100$\overset{\circ}{\text{A}}$ and 0.98 near 2500$\overset{\circ}{\text{A}}$.

(3) Huggins System (3500-3000$\overset{\circ}{\text{A}}$)

   These ozone bands were first discovered by Huggins (1890) in the spectrum of
   Sirius and hence the name. Fowler and Strutt (1917) later identified this
   group of bands in the spectrum of the low sun. Detailed laboratory investiga-
   tions on the structure and absorption cross sections were later made by
   Jakovleva and Kondratiev, 1932; Vassy, 1937; Vigroux, 1953; Inn and Tanaka,
   1953; Griggs, 1968. The system consists of numerous diffuse and weak bands
   lying in the spectra region 3500-3000$\overset{\circ}{\text{A}}$. The short wave end of this system is
   overlapped by the Hartley continuum. These bands are relatively weak compared
   with the Hartley band and, within the short spectral span of about 500$\overset{\circ}{\text{A}}$ the
   absorption coefficient changes about 200-fold; i.e., about 5 cm^{-1} at 3000$\overset{\circ}{\text{A}}$ to
   about 0.01 at 3430$\overset{\circ}{\text{A}}$ and .0003 at 3650$\overset{\circ}{\text{A}}$ (Vigroux, 1953). The data of Inn and
   Tanaka (1953), which are almost the same as reported by Griggs (1968), are
   depicted in figure (9-33). Absorption in the Huggins bands is quite sensitive
   to temperature variation. Extensive measurements in this regard were made by
   Wulf and Melvin, 1931; Vassy, 1937; Eberhardt and Shand, 1946; Barbier and
   Chalonge, 1942; and Vigroux, 1953. A striking effect at low temperatures is
   the sharpening of the bands. This may be due in part to the shortening of the
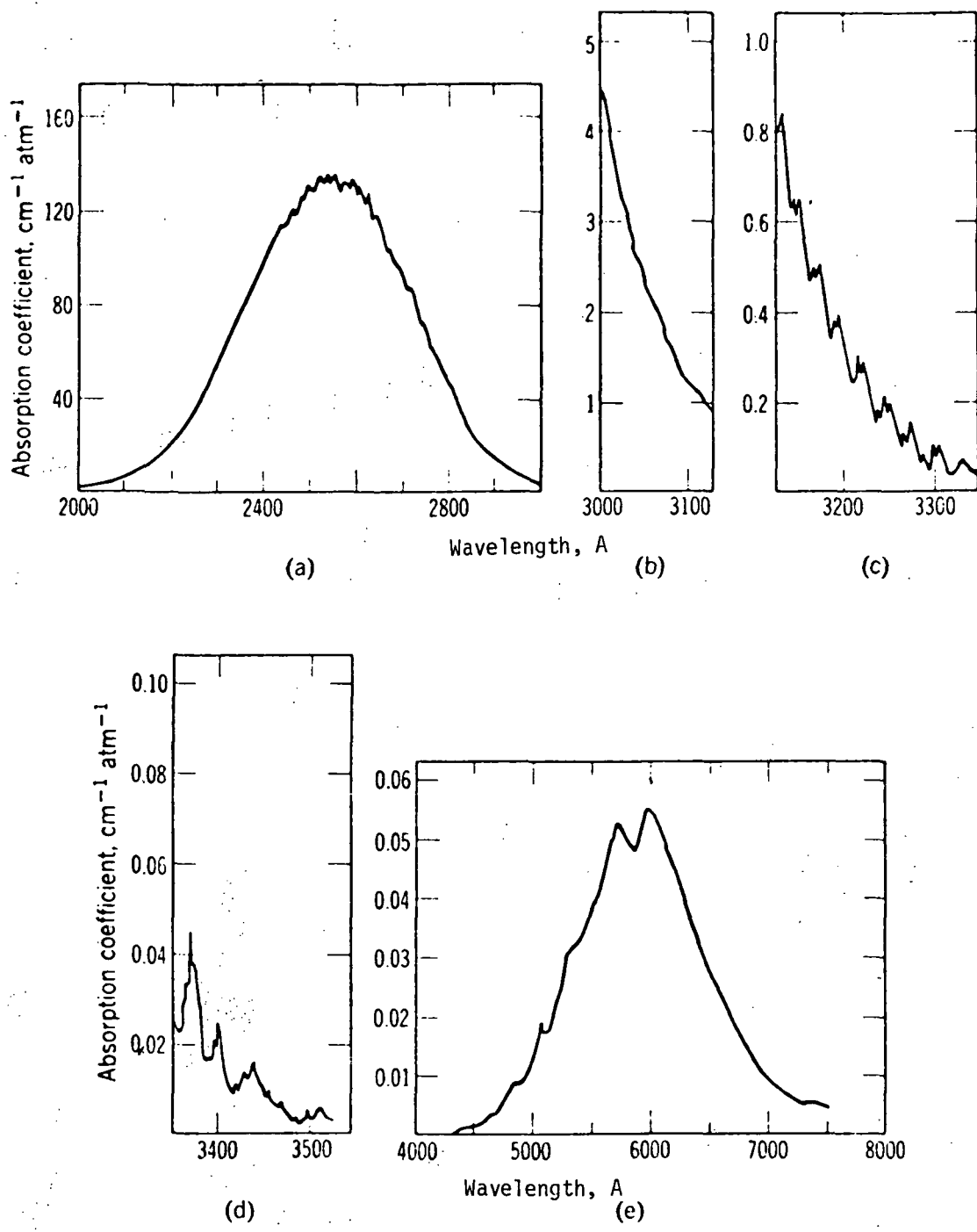   rotational branches in the bands but it may also be due to the absence of 1-1

Figure (9-33). Absorption coefficient profiles of O_3 for the region 7500-2000Å. [Inn and Tanaka (1953)]

and 2-2 bands in the bending fundamental which accompany every main band of the system. Jakovleva and Kondratiev (1932) had found several progressions in the diffuse bands overlapping the Hartley continuum. The spacing of 300 cm^{-1} in these progressions probably corresponds to the bending vibration v_2' in the upper state. The large extent of the Huggins and Hartley bands strongly suggests that there is an appreciable change of angle between the upper and lower state. The possibility that both band systems really represent only one electronic transition can not, however, be ruled out altogether.

(4) Chappuis System (8500-4400Å)

Chappuis bands form the main visible band system of the ozone absorption and occupy the spectral region 6100-5500Å. At long path lengths, the spectrum extends to shorter wavelengths merging into a weak continuum around 4000Å. The two strongest bands of the system are at 6020 and 5730Å (Wolf, 1930) and under high resolution they have been found to be genuinely diffuse (Humphry and Badger, 1947). The occurrence of predissociation at this long wavelength is quite possible in view of the dissociation energy of the molecule being around 1 eV. Absorption cross sections in this region have been measured by Vigroux, 1953; Inn and Tanaka, 1953; and recently, by Griggs, 1968. The very low absorption cross section in this region, however, renders the measurements difficult, the maximum absorption cross section being only 5 x 10^{-21} cm^{-2}. No satisfactory vibrational analysis of these bands has been proposed so far. Figure (9-34)
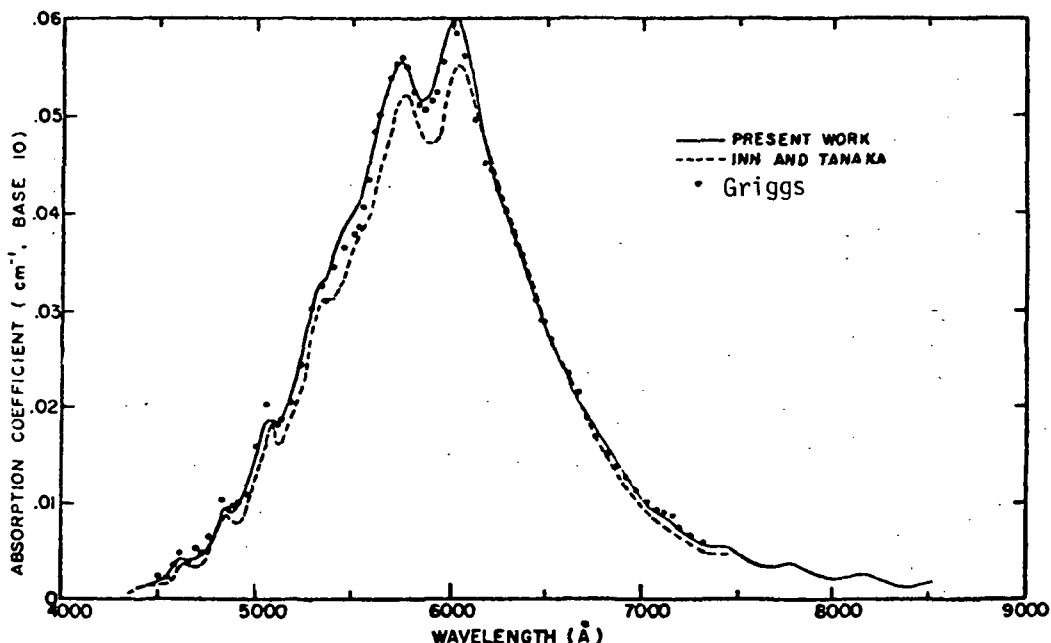

Figure (9-34). Absorption coefficient profile of O_3 for the wavelength region 8500-440Å. [Griggs (1968)]

172

depicts the absorption profile of this system, according to Vigroux, 1953. Inn and Tanaka's (1953) results for this spectrum are about 9% lower than those of Vigroux (1953). Griggs (1968) results support Vigroux (1953). Numerical data on the absorption coefficients of O_3 for the region below 3000Å can be found in Sullivan and Holland (1966) and Hudson (1971).

(5) Near Infrared System (10,000-7000Å)

Ozone gives a number of weak electronic bands in the near infrared out to 10,000Å, though the long wave limit of this absorption has not been established as yet. Wulf (1930) was probably the first to report a progression of ten members with a spacing of 567 cm^{-1}, the first one being at 10,000 cm^{-1}. Observations by Lefebvre (1934) confirm these findings. The experimental knowledge of the various excited electronic states of ozone is only limited and most of the present understanding comes from theoretical calculations. Papers by Mulliken, 1942; Mulliken, 1958; Phillips, Hunter and Sutton, 1945; Walsh, 1953; Fisher-Jhalmar, 1957; Peyerimhoff and Buenker, 1967; Hay and Goddard, 1972; Hay, Dunning and Goddard, 1973; Wang and Overend, 1974; Grimbert and Devaquet, 1975, are noteworthy in this context. Mulliken (1942) proposed the following electronic configuration for O_3.

$$(\sigma_g 2s)^2 (2s)^2 (\sigma_u 2s)^2 (\sigma_g 2P)^2 (\pi_u 2P)^2 (\pi_u 2P)^2 (2P_y)^2 (2P_x)^2 (2P_z)^2 (\pi_g 2P)^0 (\pi_g 2P)^0 (\sigma_u 2P)^0$$

$1a_1^2$	$2a_1^2$	$1b_2^2$	$3a_1^2$	$4a_1^2$	$1b_1^2$	$2b_2^2$	$2b_1^2$	$5a_1^2$	$1a_2^0$	$3b_2^0$	$4b_2^0$
		18.5	17.5	16.5	13.5	13	12.5	11.5	10.8	4.5	

The first line gives the molecular orbitals of O_2 and O_2^+, interspersed with atomic orbitals of O or O^-, in the order of ionization energy. In the second lines, symbols appropriate when there is considerable mutual interaction, are given. The third line gives the estimated ionization energies which are based on the known values for O_2 (12 eV for πg 2P, 16 eV for $\pi_u 2P$, 18 eV for $\sigma_g 2P$) and for the O atom (about 14.7 eV for an uncoupled 2P electron in O or less in O^-) after allowance for the O_2-O mutual perturbations. All of these states are depicted in figure (9-35). Recently Hay, Dunning and Goddard (1973) made extensive configuration interaction calculations on ozone for its various excited states as a function of bond length and bond angle. Reasonably accurate estimates of the vertical and adiabatic excitation energies of the equilibrium geometries of excited states were reported. Figure (9-36) schematically represents these results.
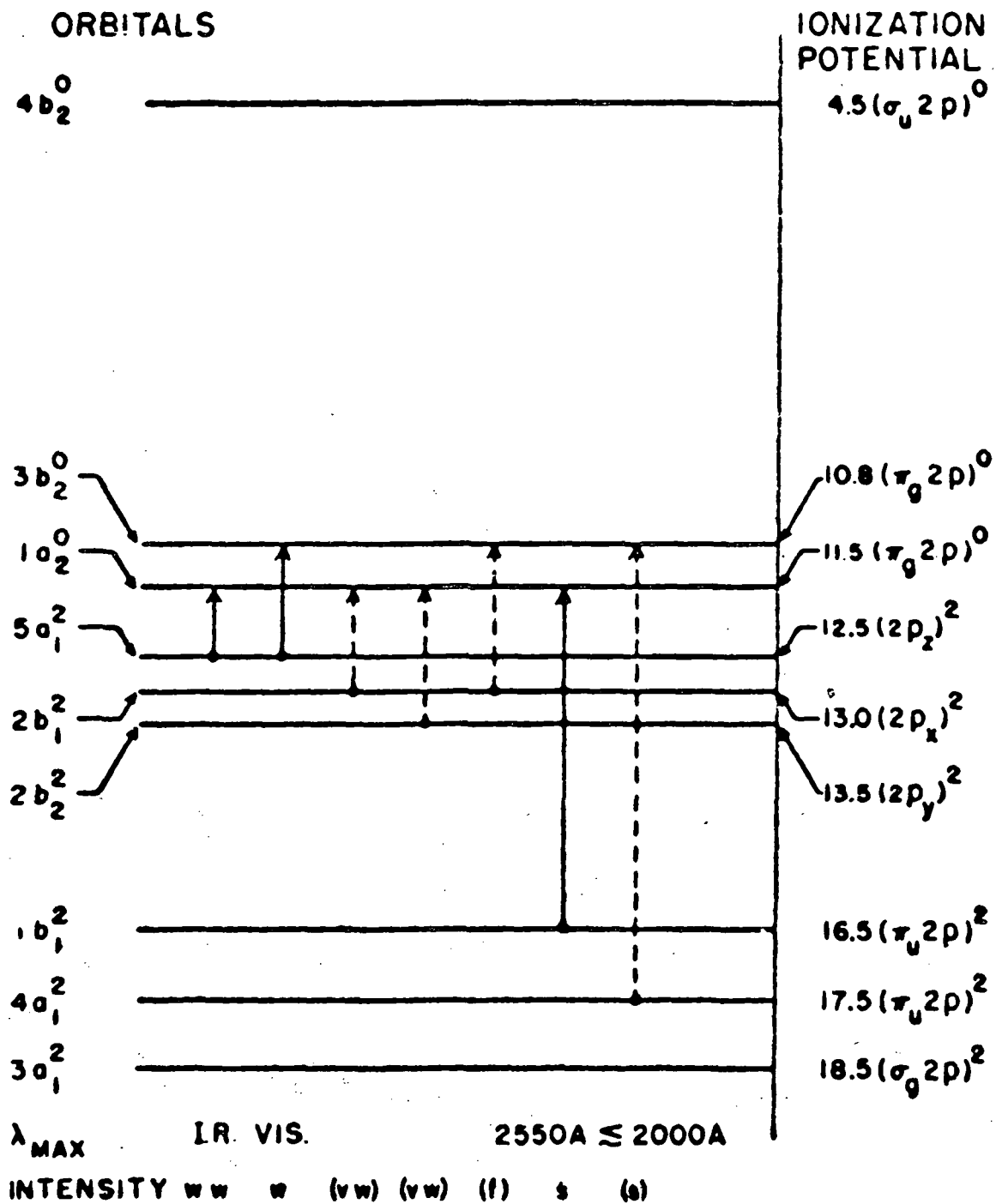
Figure (9-35). Predicted and observed electronic transitions for O_3.
[Mulliken (1942)]

Figure (9-36). Schematic showing equilibrium geometries of the various excited states of O_3 as a function of bond angle. [Hay, Dunning and Goddard (1973)]

Vibration-Rotation Spectrum. - Gaseous ozone exhibits an extensive vibration-rotation absorption spectrum. Besides the three fundamental frequencies, v_1, v_2, and v_3, a number of overtones and combinational frequencies have been identified in the region 3100-700 cm^{-1}.

Early infrared studies of ozone spectra were carried out by Lefebvre, 1935; Adel and Dennison, 1946; Wilson and Badger, 1948; Klein, Cleveland and Meister, 1951; Kaplan, Migeotte, and Neven, 1956. Vigroux, Migeotte, Neven and Swenson (1958) published a photometric atlas containing high resolution infrared spectra of ozone from 3.2 to 10.2μ. Five bands, viz., 3.27μ ($3v_3$); 3.59μ ($v_2 + 2v_3$); 4.5μ ($v_1 = v_3$); 9.01μ (v_1) and 9.59μ (v_3)

of O_3 have been detailed in this document. McCaa and Shaw (1968) recorded as many as 14 vibration-rotation bands due to O_3 but, because of poor resolution, no satisfactory analysis could be obtained. Four bands recorded in high resolution have been analyzed: ν_1 and ν_3 by Clough and Knezys, 1966; $\nu_1 + \nu_3$ by Trajmar and McCaa, 1964; and $\nu_1 + \nu_2 + \nu_3$ by Snider and Shaw, 1972. Recently, Barbe, Secroun and Jouve, 1974, recorded the infrared spectra of gaseous $^{16}O_3$ and fifteen for $^{18}O_3$. Some of the observed bands clearly present the following features:

(1) $(\nu_2 + \nu_3)$; $(\nu_1 + \nu_2 + \nu_3)$; $(2\nu_2 + \nu_3)$; $(2\nu_2 + \nu_1 + \nu_3)$; and $(2\nu_1 + \nu_3)$ exhibit characteristic Q branches, although $(2\nu_2 + \nu_3)$ and $(2\nu_2 + \nu_1 + \nu_3)$ are weak.

(2) ν_2, ν_1, $(\nu_1 + \nu_2)$, $2\nu_3$, $2\nu_1$, $(2\nu_3 + \nu_2)$ and $(2\nu_3 + \nu_1)$ correspond to the type B bands (tables 9-XIX and 9-XX). For detailed data on the rotational lines forming the various bands, one may refer to the original paper (Barbe, Secroun and Jouve, 1974). It may be mentioned here that the ν_3 fundamental (1043 cm^{-1}, 9.6μ) is the strongest of all the observed frequencies of O_3 when considering solar radiation absorption by the earth's atmosphere. It is of considerable meteorological interest because of its role in the heat balance of the upper stratosphere. This band is also instrumental to some extent in reducing the escape of terrestrial heat radiation into space and thus adding to the greenhouse effect of our atmosphere.

Rotational Spectrum. - O_3 molecule has a large dipole moment of about 0.58 Debye units and thus it exhibits an intense pure rotational spectrum in the microwave region. Hughes (1952) was probably the first to report on the microwave spectrum of the ozone molecule. Such transitions were studied more elaborately later by Trambarulo, Ghosh, Barus and Gordy (1953a, 1953b) and also by Hughes (1953). Hughes (1956) obtained quite extensive rotational spectra of six isotopic ozone molecules in the microwave region (9000-45000 MHz) and presented a satisfactory analysis, which gave remarkable consistency between the parameters for the different isotopic molecules. Hughes data are presented in Table (9-XXI). Details of the spectra of isotopic ozone molecules may be seen in the original paper (Hughes, 1956).

TABLE (9-XIX) INFRARED SPECTRUM OF $^{16}O_3$

Assignment	Observed Wave Number (cm^{-1})	Calculated (cm^{-1})	Δobs - calc (cm^{-1})
ν_2	700.93		0.0
ν_3	1042.096		0.0
ν_1	1103.15		0.0
$\nu_2 + \nu_3$	1726.4	1726.0	0.4
$\nu_1 + \nu_2$	1795.3	1795.0	0.3
$\{2\nu_3$	2058.0	$\{2057.8$	0.2
$\{2\nu_1$	2201.3	$\{2201.6$	0.3
$\nu_1 + \nu_3$	2110.79	2110.5	0.3
$2\nu_2 + \nu_3$	2409.5	2408.0	1.5
$\{2\nu_3 + \nu_2$	2725.6	$\{2725.5$	0.1
$\{2\nu_1 + \nu_2$		$\{2884.2$	
$\nu_1 + \nu_2 + \nu_3$	2785.24	2785.2	0.04
$\{3\nu_3$	3046.0	$\{3045.2$	0.8
$\{2\nu_1 + \nu_3$	3185.7	$\{3186.5$	0.8
$\{2\nu_3 + \nu_1$	3084.1	$\{3085.2$	1.1
$\{3\nu_1$		$\{3291.3$	
$2\nu_2 + \nu_1 + \nu_3$	3457.5	3458.1	0.6
$\{3\nu_3 + \nu_2$	3697.1	$\{3697.1$	0.0
$\{2\nu_1 + \nu_2 + \nu_3$	3849.4	$\{3850.2$	0.8
$\{3\nu_3 + \nu_1$	4026	$\{4026.9$	0.9
$\{3\nu_1 + \nu_3$		$\{4252.3$	

TABLE (9-XX)   INFRARED SPECTRUM OF $^{18}O_3$

Assignment	Observed Wave Number (cm^{-1})	Calculated (cm^{-1})	Δobs $-$ calc (cm^{-1})
ν_2	661.7	661.7	0.0
ν_3	984.6	984.6	0.0
ν_1	1041.9	1041.9	0.0
$\nu_2 + \nu_3$	1631.2	1631.5	0.3
$\nu_1 + \nu_2$	1695.9	1695.9	0.0
$\begin{cases}2\nu_3\end{cases}$	1945.4	1946.0	0.6
$\begin{cases}2\nu_1\end{cases}$	2079.4	2079.6	0.2
$\nu_1 + \nu_3$	1995.1	1995.1	0.0
$\begin{cases}2\nu_3 + \nu_2\end{cases}$	2579.5	$\begin{cases}2578.4$	1.1
$\begin{cases}2\nu_1 + \nu_2\end{cases}$		$2725.6\end{cases}$	
$\nu_1 + \nu_2 + \nu_3$	2634.3	2634.3	0.0
$\begin{cases}3\nu_3\end{cases}$	2883.2	$\begin{cases}2882.3$	1.1
$\begin{cases}2\nu_1 + \nu_3\end{cases}$	3012.6	$3011.9\end{cases}$	0.9
$2\nu_2 + \nu_1 + \nu_3$	3271.0	3271.7	0.7
$\begin{cases}3\nu_3 + \nu_2\end{cases}$	3501.4	$\begin{cases}3501.2$	0.2
$\begin{cases}2\nu_1 + \nu_2 + \nu_3\end{cases}$		$3642.0\end{cases}$	
$\begin{cases}3\nu_3 + \nu_1\end{cases}$	3814.1	$\begin{cases}3815.2$	1.1
$\begin{cases}3\nu_1 + \nu_3\end{cases}$		$4020.0\end{cases}$	

TABLE (9-XXI) MICROWAVE SPECTRUM OF OZONE $^{16}O_3$

Identification	Observed Frequency (MHz)	Calculated Frequency (MHz)	Difference
$21_{2,20} \rightarrow 20_{3,17}$	9.201	9.228	+ 27
$9_{2,8} \rightarrow 10_{1,9}$	10.226	10.209	- 17
$3_{1,3} \rightarrow 4_{0,4}$	11.073	11.073	0
$24_{3,21} \rightarrow 23_{4,20}$	15.116	14.795	-321
$26_{4,22} \rightarrow 27_{3,25}$	16.413	16.219	-194
$19_{2,15} \rightarrow 18_{3,15}$	23.861	23.912	+ 51
$46_{6,40} \rightarrow 45_{7,39}$	25.300	25.235	- 65
$39_{5,35} \rightarrow 38_{6,32}$	25.511	25.790	+279
$17_{1,17} \rightarrow 16_{2,14}$	25.649	25.634	- 15
$40_{6,34} \rightarrow 41_{5,37}$	27.862	28.246	+384
$25_{3,23} \rightarrow 24_{1,20}$	28.960	29.060	+100
$16_{2,14} \rightarrow 15_{3,13}$	30.052	30.096	+ 44
$15_{1,15} \rightarrow 14_{2,12}$	30.181	30.141	- 40
$19_{1,19} \rightarrow 18_{2,16}$	30.525	30.578	+ 53
$22_{3,19} \rightarrow 23_{2,22}$	36.023	36.000	- 23
$17_{3,15} \rightarrow 18_{2,16}$	37.832	37.962	+130
$2_{0,2} \rightarrow 1_{1,1}$	42.833	42.833	0
$13_{1,13} \rightarrow 12_{2,10}$	43.654	43.621	- 33

Nitrous Oxide (N_2O)

Dipole Moment, M: 0.166 Debye

Ionization Potential, I.P.: 12.89 eV

Dissociation Energies: D (N_1-O) - 1.677 eV; D_2(N-NO) - 4.930 eV

Ground Electronic State Configuration: $\sigma^2\sigma^2\pi^4\pi^4 - {}^1\Sigma^+$

Fundamental Vibration Frequencies:

ν_1	ν_2	ν_3
1284.9	588.8	2223.8 (cm^{-1})

Rotational Constants:

B_0	r_0(N-N)	r_0(N-O)
0.419 cm^{-1}	1.128Å	1.184Å

Nitrous Oxide, commonly known as "laughing gas" is a colorless gas with a faint smell. It condenses to a colorless limpid liquid at 0°C under 30 atm. pressure. Gaseous nitrous oxide resembles oxygen in its behavior towards combustion; therefore, it is sometimes mistaken for oxygen in that respect.

Nitrous oxide molecule (N_2O) is a linear, non-symmetrical triatomic molecule, characterized by the point group symmetry $C_{\infty v}$. It possesses 16 valence electrons and two characteristic single bonds, viz., N-N and N-O. Its geometrical disposition is illustrated in figure (9-37).

$$\overset{N}{\circ} \; r_e \text{ (N-N)} \; \overset{N}{\circ} \; r_e \text{ (N-0)} \; \overset{0}{\circ}$$

Figure (9-37). Geometrical configuration of N_2O.

There exists as many as twelve stable isotopic forms of nitrous oxide formed by the different combinations of N^{14}, N^{15}, N^{16}, and O^{16}, O^{17}, O^{18} atomic isotopes of nitrogen and oxygen, respectively. The most abundant species is $N_2^{14}O^{16}$.

Molecular Spectrum

The observed spectra of N_2O can be classified into the following three groups:
(1) Electronic Spectrum, (2) Vibration-Rotation Spectrum, and (3) Rotational Spectrum.

Electronic Spectrum. - Nitrous oxide exhibits a fairly rich electronic spectrum that extends from 3100Å through 100Å in the extreme vacuum ultraviolet. The spectral features are mostly characterized by several continua, superimposed by banded structures in some cases. Several workers in the past carried out extensive investigations on these features

(Leifson, 1926; Dutta, 1932; Henry, 1934; Sen Gupta, 1935; Duncan, 1936; Sponer and Bonner, 1940; Romand and Mayence, 1949, 1955; Zelikoff, Watanabe and Inn, 1953; Astoin and Mayence, 1955; Walker and Weissler, 1955; Astoin, 1957; Young, 1960; Tanaka, Jursa and LeBlanc, 1960; Thompson, Harteck and Reeves, Jr., 1963; Cook and Ching, 1965; and Cook, Metzger and Ogawa, 1967, 1968).

For the sake of convenience in discussion, we can divide the observed spectra in the following spectral regions:

(1) 3065-2100Å

Dutta (1932) was probably the first to observe the tail of an absorption continuum near 2600Å in this region. Sponer and Bonner (1940) reported three absorption continua in this region, viz., (a) starting at 3065Å with a flat maximum near 2900Å, (b) starting at 2820Å with $\lambda_{max} \sim 2730$Å, and (c) starting at 2600Å with $\lambda_{max} \sim 1820$Å. The third continuum, superimposed by a few weak diffuse bands, was later found by Zelikoff, Watanabe and Inn (1953), who also pointed out that these features might involve an electronic transition that is quite different from the one responsible for the continuum. These continua have been correlated with the following dissociation processes of N_2O (Sponer and Bonner, 1940; Zelikoff, et al., 1953).

(a) N_2O ($^3\Pi$ or $^3\Sigma$) → N_2 ($^1\Sigma$) + O(^3P) - - - (1.71 eV)

(b) N_2O ($^1\Sigma$, $^1\Pi$ or $^1\Delta$) → N_2 ($^1\Sigma$) + O(^1D) ⎤
         or   ⎥ - - - - (3.68 eV)
    N_2O ($^3\Pi$) → NO ($^2\Pi$) + N(^4S)   ⎦

(c) N_2O ($^1\Sigma$) → N_2 ($^1\Sigma$) + O(^1S) - - - (5.9 eV)
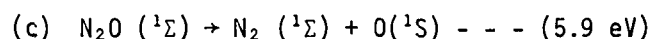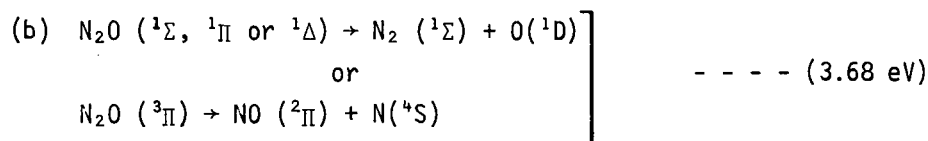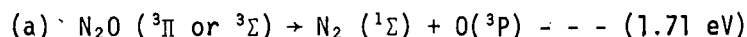
(2) 2100-1600Å

This spectral region is occupied by a weak continuum superimposed by a few weak diffuse bands for which no satisfactory analysis has been proposed so far. The weak character of these bands indicates that perhaps this transition is forbidden. In this case too, it may be that two different transitions are involved; i.e., one giving rise to the banded structure and other to the weak continuum (Duncan, 1936; Zelicoff et al., 1953; Thompson et al., 1963).

(3) 1600-1380Å

Absorption in this spectral region is characterized by a broad continuum on which are superimposed a number of diffuse bands, Table 9-XXII (Duncan, 1936; Zelikoff, et al., 1953) give the details. ν_{max} values for these bands could be represented by the following equation:

$$\nu = 59590 + 1005n - 30.0n^2 + 0.53n^3 \text{ where } n - 0, 1, 2, - -$$

The band spacing in the progression is found to be 800 cm^{-1} at the long nd and 400 cm^{-1} at the short end. The strongest absorption lies at $\nu = 6\cdot 30\ cm^{-1}$. The continuum is broad and symmetrical, with λ_{max} at 68940 cm^{-1}.

TABLE 9-XXII ABSORPTION OF N_2O IN THE SPECTRAL REGION 1600-1380Å

n	Calculated	Observed	$\Delta\nu$	Relative Intensity
0	59,590	59,520	70	0.06
1	60,565	60,510	55	0.08
2	61,484	61,580	-96	0.18
3	62,349	62,460	-111	0.20
4	63,164	63,250	-86	0.68
5	63,931	64,020	-89	1.68
6	64,654	64,720	-66	1.60
7	65,337	65,360	-23	5.0
8	65,981	65,980	1	8.0
9	66,591	66,580	11	24
10	67,173	65,160	13	43
11	67,720	67,700	20	70
12	68,246	68,210	36	102
13	68,749	68,730	19	102
14	69,234	69,230	4	69
15	69,703	69,710	-7	44
16	70,160	70,180	-20	17
17	70,609	70,650	-41	1
18	71,050	71,100	-50	1
19	71,490	71,530	-40	1
20	71,930	71,940	-10	1

(4) 1380-1215Å

Absorption in this region is characterized by a number of weak diffuse bands and also a sharp band, superimposed over a broad continuum (Zelikoff, Watanabe and Inn, 1953). Duncan (1936) earlier had reported only a structureless smooth continuum for this region. Wave numbers of these bands are:

(a) 77100 cm^{-1}

(b) 76250 cm^{-1} Diffuse Bands

(c) 75600 cm^{-1}

(d) 75100 cm^{-1}

(e) 77400 cm^{-1} Sharp Band

The underlying continuum is quite symmetrical with $\lambda_{max} \sim 77900$ cm^{-1}. According to Zelikoff, Watanabe and Inn (1953), the sharp band might be the first member (n = 3) of a Rydberg series represented by the following equation:

$$\nu = 102567 - \frac{R}{(n - 0.92)^2} \quad \text{where } n = 3, 4, 5.$$

Duncan (1936) classified the continuum peak to correspond to this Rydberg series rather than the band peak. It is probable that more than one excited state is involved in the appearance of these features; and one state may be repulsive which accounts for the continuum.

(5) 1215-1080Å

Numerous diffuse bands superimposed over a broad continuum characterize the absorption profile of N_2O in this region. Approximate wavenumbers of the various band peaks are: (a) 85450 cm^{-1}; (b) 85800 cm^{-1}; (c) 86200 cm^{-1}; (d) 86700 cm^{-1}; (e) 87500 cm^{-1}; (f) 88500 cm^{-1}; (g) 89450 cm^{-1}; (h) 90400 cm^{-1}; (i) 91000 cm^{-1}; and (j) 91800 cm^{-1}. The underlying continuum is asymmetric with a maximum, most probably, at 1080Å. Its intensity falls rapidly from 1080 to 1060Å. According to Duncan (1936), who proposed a tentative analysis of the various spectral features of N_2O absorption in this region, this underlying continuum corresponds to an electronic transition which is different from the one that is involved in the banded structure. Apart from the above mentioned weak bands, there appears another band at 84,900 cm^{-1} (λ_{max}) which is the strongest of all the known ultraviolet absorption bands for N_2O. Its absorption coefficient at λ_{max} is estimated to be 3010 cm^{-1}. Whether the diffuse bands form two different Rydberg series or represent other electronic transitions cannot be ascertained in view of the uncertain measurements on account of diffuseness. The absorption cross section profiles for the region 2100-1080Å in four wavelength segments is presented in figure (9-38).

(6) Below 1000Å

The absorption spectrum of N_2O in the spectral region below 1000Å consists of several series of Rydberg bands and also a few progressions of non-Rydberg bands, superimposed on underlying ionization and dissociation continua (Dunca, 1936; Walker and Weissler, 1955; Astoin and Mayence, 1955;
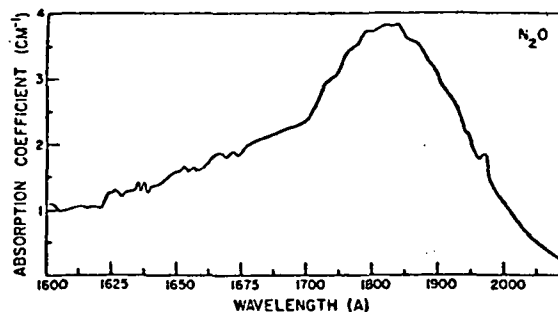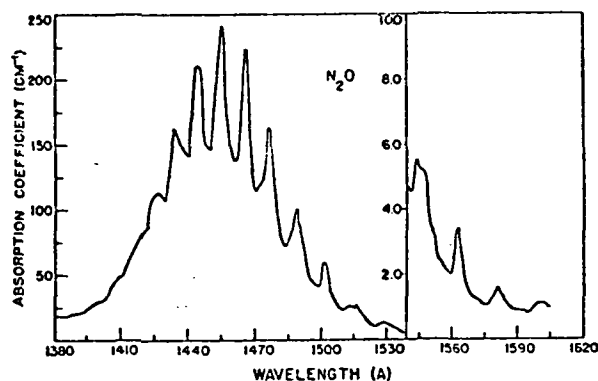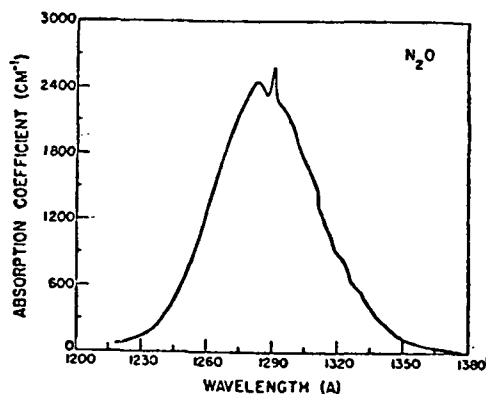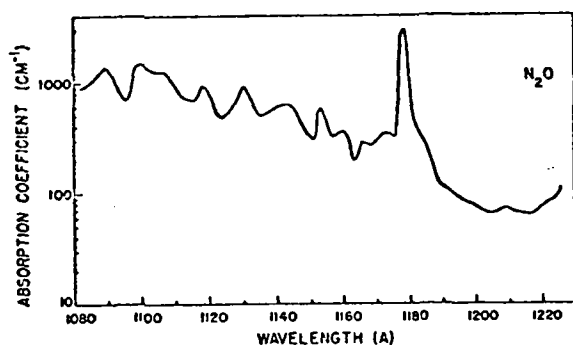
Figure (9-38). Absorption coefficient profiles of N_2O for the wavelength region (1080-2100Å). [Watanabe et al. (1953) AFCRL Report]

Astoin, 1957; Tanaka, Jursa and LeBlanc, 1960; Cook and Ching, 1965; Cook, Metzger and Ogawa, 1968). Following are the results of the paper of Cook, et al., which agree fairly well with those of Tanaka, et al. It may be mentioned here that while the former group used a photoelectric method for scanning the absorption, the latter employed the high resolution photographic technique. These results with regard to different wavelength segments are discussed as follows.

(a) 1000-960Å

There exist two Rydberg series (I and II) in this region which converge to the first ionization limit of N_2O. Tanaka, et al., (1960) had represented these series by the following formulae:

184

$$\nu(I) \ = \ 10400 - R/(n - 0.60)^2$$

$$\nu(II) = 104300 - R/(n - 0.68)^2$$

and identified members up to n = 13 in series (I) and n = 9 in series (II).
The corresponding bands. with the same n in both the series form close
doublets and converge to 12.89 eV and 19.93 eV, respectively. The values.
approximate to the first ionization potential of N_2O. The 300 cm^{-1}
difference in the two series limits perhaps indicates that the ground
state of N_2O^+ is $^2\Pi$ and that its doublet separation is about this
magnitude. Ogawa, et al., (1968) identified members up to n = 9 in both
the series and in addition identified two rather strong bands with 990.5Å
and 966.0Å, respectively. The onset of the ion current occurring at
961.8Å is in good agreement with the convergence limit of Series I as
reported by Tanaka, et al. No verification could be obtained about
Tanaka's series II limit although numerous bands of this series could
be clearly identified.

(b) 960-850Å

This region is covered by a continuum rising from k = 340 cm^{-1} at
960Å to k = 850 cm^{-1} at 850Å. Overlapping the continuous absorption
are several discrete bands belonging to two progressions called P(4)
and P(5).

(c) 850-750Å

The following three Rydberg series (series III, IV and V) bands
identified in this spectral region by Tanaka, et al. (1960), are
represented by the following equations:

$$\nu(III) = 132210 - \frac{R}{(n - 1.0)^2}$$

$$\nu(IV) = 132250 - \frac{R}{(n - .22)^2}$$

$$\nu(V) = 133490 - \frac{R}{(n - .11)^2}$$

While in series III, and IV, members from n = 3 to 13 and n = 3 to 8,
respectively, have been identified, in series V only the members from
n = 8 to 12 could be located. Series V may be the vibration series
associated with series IV. These series converge to the second ioniza-
tion potential of N_2O (16.39 eV). Series III is stronger than series
IV and their individual bands showed almost no shading. The vibration
frequencies of the upper states in both series are about 1300 cm^{-1}

which approaches the value $\nu_1 = 1288\ cm^{-1}$ for the ground state of the molecule.. Ogawa, et al., identified most of the bands in these series. The n = 3 member of series III (836.$\overset{\circ}{A}$) was found to have an especially strong absorption coefficient equal to 2780 cm^{-1}.

(d) 750-600$\overset{\circ}{A}$

This spectral region is occupied by bands belonging to Rydberg series VI, VII, VIII and IX and in the longer wavelength range by several unidentified bands. According to Tanaka, et al., (1960) these Rydberg series are expressed by the following relations:

$$\nu(VI) = 162130 - \frac{R}{(n - .31)^2} \; ; \; n = 3, 4, 5 - - -$$

$$\nu(VII) = 162200 - \frac{R}{(n - .06)^2} \; ; \; n = 3, 4, 5 - - -$$

$$\nu(VIII) = 162200 - \frac{R}{(n - .58)^2} \; ; \; n = 3, 4, 5, 6 - -$$

$$\nu(IX) = 162200 - \frac{R}{(n - .68)^2} \; ; \; n = 3, 4 - - -$$

The absorption and photoionization coefficients for the wavelength segments (a) 810-600$\overset{\circ}{A}$ and (b) 1000-790$\overset{\circ}{A}$ are presented in figures (9-39) and (9-40). Figure (9-41) presents the overall absorption profile for the entire region 1000-600$\overset{\circ}{A}$. Further, while series VI and VIII are absorption series, series VIII and IX have been designated by Tanaka et al., as "Apparent Emission Series." The bands in these two series give an appearance of emission bands, though recorded in absorption experiments. In fact, they are the reduced absorption bands in the ionization continua. All these series converge to a frequency which corresponds to the third ionization limit of N_2O (20.1 eV). Series VII is stronger than series VI and the doublet separation in both cases diminishes rather rapidly as n increases. Ogawa, et al., (1968) identified lower members of these four series in their absorption and ionization measurements. However, because of overlapping of the apparent emission bands and the absorption bands, no reliable data could be obtained.

(e) Below 600$\overset{\circ}{A}$

Astoin and Mayence (1955) extended the study of N_2O absorption to 150$\overset{\circ}{A}$ in the vacuum ultraviolet. The absorption spectrum consists of three band systems superimposed on a continuum in each case in the region 1000-150$\overset{\circ}{A}$. The first continuum (600,000-400,000 cm^{-1}) is very weak at the shorter wavelength side of the spectrum. On the longer wavelength side, it starts with a discontinuity near 380,000 cm^{-1} (47.5 eV), which may be ascribed to

an ionization potential of the N_2O molecule. The second continuum is of a more symmetrical shape and the third, beyond 500Å, shows an absorption discontinuity near 104,000 cm^{-1}, which agrees closely with the first ionization potential of N_2O (12.9 eV) observed in electron impact experiments. Figure (9-42) depicts the absorption cross section profile for this region. Figure (9-43) presents a schematic showing different potential energy curves of N_2O (Zelikoff et al., 1953).
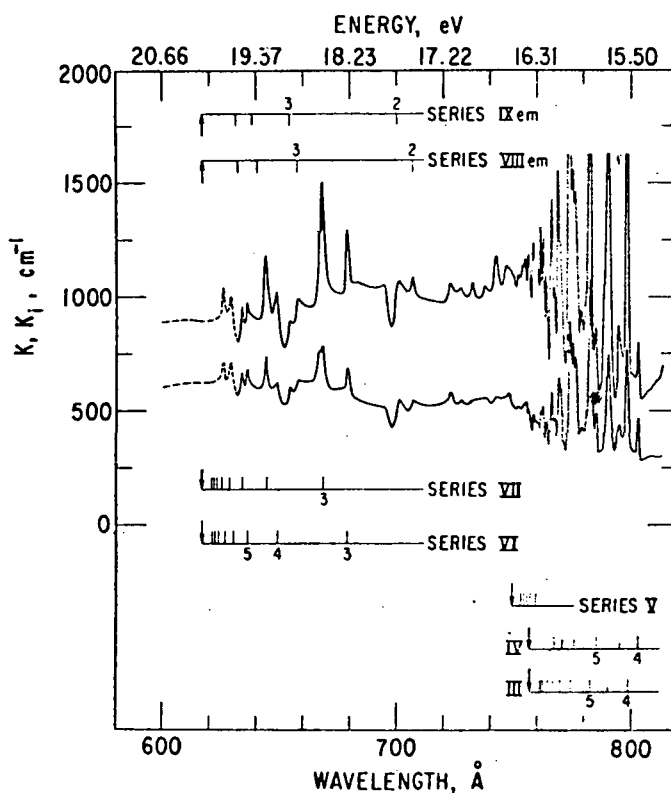

Figure (9-39). Absorption and photoionization coefficient of N_2O in the region 810-600Å. [Cook et al., 1968]
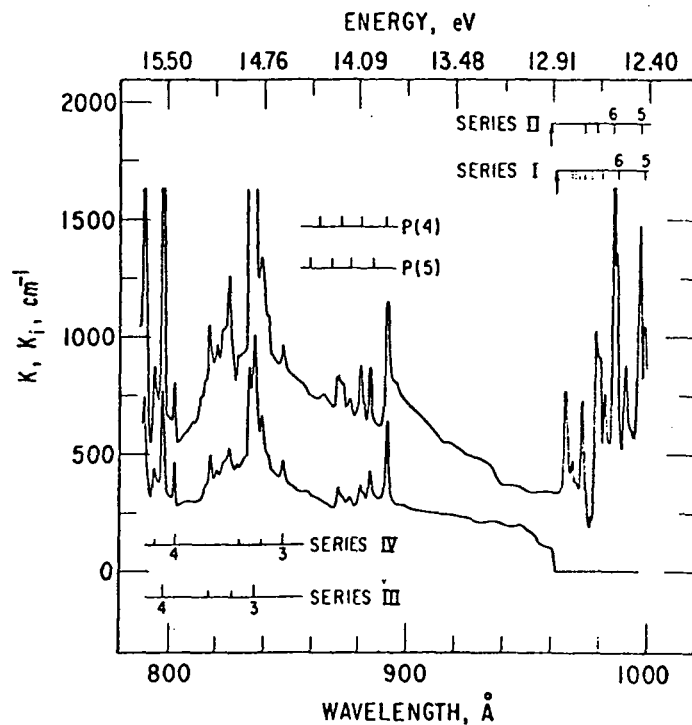
Figure (9-40). Absorption and photoionization coefficients at N_2O in the region 1000-790Å. [Cook et al., 1968]
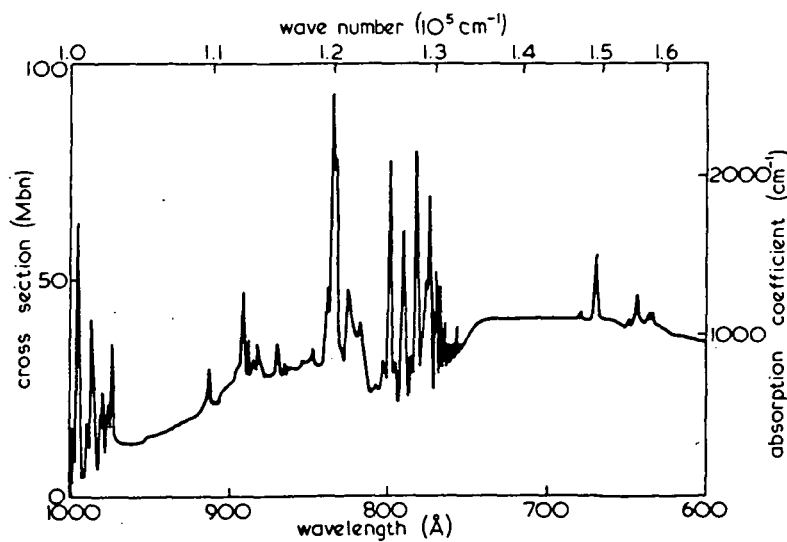
Figure (9-41). Total absorption cross sectional profile of N_2O for the entire region 1000-600Å. [Cook and Ching, 1965]
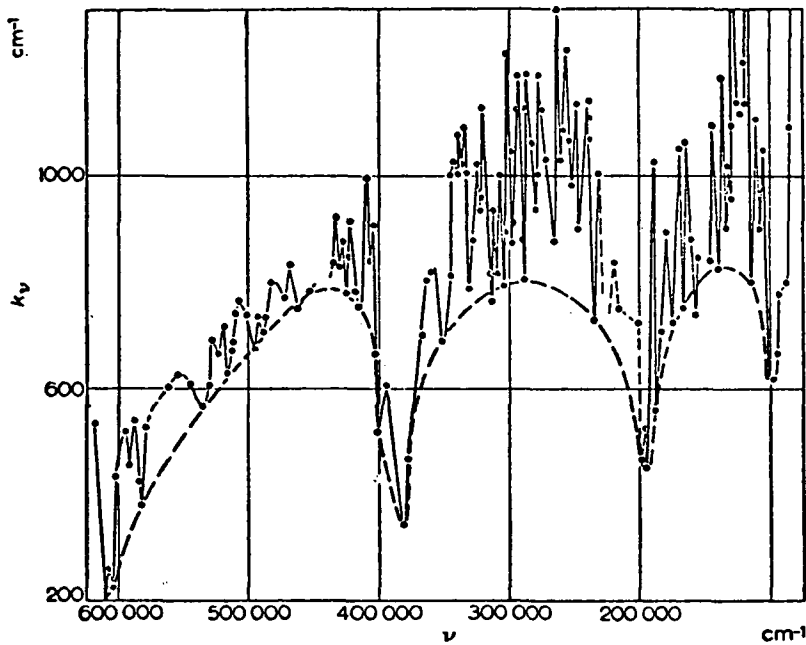
Figure (9-42). Absorption cross section profile of N₂0 for the region 1000-150Å.
[Astoin and Granier - Mayence, 1955]

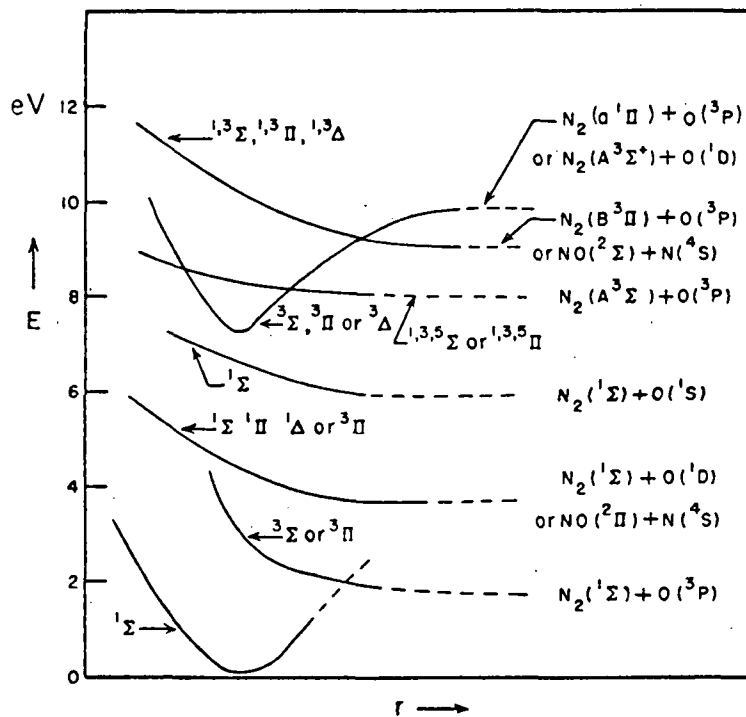Figure (9-43). Schematic showing different potential energy curves of N₂0.
[Zelikoff et al. (1953)]

Vibration-Rotation Spectrum. - Nitrous oxide (N_2O) exhibits a rich vibration-rotation spectrum that covers a wide spectral range in the infrared region. While most of this spectrum has been studied in absorption, quite a number of these transitions have been observed in emission as well.

In addition to the three fundamental frequencies, viz., ν_1, ν_2 and ν_3, which are both infrared and Raman active, many overtones; combinational frequencies and higher state bands have been reported in the laboratory spectra. These bands lie in the region from 500 cm^{-1} through 10,000 cm^{-1}. Prominent band frequencies are tabulated in Table (9-XXIII). The solar spectrum also exhibits some of these bands (Table 9-XXIV).

Important references that cover most of the work on the infrared absorption of N_2O are: Herzberg and Herzberg, 1950; Thompson and Williams, 1951; Thompson and Williams, 1953; Douglas and Mollar, 1954; Lakshmi and Shaw, 1955; Lakshmi, Rao and Nielsen, 1956; Plyler, Tidwell and Allen, 1956; Clough, McCarthy and Howard, 1959; Tidwell, Plyler and Benedict, 1960; Rank, Eastman, Rao and Wiggins, 1961; Fraley, Brim and Rao, 1962; Gross and McCubbin, 1964; Pliva, 1964; Plyler, Tidwell and Maki, 1964; Gordon and McCubbin, 1964; Pliva, 1968; Griggs, Rao, Jones and Potter, 1968; Mantz, Rao, Jones and Potter, 1969; Pearson, Sullivan and Frenkel, 1970. Burch, Gryvnak and Pembrook (1972) have presented a survey of most of this work.

Lately, Krell and Sams (1974) reported a detailed study of the N_2O infrared absorption in the region 2265-2615 cm^{-1} and presented extensive data on the rotational constants for a large number of vibrational states. Farreng, Gaultier and Rossetti (1974); and Farreng and Dupre-Maquaire (1974) reported high resolution measurements on the vibrational luminescence of N_2O as obtained in a N_2O - N_2 plasma discharge and identified as many as 15 vibrational transitions in the spectral range of the fundamental (4.7μm).

Amiot and Guelachvili (1974) recorded the $N_2^{14}O^{16}$ infrared absorption (1.2 - 3.3μ) using the Fourier transform technique and presented extensive data on a large number of bands. Rotational constants for as many as 51 vibrational states have been presented. For details, refer to the original articles.

Rotational Spectrum. - Pure rotational transitions in nitrous oxide have been studied up to J 19 → 20 in the microwave region at 25123 MHz (Bloor et al., 1961). These authors made precise measurements on a number of rotational transitions; e.g., J 14 → 15; J 15 → 16; J 16 → 17; J 17 → 18; J 18 → 19 and J 19 → 20 in the region 600-800 cm^{-1}.

Earlier investigations that cover mostly the lower transitions are those of Coles., et al., 1947; Smith et al., 1948; Coles and Hughes, 1949; Jen, 1949; Townes, et al., 1949; Shulman, et al., 1949, 1950; Johnson et al., 1951; Tetenbaum, 1952; Douglas and Moller, 1954; Palik and Rao, 1956; Burrus and Gordy, 1956; White, et al., 1957; Costain, 1958; Pierce, 1959; Brit, et al., 1961. Details may be seen in the original papers.

TABLE (9-XXIII) N₂O BANDS IN THE SPECTRUM

$\nu_1\nu_2{}^l\nu_3 \rightarrow \nu_1\nu_2{}^l\nu_3$		Obs. ν and Band Type		Calc. ν
0000	0110	589.0	'	*
	0200	1167.3	"	*
	1000	1285.4	"	*
	1110	1868	"	1869.6
	0001	2224.1	"	*
	1200	2462.2	"	*
	2000	2564.2	"	*
	0111	2799.1	'	2799.2
	0201	3366.5	"	*
	1001	3482.2	"	*
	0002	4420.7	"	*
	200ī	4736.0	"	4733.7
0110	0200	579.5	'	578.3
	0220	590.5	'	*
	1220	1845	'	1866.4
	1200	1829	'	1854
	0201	2777	'	2777.4
	0221	2786	'	2789.7
0000	1000	1283	Raman	1285.4
	0001	2226	Raman	2224.1

TABLE (9-XXIV) N₂O BANDS IN THE SOLAR SPECTRUM

cm^{-1}	μ	Transition	Type	Molecular Band Strength Under Standard Conditions (cm)
4730.86	2.11	00°0-20°1	Parallel	
4630.31	22.16	00°0-12°1	"	
4417.51	2.27	00°0-00°2	"	
4389.06	2.28	01¹0-01¹2	"	
3481.2	2.87	00°0-10°1	"	$1.29.10^{-18}$
3365.6	2.97	00°0-02°1	"	
2798.6	3.57	00°0-01¹1	Perpendicular	9.10^{-20}
2577	3.88	01¹0-21¹0	Parallel	
2563.5	3.90	00°0-20°0	"	$1.6.10^{-18}$
2461.5	4.06	00°0-12°0	"	$4.3.10^{-10}$
2223.5	4.50	00°0-00¹1	"	$6.88.10^{-17}$
2210	4.52	01¹0-01°1	"	
1285.0	7.78	00°0-10°0	"	$9.78.10^{-18}$
1167.0	9.56	00°0-02°0	"	$4.08.10^{-19}$
588.8	17.0	00°0-01¹0	Perpendicular	$7.75.10^{-19}$

Hydrogen (H_2)

Dipole Moment, M: Zero

Ionization Potential, I.P.: 15.422 eV

Dissociation Energy, D(H-H): 4.476 eV

Ground Electronic State Configuration: $(1s\sigma)^2 - {}^1\Sigma_g^+$

Ground State Vibration Frequency and Anharmonicity Constants: ω_e = 4403.186 cm^{-1};

$\omega_e x_e$ = 121.34 cm^{-1};

$\omega_e y_e$ = 0.8129 cm^{-1}

Rotational Constants:

B_e	α	r_e(H-H)
60.8679 cm^{-1}	3.0622 cm^{-1}	0.74116Å

Hydrogen is a colorless, odorless, tasteless gas, which is lighter than air. It is combustible but does not support combustion. The critical temperature for hydrogen is about -240°C and just below this point, a pressure of about 20 atm. turns the gas into a clear and colorless liquid of density 0.07 gm/ml. If liquid hydrogen is evaporated in a partial vacuum, we get solid crystalline hydrogen, which is white in color, and has a specific gravity 0.08.

Hydrogen (H_2) is perhaps the simplest stable molecule known in nature. Basically it is composed of four elementary particles viz., two protons and two electrons held together by electrostatic forces. If the spins of the two electrons are aligned in such a way that the electron moments are anti-parallel, the two hydrogen atoms form a stable molecule but in the case where these moments are parallel, the two H-atoms fly apart and we do not have any molecular formation.

Two types of molecular hydrogen exist in nature, viz., ortho-hydrogen and para-hydrogen. At room temperatures, molecular hydrogen which has its ortho and para forms in equilibrium contains about 75% ortho and 25% para varieties. Hydrogen occurs in the following principal isotopic forms; H_2, D_2, T_2, HD, HT, DT (D = ^{2}H; T = ^{3}H).

Molecular Spectrum

In spite of having a simple structure, hydrogen exhibits a very complicated electronic spectrum consisting of thousands of lines. Since H_2 does not possess a permanent electric dipole moment, it does not exhibit any vibration-rotation or pure rotational spectrum under normal conditions. Certain pressure-induced and quadrupole rotation vibration transitions have, however, been observed. Isotopically substituted molecules such as HD and HT have a lower symmetry however, and therefore, the electric dipole moment in the free molecule is not zero. Vibration-rotation and pure rotational

transitions in respect of such forms of molecular hydrogen have been obtained and studied quite extensively (Herzberg, 1950; Wu, 1952; Durie and Herzberg, 1960; Trefler and Gush, 1968; Bunker, 1973; McKellar, 1973; Bejar and Gush, 1974).

The observed spectra of molecular hydrogen can be classified under the following subheads: (1) Electronic Spectrum, (2) Vibration-Rotation and Pure Rotational Spectra, and (3) Quadrupole Vibration-Rotation Spectrum.

Electronic Spectrum. - Electronic spectrum of molecular hydrogen and its various isotopic forms has long been subject to many detailed investigations, both experimental and theoretical. The books by Richardson (1934) and Herzberg (1950) and the paper by Tanaka (1944) present a nice survey of most of the early work. There has been a heavy and continuous influx of research papers on this subject all along and it is not feasible here to mention all of them. Following are a few of the important references: Herzberg and Howe, 1959; Herzberg and Monfils, 1960; Monfils, 1961, 1962, 1965, 1968a, 1968b; Namioka, 1964a, 1964b; Wilkinson, 1968; Herzberg and Jungen, 1972; Bredohl and Herzberg, 1973; Miller and Green, 1974; Brottcher and Dockey, 1974; Dabrowski and Herzberg, 1974. We can classify the observed spectrum in the following two categories:

(1) Singlet-Singlet Transitions

As many as 32 singlet-singlet electronic transitions have been identified in the electronic spectrum of molecular hydrogen. These are listed in Table (9-XXV). While the transitions (1) and (2) have been studied in both absorption and emission, transitions (3), (4), (5), and (7) could be studied only in absorption. Transitions (8) through (32) have been identified in emission only. Further, while emission features have been observed in the region 13000-1000Å, absorption observations were confined to only 1100-750Å. System (1), $[B \, ^1\Sigma_u^+ - X \, ^1\Sigma_g^+]$ which is also called the Lyman System, is the strongest of all. The other strong systems are the Werner System (2) and the Hopfield-Beutler System (4). Almost all the systems which are found to involve the ground state $^1\Sigma_g^+$ exhibit strong perturbations.

(2) Triplet-Triplet Transitions

The spectral features that correspond to this type of electronic transitions lie in the spectral region (15000-8000Å) and have been observed only in emission. These have been classified into as many as 18 different transitions and listed in Table 9-XXVI.

Rosen (1970) has compiled details of the relevant data in respect of all these transitions. Figure (9-44) presents a schematic showing various known singlet and triplet electronic states of H_2 (Herzberg, 1950).

Absorption and photoionization cross sections of H_2 were measured by a number of workers in the past, particularly in the vacuum ultraviolet region (Weissler, 1952; Wainfan et al., 1955; Bunch et al., 1958; Cook and Metzger, 1964). The results of Cook

TABLE (9-XXV) VARIOUS OBSERVED ELECTRONIC TRANSITIONS OF MOLECULAR HYDROGEN

S.N.	Transitions	Designation	γ_{00}	Degradation
(1)	$B\ ^1\Sigma_u^+ \rightleftarrows X\ ^1\Sigma_g^+$	Lyman System	90203.55	R
(2)	$C\ ^1\Pi_u^- \leftarrow X\ ^1\Sigma_g^+$	Werner System	99081.72	R
(3)	$B\ ^1\Sigma_u^+ \leftarrow X\ ^1\Sigma_g^+$		110478.54	R
(4)	$D\ ^1\Pi_u^+ \leftarrow X\ ^1\Sigma_g^+$	Hopfield-Beutler	112871.74	R
(5)	$B''\ ^1\Sigma_u^+ \leftarrow X\ ^1\Sigma_g^+$		116882.00	R
(6)	$D'\ ^1\Pi^- \leftarrow X\ ^1\Sigma_g^+$		117834.65	R
(7)	$D''\ ^1\Pi_u^- \leftarrow X\ ^1\Sigma_g^+$		120172.21	R
(8)	$E\ ^1\Sigma_g^+ \rightarrow B\ ^1\Sigma_u^+$		8961.2	V
(9)	$F\ ^1\Sigma_g^+ \rightarrow B\ ^1\Sigma_u^+$		~14000	R
(10)	$Q\ \rightarrow B\ ^1\Sigma_u^+$		21151	R
(11)	$K\ \rightarrow B\ ^1\Sigma_u^+$		21425.4	R
(12)	$G\ ^1\Sigma_g^+ \rightarrow B\ ^1\Sigma_u^+$		(21609)	V
(13)	$I\ ^1\Pi_g \rightarrow B\ ^1\Sigma_u^+$		21813	V
(14)	$J\ ^1\Delta_g \rightarrow B\ ^1\Sigma_u^+$		22150	V
(15)	$H\ ^1\Sigma_g^+ \rightarrow B\ ^1\Sigma_u^+$		22754.1	V
(16)	$L\ ^1\Sigma_g^+ \rightarrow B\ ^1\Sigma_u^+$		23054.8	
(17)	$M\ ^1\Sigma_g^+ \rightarrow B\ ^1\Sigma_u^+$		23190	
(18)	$N\ ^1\Sigma_g^+ \rightarrow B\ ^1\Sigma_u^+$		24896	
(19)	$T\ ^1\Sigma_g^+ \rightarrow B\ ^1\Sigma_u^+$		27130	
(20)	$P\ ^1\Sigma_g^+ \rightarrow B\ ^1\Sigma_u^+$		27148	
(21)	$R\ ^1\Pi_g \rightarrow B\ ^1\Sigma_u^+$		~27400	
(22)	$S\ ^1\Delta_g \rightarrow B\ ^1\Sigma_u^+$		27460	
(23)	$O\ ^1\Sigma_g^+ \rightarrow B\ ^1\Sigma_u^+$		27487	
(24)	$K\ \rightarrow C\ ^1\Pi_u^-$		12541.2	R
(25)	$G\ ^1\Sigma_g^+ \rightarrow C\ ^1\Pi_u^-$		12725	R
(26)	$I\ ^1\Pi_g \rightarrow C\ ^1\Pi_u^-$		12925	R
(27)	$J\ ^1\Delta_g \rightarrow C\ ^1\Pi_u^-$		13264	R
(28)	$H\ ^1\Sigma_g^+ \rightarrow C\ ^1\Pi_u^-$		13866.6	R
(29)	$P\ ^1\Sigma_g^+ \rightarrow C\ ^1\Pi_u^-$		18260	
(30)	$R\ ^1\Pi_g \rightarrow C\ ^1\Pi_u^-$		~18400	
(31)	$D\ ^1\Pi_u^- \rightarrow E\ ^1\Sigma_g^+$		13713.3	R
(32)	$X\ ^1\Sigma_g^+ \rightarrow E\ ^1\Sigma_g^+$		~137000	

TABLE (9-XXVI)   VARIOUS OBSERVED ELECTRONIC TRANSITIONS OF MOLECULAR HYDROGEN

S.N.	Transitions	Designation	ν_{OO}	Degradation
(1)	$e\ ^3\Sigma_u^+ - a\ ^3\Sigma_g^+$		11605.7	R
(2)	$d\ ^3\Pi_u - a$	Fulcher (α)	16619.0	R
(3)	$f\ ^3\Sigma_u^+ - a$		20526.0	R
(4)	$k\ ^3\Pi_u - a$	(β)	22271.5	R
(5)	$m\ ^3\Sigma_u^+ - a$		23295.1	
(6)	$n\ ^3\Pi_u - a$	(γ)	24847.5	R
(7)	$t\ ^3\Sigma_u - a$		25343	R
(8)	$u\ ^3\Pi_u - a$	(δ)	26232.5	R
(9)	$a\ ^3\Sigma_g^+ - b\ ^3\Sigma_u^+$	Continuum 5000 > λ > 1600Å		
(10)	$g\ ^3\Sigma_g^+ - c\ \Pi_u^+$		16926	
(11)	$h\ ^3\Sigma_g^+ - c$		16990	R
(12)	$i\ ^3\Pi_g - c$		17162	
(13)	$j\ ^3\Delta_g - c$		17355	
(14)	$p\ ^3\Sigma_g^+ - c$		22588	
(15)	$D\ ^3\Delta_g - c$		22626	
(16)	$r\ ^3\Pi_g - c$		22699	
(17)	$v^3\ - c$		22487	R
(18)	$q^3\ - c$		25220	R

195

E (cm⁻¹) — Singlets | Triplets — Volts

Singlets: $ns\sigma$ $np\sigma$ $np\pi$ $nd\sigma$ $nd\pi$ $nd\delta$ — doubly excited levels
$^1\Sigma_g^+$ $^1\Sigma_u^+$ $^1\Pi_u$ $^1\Sigma_g^+$ $^1\Pi_g$ $^1\Delta_g$

Triplets: $ns\sigma$ $np\sigma$ $np\pi$ $nd\sigma$ $nd\pi$ $nd\delta$ $nf\sigma$ — doubly excited levels
$^3\Sigma_u^+$ $^3\Sigma_u^+$ $^3\Pi_u$ $^3\Sigma_g^+$ $^3\Pi_g$ $^3\Delta_g$ $^3\Sigma_u^+$

124,429

$2p\pi 3p\pi\ ^1\Sigma_g$
$2s\sigma 3s\sigma\ ^1\Sigma_g$
$(2s\sigma)^2\ ^1\Sigma_g$ $2p\sigma 2p\pi\ ^1\Pi_g$
$(2p\pi)^2\ ^1\Sigma_g$
$(2p\sigma)^2\ ^1\Sigma_g$ $2p\sigma 3p\sigma\ ^1\Sigma_g$

$2p\sigma 4p\pi\ ^3\Pi_g$
$2p\sigma 3d\sigma\ ^3\Sigma_u$
$2p\sigma 3d\pi\ ^3\Pi_u$

100,000

50,000

0
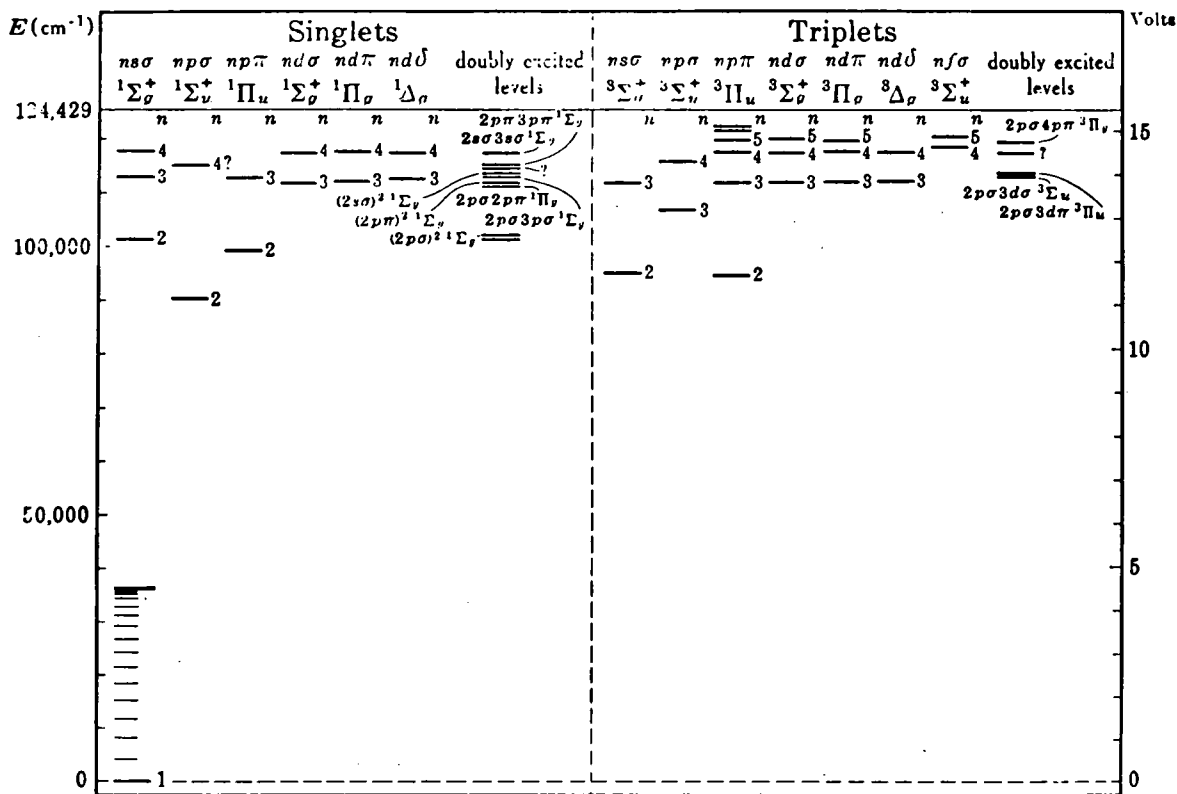
Figure (9-44). Schematic showing various known singlet and triplet electronic states of the molecule H_2. [Herzberg, 1950]

and Metzger (1964) which cover the spectral region (1000-580Å) are presented in figures (9-45 and 9-46). The most prominent features of this study are: (a) weak band absorption between 970Å and 860Å with $k_{max} \simeq 20\ cm^{-1}$ and $k_{min} \simeq 1\ cm^{-1}$, (b) a predissociation continuum, (c) an ionization continuum with k_{max} approximately equal to 300 cm^{-1} for the underlying continuum, and (d) superimposed on these two continua strong absorptions due to the D - X system with variations in k value from 680 cm^{-1} for the v' = 3 band to 330 cm^{-1} for the v' = 8 band. The ionization coefficient rises from k_i = 10 cm^{-1} at 808Å to k_i = 150 cm^{-1} at 780Å and approaches the absorption coefficient value at shorter wavelengths, where the ionization efficiency is 100%.

There is a strong continuous spectrum of H_2 which has a long wavelength limit in the neighborhood of 4500-5000Å. It increases in intensity towards the ultraviolet with a maximum at about 2500Å, after which the intensity falls off again. The conditions which favor the excitation of α-system of the triplet spectrum favor also the continuous spectrum. There is a pressure discrimination with respect to its excitation when the compari-
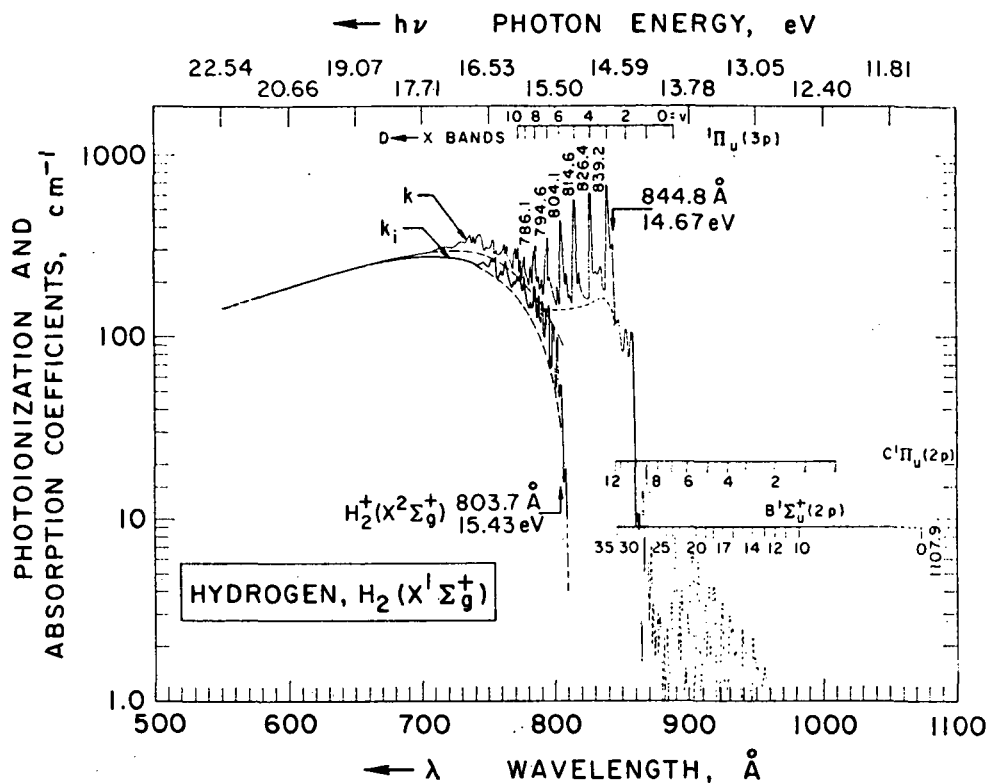
196

PHOTON ENERGY, eV

$\leftarrow h\nu$

22.54   19.07   16.53   14.59   13.05   11.81
    20.66   17.71   15.50   13.78   12.40

PHOTOIONIZATION AND ABSORPTION COEFFICIENTS, cm^{-1}

1000

100

10

1.0

500   600   700   800   900   1000   1100

$\leftarrow \lambda$ WAVELENGTH, Å

10 8 6 4 2 0:v
D $\rightarrow$ X BANDS

$^1\Pi_u(3p)$

786.1
794.6
804.1
814.6
826.4
839.2

844.8 Å
14.67 eV

k

k$_i$

$H_2^+(X^2\Sigma_g^+)$ 803.7 Å
15.43 eV

HYDROGEN, $H_2(X^1\Sigma_g^+)$

C$^1\Pi_u$(2p)

B$^1\Sigma_u^+$(2p)

12 8 6 4 2

35 30 25 20 17 14 12 10   1107.9
0

Figure (9-45). Photoionization and absorption coefficients of H_2 for the wavelength region 1000-580A. [Cook and Metzger, 1964]

PHOTON ENERGY, eV

$\leftarrow h\nu$

20   18   16   14   12

3.0

i_g, ION CHAMBER CURRENT (10^{12} A)

10.0

8.0

6.0

4.0

2.0

0

HYDROGEN: H_2
i_{Pt}: ABSORPTION SPECTRUM
i_g: PHOTOIONIZATION SPECTRUM
i_{Pt}^0: HOPFIELD CONTINUUM
PATH LENGTH $\ell = 40.6$ cm
PRESSURE p = 0.036 mm Hg

i_{Pt}^0

i_{Pt}

i_g

2.4

1.8

1.2

0.6

0

i_{Pt} AND i_{Pt}^0, PHOTOELECTRIC CURRENT (10^{12} A)

500   600   700   800   900   1000

WAVELENGTH, Å $\lambda \longrightarrow$
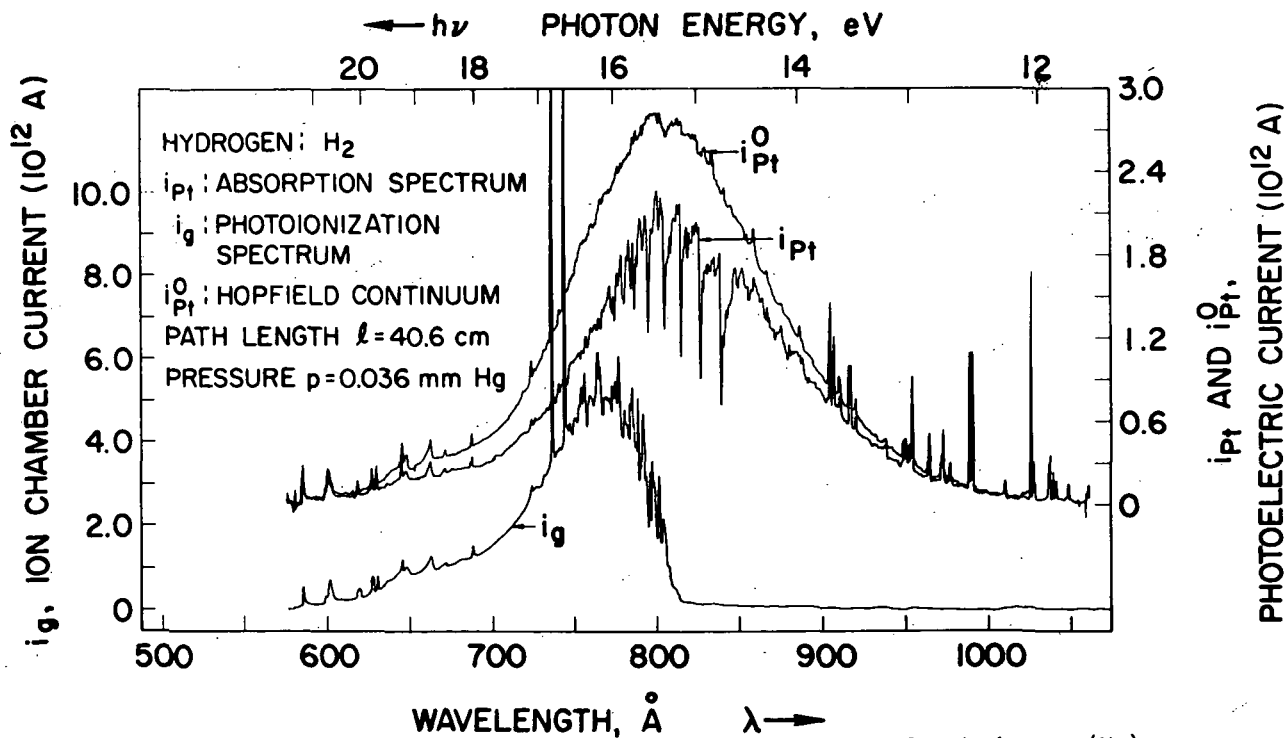
Figure (9-46). Absorption and photoionization spectra of molecular hydrogen (H_2). [Cook and Metzger, 1964]

197

son is confined to the lines of the α-system. The lines are enhanced relative to the continuous spectrum at low pressures while high pressures favor the continuous spectrum. A minimum potential is required for its excitation by electron impact (12.6 eV). Figure (9-47) presents potential energy curves for a few important electronic states of H_2. The transition $C \rightarrow A$ corresponds to this continuum.

Hydrogen exhibits yet another continuum which shows up in spark discharges in hydrogen gas at high pressures. This is most probably caused by an interatomic stark effect on the Balmer lines of the atomic spectrum (Finkelburg, 1931).
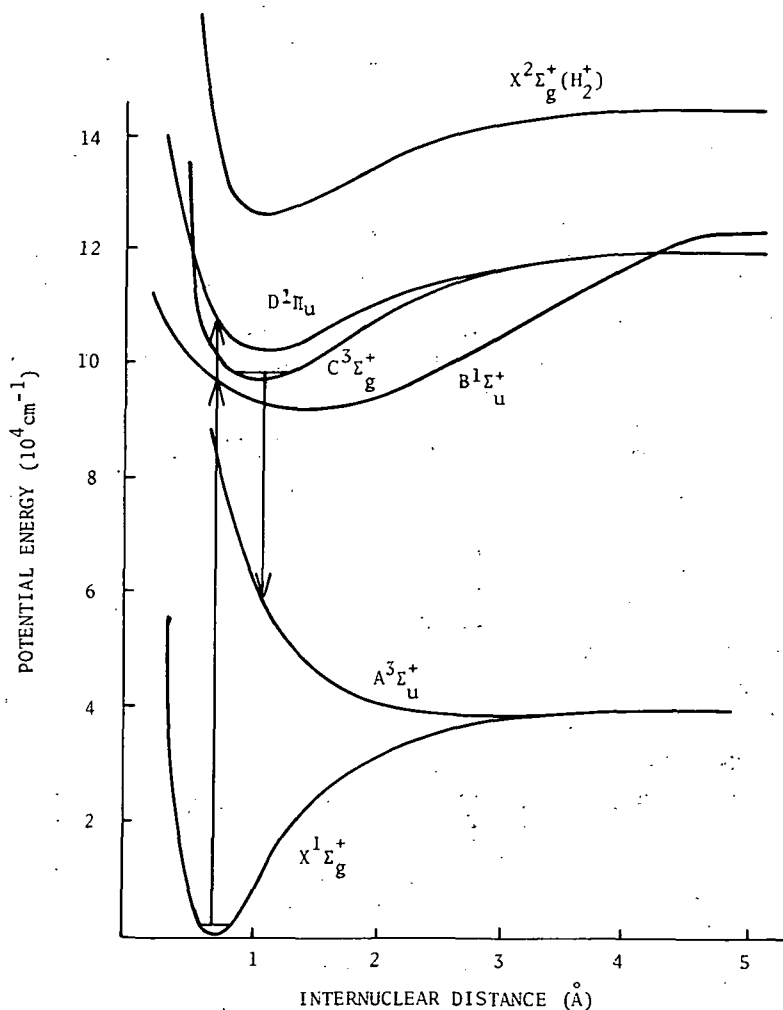
Figure (9-47). Potential energy curves for a few important electronic states of molecular hydrogen. Transitions $B \leftarrow X$ and $D \leftarrow X$ correspond to the important absorption bands at 1109 and 1002Å. $C \rightarrow A$ corresponds to the well known H_2 ultraviolet continuum.

<u>Vibration-Rotation and Pure Rotation Spectra</u>. - H$_2$ does not exhibit any vibration-rotation of pure rotational spectral features under normal conditions on account of symmetry considerations. However, it does exhibit quadrupole vibration-rotation absorption features and in the compressed state, certain pressure-induced dipole transitions in the infrared. Besides laboratory interest, both these types of spectra are quite important from the viewpoint of planetary spectroscopy.

Pressure induced dipole features show up only when the hydrogen is in the compressed form. The intermolecular forces operative during collisions produce a distortion in the normal electron distribution of the molecule. The resulting electric dipole of the system is modulated by the vibration and rotation of the colliding molecules, so that frequencies which are otherwise inactive in a free molecule appear in the infrared absorption. At such pressures where only binary collisions are important, the intensity of the induced absorption is proportional to the square of the density of the pure gas. This induced absorption is explained in terms of electron overlap and quadrupole interactions. The overlap interaction produces mainly those transitions for which $\Delta J = 0$, i.e., Q lines. The quadrupole interaction on the other hand is strongly dependent on the mutual orientation of the molecules in a pair and produces transitions for which $\Delta J = \pm 2$, i.e., S and O branches and in addition also contributes a little towards the Q lines. Details on the theory of pressure-induced transitions may be seen in the articles by Van Kranendonk and Bird, 1951; Van Kranendonk, 1952, 1957, 1958; and also by Britton and Crawford, 1958. The fundamental vibrational band of H$_2$ at pressures in the range 100 atm. has been studied by Welsh (1969) in pure H$_2$ and in mixtures of H$_2$ with N$_2$, Ar and He. These results are presented in figure (9-48). Figure (9-49) depicts the results of Hare and Welsh (1958) who studied the fundamental absorption band of hydrogen in H$_2$ - N$_2$ mixture at various total pressures in the range 1137-4665 atm.

Kuiper (1952) was probably the first to report a diffuse feature at 8260Å in the spectrum of Uranus which was later on identified as the pressure-induced dipole absorption due to H$_2$ (Herzberg, 1952). Similar induced dipole absorptions of H$_2$ were identified in the spectra of Neptune and Uranus. Belton and Spinrad (1973) found that the S$_3$(O) line of the pressure induced 3-0 band was roughly of the same shape and strength in both planets suggesting close similarities of the two atmospheres.

Danielson (1966) and Moroz (1966) reported characteristic absorption in the case of Jupiter near 2.2µ which they attributed to the (1-0) pressure induced dipole transition of H$_2$.

In addition to induced vibration-rotation transitions, hydrogen also exhibits pure rotational transitions (Ketelaar, Colpa and Hooge, 1955; Colpa and Ketelaar, 1958; Kiss, Gush and Welsh, 1959). The Raman spectrum of H$_2$ shows four rotational lines S(J) with J = 0, 1, 2, 3, at 354.4, 587.1, 814.4 and 1034.7 cm^{-1}, J = 0 → 2, 1 → 3, 2 → 4, 3 → 5 respectively (Stoicheff, 1957). In the induced spectrum of H$_2$ all these lines have been
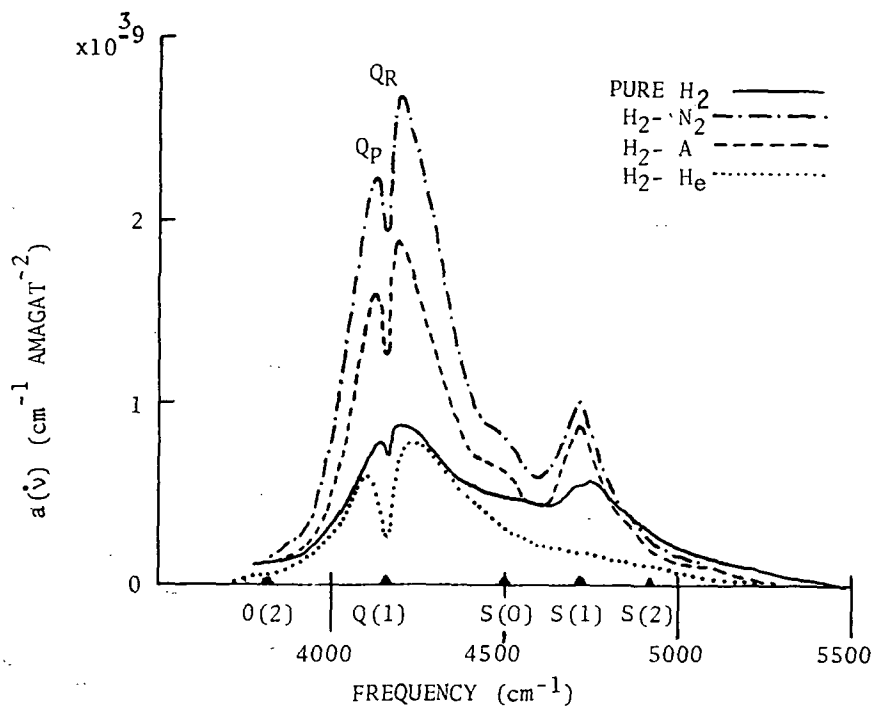
Figure (9-48). Specific absorption profiles of the induced fundamental vibrational band of H_2 for the pure gas and mixtures with some foreign gases at 300K. The shapes of the profiles correspond to total pressure of 100 atm. The triangles on the abscissa axis show the frequencies of the transitions as calculated from the constants of the free molecule. [After Welsh (1969)]
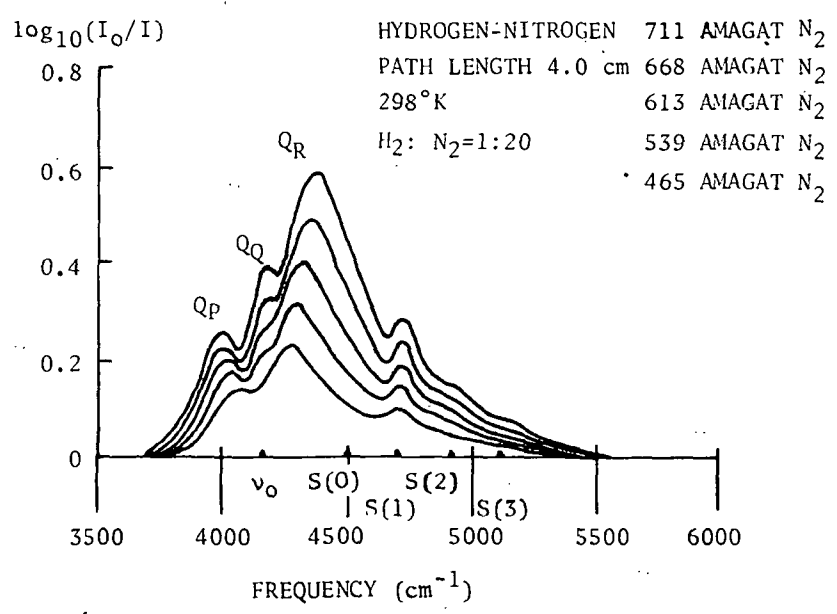

Figure (9-49). The fundamental absorption of hydrogen in a hydrogen-nitrogen mixture at various total pressures in the range 1137-4665 atm. [After Hare and Welsh (1958)]

identified in the region of the CsBr optics. Figure (9-50) and (9-51) depict these induced features (Kiss, Gush and Welsh, 1959).
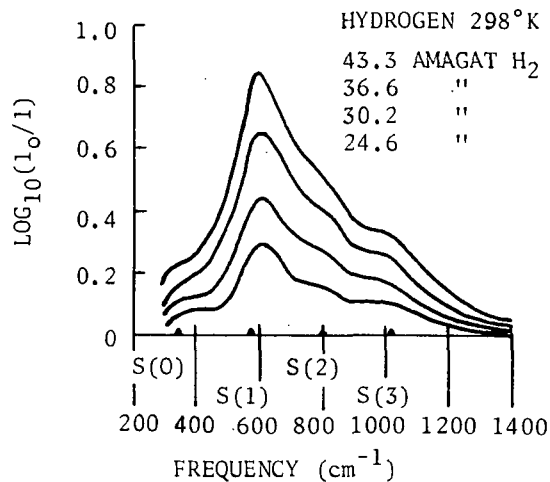
Figure (9-50). Absorption of pure H_2 in the frequency range 300-1400 cm^{-1} at room temperature (298°K). [Kiss, Gush and Welsh (1959)]
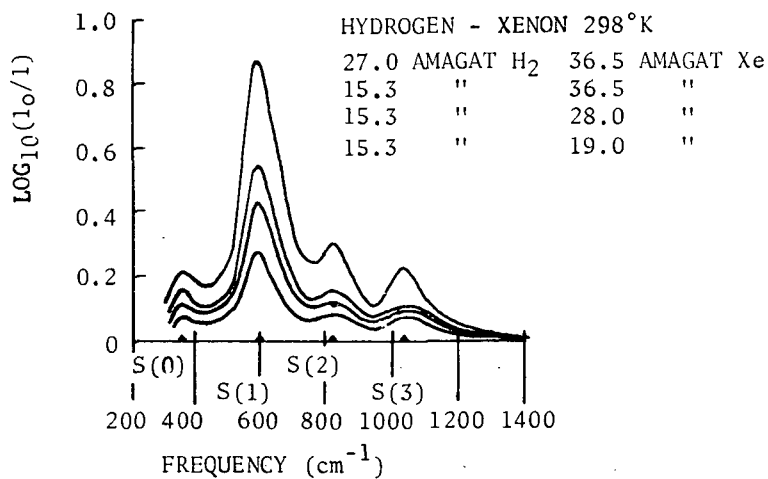
Figure (9-51). Absorption of H_2-X_e mixtures in the region 300-1400 cm^{-1} at room temperature (298°K). [Kiss, Gush and Welsh (1959)]

201

Quadrupole Vibration-Rotation Spectrum. - Molecular hydrogen (H_2) exhibits numerous quadrupole absorption features in the infrared region. Herzberg (1949) was probably the first to observe the first and second overtone of the H_2 vibration using a long path multiple reflection absorption cell. Extensive laboratory investigations on this type of transitions have been reported by Rank, Fink and Wiggins (1966). Karl and Poll (1967) presented new calculations of the quadrupole moments using rigorous wave functions and the calculated line strengths are in good agreement with the experimental results (Table 9-XXVII).

TABLE (9-XXVII) EXPERIMENTAL AND CALCULATED VALUES OF THE
QUADRUPOLE-MOMENT MATRIX ELEMENTS

	A_0 (cm^{-1}/km amagat)	ν (cm^{-1})	Qexptl (D - Å)	Qcalo (D - Å)
$S_1(0)$	2.8×10^{-2}	4497.8	0.103	0.105
$S_1(1)$	9.0×10^{-2}	4712.9	0.0989	0.0969
$S_1(2)$	1.4×10^{-2}	4917.0	0.0945	0.0886
$S_1(3)$	8.4×10^{-3}	5108.4	0.0833	0.0804
$Q_1(1)$	4.5×10^{-2}	4155.3	0.103	0.118
$Q_1(2)$	6.5×10^{-3}	4143.5	0.112	0.119
$Q_1(3)$	4.4×10^{-3}	4125.9	0.111	0.119
$S_2(1)$	1.4×10^{-2}	8604.2	0.0158	0.0159
$Q_2(1)$	7.8×10^{-3}	8075.3	0.0159	0.0151
$S_3(1)$	1.3×10^{-3}	12265.5	0.00283	0.00282

Table (9-XXVIII) presents the laboratory data on the various known quadrupole lines of 3-0 and 4-0 bands of H_2 (Rank, Fink and Wiggins, 1966). Table (9-XXIX) gives wave numbers (calculated) for the various quadrupole lines as might be expected (Herzberg, 1938).

Kiess, Corliss, and Kiess (1960) first identified four quadrupole absorption lines of hydrogen in the spectrum of Jupiter. Later a number of other workers identified numerous quadrupole lines in the spectrum of Jupiter and other giant planets (Zabriskie, 1962; Spinrad and Trafton, 1963; Foltz and Rank, 1963; Owen and Mason, 1968). Most of these investigations have been primarily based on observations of the 3-0 and 4-0 quadrupole bands. The (2-0) and (1-0) bands are badly blended with methane and ammonia absorption lines. In a quadrupole spectrum, one has S, Q and O branches and for the temperatures in the Jovian atmosphere, the strongest lines should be S(0), S(1), S(2) and Q(1). All these four lines have been reported by Kiess et al. (1960) in the case of 3-0 quadrupole band. The S(1) line is purer than others, i.e., this line is more free from serious blending with telluric or solar absorptions than others. In the case of 4-0 band only S(1) has been reported in the spectrum of Jupiter. S(0) is highly blended with NH_3 lines and Q(1) is not yet detected; S(2) has been predicted to be too weak to be visible (Spinrad and Trafton, 1963).

TABLE (9-XXVIII) WAVELENGTHS AND STRENGTHS OF H_2 QUADRUPOLE LINES

Band	Line	λ Air (Å)	S_o
3-0	Q(1)	8497.5	4.2×10^{-4}
	S(0)	8272.7	3.2×10^{-4}
	S(1)	8150.7	1.3×10^{-3}
	S(2)	8046.4	2.4×10^{-4}
4-0	Q(1)	6565.0*	3.7×10^{-5}
	S(0)	6435.1†	3.5×10^{-5}
	S(1)	6367.8	1.6×10^{-4}

* Predicted Value Blended with Ammonia
† Predicted Value

TABLE (9-XXIX) QUADRUPOLE R-V SPECTRUM OF H_2 (CALCULATED VALUES IN cm^{-1})
(Herzberg, 1938)

	1-0			2-0		
K	S	Q	0	S	Q	0
0	4498	--	--	8403	--	--
1	4713	4155	--	8101	8072	--
2	4917	4143	3807	8782	8048	7729
3	5108	4126	3568	8945	8014	7485
4	5280	4103	3339	9090	7968	7234
5	5448	4074	3091	9213	7911	6979

	3-0			4-0		
K	S	Q	0	S	Q	0
0	12080	--	--	15530	--	--
1	12264	11760	--	15695	15222	--
2	12420	11725	11423	15832	15176	14890
3	12556	11674	11173	15940	15108	14635
4	16667	11605	10911	16018	15017	14362
5	12753	11521	10639	16066	14905	14073

Nitrogen (N_2)

Dipole Moment, M: Zero

Ionization Potential, I.P.: 15.576 eV

Dissociation Energy, D(N-N): 9.760 eV

Ground Electronic State Configuration: $(1s\sigma)^2 (2p\sigma)^2 (2s\sigma)^2 (3p\sigma)^2 (2p\pi^4) (3d\sigma^2)$ - - $^1\Sigma_g^+$

Fundamental Vibration Frequency and Anharmonicity Constants: ω_e = 2358.027 cm^{-1};

$\omega_e x_e$ = 14.1351 cm^{-1};

$\omega_e y_e$ = -1.7510 x 10^{-2} cm^{-1}

Rotational Constants:

B_e	α_e	r_e(N-N)
1.9980 cm^{-1}	0.01772	1.0977Å

Nitrogen is a colorless, odorless and tasteless diatomic gas, constituting about four-fifths of the earth's atmosphere. Its presence in trace amounts has also been postulated in certain other planetary atmospheres too. Except when heated to high temperatures where it combines with most metals to form nitrides, it is an extremely inert gas.

N_2 is a simple homonuclear diatomic molecule formed of two atoms of nitrogen joined together by a covalent bond of about 1Å in length. The most abundant isotopic species of nitrogen is the $^{14}N_2$; the other much less abundant species are $^{15}N_2$ and $^{15}N^{14}N$.

Molecular Spectrum

Nitrogen (N_2) exhibits only such spectra that arise as a result of electronic transitions. Pure rotational and vibration-rotation transitions do not show up in this case because of symmetry considerations.

Electronic Spectrum. - Molecular nitrogen exhibits a very rich and widespread electronic spectrum. As many as 35 electronic transitions involving 22 distinct electronic states are known. Most of these transitions show up in emission only and there are only a few that appear simultaneously or exclusively in absorption. As a matter of fact, molecular nitrogen is a very weak absorber in the wavelength range beyond 900Å upwards.

Lofthus (1960) has presented an exhaustive review of most of these transitions and another review by the same author is forthcoming in 1976. We are therefore not presenting details of all the known transitions here. A brief account of those transitions which appear prominently in absorption is however presented in view of their significance in aeronomy.

N_2 absorption can be classified into the following three wavelength segments: (1) 2600-1000Å; (2) 1000-600Å; and (3) Below 600Å.

(1)   2600-1000Å

Since almost all the known electronic states of molecular nitrogen having excitation energies less than 12.5 eV (1000Å) are of valence type and their

radiative combinations with the ground state are forbidden by electric dipole selection rules, the resulting spectra are usually very weak. Worley, 1953; Wilkinson, 1956; Wilkinson and Mulliken, 1959; Ogawa and Tanaka, 1959; Ogawa and Tanaka, 1960; Tanaka, Ogawa and Jursa, 1964; Tilford and Wilkinson, 1964; Vanderslice, Tilford and Wilkinson, 1965; Tilford, Vanderslice and Wilkinson, 1965; Miller, 1966; Joshi, 1966; Dressler and Lutz, 1967; Carroll and Yoshino, 1967; Dressler, 1969 made important contributions in our understanding of this segment of N_2 spectrum. The following band systems have been reported in absorption which lie in this region:

(a) Wilkinson (1690-1630Å): $B\,^3\Pi_g \leftarrow X\,^1\Sigma_g^+$

(b) Ogawa-Tanaka-Wilkinson (2240-1120Å): $B'\,^3\Sigma_u^- \leftarrow X\,^1\Sigma_g^+$

(c) Lyman-Birge-Hopfield (2600-1090Å): $a\,^1\Pi_g \leftarrow X\,^1\Sigma_g^+$

(d) Ogawa-Tanaka-Wilkinson-Mulliken (2000-1080Å): $a'\,^1\Sigma_u^- \leftarrow X\,^1\Sigma_g^+$

(e) Tanaka (1400-1140Å): $w\,^1\Delta_u \leftarrow X\,^1\Sigma_g^+$

(f) Tanaka (1130-1070Å): $C\,^3\Pi_u \leftarrow X\,^1\Sigma_g^+$

(g) Dressler-Lutz (~1009Å): $a''\,^1\Sigma_g^+ \leftarrow X\,^1\Sigma_g^+$

Transition (f) was first predicted by Mulliken (1957), and it was experimentally identified later by Dressler and Lutz (1967).

(2) 1000-600Å

The spectrum of molecular nitrogen in the region 1000-830Å is quite strong but very complex. Dressler (1969) and Carroll and Collins (1969) have interpreted these features in terms of the following transitions.

(a) $b\,^1\Pi_u \leftarrow X\,^1\Sigma_g^+$; (995-855Å)

(b) $b'\,^1\Sigma_g^+ \leftarrow X\,^1\Sigma_g^+$; (965-830Å)

(c) $c\,^1\Pi_u \leftarrow X\,^1\Sigma_g^+$; (960-865Å)

(d) $c'\,^1\Sigma_u^+ \leftarrow X\,^1\Sigma_g^+$; (960-840Å)

(e) $o\,^1\Pi_u \leftarrow X\,^1\Sigma_g^+$; (950-880Å)

Besides, four Rydberg series have been identified in the absorption spectrum of N_2 in the spectral region below 960Å. These are:

(a) Worley-Jenkins [$X\ ^1\Sigma_g^+\ (N_2^+) \leftarrow X\ ^1\Sigma_g^+$]

(b) Carroll-Yoshino [$X\ ^2\Sigma_g^+\ (N_2^+) \leftarrow X\ ^1\Sigma_g^+$]

(c) Worley [$A\ ^2\Pi_u\ (N_2^+) \leftarrow X\ ^1\Sigma_g^+$]

(d) Hopfield [$B\ ^2\Sigma_u^+\ (N_2^+) \leftarrow X\ ^1\Sigma_g^+$]

(3) Below 600Å

N$_2$ absorption below 600Å exhibits a continuum overlapped by a weak banded structure in the wavelength range (570-470Å). The structure corresponds to two autoionizing states, members of a Rydberg series, converging to the C state of N_2^+ at 23.6 eV.

Table (9-XXX) gives spectroscopic constants for the different known electronic states and (9-XXXI) presents a resume of all the known radiative transitions so far observed. Figure (9-52) depicts relative disposition of these states and various radiative transitions. Absorption cross sections of N$_2$ have also been measured by many workers in the past, particularly below 1450Å through 200Å (Clark, 1952; Weissler et al., 1952; Curtis, 1954; Lee, 1955; Watanabe and Marmo, 1956; Astoin and Granier, 1957; Watanabe, 1961; Itamoto and McAllister, 1961; Huffman et al., 1963; Cook and Metzger, 1964; Samson and Cairns, 1964). Figures (9-53), (9-54), (9-55), and (9-56) present the results of Huffman et al. which cover the spectral region 1000-600Å.

TABLE (9-XXX) SPECTROSCOPIC CONSTANTS FOR KNOWN ELECTRONICS STATES

States	T_0	ω_e	$x_e\omega_e$	B_e	α_e	$D_e 10^6$	r_e
$z\ ^1\Delta_g$	115365.9	(1700)	-	(1.76)	(0.0153)	-	(1.16)
$y\ ^1\Pi_g$	114166.3	1707.9	-	1.78	-	-	1.16
$x\ ^1\Sigma_g^-$	113212.1	1910.0	20.7	1.750	0.0225	5.88	1.168
$d'\ ^1?_u$	111333	-	-	-	-	-	-
$o\ ^1\Pi_u$	105682	2020.0	32.28	1.694	-	-	1.19
$c'\ ^1\Sigma_u^+$	104322.4	2046	-	1.929	-	-	1.12
$c\ ^1\Pi_u$	104139.2	2410	-	1.50	-	-	1.27
$b'\ ^1\Sigma_u^+$	103672	746	-	1.154	0.0048	-	1.444
$D\ ^3\Sigma_u^+$	103573	-	-	1.961	-	20	1.108
$b\ ^1\Pi_u$	100816.9	635	-	1.448	-	29	1.230
$a''\ ^1\Sigma_g^+$	99032	-	-	-	-	-	-
$C'\ ^3\Pi_u^+$	97580	-	-	1.0496	-	10.9	1.508
$E\ ^3\Sigma_g^+$	95771	2185	-	-	-	-	-
$C\ ^3\Pi_u$	88977.9	2047.178	28.4450	1.82473	0.018683	5.80	1.1487
$W\ ^1\Delta_u$	71698.8	1559.236	11.8874	1.498	0.0166	5.53	1.2678
$a\ ^1\Pi_g$	68951.2	1694.208	13.9491	1.61688	0.017933	5.89	1.2203
$a'\ ^1\Sigma_u^-$	67739.3	1530.254	12.0747	1.47988	0.016574	5.54	1.2755
$B'\ ^3\Sigma_u^-$	65852.4	1516.883	12.1810	1.47359	0.016861	5.56	1.2782
$W\ ^3\Delta_u$	59328	1539	17	-	-	-	-
$B\ ^3\Pi_g$	59306.8	1733.391	14.1221	1.6374	0.01791	5.84	1.2126
$A\ ^3\Sigma_u^+$	49754.8	1460.518	13.8313	1.45455	0.018009	5.77	1.2866
$X\ ^1\Sigma_g^+$	0	2358.027	14.1351	1.9980	0.01772	5.74	1.0977

206

TABLE (9-XXXI) OBSERVED ELECTRONIC TRANSITIONS OF THE MOLECULE N_2

| S.N.	Band System	Electronic Transition	Favorable Sources	Wavelength	Limits	Characteristic Bands, A	Remarks
1	Vegard-Kaplan	$A^3\Sigma^+_u \leftrightarrow X^1\Sigma^+_g$	Residual Luminescence	5060-2100Å	R	2760.8(0,6)	Single headed
2	Wilkinson	$B^3\Pi \leftarrow X^1\Sigma^+_g$	Absorption	1690-1630Å	R		
3	First Positive	$B^3\Pi^-_g \rightarrow A^3\Sigma^+_u$	Positive column	IR-4700	V	10510.1(0,0); 8912.40(1,0)	Triple headed
4	Wu-Benesch	$W^3\Delta_u \leftrightarrow B^3\Pi_g$	Discharge	41000-22000		-	Bands Unresolved
5	Ogawa-Tanaka-Wildinson	$B'^3\Sigma^-_u \leftarrow X'\Sigma^+_g$	Absorption ($N_2 + X_e$)	2240-1120	R	-	Double headed
6	Infrared residual Luminescence	$B'^3\Sigma^-_u \rightarrow B^3\Pi_g$	Residual Luminescence High Tension discharge	8920-6060	R	-	Complex structure
7	Lyman-Birge Hopfield	$a^1\Pi_g \leftrightarrow X^1\Sigma^+_g$	Absorption, Low pressure discharge	2600-1090	R	2125.9(5, 14) 2041.2(5,13)	O,P,Q,R,S branches
8	Ogawa-Tanaka Wilkinson-Mulliken	$a'\Sigma^-_u \leftrightarrow X'\Sigma^+_g$	Absorption (N_2+Ar)	2000-1080	R	-	Q branch only
9	Tanaka	$W'\Delta_u \leftarrow X^1\Sigma^+_g$	Absorption	1400-1140	R	-	Heads ill-defined
10	MacFarlane IR	$a^1\Pi_g \rightarrow a'^1\Sigma^-_u$	Laser	82000-33000		-	Principal Q Lines
11	MacFarlane IR	$W'\Delta_u \rightarrow a^1\Pi_g$	Laser	36500		-	Principal Q lines
12	Tanaka	$C^3\Pi_u \leftarrow X^1\Sigma^+_g$	Absorption	1130-1070	R		Five heads
13	Second positive	$C^3\Pi_u \rightarrow B^3\Pi_g$	Positive Column	5450-2680		3576.9(0,1); 3371.3(0,0)	Triple headed
14	Herman-Kaplan	$E^3\Sigma^+_g \rightarrow A^3\Sigma^+_u$	Residual Luminescence	2740-2130	V	2471.4(0,4) 2391.6(0,3)	Bands unresolved
15	Goldstein-Kaplan	$C'^3\Pi_u \rightarrow B^3\Pi_g$	Residual Luminescence	5060-2860	R	4728.0(0,11)	Multi-headed
16	Fourth Positive	$D^3\Sigma^+_u \rightarrow B^3\Pi_g$	Residual Luminescence Ordinary discharge	2910-2250	V	2448.0(0,2)	Five-headed
17	Dressler-Lutz	$a''^1\Sigma^+_g \leftarrow X^1\Sigma^+_g$	Absorption	1009		-	Unresolved
18	-	$b^1\Pi_u \leftrightarrow X^1\Sigma^+_g$	Absorption ordinary discharge	995-855	R	-	Unresolved
19	-	$b'^1\Sigma^+_g \leftrightarrow X^1\Sigma^+_g$	Absorption ordinary discharge	965-830	R		
20	-	$c^1\Pi_u \leftrightarrow X^1\Sigma^+_g$	Absorption ordinary discharge	960=865	R		
21	-	$c'^1\Sigma^+_u \leftrightarrow X^1\Sigma^+_g$	Absorption ordinary discharge	960-860	R		
22	-	$O^1\Pi_u \leftrightarrow X^1\Sigma^+_g$	Absorption ordinary discharge	950-880	R		
23	Gaydon-Herman	$b^1\Pi_u \rightarrow a^1\Pi_g$		3420-2740	R		
24	Gaydon Herman	$b'^1\Sigma^+_u \rightarrow a^1\Pi_g$	Ordinary discharge	2500	R	-	
25	Gaydon Herman	$C^1\Pi_u \rightarrow a^1\Pi$		3010-2220R	V		
27	Gaydon Herman	$d^3(\ ) \rightarrow a^1\Pi_g$		2550-2350			
28	Gaydon Herman	$O^1\Pi_u \rightarrow a^1\Pi_g$		2860-2720	R		
29	Fifth positive	$x^1\Sigma^-_g \rightarrow a'^1\Sigma^-_u$	Ordinary Discharge	2850-2030	V	2411.7(1,4)	Single headed
30	Kaplan (I)	$y^1\Pi_g \rightarrow a'^1\Sigma^-_u$	Ordinary discharge	2470-2070	V	2225.9(0,1)	Single headed
31	Kaplan (II)	$y^1\Pi_g \rightarrow \omega^1\Delta_u$	Ordinary discharge	2860-2260	V	2536.6(0,2)	Single headed
32	-	$z^1\Delta_g \rightarrow \omega^1\Delta_u$	Ordinary discharge	2480-2360	V		Single headed
33	Gaydon (Green)	-	High pressure discharge Electron-bombardment	6340-5040	V	5815 (0,1)	Not well resolved
34	Herman (IR)		Low temperature discharge	8550-7000	V	8057(0,0)	Six headed
35	Rydberg	-	Absorption	< 960			
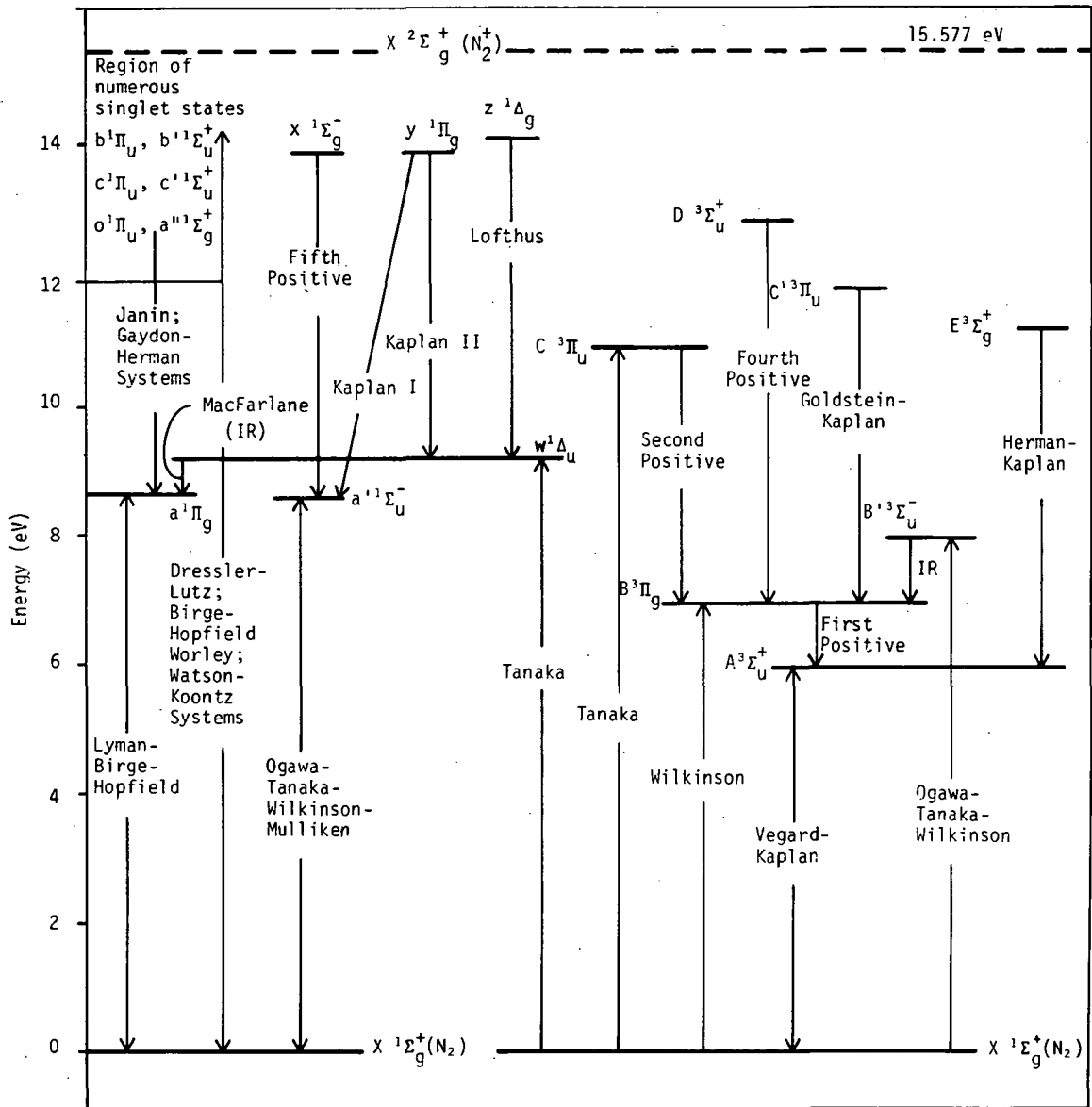
Figure (9-52). Schematic showing various known electronic states of N_2 molecule and radiative transitions.
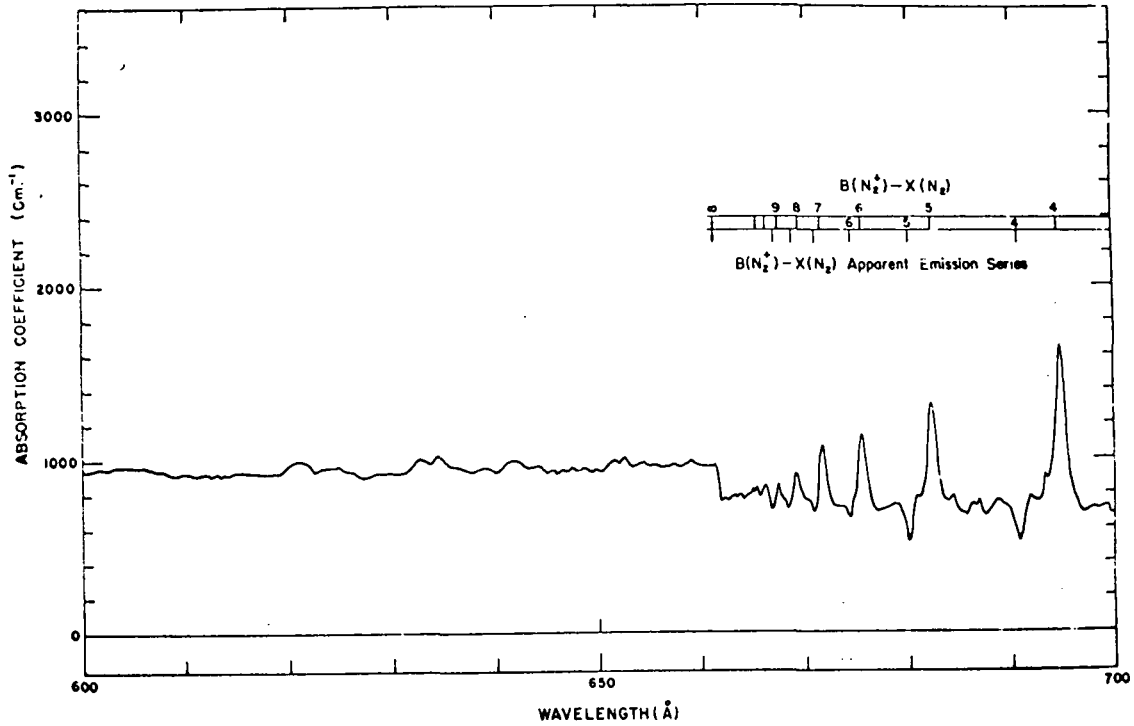
Figure (9-53). Absorption coefficient of N_2 for the wavelength region 700-600Å. [Huffman et al. (1963)]
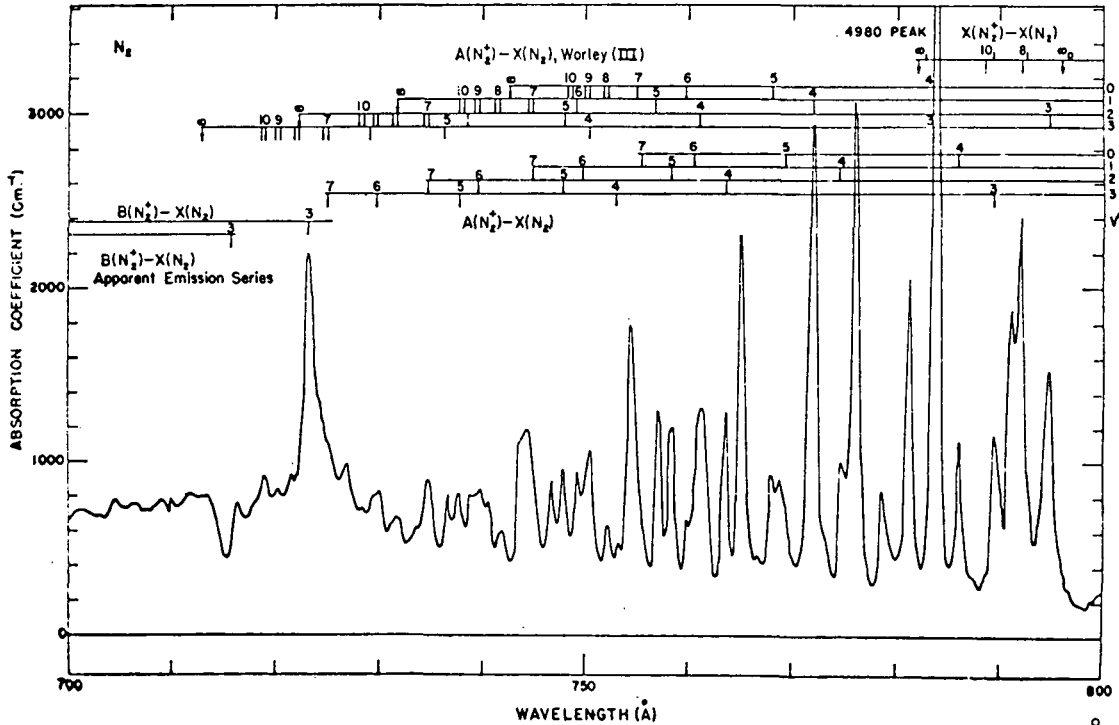

Figure (9-54). Absorption coefficient of N_2 for the wavelength region 800-700Å. [Huffman et al. (1963)]
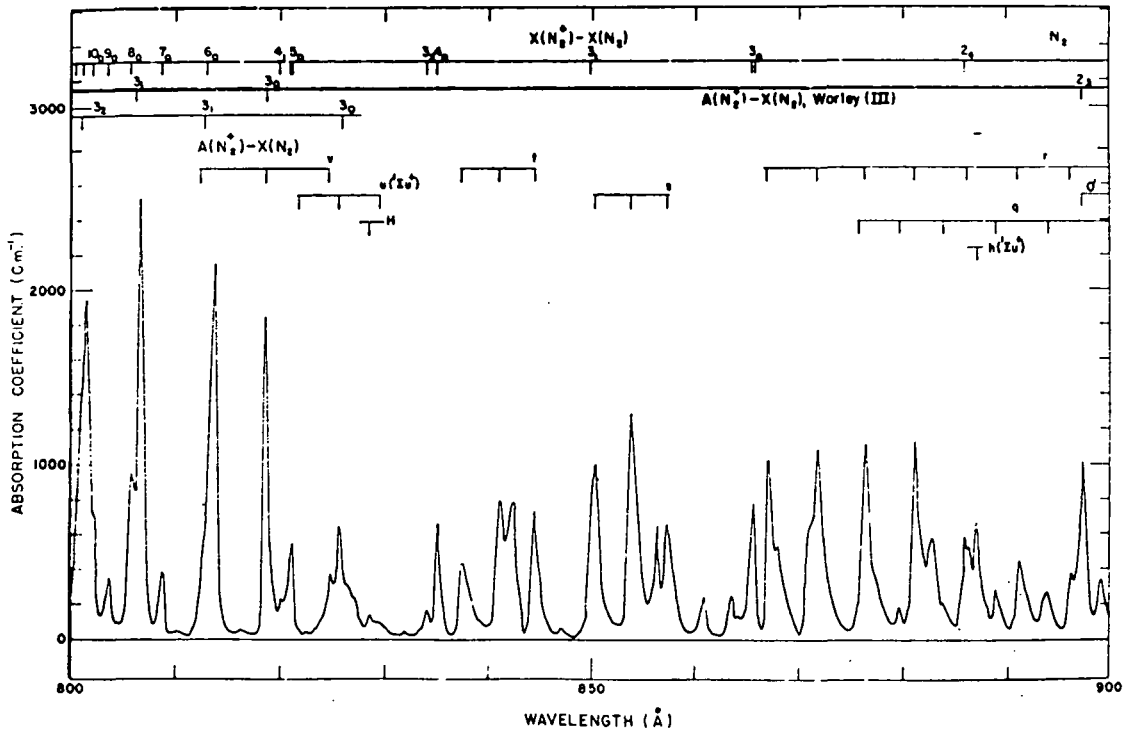
Figure (9-55). Absorption coefficients of N_2 for the wavelength region 900-800Å. [Huffman et al. (1963)]
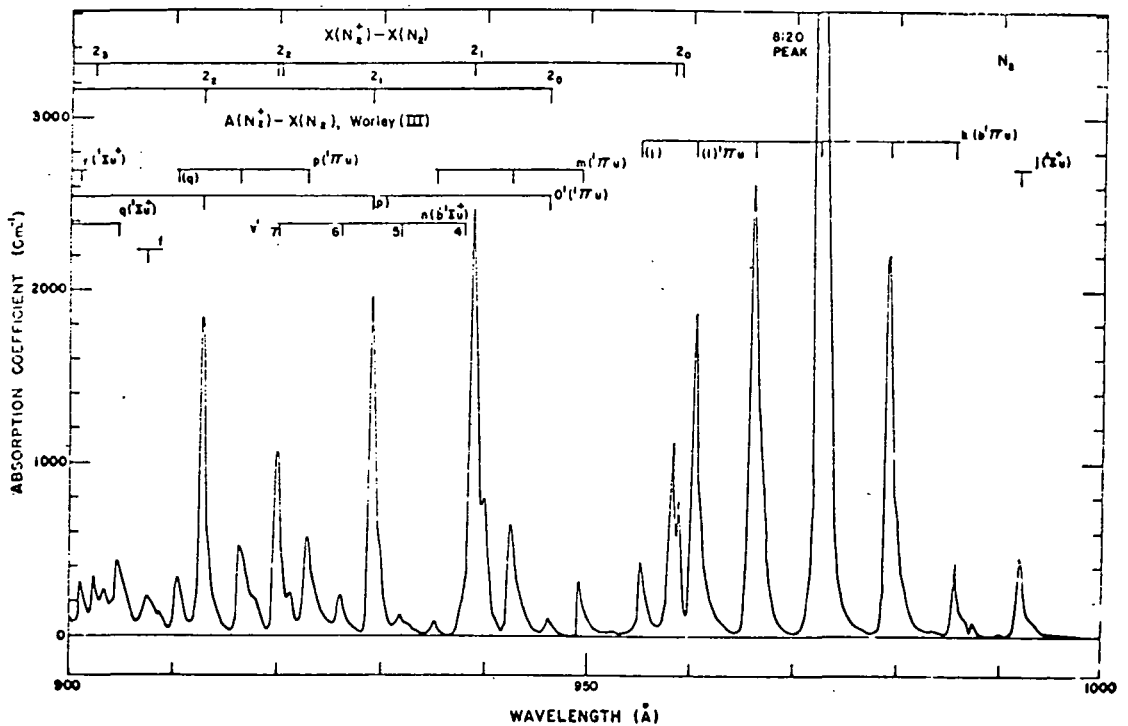

Figure (9-56). Absorption cross section of N_2 for the wavelength region 1000-900Å. [Huffman et al. (1963)]

Oxygen (O_2)

Dipole Moment, M: Zero

Ionization Potential, I.P.: 12.075 eV

Dissociation Energy, D(0-0):- 5.114 eV

Ground Electronic State and Configuration: $KK(2\sigma_g)^2 (2\sigma_u)^2 (3\sigma_g)^2 (1\pi_u)^4 (1\pi_g)^2$ - - $^3\Sigma_g^-$

Fundamental Vibration Frequency and Anharmonicity Constants: ω_e = 1580.2

$\omega_e x_e$ = 11.98

$\omega_e y_e$ = 0.0474 (cm^{-1})

Rotational Constants:

B_e	α_e	r_e(0-0)
1.446 cm^{-1}	0.0159 cm^{-1}	1.2075Å

Oxygen is a colorless, odorless gas at ordinary temperatures. It is the second most abundant constituent of the earth's atmosphere and happens to be an important species of certain stellar and possibly of certain planetary atmospheres. Gaseous O_2 condenses on cooling below its critical point to a bluish liquid, which freezes to solid form around 54°K. Liquid oxygen is made up of polymeric O_4 molecules in equilibrium with the simple O_2 molecules.

O_2 is a highly paramagnetic diatomic molecule. Due to the presence of two unpaired electrons in its configuration, the molecule has a permanent magnetic moment in its ground state. The principal isotopic forms of oxygen are the various combinations of its atomic isotopes O^{16}, O^{17} and O^{18}, the most abundant being O_2^{16}.

Molecular Spectrum

The observed spectral features of O_2 molecule can be classified into the following groups: (1) Electronic Spectrum, and (2) Microwave Spectrum.

Electronic Spectrum. - O_2 is a weak light emitter because for most of its excited states, transitions to the ground state are strongly forbidden by the electric dipole selection rules. Further, since $^{16}O_2$ has zero nuclear spin, alternate lines in the rotational structure of the electronic bands do not show up. A brief account of the prominent transitions so far identified in the O_2 spectrum is presented.

(1) a $^1\Delta_g \rightleftarrows$ X $^3\Sigma_g^-$ Infrared Atmospheric System (15,800-9240Å)R

This system of bands corresponds to a magnetic dipole intercombinational transition. It is a weak system and consists of red-degraded bands which are characterized by O, P, R, S, and Q branches. These bands have been identified in liquid oxygen absorption spectrum, solar spectrum, day and night airglow and nightsky spectra (Ellis and Knesser, 1933; Herzberg and Herzberg, 1947; Babcock and Herzberg, 1948; Gush and Buijs, 1964).

(2) b $^1\Sigma_g^+ \rightleftarrows$ X $^3\Sigma_g^-$ Atmospheric System (9970-5380Å)R

This band system also corresponds to a magnetic dipole intercombinational transition. The constituent bands are red-degraded and are characterized by doublet P and R branches, i.e., P, ^PQ, R and ^RQ branches. The most extensive measurements on these bands are of Babcock and Herzberg (1948), who studied them in long column air absorption in the laboratory as well as in solar absorption by the earth's atmosphere. Earlier, work on these bands was done by Dieke and Babcock, 1927; Babcock, 1929; Mulliken, 1928; Giaugne and Johnston, 1929; Ossenbrugen, 1928; Curry and Herzberg, 1934.

(3) b $^1\Sigma_g^+ \rightarrow$ a $^1\Delta_g$ Noxon System (19,080Å)

Noxon (1961) reported an emission band at 19080 ± 30Å in the spectrum of a low pressure discharge through helium containing traces of oxygen. He ascribed it as the (0,0) band of an electric quadrupole electronic transition $^1\Sigma_g^+ - {}^1\Delta_g$. Since $\Delta\Lambda = 2$ in this case, such a transition is not allowed even by magnetic dipole selection rules.

(4) c $^1\Sigma_u^- \rightleftarrows$ X $^3\Sigma_g^-$ Herzberg II System: (4790-4490Å); (2715-2540Å)

This system represents a weak spin-forbidden transition first identified by Herzberg (1953). The bands which are red-degraded lie overlapping the stronger bands of Herzberg System I (A $^3\Sigma_u^+$ - X $^3\Sigma_g^-$). They possess fine structure similar to that of the atmospheric system b $^1\Sigma_u^-$ - X $^3\Sigma_g^-$ bands but are weaker by a factor of 10^3. Herzberg (1953) and later Degan (1968) studied the fine structure of many of these bands.

(5) C $^3\Delta_u$ - X $^3\Sigma_g^-$ Herzberg III System (2630-2570Å)R

High Pressure Bands (2924-2440Å)

These are the fragments of two very weak and triple headed bands identified by Herzberg (1953) using a 350 meter absorption column at about 2.7 atm. pressure. These underlie the far stronger A $^3\Sigma_u^+ \leftarrow$ X $^3\Sigma_g^-$ bands.

(6) C $^3\Delta_u \rightarrow$ a $^1\Delta_g$ Chamberlain System (4380-3700Å)R

This represents an intercombinational electric dipole transition. Chamberlain (1958) observed about 27 weak bands in the spectrum of airglow which he ascribed to O_2. Identification of these bands is, however, uncertain.

(7) A $^3\Sigma_u^+ \rightleftarrows$ X $^3\Sigma_g^-$ Herzberg I System (4880-2430Å)R

This is a forbidden electric dipole transition first reported by Herzberg (1932). The bands are quite weak and degraded to the red. The dominant Q-branch lines consist of six components $^QQ_3$, $^QP_{32}$, $^QQ_1$, $^QR_{12}$, $^QR_{23}$, $^QP_{21}$ and $^OP_{23}$ which was observed only in the case of the strongest bands. Faint branches $^SR_{21}$, $^OQ_{13}$, $^OP_{12}$ and $^OP_{23}$ were also observed in certain bands (Herzberg, 1953). Dufay (1941) identified some of the bands of the ultra-violet night airglow (3800-3100Å) as members of this system. Chamberlain (1955)

confirmed these identifications by fine structure analysis of the bands. Broida and Gaydon (1954) produced these bands in laboratory afterglow too. Barth (1957, 1958, 1959) observed this system in oxygen-nitrogen afterglow in the region (4500-2500Å).

(8) B $^3\Sigma_u^-$ $\rightleftarrows$ X $^3\Sigma_g^-$ Schumann-Runge System (5350-1750Å)R and (1750-1300Å) Continuum. This system consists of a large number of strong single-headed bands which appear readily both in absorption as well as emission. The discrete band structure merges into an intense dissociation continuum extending almost up to 1250Å. Starting from the early studies by Schumann (1903) and Runge (1921), this spectrum has been extensively studied by numerous workers (Fuchtbauer and Holm, 1925; Ossenbruggen, 1928; Lochte-Holtgreven and Dieke, 1929; Fesefeldt, 1927; Pulskamp, 1929; Curry and Herzberg, 1934; Knauss and Ballard, 1935; Millon and Herman, 1944; Feast, 1949; Lal, 1948; Feast, 1950; Garton and Feast, 1950; Herczog and Wieland, 1950; Durie, 1952; Brix and Herzberg, 1954; Rakotoarijimy et al., 1958; Ogawa, 1966; Ogawa and Chang, 1968; Hudson and Carter, 1968; Ackerman and Biaume, 1970).

(9) Miscellaneous Absorption Transitions: (1585-1140Å)

   (a) AAD (Alberti-Ashby and Douglas) bands α $^1\Sigma_u^+$ $\leftarrow$ b $^1\Sigma_g^+$ (1585-1538Å) V

   (b) Tanaka Progression II α $^1\Sigma_u^+$ $\leftarrow$ X $^3\Sigma_g^-$ (1280-1196Å) V

   (c) Tanaka Progression I β $^3\Sigma_u^+$ $\leftarrow$ X $^3\Sigma_g^-$ (1294-1181Å) V

   (d) One Single Band $^1\Delta_u$ $\leftarrow$ a $^1\Delta_g$ (1243.8Å)

   (e) One Single Band $^1\Pi_u$ $\leftarrow$ a $^1\Delta_g$ (1229.0Å)

   (f) Ogawa-Yamawaki Band $^3\Sigma_u^+$ $\leftarrow$ X $^3\Sigma_g^-$ (1144.6Å)

Besides early work on the ultraviolet absorption of O_2 by Tanaka (1952), Alberti, Ashby and Douglas (1968) lately carried out extensive studies of O_2 absorption in the region (1585-1195Å). They identified as many as sixteen bands, some of them quite weak, but almost all of them overlapped by a strong continuum. Some of these bands were assigned a new electronic transition $^1\Sigma_u^+$ $\leftarrow$ $^1\Sigma_g^+$ (1585-1538Å) and several of them were the same as of Tanaka's progressions I and II. In addition to the two single bands at 1243.8Å and 1229.0Å, Ogawa-Yamawaki (1969) reported yet another band at 1144.6Å whose upper state was designated as $^3\Sigma_u^+$. It is perhaps a member of the Rydberg series converging to the X $^2\Pi_g$ state of O_2^+.

(10) Rydberg Series

Numerous Rydberg series whose convergence limits are the various states of O_2^+ are known in the VUV absorption spectrum of O_2. Significant contributions to the study of these series are of Price and Collins (1935); Cook and Metzger

(1964); Huffman, Larrabe and Tanaka (1964). These are summarized below:

(a) $X\ ^2\Pi_g\ (0_2^+) \leftarrow X\ ^3\Sigma_g^-\ (0_2)\quad (1290\text{-}1180\text{\AA})\ V$

(b) $b\ ^4\Sigma_g^-\ (0_2^+) \leftarrow X\ ^3\Sigma_g^-\ (0_2)\quad (730\text{-}660\text{\AA})\ R$

(c) $B\ ^2\Sigma_g^-\ (0_2^+) \leftarrow X\ ^3\Sigma_g^-\ (0_2)\quad (650\text{-}600\text{\AA})\ R$

(d) $c\ ^4\Sigma_g^-\ (0_2^+) \leftarrow X\ ^3\Sigma_g^-\ (0_2)\quad (595\text{-}510\text{\AA})$

Lately, Lindham (1969) has reported a number of new Rydberg series and re-interpreted others.

Detailed information with regard to band head data and spectroscopic constants in respect to all these transitions are compiled by Krupenie (1972). Table (9-XXXII) gives spectroscopic constants for the different known electronic states. Figure (9-57) presents a schematic showing relative disposition of these electronic states and the important transitions, and Table (9-XXXIII) provides a summary of all the known radiative transitions so far observed.

TABLE (9-XXXII) SPECTROSCOPIC CONSTANTS FOR KNOWN ELECTRONIC STATES

States	T_0	ω_e	$\omega_e x_e$	B_e	$\alpha_e \cdot 10^2$	r_e
$^1\Pi_u$	89244.8	-	-	1.451	-	-
$^1\Delta_u$	88278.4	-	-	1.446	-	-
$\beta\ ^3\Sigma_u^+$	79228	1844	-	1.65	-	-
$\alpha\ ^1\Sigma_u^+$	76262.4	1889.2	~20	1.691	-	-
$B\ ^3\Sigma_u^-$	49358.15	709.31	10.65	0.81902	12.06	-
$A\ ^3\Sigma_u^+$	35007.15	799.08	12.16	0.9106	1.416	-
$C\ ^3\Delta_u$	-	(~750)	(~14)	-	-	-
$c\ ^1\Sigma_u$	33057.3	794.29	12.736	0.9155	1.391	1.517
$b\ ^1\Sigma_g^+$	13120.9080	1432.6874	13.95008	1.4004	1.8170	1.22685
$a\ ^1\Delta_g$	7882.39	(1509.3)	(12.9)	1.4264	1.71	1.2157
$X\ ^3\Sigma_g^-$	0	1580.211	11.99	1.445572	1.581	-

Rydberg-Series

(i) $X\ ^2\Pi_g\ (O_2^+) \leftarrow X\ ^3\Sigma_g^-$

(ii) $b\ ^4\Sigma_g^-\ (O_2^+) \leftarrow X\ ^3\Sigma_g^-$

(iii) $B\ ^2\Sigma_g^-\ (O_2^+) \leftarrow X\ ^3\Sigma_g^-$

(iv) $c\ ^4\Sigma_u^-\ (O_2^+) \leftarrow X\ ^3\Sigma_g^-$

20

12

11

10

9

8

7

6

5

4

3

2

1

Energy (eV)

$c\ ^4\Sigma_u^-\ (O_2^+)$

(iv)

$B\ ^2\Sigma_g^-\ (O_2^+)$

(iii)

$C\ ^2\Delta_g\ (O_2^+)$

$b\ ^4\Sigma_g^-\ (O_2^+)$

$A\ ^2\Pi_u\ (O_2^+)$

$a\ ^4\Pi_u\ (O_2^+)$

(ii)

$X\ ^2\Pi_g\ (O_2^+)$

$^1\Pi_u$

$^1\Delta_u$

$^1\Sigma_u^+$

(i)

$\alpha\ ^1\Sigma_u^+$

$c\ ^1\Sigma_u^-$

Herzberg II

$b\ ^1\Sigma_g^+$

Noxon

Atmos

IR-Atm.

$a\ ^1\Delta_g$

$X\ ^3\Sigma_g^-$

Broida-Gaydon

Chamberlain

$^3\Sigma_u^+$

$B\ ^3\Sigma_u^+$

$B\ ^3\Sigma_u^-$

$A\ ^3\Sigma_u^+$

$C\ ^3\Delta_u$

Schumann Runge

Herzberg III

Herzberg I

$X\ ^3\Sigma_g^-$
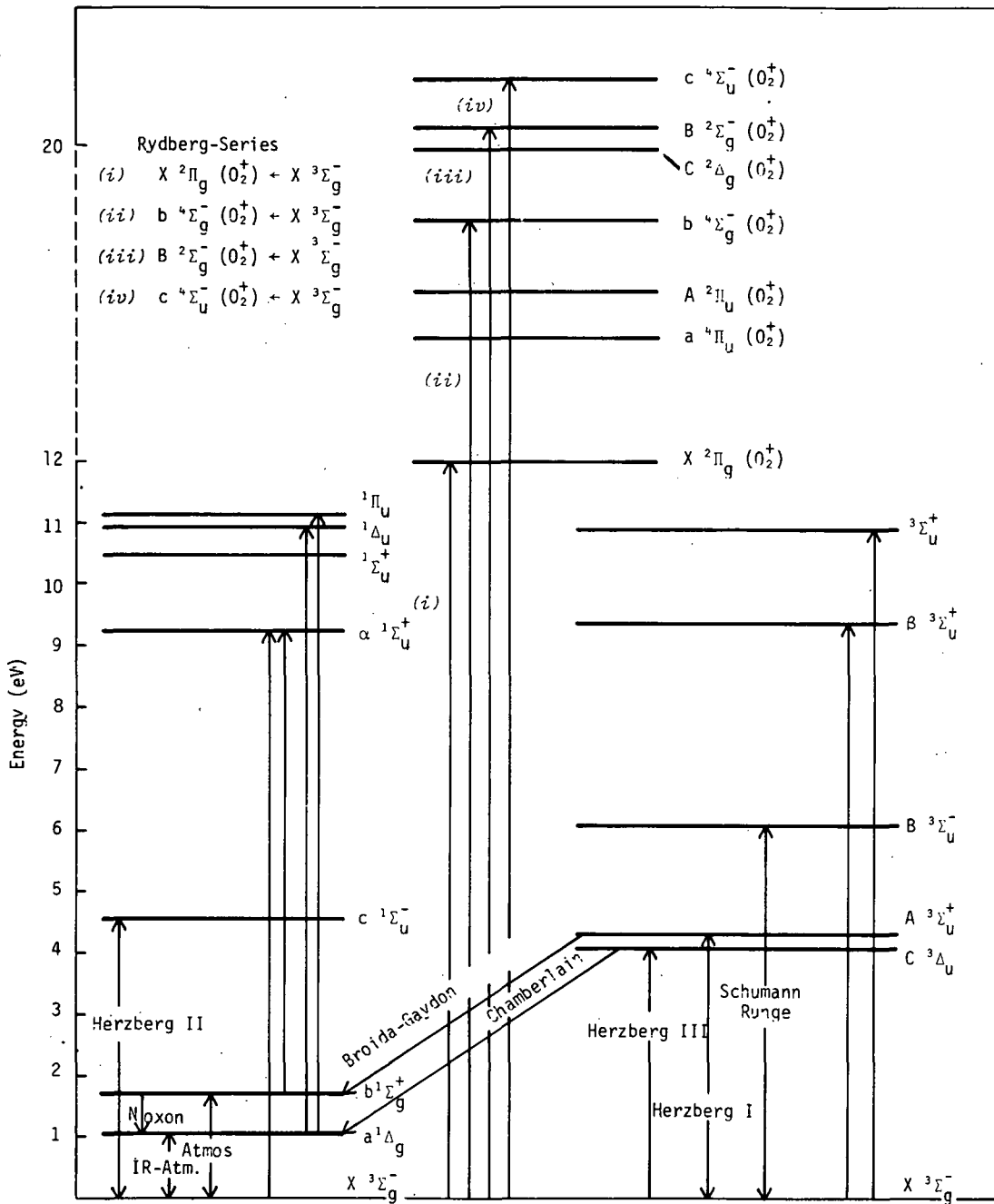
Figure (9-57).   Schematic showing various known electronic states of O_2 and important radiative transitions.

TABLE (9-XXXIII) OBSERVED ELECTRONIC TRANSITIONS OF THE MOLECULE O_2

S.N.	Band System	Electronic Transition	Favorable Sources	Wavelength	Limits	Characteristic Bands (cm^{-1})	Remarks
1	IR (Atmospheric)	$a^1\Delta_g \leftrightarrow X^3\Sigma_g^-$	Absorption; Emission	15800-9240	R	7882.39 (0,)	
2	Atmospheric bands	$b^1\Sigma_g^+ \leftrightarrow X^3\Sigma_g^-$	Numerous sources	9970-5380	R	13120.908 (0,0)	
3	Noxon	$b^1\Sigma_g^+ \rightarrow a^1\Delta_g$	Discharge in $H_e + O_2$ Traces	19080	$\overset{\circ}{A}$	5240 (0,0)	Band heads
4	Herzberg II	$c^1\Sigma_u^- \leftrightarrow X^3\Sigma_g^-$	Luminescence: Absorption	4790-4490 2715-2540	R	32664.1 (0,0) (calculated)	
5	Herzberg III (High Pressure bands)	$C^3\Delta_u^- \leftarrow X^3\Sigma_g^-$	Absorption 1<b<600 atm.	2630-2570) 2924-2440)	R	34319 (0,)	Band head
6	Chamberlain	$C^3\Delta_u \rightarrow a^1\Delta_g$	Luminescence	4380-3700	R		
7	Herzberg I	$A^3\Sigma_u^+ \leftrightarrow {}^3\Sigma_g^-$	Absorption; Luminescence	4880-2430	R	35007.15 (0,0) (Calculated)	
8	Schumann-Runge	$B^3\Sigma_u^- \leftrightarrow X^3\Sigma_g^-$	Numerous Sources	5350-1750 1750-1300 continuum	R		
9	Rydberg series	$X^2\Pi_g(O_2^+) \leftarrow X^3\Sigma_g^-$		1290-1180	V		
		$b^3\Sigma_g^-(O_2^+) \leftarrow X^3\Sigma_g^-$	Absorption	730-660	R		
		$B^2\Sigma_g^-(O_2^+) \leftarrow X^3\Sigma_g^-$		650-600	R		
		$c^4\Sigma_u^-(O_2^+) \leftarrow X^3\Sigma_g^-$		595-510			
10		$\alpha^1\Sigma_u^+ \leftarrow b^1\Sigma_g^+$		1585-1538	V	63141.5	
		$B^3\Sigma_u^+ \leftarrow X^3\Sigma_g^-$	Absorption	1280-1196	V		
		$^1\Delta_u \leftarrow a^1\Delta_g$		1243.8		80396.0	
		$^1\Pi_u \leftarrow a^1\Delta g$		1229.0		81362.5	
		$^3\Sigma_u^+ \leftarrow X^3\Sigma_g^-$		1144.6	V	87369.1	

Numerous unclassified bands

High Pressure Bands of Oxygen. -. The observed spectral features of compressed oxygen
are normally divided into the following four groups:

(1) $3.3\mu m$ and $6.4\mu m$ induced infrared absorption corresponding to O_2 fundamental
     and first overtone.

(2) $12600-6800\overset{o}{A}$: Intensity proportional to pressure. Includes bands of O_2
     (a-x, b-x) transitions as well as bands of $(O_2)_2$.

(3) $6800-3000\overset{o}{A}$: Intensity proportional to $(Pressure)^2$. Simultaneous transitions
     in coupled O_2 molecules, e.g., $(^1\Delta_g + ^1\Delta_g) - (^3\Sigma_g^- + ^3\Sigma_g^-)$.

(4) $2900-2400\overset{o}{A}$: Bands whose frequencies are tentatively correlated with
     $^3\Delta_u - ^3\Sigma_g^-$, O_2.

A brief description of these features is presented.

O_2 does not exhibit any rotation-vibration spectrum on account of symmetry considera-
tions. Crawford, Welsh and Locke (1949) and Shapiro and Gush (1966), however, observed
both fundamental and the first overtone O_2 bands appearing at high pressures. Smith and
Johnston (1952) found a shoulder at 1610 cm^{-1} in the case of infrared band of condensed
oxygen, which is consistent with a possible vibration in $(O_2)_2$.

Ellis and Kneser (1933) while studying optical absorption of liquid oxygen observed
bands in the region $(6800-3000\overset{o}{A})$ which were attributed to simultaneous transitions in
the collision-complex $O_2 - O_2$. Some of these bands have also been identified in the
spectrum of gas phase oxygen under pressures less than 10 atmospheres (Herzberg, 1952;
Herzberg, 1952b). These bands were diffuse and showed no fine structure. Several of
these bands have been identified in the atmospheric absorption during sunset (Herman,
1939; Vassy and Vassy, 1939; Dufay, 1942). More detailed studies on the high pressure
absorption of oxygen by Dianov-Klokov (1964) and Cho et al. (1963) indicate the pressure
induced effects above 1.5 atm. pressures. Robin (1959) identified some of these bands at
oxygen pressures up to 5000 atm.

Cho, Allin and Welsh (1956) observed simultaneous transitions $2(^1\Delta_g) - 2(^3\Sigma_g^-)$ lying
close to O_2, $^1\Sigma_g^+ - X ^3\Sigma_g^-$ transitions in the absorption spectrum of $O_2 - N_2$ liquid measures.
Landan, Allin and Welsh (1962) observed violet degraded bands involving simultaneous
transitions superimposed on a continuous distribution of lattice frequencies. They all
refer to the induced absorption features in the condensed phase of oxygen.

According to Diano-Klokov (1959) all the absorption bands in the $12600-3000\overset{o}{A}$ region
in liquid and condensed oxygen are fundamentally related to intermolecular interaction and
that the spectra correspond to induced dipole transitions in the $(O_2)_2$ complexes. Accord-
ing to Rettschnick and Hoytink (1967), the simultaneous transitions in a $(O_2 - O_2)$ complex
arises due to electron exchange between the two oxygen molecules during collisions.
Studies by Jorden et al., 1964; Cairns and Pimentel, 1965; Barrett, Meyer and Wesserman,
1967; Blickensderfer and Ewing, 1967; on condensed oxygen further support the formation
of the collision complexes like $(O_2 - O_2)$.

Finkelnburg and Steiner (1932) observed the high pressure bands of oxygen in the region 2900-2300Å. In oxygen absorption at pressures of 60-600 atm. they observed a long progression of diffused, almost headless and red-degraded bands, which do not appear at lower pressures. The convergence limits of these bands was roughly coincident with the dissociation limit of O_2. This together with the quadratic increase of absorption with pressure suggested that the bands originated from a collision induced forbidden transition in $O_2(^3\Delta_u \leftarrow X\ ^1\Sigma_g^-)$. Herman (1939) studied the variation of absorption of oxygen with pressure up to 30 atmospheres. The triplet bands were shown to be independent of the Herzberg system (3000-2400Å) of O_2 and were attributed to (O_2 - O_2). Studies by Blickensderfer and Ewing, 1969; Krishna and Cassen, 1969; Robinson, 1967; Tsai and Robinson, 1969; Tabisz, 1969; are significant in this context.

There is no doubt that many spectral features of compressed or condensed oxygen do not show up in the low pressure gas. The simultaneous transitions can be considered as if induced by collisions or due to the formation of unstable collision-complexes. However, the virtually unchanged infrared spectrum is not consistent with the idea of dimer formation but the shoulder at 1610 cm^{-1} could represent vibration in $(O_2)_2$.

The triplet bands (2900-2400Å) are also now assigned to O_2. The quadratic pressure dependence on the intensities of simultaneous transitions as observed by some only indicated dependence on initial reactants; i.e., two O_2 molecules, but does not indicate whether or not the final product is a $(O_2)_2$ molecule. The slight displacement of band frequencies as compared with low pressure O_2 indicates only a very weak interaction between the pairs of O_2 molecules. It may, however, be remarked here that though various physical properties provide some evidence for a stable (O_2 - O_2) collision dimer, the matter has not been solved unequivocally.

Absorption cross section measurements on molecular oxygen (O_2) have been made by many workers (Schneider, 1937; Weissler and Lee; 1952; Ditchburn and Heddle, 1953; Watanabe et al., 1953; Wainfan et al, 1955; Watanabe and Marmo, 1956; Wilkinson and Mulliken, 1957; Ditchburn and Young, 1962; Thompson et al., 1963; Huffman et al., 1964; Cook and Metzger, 1964; Samson and Cairns, 1964, 1965; Cook and Ching, 1967; Goldstein and Mastrup, 1966; Matsunaga and Watanabe, 1967; and many others). The results of most of these investigations have been reviewed by McNesby and Okabe, 1964; Sullivan and Holland, 1966; Huffman, 1969; and recently by Hudson, 1971.

Figures (9-58), (9-59), (9-60), and (9-61) present the absorption cross section profiles of O_2 for the spectral region 2500-800Å. Figures (9-62) and (9-63) depicts the absorption cross sectional curves for the Herzberg and Schumann Runge continua respectively. Figures (9-64), (9-65), (9-66), and (9-67) present the absorption cross section profiles for the region 1000-600Å.
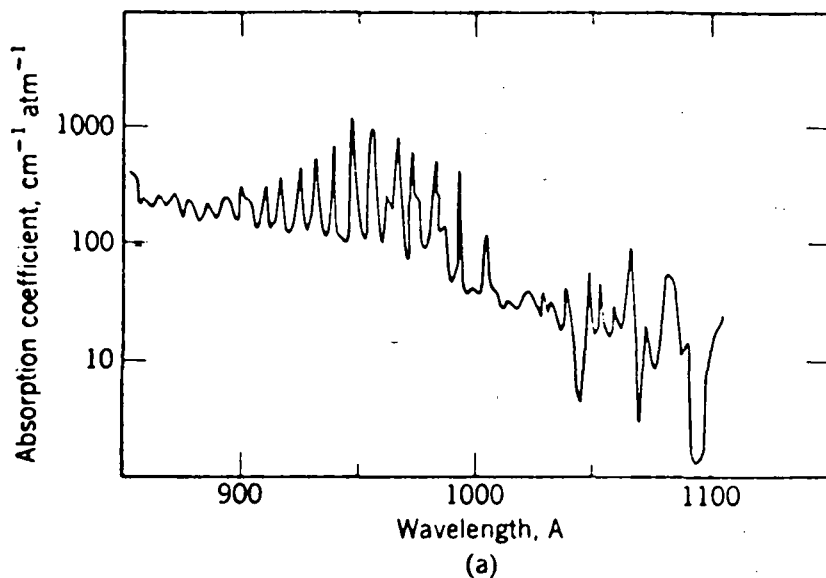
Figure (9-58).   Absorption coefficients of O_2 for the wavelength region 1100-850Å.
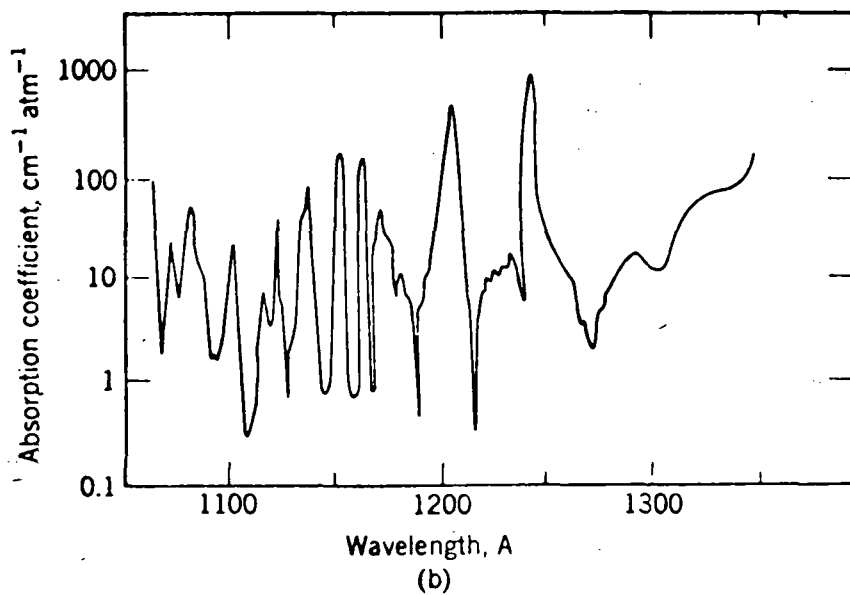[Watanabe and Marmo (1956)]

Figure (9-59).   Absorption coefficients of O_2 for the wavelength region 1350-1050Å.
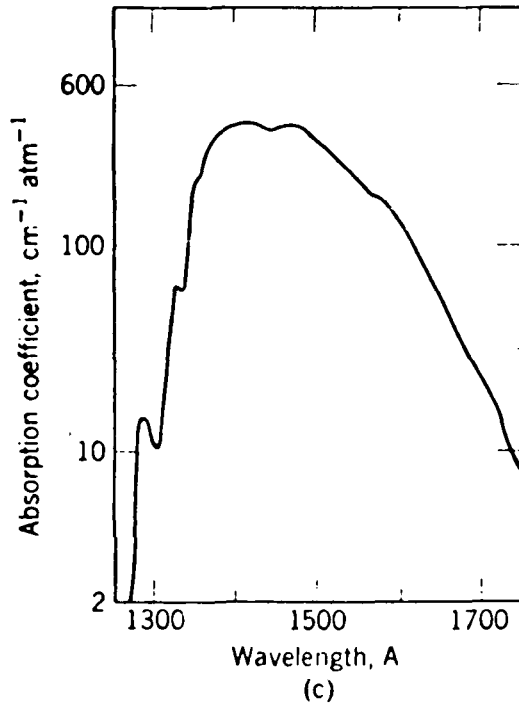[Watanabe, Inn & Zelikoff (1953)]

219

Figure (9-60). Absorption coefficients of O_2 for the wavelength region 1750-1250Å. [Watanabe, Inn and Zelikoff (1953)]
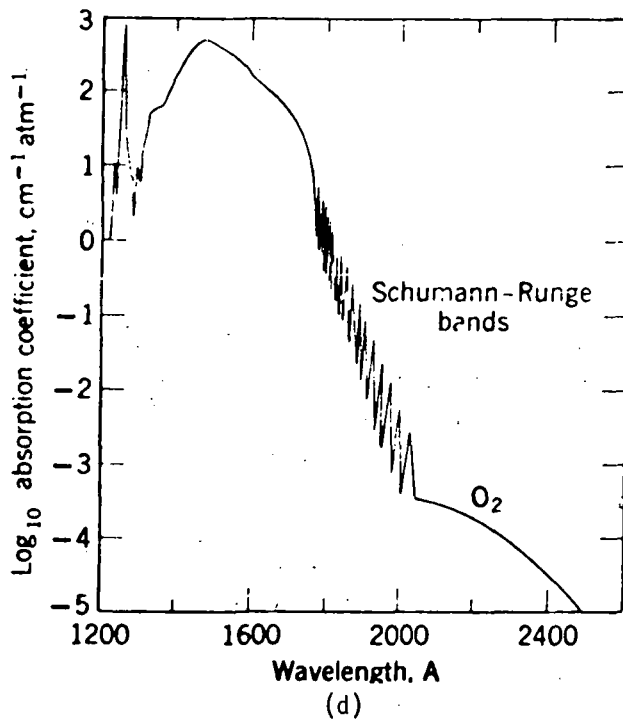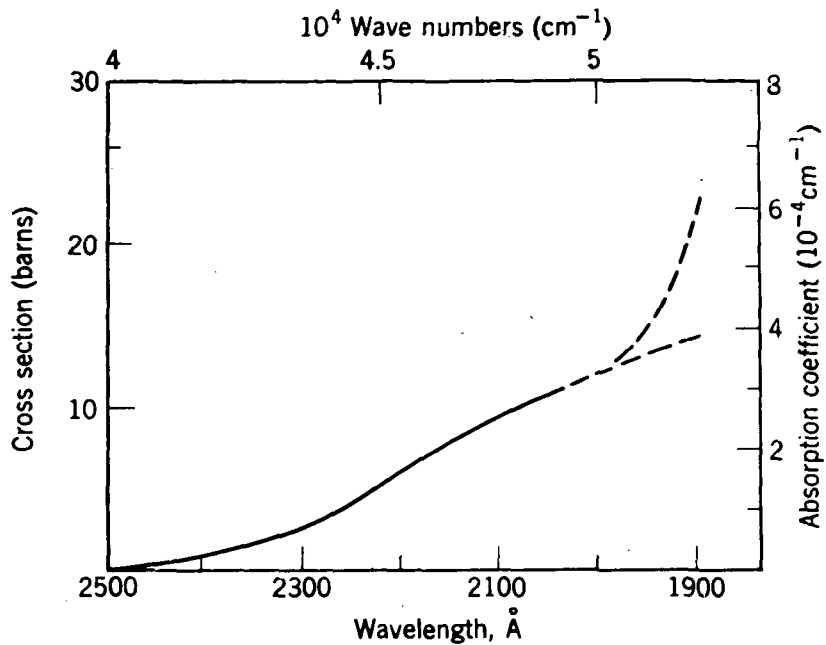

Figure (9-61). Absorption coefficients of O_2 for the wavelength region 2500-1200Å. [McNesby and Okabe (1964)]

Figure (9-62). Herzberg dissociation continuum cross sectional curve.
[Ditchburn and Young (1962)]
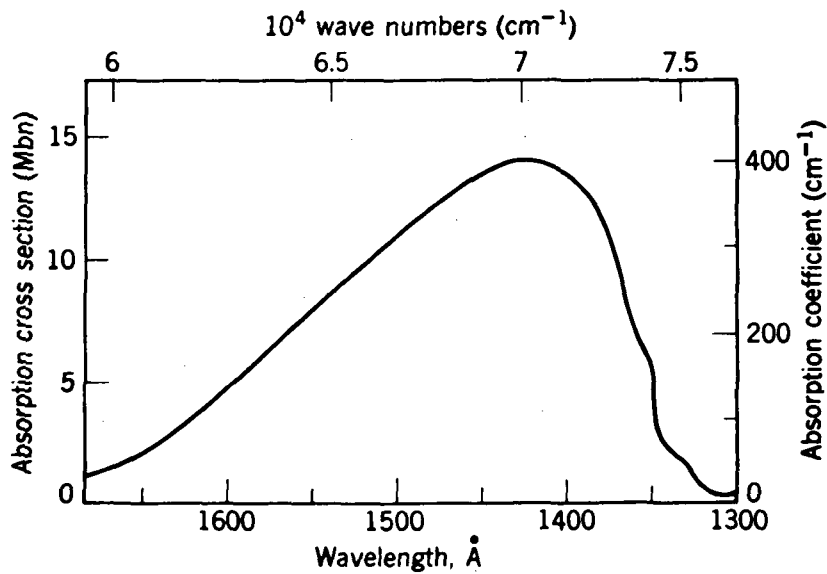
Figure (9-63). Schumann-Runge dissociation continuum cross sectional curve.
[Metzger and Cook (1964)]

221
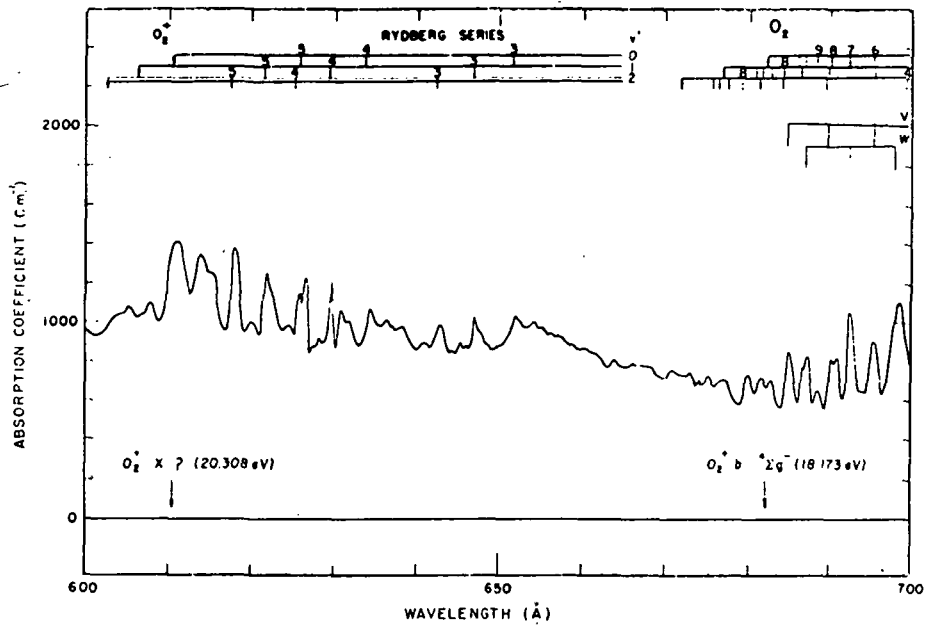
Figure (9-64). Absorption coefficients of O_2 for the wavelength region 700-600Å. [Huffman et al. (1964)]
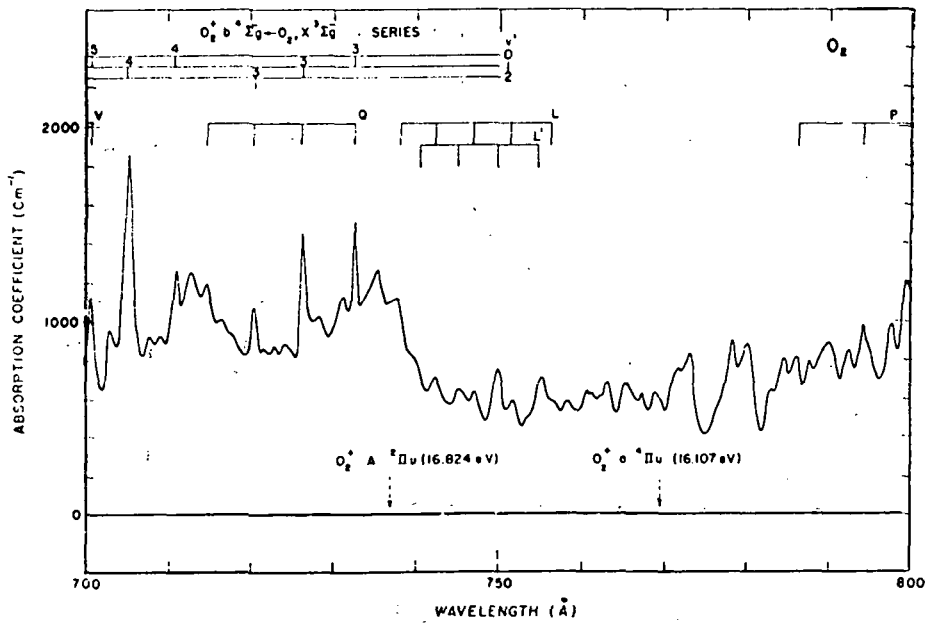
Figure (9-65). Absorption coefficients of O_2 for the wavelength region 800-700Å. [Huffman et al. (1964)]
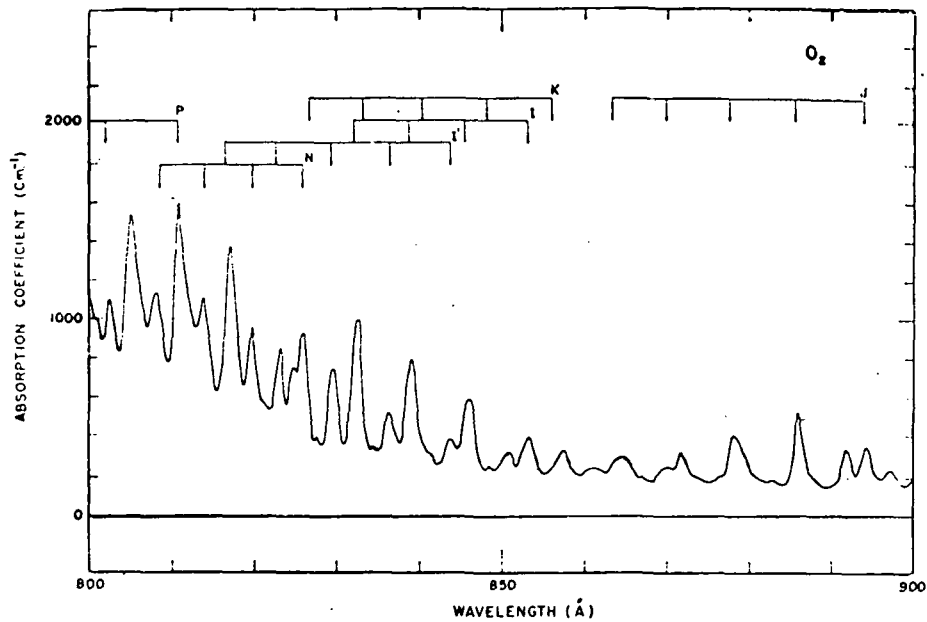
Figure (9-66). Absorption coefficients of O_2 for the wavelength region 900-800Å. [Huffman et al. (1964)]
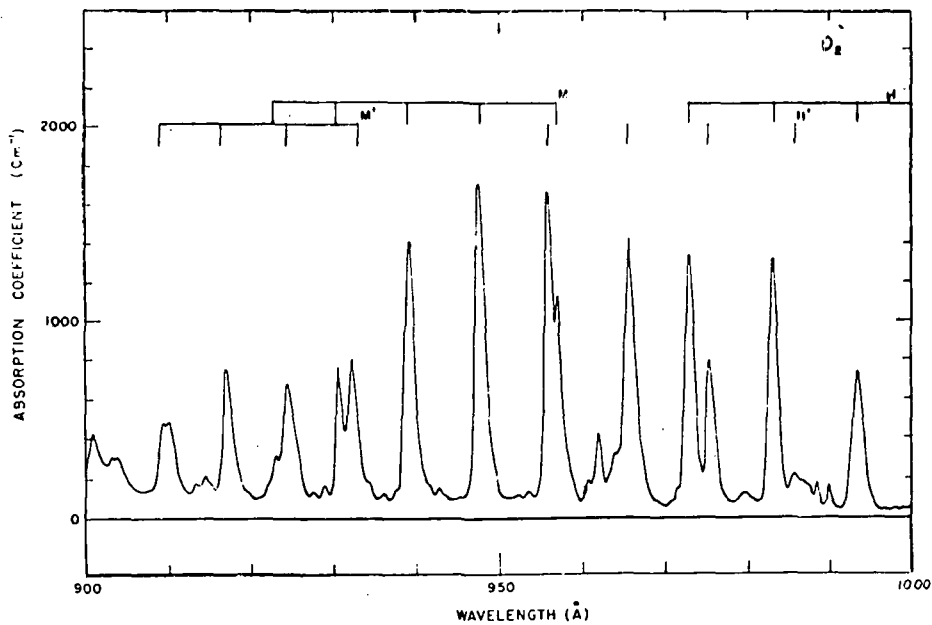
Figure (9-67). Absorption coefficients of O_2 for the wavelength region 1000-900Å. [Huffman et al. (1964).

<u>Microwave Spectrum</u>. - The O_2 molecule, though it is electrically non-polar, possesses a permanent magnetic moment associated with the aligned spins of two unpaired electrons. Consequently, magnetic dipole transitions ($\Delta N = 0$, $\Delta J = \pm 1$) are allowed.

Beringer (1946) first observed weak absorption corresponding to such transitions. It was followed by detailed investigations made by Burkhalter et al., 1950; Anderson, Johnson and Gordy, 1951; Zimmerer and Mizushima, 1961; West and Mizushima, 1966; McKnight and Gordy, 1968; Wilheit and Barrett, 1970; Tankham, 1954; Tinkham and Stranberg, 1955a, b, c; Gebbie et al., 1966; Miller, Javan and Townes, 1951; Miller and Townes, 1953. For details one may refer to the original papers.

Carbon Monoxide (CO)

Dipole Moment, M: 0.1 Debye

Ionization Potential, I.P.: 14.013 eV

Dissociation Energy, D(C-O): 11.09 eV

Ground Electronic State Configuration: $(1\sigma)^2 (2\sigma)^2 (3\sigma)^2 (4\sigma)^2 (1\pi)^4 (5\pi)^2$ - - - $^1\Sigma^+$

Ground State Vibration Frequency and Anharmonicity Constants: ω_e = 2169.826

$$\omega_e x_e = 13.295$$
$$\omega_e y_e = 0.0115 \text{ (cm}^{-1})$$

Rotational Constants:

B_e	α_e	r_e
1.93127 cm^{-1}	0.0175 cm^{-1}	1.1283Å

Carbon monoxide is a fairly stable, light and toxic gas. In earth's atmosphere, it exists as a major pollutant. Its presence has been confirmed in certain other planetary atmospheres, e.g., Venus and Mars, as well as in stellar atmospheres, comet tails and the solar chromosphere.

CO is a simple heteronuclear polar diatomic molecule, composed of one atom of carbon and one atom of oxygen joined together by a covalent bond of length approximately 1Å in its ground electronic state. Carbon monoxide is normally available in the following isotopic forms: $C^{12}O^{16}$; $C^{12}O^{17}$; $C^{13}O^{16}$; $C^{13}O^{18}$; $C^{14}O^{16}$.

Molecular Spectrum

Carbon monoxide exhibits a fairly rich and extensive spectrum ranging from microwave to the vacuum ultraviolet. The observed spectral features can be grouped into three categories: (1) Electronic Spectrum, (2) Vibration-Rotation Spectrum, and (3) Rotational Spectrum.

Electronic Spectrum. - Electronic bands of carbon monoxide cover a wavelength span of about 8000Å in the region 8600-600Å. As many as 31 electronic transitions involving 24 electronic states of the molecule are now known. A number of Rydberg series have also been identified. Birge, 1926; Krupenie, 1966; and lately, Tilford and Simmons, 1972; have presented exhaustive reviews covering various aspects of these features. Table (9-XXXIV) presents a classified resumé of all the electronic transitions so far identified for ready reference. Brief description of the spectral features of each of these transitions follows:

(1) a $\Pi_r \rightleftarrows$ X $^1\Sigma^+$ Cameron System (2580-1760Å)R

The Cameron band system is an electric dipole forbidden system consisting of red-degraded quintupole headed bands covering the spectral region 25800-1760Å. The system is heavily overlapped by the stronger Fourth positive system (discussed later) that covers a wider range 2800-1140Å and also by

TABLE (9-XXXIV) OBSERVED ELECTRONIC TRANSITIONS OF THE MOLECULE CO

S.N.	Band System	Electronic Transition	Favorable Sources	Wavelength Limits		Characteristic Bands, Å	Remarks
1	Cameron	$a^3\Pi_r \leftrightarrow X^1\Sigma^+$	Absorption, Discharges (low pressure)	2580-1760Å	R	2575.3(4,8)	Five headed
2	Hopfield-Birge	$a'^3\Sigma^+ \leftarrow X^1\Sigma^+$	Absorption	1810-1280Å	R	1439.0(13,0)	
3	Asundi	$a'^3\Sigma^+ \rightarrow a^3\Pi_r$	Positive column	8600-3900Å	R	6513.5(9,1)	Many Headed
		$d^3\Delta_i \leftarrow X^1\Sigma^+$	Absorption	1620-1230Å	R	1402.8(10,0)	Simple Heads
5	"Triplets"	$d^3\Delta_i \rightarrow a^3\Pi_r$	Discharge (CO + He)	7500-3770Å	R	6464.6 / 6433.1 (3,0) / 6401.0	Triple headed
		$e^3\Sigma^- \leftarrow X^1\Sigma^+$	Absorption	1575-1240Å	R	1542.8(1,0)	
7	Herman	$e^3\Sigma^- \rightarrow a^3\Pi_r$	Discharge (CO + rare gases)	5430-4270Å	R		Dense Heads
8	Fourth Positive	$A^1\Pi \leftrightarrow X^1\Sigma^+$	Absorption positive column	2800-1140Å	R	2089.9(5,12) 2067.6(4,11) 2046.3(3,10)	Simple heads
9		$I^1\Sigma^- \leftarrow X^1\Sigma^+$	Absorption	1550-1260Å	R		Only Q
10		$f^3\Sigma^+ \rightarrow a^3\Pi_i$	Geissler tube	2980-2670Å	R		
11	Hopfield-Birge	$b^3\Sigma^+ \leftrightarrow X^1\Sigma^+$	Absorption	1190-1130Å	V		
12	Third Positive	$b^3\Sigma^+ \rightarrow a^3\Pi_r$	Positive column	3830-2260Å	V	2833.1(0,0)	Five headed
13	Hopfield-Birge	$B^1\Sigma^+ \leftrightarrow X^1\Sigma^+$	Absorption	1150-1100Å	V		
14	Ångström	$B^1\Sigma^+ \leftrightarrow A^1\Pi$	Positive Column	6620-4120Å	V	4510.9(0,0)	Simple heads
15	Kaplan	$K \rightarrow a^3\Pi_r$	Discharge	2750-2520Å	V		
16		$Eo^1\Sigma^+ \rightarrow X^1\Sigma^+$	High Pressure discharge	1310-1100Å	R		
17		$j^3\Sigma^+ \leftarrow X^1\Sigma^+$	Absorption	1100-1070Å	R		
18	Hopfield-Birge	$C^1\Sigma^+ \leftrightarrow X^1\Sigma^+$	Absorption	1100-1060Å	V		
19	Knauss	$C^1\Sigma^+ \rightarrow a'^3\Sigma^+$	r.f. discharge	3250-2930Å			
20	Herzberg	$C^1\Sigma^+ \rightarrow A^1\Pi$	Positive Column	5710-3680Å	V	3893.1(0,1)	Simple heads
21	"3A"	$c^3\Pi \rightarrow a^3\Pi_r$	Geissler tube	2710-2300Å	V	2389.7(0,1)	Multiple heads
22	Tilford	$c^3\Pi \leftarrow X^1\Sigma^+$	Absorption	1086Å	V		
23	Hopfield-Birge	$E^1\Pi \leftrightarrow X^1\Sigma^+$	Absorption	1080-1050Å	V		
24		$^1\Sigma \rightarrow X^1\Sigma^+$	Absorption	1130-1010Å	R		
25	Hopfield-Birge	$F(^1\Sigma^+) \leftarrow X^1\Sigma^+$	Absorption	1000Å	R		
26	Hopfield-Birge	$G(^1\Pi) \leftarrow X^1\Pi^+$	Absorption	950Å	R		
27	Tanaka	$P \leftarrow X^1\Sigma^+$ $Q \leftarrow X^1\Sigma^+$ $R \leftarrow X^1\Sigma^+$ $S \leftarrow X^1\Sigma^+$ $T \leftarrow X^1\Sigma^+$	Absorption	790-730Å 780-740Å 780-730Å 690-670Å 650-640Å	R R R R R		
28	Rydberg	Rydberg	Absorption	950-600Å	R		

the B $^2\Sigma^+$ - X $^2\Sigma^-$ First negative bands of CO$^+$. Cameron (1926) first dis-
covered these bands in an uncondensed discharge in neon gas with traces
of carbon monoxide and hence the name. Hopfield and Birge (1927) later
observed them in absorption. It was followed by more detailed investigations
by Knauss and Cotton, 1931; Gero, Herzberg and Schmid, 1937; Schmid and Gero,
1937; Gero, 1938; Herman, 1947; Rao, 1949; Tanaka, Jursa and LeBlanc, 1957;
Krupenie, 1966.

(2) a' $^3\Sigma^+$ - X $^1\Sigma^+$ Hopfield-Birge System (1810-1280Å)R

This system arises out of a forbidden electric dipole transition. Hopfield
and Birge (1927) first reported a group of five red-degraded bands with the
one at 1696.9Å as the (0,0) band of the system. The system was later studied
by Estey, 1930; Beer, 1937; and lately by Herzberg and Hugo, 1955; Tanaka,
Jursa, and LeBlanc, 1957. High resolution studies are due to Herzberg et al.,
1955; and Simmons et al., 1972.

(3) a' $^3\Sigma^+$ - a $^3\Pi_r$ Asundi System (8600-3900Å)R

This system consists of numerous multiheaded red-degraded bands stretching
right through deep red. Asundi (1929) first discovered these bands in a
gaseous discharge through carbon monoxide. Studies by Beer, 1937; Schmid
and Gero, 1937; Gero and Lorinezi, 1939; Garg, 1949; Herzberg and Hugo, 1955;
are worth mentioning in this context.

(4) d $^3\Delta_i$ - X $^1\Sigma^+$ Transition (1620-1230Å)R

This is a weak progression of single-headed and red degraded bands extending
to high v' values and assumed to correspond to the R-heads of the transition.
The system was first reported by Tanaka, Jursa and LeBlanc, 1957; and lately
studied by Herzberg, Hugo and Tilford, 1970.

(5) d $^3\Delta_i$ - a $^3\Pi_r$ "Triplets" (7500-3770Å)R

The d $^3\Delta_i$ - a $^3\Pi_r$ "Triplet" bands form a fairly extensive system of moderate
intensity and cover almost the entire visible region. Merton and Johnson,(1923)
first observed two progressions of this system in a gaseous discharge in helium
with traces of carbon monoxide. Later, these bands were produced and studied
using different sources in emission (Birge, 1925; Gero and Szabo, 1939; Asundi,
1940; Herman and Herman, 1947, 1948; Mulliken, 1958; Sato, 1960, 1962; Carroll,
1962; Kovács, 1964).

(6) e $^3\Sigma^-$ - X $^1\Sigma^+$ Transition (1570-1240Å)

This band system also corresponds to a forbidden transition and lies in the
vacuum ultraviolet. Herzberg and Hugo (1955) first observed a long progression
(v' = 0) of weak, red-degraded single headed bands in absorption which con-
stitutes this system. Later, Tanaka, Jursa and LeBlanc (1957) and also Simmons
and Tilford (1971) studied these bands in detail.

(7) e $^3\Sigma^-$ - a $^3\Pi_r$ Herman System (5430-4270Å)R

This system is composed of closely spaced red-degraded bands. Though Merton and Johnson (1923) first observed some of these bands, it was Herman and Herman (1947, 1948) who identified them forming as a separate system. Later Herzberg and Hugo (1955) and Tanaka, Jursa and LeBlanc (1957) studied these bands in absorption. Barrow (1961) and Simmons, Bass and Tilford (1965) presented a modified analysis.

(8) A $^1\Pi$ - X $^1\Sigma^+$ Fourth Positive System (2800-1140Å)R

This is the most prominent group of bands in the electronic spectrum of carbon monoxide. It consists of a large number of single-headed, red-degraded bands lying in the region 2800-1140Å. Besides early studies by Birge (1923), these bands have been studied by many workers (Leifson, 1926; Birge, 1927; Estey, 1930; Headrick and Fox, 1930; Read, 1934; Gero, 1936; Schmid and Gero, 1936; Tschulanowsky and Stepanow, 1936; McCulloh, 1951; McCulloh and Glocker, 1953; Tanaka, Jursa and LeBlanc, 1957; Tanaka, 1957; Simmons, Bass and Tilford, 1969). Detailed line structure study of the various bands has been recently made by Tilford and Simmons (1972).

(9) I $^1\Sigma^-$ - X $^1\Sigma^+$ Transition (1550-1260Å)R

This is a smaller group consisting of three red-degraded bands showing only Q-heads. It appears only in absorption. It was first identified as a separate system by Herzberg et al. (1966). Recently Simmons and Tilford (1971) studied these bands quite extensively.

(10) f $^3\Sigma^+$ - a $^3\Pi_i$ Transition (2980-2670Å)R

This is a relatively weak system consisting of several red-degraded bands lying very near to the (1,0) and (0,1) violet degraded bands of the Third positive system. Schmid and Gero (1937) who first observed these bands, ascribed them to the electronic transition, $^3\Sigma^+$ - $^3\Pi$. Gero (1938) also performed rotational analysis of two of these bands. The system was studied more extensively later by Garg, 1949; Stepanov, 1940; Gaydon, 1953; and Herzberg, 1961.

(11) b $^1\Sigma^+$ $\rightleftharpoons$ X $^1\Sigma^+$ (1190-1130Å)

Discussed later under the heading "Hopfield-Birge Singlet-Singlet Transitions".

(12) b $^3\Sigma^+$ - a $^3\Pi_r$ Third Positive System (3830-2260Å)V

This system is composed of strong quintet-headed red degraded bands characterized by intensity fluctuations. First systematic measurements on these bands date back to 1888 by Deslandres who observed them in a gaseous discharge in carbon monoxide. Johnson (1926) made first assignment of the vibrational quantum numbers for the various bands in the system and identified the lower state of the transition with the upper state of the Cameron bands.

Detailed investigations were later made by Birge, 1926; Duffendack and Fox, 1926, 1927; Asundi, 1929; Dieke and Mauchly, 1932; Schmid and Gero, 1935; Gero, 1936; Beer, 1937; Stepanov, 1940.

(13) $B\ ^1\Sigma^+ \rightleftarrows X\ ^1\Sigma^+$ (1150-1100Å)

Discussed later under the heading "Hopfield-Birge Singlet-Singlet Transitions."

(14) $B\ ^1\Sigma^+ - A\ ^1\Pi$ Angstrom System (6620-4120Å)V

This band system is composed of fairly strong single-headed and violet degraded bands, characterized by numerous perturbations and predissociations. The first rotational analysis of some of these bands was carried out by Hulthen (1923) and Jasse (1926). Later, Rosenthal and Jenkins, 1929; Schmid and Gero, 1935; Johnson and Asundi, 1936; Coster and Brons, 1934; McCulloh, 1951; McCulloh, and Glockler, 1953; Douglas and Moller, 1953; studied this spectrum under high dispersion and resolution and using better sources of emission.

(15) $K - a\ ^3\Pi_r$ Kaplan System (2750-2520Å)V

Kaplan (1930) observed three bands forming a new system when a trace of carbon monoxide gas was excited in a long atomic hydrogen tube. The bands were violet degraded and each showed six subheads. They resembled quite closely with the "3A" bands. Kaplan attributed the system to a transition $K-a\ ^3\Pi_r$, the upper state being most probably a metastable quintet.

(16) $E_0\ ^1\Sigma^+ - X\ ^1\Sigma^+$ "High Pressure Bands " (1310-1100Å)R

These are weak red degraded bands and were first observed by Tschulanowsky and Gassilewitch (1937) in the region 1200-930Å in a high pressure discharge in carbon monoxide. Tschulanowsky (1939) classified these bands as belonging to a new system $E_0\ ^1\Sigma^+ - X\ ^1\Sigma^+$.

(17) $j\ ^3\Sigma^+ - X\ ^1\Sigma^+$ Transition (1100-1070Å)R

This system of red-degraded bands was discovered by Tilford and Vanderslice (1968). It consists of mainly two bands at 1073.5Å and 1099Å, respectively.

(18) $C\ ^1\Sigma^+ \rightleftarrows X\ ^1\Sigma^+$ (1110-1060Å)

Discussed later under the heading "Hopfield-Birge Singlet-Singlet Transitions."

(19) $C\ ^1\Sigma^+ - a'\ ^3\Sigma^+$ Knauss System (3250-2930Å)V

Knauss (1931) observed four violet degraded bands in an electrodeless discharge through carbon monoxide. These bands were ascribed to an entirely new transition $C\ ^1\Sigma^+ - a'\ ^3\Sigma^+$. More recent data on the vibrational structure of the state $a'\ ^3\Sigma$ indicated that the v'' values as proposed by Knauss should be raised by 2.

(20) $C\ ^1\Sigma^+ - A\ ^1\Pi$ Herzberg System (5710-3680Å)V

This system, which partly overlaps the Angstrom system, consists of only a few bands of the $v'' - 0$ progression. Three bands of this system were first observed by Duffendack and Fox (1927) who perhaps wrongly identified them as

part of the Angström system on account of their similar structure. Herzberg, (1929) observed eight bands of this group and identified them as arising out of a new transition, now designated as $C\ ^1\Sigma^+ - A\ ^1\Pi$. The system was later studied in detail by Asundi, 1929; Asundi and Johnson, 1929; Schmid and Gero, 1935.

(21) $C\ ^3\Pi - a\ ^3\Pi_r$. 3A System (2710-2300Å)V

This system is composed of fairly strong multi-headed and violet degraded bands lying in the region 2710-2300Å. Five of the bands assigned to this system were first observed by Duffendack and Fox (1926, 1927). Later studies were made by Asundi, 1929; Schmid and Gero, 1937; Gero, 1938; and lately by Tilford, 1969; and Ginter and Tilford, 1969. These bands have the same final state as the Third positive system $b\ ^3\Sigma^+ - a\ ^3\Pi$ but originate from a state about 1.02 eV above the b state.

(22) $c\ ^3\Pi - X\ ^1\Sigma^+$ Tilford System (~1086Å)V

Tilford (1969) first identified this transition. It is composed of only one violet degraded band, the (0,0) band located at 92076.8 cm^{-1}.

(23) $E\ ^1\Pi \overset{\rightarrow}{\leftarrow} X\ ^1\Sigma^+$ (1080-1050Å)

Discussed later under the heading "Hopfield-Birge Singlet-Singlet Transitions."

(24) $^1\Pi - X\ ^1\Sigma^+$ Transition (1130-1010Å)R

Tschulanovsky (1939) reported a group of weak and overlapping red degraded bands in the region 1100-1000Å, which form a new $^1\Pi - X\ ^1\Sigma^+$ system. The best resolved band is the (0,1) band located at 1034.65Å which shows longer and stronger P and R branches than the Q branch.

(25) $F\ (^1\Sigma^+) \leftarrow X\ ^1\Sigma^+$ (1000Å)

Discussed later under the heading "Hopfield-Birge Singlet-Singlet Transitions."

(26) $G\ (^1\Pi) \rightarrow X\ ^1\Sigma^+$ (950Å)

Discussed later under the heading "Hopfield-Birge Singlet-Singlet Transitions."

(27) P, Q, R, S, T $- X\ ^1\Sigma^+$ Tanaka Absorption Systems (800-630Å)R

(a) $P \leftarrow X\ ^1\Sigma^+$ (790-730Å)R

(b) $Q \leftarrow X\ ^1\Sigma^+$ (780-740Å)R

(c) $R \leftarrow X\ ^1\Sigma^+$ (780-730Å)R

(d) $S \leftarrow X\ ^1\Sigma^+$ (690-670Å)R

(e) $T \leftarrow X\ ^1\Sigma^+$ (650-640Å)R

Tanaka (1942) observed in absorption five new progressions of red degraded bands with approximately constant differences of frequency. These progressions were ascribed by Tanaka to the electronic transitions from the ground state to the P, Q, R, S and T states. Weissler et al. (1959), and later Kaneko (1961), identified some of these states in the photoionization and electron impact experiments.

(28) Rydberg Series (950-600Å)

Five Rydberg series have been identified in the absorption spectrum of carbon monoxide in the vacuum ultraviolet region (950-600Å) (Henning, 1932; Tanaka, 1942; Anand, 1942; Takamine, Tanaka and Iwata, 1943; Woods, 1943; Ogawa, 1965; Ogawa and Ogawa, 1972). These are as follows:

$$\nu = 113029 - \frac{R}{(n - 1.88)^2} \; ; \quad n = 6 - - - 14 \quad \text{Takamine-Tanaka-Iwata;} \quad X\ ^2\Sigma^+\ (CO^+) \leftarrow X\ ^1\Sigma^+$$

$$\nu = 133380 - \frac{R}{(n - 1.69)^2} \; ; \quad n = 5 - - - 9 \quad \begin{array}{l}\text{Tanaka} \\ \alpha \text{ Series;}\end{array} \quad A\ ^2\Pi_i\ (CO^+) \leftarrow X\ ^1\Sigma^+$$

$$\nu = 158692 - \frac{R}{(n - 1.68)^2} \; ; \quad n = 4 - - - 12 \quad \begin{array}{l}\text{Tanaka} \\ \beta \text{ Series;}\end{array} \quad B\ ^2\Sigma^+\ (CO^+) \leftarrow X\ ^1\Sigma^+$$

$$\nu = 158670 - \frac{R}{(n - .93)^2} \; ; \quad n = 4 - - - 9$$

$$\text{Ogawa;} \quad B\ ^2\Sigma^+\ (CO^+) \leftarrow X\ ^1\Sigma^+$$

$$\nu = 158680 - \frac{R}{(n - .20)^2} \; ; \quad n = 3 - - - 7$$

(29) Hopfield-Birge Singlet-Singlet Transitions (11, 13, 18, 23, 25, 26)

(a) $b\ ^1\Sigma^+ \rightleftarrows X\ ^1\Sigma^+$ (1190-1130Å)
(b) $B\ ^1\Sigma^+ \rightleftarrows X\ ^1\Sigma^+$ (1150-1100Å)
(c) $C\ ^1\Sigma^+ \rightleftarrows X\ ^1\Sigma^+$ (1110-1060Å)
(d) $E\ ^1\Pi \rightleftarrows X\ ^1\Sigma^+$ (1080-1050Å)
(e) $F\ (^1\Sigma^+) \leftarrow X\ ^1\Sigma^+$ (1000Å)
(f) $G\ (^1\Pi) \rightarrow X\ ^1\Sigma^+$ (950Å)

Hopfield, 1927; and Hopfield and Birge, 1927; reported these band systems, a majority of them appearing both in absorption and emission. Full details of this work was never published, though several of these bands have since been observed elsewhere and studied (Read, 1934; Tanaka et al., 1957; Tilford, et al., 1965; Tilford, Vanderslice and Wilkinson, 1965; Simmons and Tilford, 1966; Simmons and Tilford, 1971). Band head data in respect to all these systems can be found in the NSRDS-NBS-5 report by Krupenie (1966) and the review article by Tilford and Simmons (1972). Table (9-XXXV) gives the various spectroscopic constants for all the known radiative transitions and figure (9-68) presents a schematic showing the relative disposition of the various known states of CO and its ion, CO^+. Various radiative transitions are also indicated.

TABLE (9-XXXV) SPECTROSCOPIC CONSTANTS FOR KNOWN RADIATIVE TRANSITIONS OF CO

State Nomen-clature	T_0	ω_e	$\omega_e x_e$	B_e	α_e	$D_e \cdot 10^6$	r_e	Remarks
T	154362	(1354)	(9)	-	-	-	-	
S	144735	(1641)	(4.8)	-	-	-	-	
R	128866	1568	11.6	-	-	-	-	
Q	128738	1558	10.6	-	-	-	-	
P	126410	1567	13.6	-	-	-	-	
$G(^1\Pi)$	105266	(1097)	-	-	-	-	-	
$F(^1\Sigma^+)$	99730	2112	198	-	-	-	-	(a)
$^1\Pi$	98836	-	-	1.139[b]	-	-	1.469[c]	
$E^1\Pi$	92930.03	(2134)	-	1.9644[b]	-	6.5	1.1188[c]	(a)
$c^3\Pi$	92076.1	-	-	1.9563[b]	-	-	1.1211[c]	(a)
$C^1\Sigma^+$	91919.1	2175.92	14.76	1.9533	0.0196	5.7	1.1219	(a)
$i^3\Sigma^+$	90988.0	2196	15	1.889	0.020	-	1.141	
$E_o{}^1\Sigma^+$	-	-	-	1.182[b]	-	-	1.442[c]	
K	(89889)	-	-	-	-	-	-	
$B^1\Sigma^+$	86916.2	2212.70	15.22	1.9612	0.0261	6.1	1.1197	(a)
$b^3\Sigma^+$	83832.5	(2188)	-	1.986	0.042	-	1.113	(a)
$f^3\Sigma^+$	(83744)	-	-	(0.83)[b]	-	-	-	
$A^1\Pi$	64746.5	1515.4	17.25	1.6104	0.0205	7.3	1.2356	
$I^1\Sigma^-$	64546.65	1092.03	10.754	1.2702	0.01815	9.0	1.3913	
$e^3\Sigma^-$	63708.92	1113.67	9.596	1.2848	0.0181	6.5	1.3834	
$d^3\Delta_1$	60646.93	1152.58	7.2812	1.3099	0.01677	5.8	1.3700	
$a^3\Sigma^+$	55353.91	1230.651	11.0130	1.3453	0.01872	6.5	1.3519	
$a^3\Pi_r$	48473.97	1743.55	14.47	1.6911	0.0195	-	1.2058	
$X^1\Sigma^+$	0	2169.8233	13.2939	1.931271	0.017513	6.1198	1.128322	

(a) First member of a Rydberg series
(b) Value of B_0
(c) Value of r_0
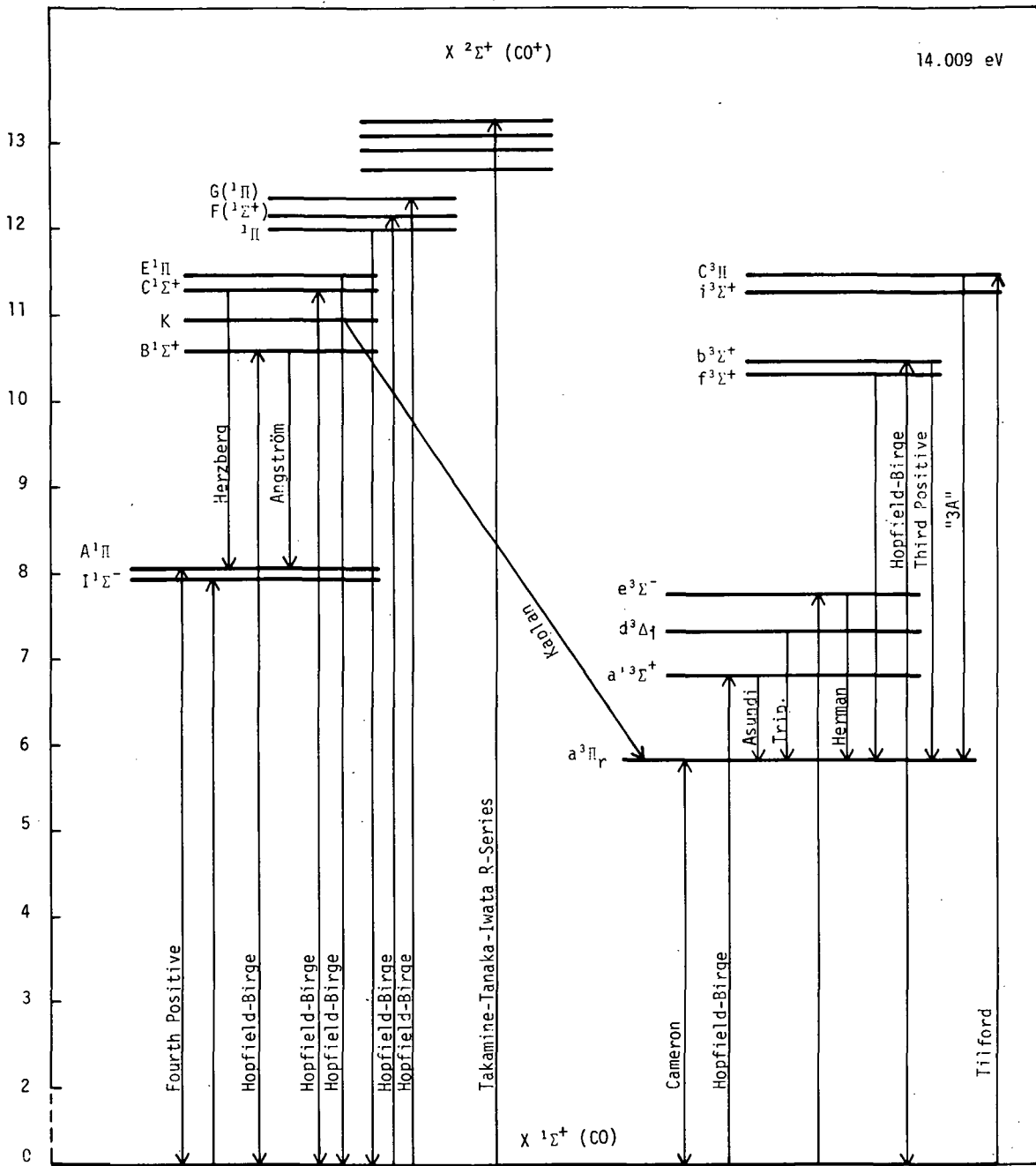
Figure (9-68). Schematic showing various known electronic states of CO and important radiative transitions.

Absorption cross sections for carbon monoxide have also been measured by different workers in different wavelength segments, especially below 2000Å (Watanabe et al., 1953; Sun and Weissler, 1955; Cairns and Samson, 1955; Huffman et al., 1964; Thompson et al., 1963; Myer and Samson, 1970). The results of Myer and Samson (1970) for the spectral region (1700-1050Å) presented in figure (9-69) and those of Huffman et al. (1964) for the region (1000-600Å) are presented in figures (9-70), (9-71), (9-72), and (9-73).

Vibration-Rotation Spectrum. - Vibration-rotation spectrum of carbon monoxide has been the subject of numerous investigations in the past. Mention may be made of the following few important references (Herzberg and Rao, 1949; Plyler et al., 1952; Goldberg and Mueller, 1953; Mills and Thompson, 1953; Locke and Herzberg, 1953; Plyler et al., 1955; Rank et al., 1957; Mould et al., 1960; Rank et al., 1961; Pierre, 1964; Rank et al., 1965; Kaplan et al., 1969).

Though most of these studies have been limited to absorption many of the vibration-rotation features have been identified in emission too in combustion or ablation of certain organic compounds. Some of the bands have been identified in sun's spectrum as well as in the spectra of certain planetary atmospheres. (Connes, 1969; Goldberg and Mueller, 1953). Mantz et al. (1970) and recently Roh and Rao (1974), and Johns et al. (1974) made extensive wavelength measurements for a large number of vibration-rotation laser lines lying in the spectral region 2000-1200 cm^{-1}

The fundamental band $1 \leftarrow 0(6\mu)$ appears as strongest of all the known vibration rotation bands of carbon monoxide. Two other weaker bands $2 \leftarrow 0$ (2.35μ) and $3 \leftarrow 0$ (1.58μ) are also of common occurrence. A list of the known vibration-rotation transitions of carbon monoxide is given in (Table 9-XXXVI). For detailed data on the fine structure of these bands, papers by Rank et al., 1957; Plyler et al., 1955; Pierre, 1964; may be referred.

Rotational Spectrum. - Pure rotational transitions in carbon monoxide have been studied both in the microwave (λ < 2.6 mm) as well as in the far infrared (600-100μ) regions (Gilliam, Johnson and Gordy, 1950; Bedard, Gallagher and Johnson, 1953; Palik and Rao, 1956; Gordy and Cowan, 1957; Rosenblum, Nethercot and Townes, 1958; Jones and Gordy, 1964; Rao, deVore and Plyler, 1963). Details can be seen in the original references.
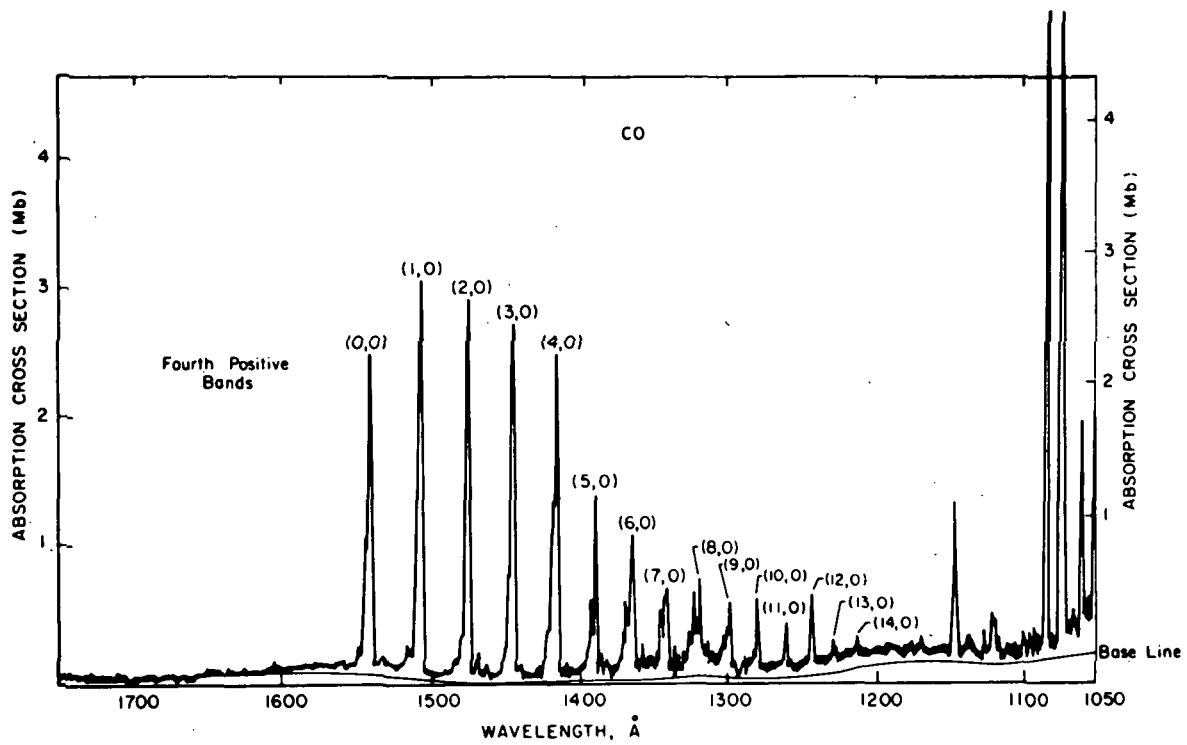
Figure (9-69).   Absorption cross sections profile of CO for the wavelength
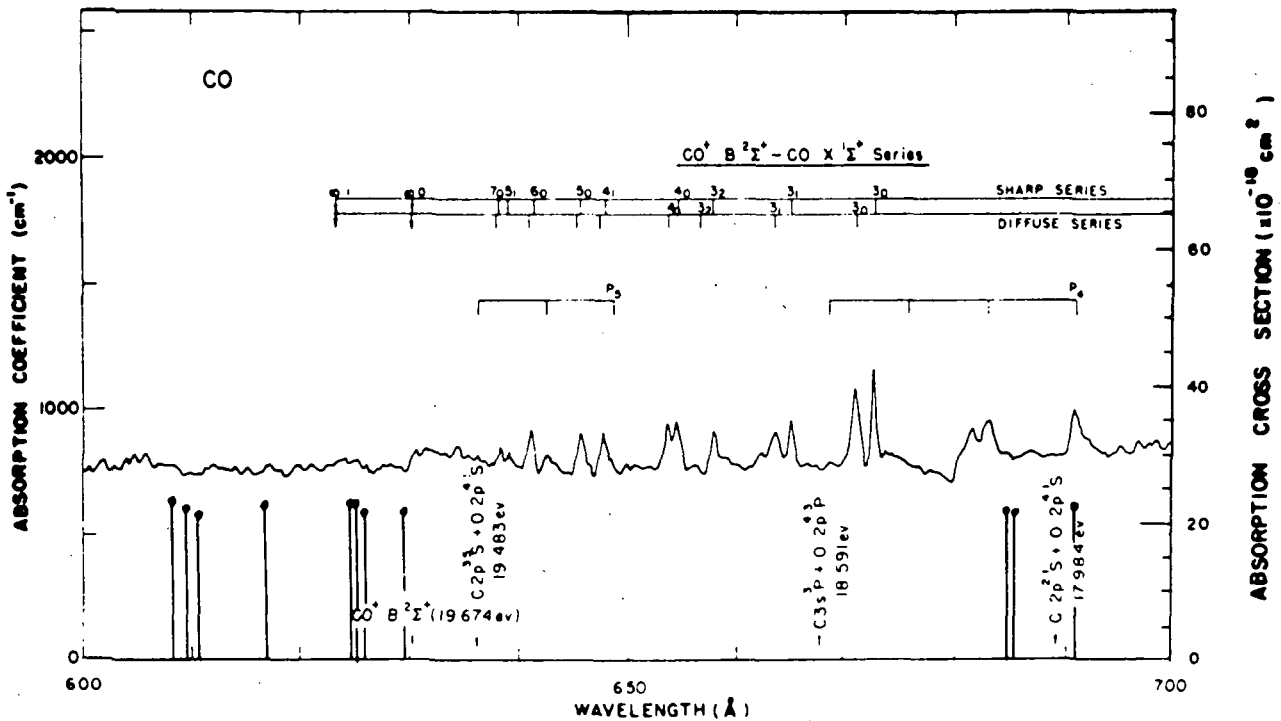region 1750-1050Å (Myer and Samson, 1970).

Figure (9-70).   Absorption coefficient of CO for the wavelength region
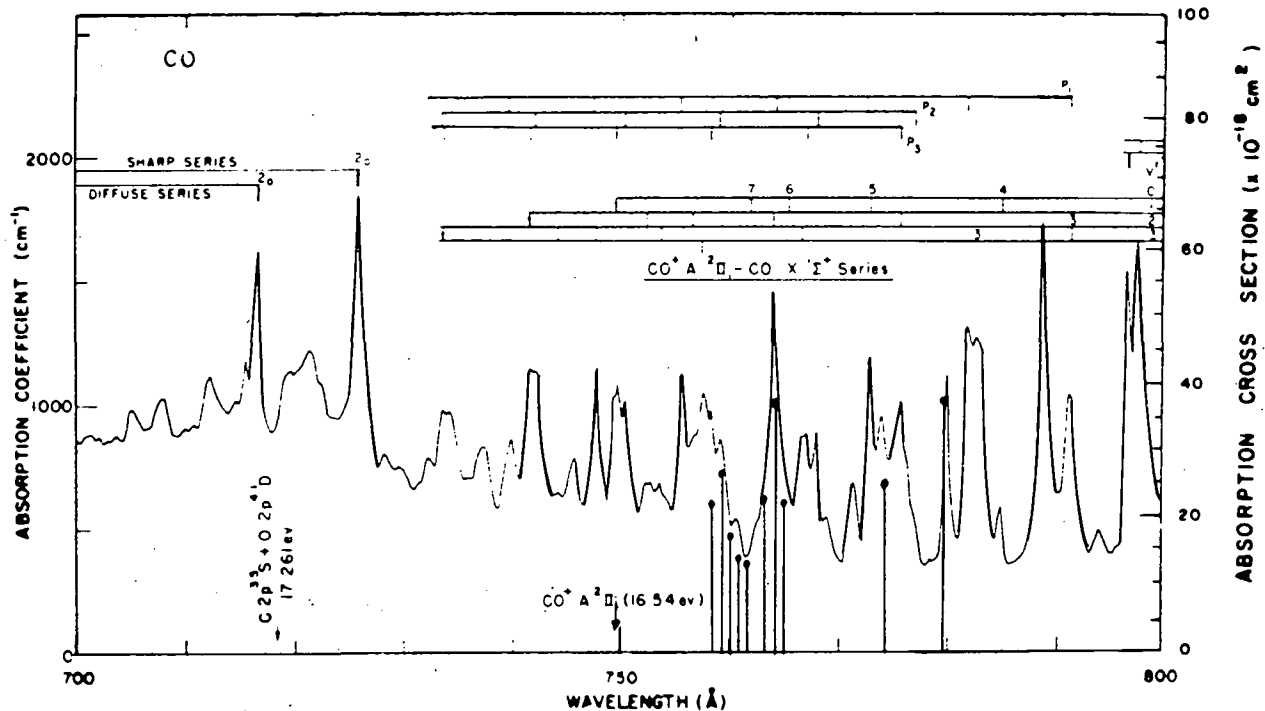700-600Å (Huffman et al, 1964).

235

Figure (9-71).   Absorption cross section of CO for the wavelength region
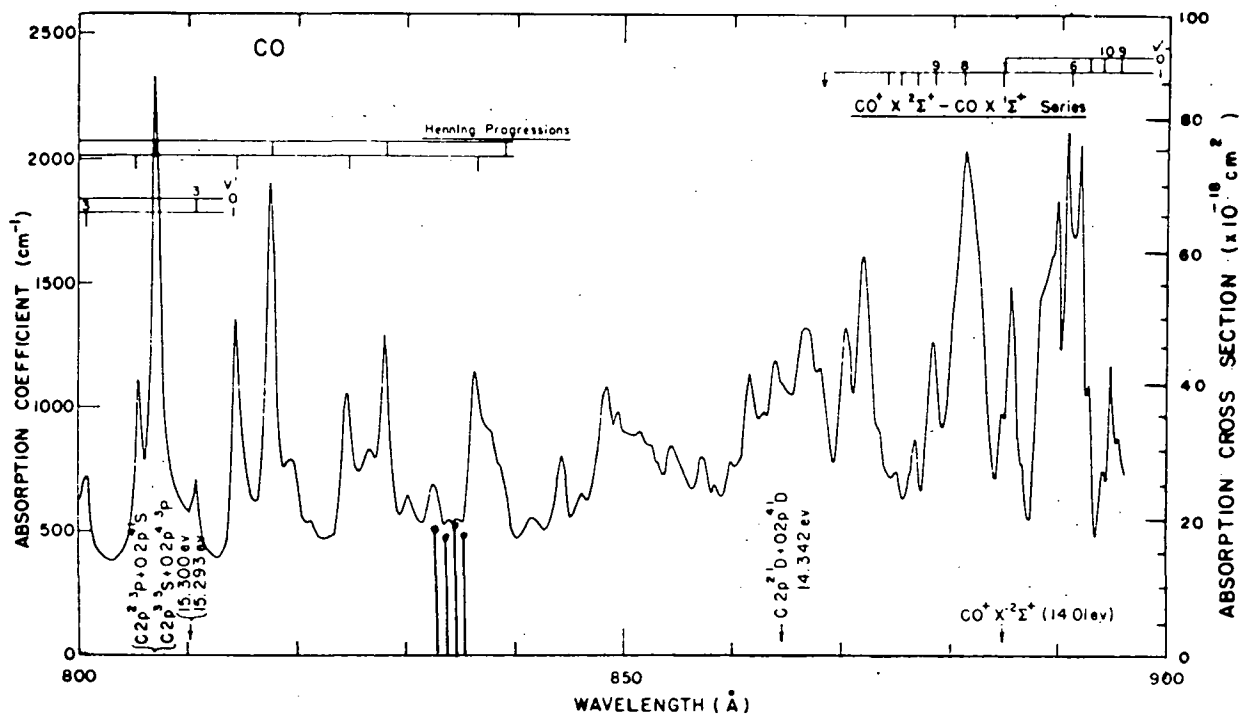800-700Å (Huffman et al., 1964).

Figure (9-72).   Absorption coefficient of CO for the wavelength region
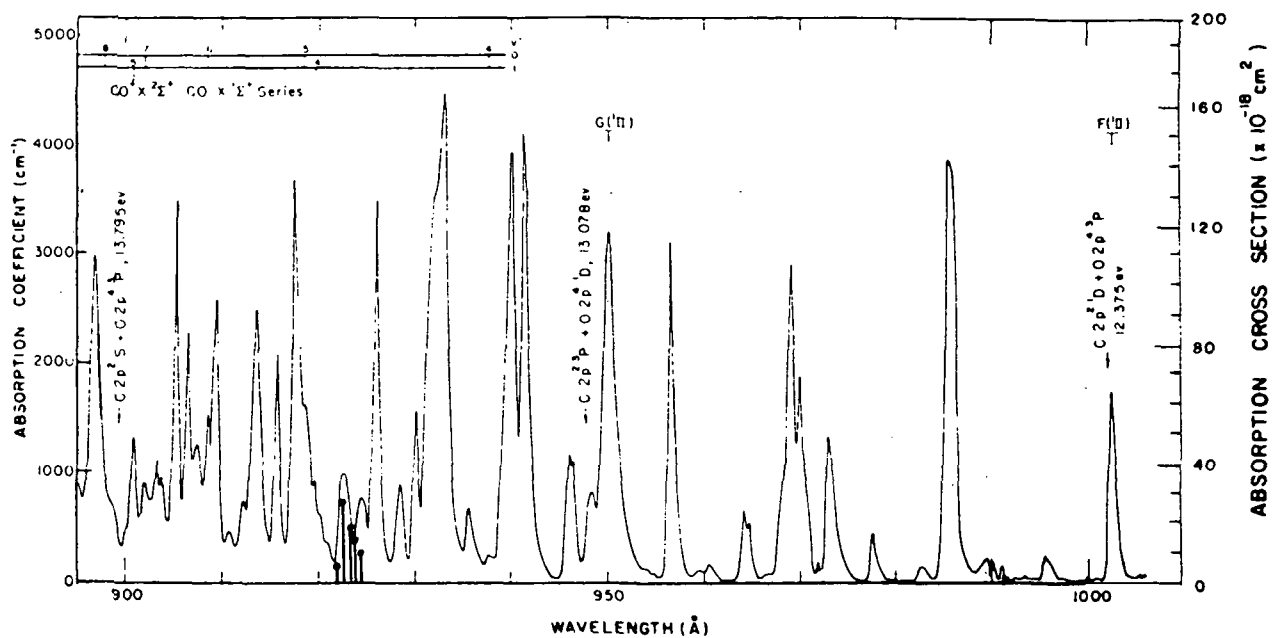900-800Å (Huffman et al., 1964).

236

Figure (9-73). Absorption coefficients of CO for the wavelength region 1000-900Å (Huffman, et al., 1964).

TABLE XXXVI. VIBRATION-ROTATION BANDS OF $C^{12}O^{16}$ IN THE INFRARED REGION

(Kruperne, 1966)

S.N.	Band Classification	ν_0(Obs.)
(1)	2-1	2116.80 cm^{-1}
(2)	1-0	2143.274
(3)	7-5	3996.88
(4)	6-4	4049.24
(5)	5-3	4101.73
(6)	4-2	4154.404
(7)	3-1	4207.168
(8)	2-0	4260.064
(9)	3-0	6350.436
(10)	4-0	8414.458

Hydrogen Chloride (HCl)

Dipole Moment, M: 1.04 Debye

Ionization Potential, I.P.: 12.74 eV

Dissociation Energy, D(H-Cl): 4.433 eV

Ground Electronic State Configuration: $KL(3s\sigma)^2(3p\sigma)^2 (3p\pi)^4 - - - {}^1\Sigma^+$

Ground State Vibration Frequency and Anharmonicity Constants: $\omega_e = 2990.95$ (cm^{-1})

$$\omega_e x_e = 52.8186$$

$$\omega_e y_e = 0.2243$$

Rotational Constants:

B_e	α_e	r_e(H-Cl)
10.5934 cm^{-1}	0.3072 cm^{-1}	1.2745Å

Hydrogen Chloride is a colorless gas denser than air. It is fairly stable at temperatures up to 1500°C, after which it dissociates into chlorine and hydrogen. It easily condenses to the liquid form by pressure alone and the liquid so formed freezes to a white solid which melts at 112°C.

HCl is a highly polar diatomic molecule composed of one hydrogen and one chlorine atom separated by a bond length about 1.27Å in its ground electronic state. Hydrogen chloride occurs in the following principal isotopic forms: ${}^1H^{35}Cl$, ${}^2H^{35}Cl$, ${}^3H^{35}Cl$, ${}^1H^{37}Cl$, ${}^2H^{37}Cl$, ${}^3H^{37}Cl$.

Molecular Spectrum

The observed spectra of gaseous hydrogen chloride can be described under the following three categories: (1) Electronic Spectrum, (2) Vibration-Rotation Spectrum, and (3) Rotational Spectrum.

Electronic Spectrum. - Besides early work by Price (1938) and Romand and Vodar (1948), many workers in recent years have investigated electronic spectrum of HCl (Jacques and Barrow, 1959; Stamper, 1962; Tilford, Ginter and Vanderslice, 1970; Myer and Samson, 1970). The observed features of the electronic spectrum include:

(1) $V {}^1\Sigma^+$ - $X {}^1\Sigma^+$ System (2375-1800Å)

Jacques and Barrow (1959) studies this system in its various details. Electrodeless discharge through hydrogen chloride vapor gave rise to a multi-line spectrum in the spectral region 2375-1800Å. Of the 2000 lines measured, about 1000 which include most of the strong lines, have been assigned to 15 bands involving $v' = 0, 1, 2$ in the $v {}^1\Sigma^+$ and $v'' = 10, 11 - - - 16$ in the ground $X {}^1\Sigma^+$ state.

(2) $V {}^1\Sigma^+$ - $Q^{1,3}\Pi$ Continuum $(\lambda_{max} \sim 2570\text{Å})$

Jacques and Barrow (1959) reported a broad continuum with $\lambda_{max} \sim 2570$Å in the electrodeless discharge spectrum of HCl. Further details about this emission continuum are not available.

238

(3) $Q^{1,3}$ - X $^1\Sigma^+$ Continuum ($\lambda_{max} \sim 1535\overset{\circ}{A}$)

Romand and Vodar (1948) reported a broad absorption continuum with $\lambda_{max} \sim 1535\overset{\circ}{A}$ in the vacuum ultraviolet region. Similar observations have been made recently by Myer and Samson (1970). It is a broad absorption band extending in the region 1800-1400$\overset{\circ}{A}$ with $\lambda_{max} \sim 1535\overset{\circ}{A}$.

(4) B [b $^3\Pi_i$] - X $^1\Sigma^+$ Band at $\lambda \sim 1340\overset{\circ}{A}$

It is a sharp band first reported by Price (1938) in the vacuum ultraviolet absorption spectrum of HCl. Studies on the absorption cross sections of HCl by Myer and Samson (1970) confirmed the existence of this band. Recently, Tilford, Ginter and Vanderslice (1970) photographed this band under high dispersion and also scanned it using photoelectric methods. A detailed rotational structure analysis of the band suggested it to be the (0,0) band of a b $^3\Pi_i$ - X $^1\Sigma^+$ transition. Table (9-XXXVII) presents the fine structure data for this band.

TABLE (9-XXXVII) WAVENUMBERS OF THE BANDS OF THE b $^3\Pi_i \leftarrow$ X $^1\Sigma^+$ TRANSITION OF HCl[a]

	$^3\Pi_2$ - X(0-0)[b]	$^3\Pi_1$ - X(0-0)[c]		$^3\Pi_0$ - X(0-0)[c]	
J	Q(J)	P(J)	R(J)	P(J)	R(J)
0			75 161.4		
1			180.8		75 531.5
2		75 100.5	198.3	75 448.8*	551.8
3	74 824.9	076.9	214.5	426.8	572.4
4	815.5	052.5	229.1	405.2	591.2
5	802.2	027.0	242.6	385.4	610.4*
6	786.0	75 000.3	255.7	363.1	630.0
7	769.3	74 972.6	266.2	340.6	647.0
8	750.2	944.0	275.0	318.3	664.5
9		913.3			681.5

[a] All branches are diffuse with the degree of diffuseness increasing with increasing rotational energy. Bands too diffuse for rotational analysis are listed in Table (9-XLI). An asterisk indicates a blended line.

[b] R-head observed at 74 917 ± 5 cm^{-1} P(5) - 74 710.7; P(6) = 74 676.7 cm^{-1}.

[c] Q-branch unresolved.

(5) C $[^1\Pi]$ - X $^1\Sigma^+$ System (1290-1210Å)

This is a very strong electronic band system of HCl. It was first identified by Price (1938). Myer and Samson (1970) measured absorption cross sections of HCl in this region and reported as many as 5 vibrational members, viz., (0,0) - 1291.1Å; (1,0) - 1247.3Å; (2,0) - 1208.7Å; (3,0) - 1175.0Å; (4,0) - 1143.8Å. The vibration analysis of these data yielded the molecular constants as ω_e = 2880 cm^{-1} and $\omega_e x_e$ = 80 cm^{-1} which differed slightly with those derived by Price (1938). Tilford, Ginter and Vanderslice (1970) studied rotational structure of (0,0) and (1,0) bands of this system and obtained rotational constants for vibrational levels up to ν = 3 of the upper state. These data are presented in Table (9-XXXVIII).

TABLE (9-XXXVIII) WAVENUMBERS OF THE BANDS OF THE C $^1\Pi \leftarrow$ X $^1\Sigma^+$ TRANSITION OF HCl[a]

J	P(J)	(0-0) Band[b] Q(J)	R(J)	(1-0) Band[c] P(J)	R(J)
0			77 503.94		80 187.4
1		77 482.89*	520.38		204.8
2	77 440.47	478.86	534.69	80 125.5	219.0
3	416.27	472.18	546.43	100.2	
4	388.58	463.34*	556.20	071.3	
5	359.93	452.29	563.20	041.3	
6	327.22	438.67	568.09	80 010.5	
7	293.22	422.86		79 976.0	
8	257.80	405.93*		938.2	
9	218.36	384.63*			
10	177.86				

[a] All branch lines are somewhat diffuse with the degree of diffuseness increasing with increasing rotational energy. An asterisk indicates a blended line.

[b] A number of very diffuse lines corresponding to higher J levels have been observed but are not reported here.

[c] Branch lines for this transition are very diffuse and no H^{35}Cl-H^{37}Cl splitting is resolved. The head of the unresolved Q-branch is at 80 170 ± 3 cm^{-1} and the R-head is observed at 80 252 ± 5 cm^{-1}.

(6) Rydberg Series (1150-1050Å)

Myer and Samson (1970) reported numerous overlapping bands, some sharp and some diffuse in the spectral region 1150-1050Å. These may be the members of some Rydberg series. The results of Myer and Samson are presented in figure (9-74). Figure (9-75) presents a schematic of the important electronic states of HCl so far known.
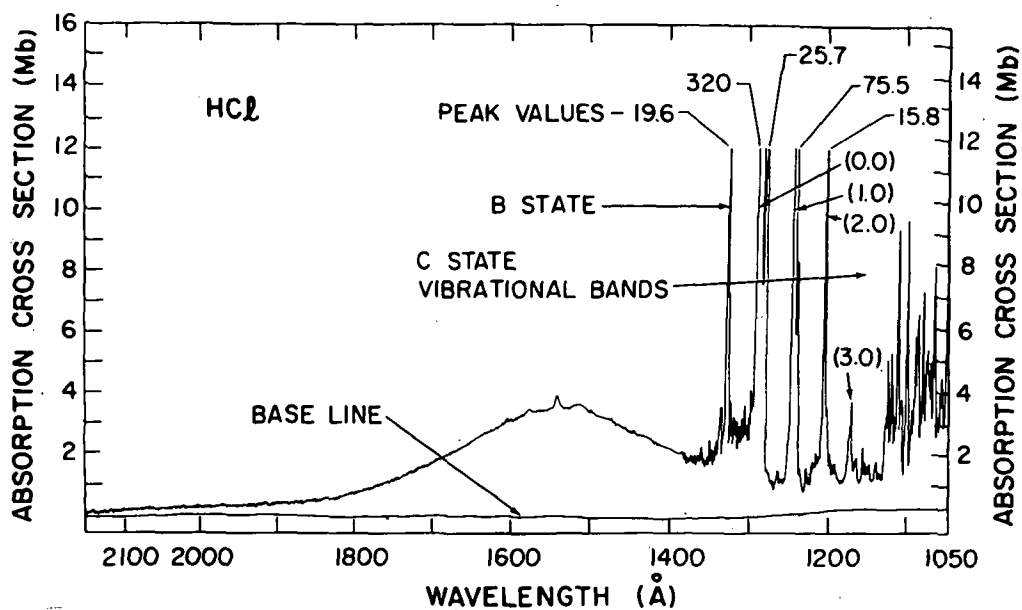
240

Figure (9-74). Absorption cross sections of HCl for the wavelength region 2150-1050Å. [Myer and Samson, 1970]
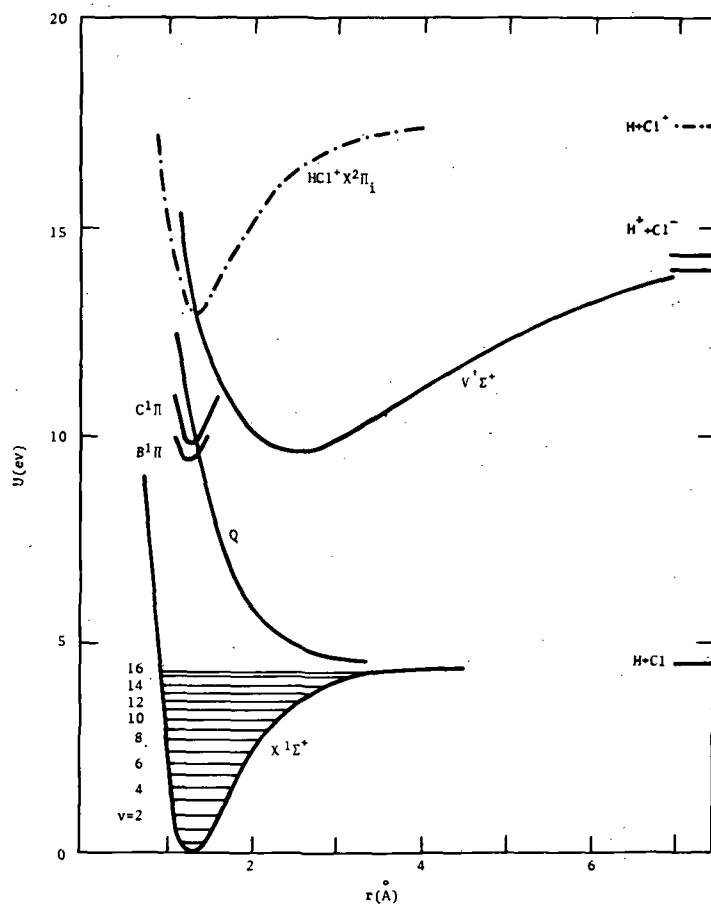

Figure (9-75). Schematic showing some important electronic states of HCl.

<u>Vibration-Rotation Spectrum</u>. - Vibration-rotation spectrum of hydrogen chloride has been the subject of numerous investigations (Randall and Imes, 1920; Meyer and Levin, 1929; Herzberg and Spinks, 1934; Lindholm, 1943; Naude and Verleger, 1950; Mills, Thompson, and Wiggins, 1960; Rank, Eastman, Rao and Wiggins, 1962; Stafford, Holt and Paulson, 1963; Rank, Rao and Wiggins, 1965; Roberts, 1966; Newman, 1952).

These bands which are degraded to the longer wavelengths lie in the spectral region (4.8 - 0.7μ) and appear in emission as well as in absorption. Table (9-XXXIX) provides the data on the rotational structure for the fundamental band.

TABLE (9-XXXIX) OBSERVED BAND ORIGINS (cm^{-1})

Band	Observed
1-0	2885.9775
2-0	5667.9841
3-0	8346.7816
3-1	5460.8041
4-2	5254.8555
5-3	5049.503
4-0	10922.803
5-0	13396.217

Data presented here for HCl^{35} are due to Rank et al. (1960, 1965) who made extensive measurements on these spectral features in absorption using high dispersion echelle spectrographs and long absorption columns of heated vapor of hydrogen chloride. Table (9-XL) gives the band origin data for the various observed bands. Detailed data can be seen in the original papers on other bands, viz., (2-0), (3-0), (3-1), (4-2), (5-3), (4-0), (5-0). Corresponding data on DCl^{35} and DCl^{37} have been presented by Van Horne and Hause (1956).

Traces of gaseous HCl have been discovered in the atmosphere of Venus by identifying numerous weak absorption lines in the spectrum of Venus that have been assigned to the (2-0) vibration-rotation band of HCl (Connes, Connes, Benedict and Kaplan, 1967). These lines have been found to be consistent with approximately 2 mm Amagat of HCl gas in the optical path at temperatures around 240°K and presssure 0.1 atm. The observed data along with accurately measured laboratory data are presented in Table (9-XLI).

Laser action in HCl spectrum was first studied by Kasper and Pinentel (1965) in a system pumped by the H_2 - Cl_2 photoflash induced explosion. It was later investigated by many workers using a variety of systems (Deutsch, 1967; Moore, 1968). Table (9-XLII) presents the HCl transitions where laser action has been observed.

TABLE (9-XL) CALCULATED AND OBSERVED FREQUENCIES IN VACUUM WAVE NUMBERS (cm^{-1}) OF THE 1-0 BAND OF HCl^{35}

J	R(J) (calc)	(obs)	calc-obs. $\times 10^3$	P(J) (calc)	(obs)	calc-obs. $\times 10^3$
0	2906.2479	.2521	− 4.2			
1	2925.8977	.8950	+ 2.7	2865.0991	.0967	+ 2.4
2	2944.9146	.9154	− 0.8	2843.6254	.6234	+ 2.0
3	2963.2866	.2865	+ 0.1	2821.5691	.5713	− 2.2
4	2981.0015	.0013	+ 0.2	2798.9433	.9401	+ 3.2
5	2998.0476	.0438	+ 3.8	2775.7609	.7602	+ 0.7
6	3014.4134	.4114	+ 2.0	2752.0353	.0363	− 1.0
7	3030.0876	.0862	+ 1.4	2727.7797	.7774	+ 2.3
8	3045.0592	.0569	+ 2.3	2703.0074	.0068	+ 0.6
9	3059.3171	.3179	− 0.8	2677.7320	.7320	0.0
10	3072.8509	.8490	+ 1.9	2651.9668	.9664	+ 0.4
11	3085.6502	.6539	− 3.7	2625.7255	.7272	− 1.7
12	3097.7048	.7034	+ 1.4	2599.0216	.0208	+ 0.8
13	3109.0050	.0026	+ 2.4	2571.8686	.8703	− 1.7
14	3119.5413	.5362	+ 5.1	2544.2801	.2817	− 1.6
15	3129.3042	.3031	+ 1.1	2516.2696	.2724	− 2.8
16	3138.2848	.2869	− 2.1	2487.8507	.8560	− 5.3
17	3146.4743	.4700	+ 4.3	2459.0367	.0406	− 3.9
18	3153.8642	.8637	+ 0.5	2429.8412	.8409	+ 0.3
19	3160.4462	.4418	+ 4.4	2400.2774	.2773[a]	+ 0.1
20	3166.2125	.2135	− 1.0	2370.3585	.3622[a]	− 3.7
21	3171.1552	.1514	+ 3.8	2340.0976	.0977[a]	− 0.1
22	3175.2670	.2644	+ 2.6	2309.5078	.5138[a]	− 6.0
23	3178.5405	.5395	+ 1.0	2278.6019	.6037[a]	− 1.8
24	3180.9690	.9669	+ 2.1	2247.3926	.3964[a]	− 3.8
25	3182.5455	.5403	+ 5.2	2215.8926	.8989[a]	− 6.3
26	3183.2635	.2574	+ 6.1	2184.1142	.1146	− 0.4
27	3183.1167	.1090	+ 7.7	2152.0696	.0775	− 7.9
28	3182.0990	.0857	+13.3	2119.7709	.7868	+14.1
29	3180.2044			2087.2299	.2392	− 9.3
30	3177.4271	.4142	+12.9	2054.4583	.4582	− 0.1
31	3173.7614	.7417	+19.7	2021.4673		

[a]Computed from $\Delta_2 F''(J)$ and corresponding R line.

TABLE (9-XLI) HCl LASER

Wavelength $\lambda_{vac}(\mu m)$	Frequency $\nu(cm^{-1})$	Transition HCl^{35}	HCl^{37}
		2-1 Band	
3.7071	2697.52	P(4)	
3.7383	2675.01	P(5)	
3.7408	2673.23		P(5)
3.7710	2651.82	P(6)	
3.7735	2650.08		P(6)
3.8050	2628.13	P(7)	
3.8074	2626.45		P(7)
3.8401	2604.09	P(8)	
3.8425	2602.48		P(8)
3.8768	2579.42	P(9)	
3.9149	2554.34	P(10)	
		3-2 Band	
3.8509	2596.79	P(4)	
3.8840	2574.70	P(5)	
3.9181	2552.26	P(6)	
3.9205	2550.70		P(6)
3.9536	2529.31	P(7)	
3.9560	2527.79		P(7)
3.9909	2505.68	P(8)	
4.0295	2481.69	P(9)	

TABLE (9-XLII) HCl LASER PURE ROTATIONAL TRANSITIONS

Wavelength $\lambda_{vac}(\mu m)$	Frequency $\nu(cm^{-1})$	Transition HCl^{35}	HCl^{37}
		$\nu = 0$	
13.8720	720.921	R(40)	
14.0994	709.279	R(39)	
14.3434	697.232	R(38)	
16.2125	616.809	R(32)	
16.6085	602.114	R(31)	
16.664	600.10		R(31)
17.0340	587.070	R(30)	
17.4923	571.686	R(29)	

Wavelength $\lambda_{vac}(\mu m)$	Frequency $\nu(cm^{-1})$	Transition HCl^{35}	HCl^{37}
17.9874	555.969	R(28)	
17.997	555.65		R(28)
18.522	539.928	R(27)	
19.122	522.96		R(26)
20.4106	489.949	R(24)	
21.1556	472.701	R(23)	
21.9706	455.175	R(22)	
22.8637	437.380	R(21)	
23.8485	419.326	R(20)	
24.9367	401.023	R(19)	
26.1462	382.483	R(18)	
27.508	363.53	R(17)	
		$\nu = 1$	
16.765	596.48		R(32)
17.125	583.94	R(31)	
17.575	568.99	R(30)	
18.035	554.48	R(29)	
18.555	538.94	R(28)	
18.593	537.84		R(28)
19.145	522.33		R(27)
19.7002	507.628	R(26)	
20.3455	491.526	R(25)	
21.0470	475.130	R(24)	
21.8127	458.449	R(23)	
22.6514	441.491	R(22)	
23.5705	424.268	R(21)	
24.6177	406.215		R(20)
24.5833	406.789	R(20)	
25.7040	389.065	R(19)	
		$\nu = 2$	
19.183	521.29	R(28)	
20.9991	476.215	R(26)	
24.3178	411.232	R(21)	
		$\nu = 3$	
19.783	505.48	R(28)?	
19.821	504.52		

<u>Rotational Spectrum</u>. Pure rotational spectrum of HCl has been studied both in absorption as well as in emission. Hansler and Oetjen (1953) and MacCubbin (1952) identified pure rotation transitions in the far infrared region (480-45). Strong (1934) had earlier studied them in the region (29-15) in the emission spectrum of H_2/Cl_2 flames. Jones and Gordy (1964) studied one of these transitions (J = 0 → 1) in the microwave region too (0.48mm).

The J = 0 → 1 transition in DCl^{35} and DCl^{37} was also studied using microwave techniques by Cowen and Gordy (1958). Details can be seen in the original papers. Laser action has also been found in a number of pure rotational transitions (Deutsch, 1967; Akitt and Yardley, 1970). Table (9-XLIII) presents a list of these features.

TABLE (9-XLIII) DCl LASER

Wavelength $(\lambda_{vac}$ (µm)	Frequency $\nu(cm^{-1})$	Transition DCl^{35}	DCl^{37}
		2-1 band	
5.0445	1982.35	P(5)	
5.0514	1979.65		P(5)
..0743	1970.72	P(6)	
5.0811	1968.08		P(6)
5.1049	1958.90	P(7)	
5.1118	1956.25		P(7)
5.1363	1946.94	P(8)	
5.1431	1944.35		P(8)
5.1688	1934.67	P(9)	
		3-2 band	
5.1511	1941.35	P(4)	
5.1811	1930.10	P(5)	
5.1879	1927.56		P(5)
5.2118	1918.73	P(6)	
5.2186	1916.24		P(6)
5.2435	1907.13	P(7)	
5.2503	1904.67		P(7)
5.2760	1895.37	P(8)	
5.2829	1892.91		P(8)
5.3097	1883.35	P(9)	
5.3443	1871.15	P(10)	
5.3799	1858.77	P(11)	
		4-3 band	
5.3244	1878.13	P(5)	
5.3562	1867.01	P(6)	
5.3629	1864.65		P(6)
5.3889	1855.66	P(7)	
5.3956	1853.36		P(7)
5.4295	1841.79		P(8)
5.4577	1832.27	P(9)	
5.4935	1820.34	P(10)	
5.5304	1808.20	P(11)	
		5-4 band	
5.5084	1815.38	P(6)	
5.5423	1804.31	P(7)	
5.5776	1792.89	P(8)	
5.6137	1781.36	P(9)	

Hydrogen Fluoride (HF)

Dipole Moment, M: 1.91 Debye

Ionization Potential, I.P.: 15.77 eV

Dissociation Energy, D(H-F): 5.85 eV

Ground Electronic State Configuration: $K(2s\sigma)^2(2p\sigma)^2(2p\pi)^4$ - - - $^1\Sigma^+$

Ground State Vibration Frequency and Anharmonicity Constants: $\omega_e = 4138.32$ (cm^{-1})

$$\omega_e x_e = 89.88$$
$$\omega_e y_e = 0.93$$

Rotational Constants:

B_e	α_e	r_e(H-F)
20.9557 cm^{-1}	0.798 cm^{-1}	0.9168Å

Hydrogen fluoride is an extremely harmonic, corrosive and hydrogen bonded gas. Even at 20°C and 745 mm pressure, about 80% of the gas is polymerized in the form (HF)$_6$. The other hydrogen halides do not exhibit this strange property. It is also highly soluble in water; the solution is called hydrofluoric acid. Anhydrous hydrogen fluoride is a limpid liquid which fumes strongly in air.

HF is a polar diatomic molecule, composed of one hydrogen and one fluorine atom, separated by a mean bond distance of about 0.92Å in its ground electronic state. The commonly occurring isotopic forms of hydrogen fluoride are: $^1H^{19}F$, $^2H^{19}F$ and $^2H^{19}F$.

Molecular Spectrum

The observed spectral features of gaseous hydrogen fluoride ($^1H^{19}F$) can be described under the following subheads: (1) Electronic Spectrum, (2) Vibration-Rotation Spectrum, and (3) Rotational Spectrum.

Electronic Spectrum. - Besides earlier investigations by Woods, 1943; Safary, Romand and Vodar, 1951; Barrow and Caunt, 1954; Johns and Barrow, 1957; more recent work on the electronic spectrum of HF molecule is of Johns and Barrow (1959). The following two transitions have been reported.

(1)   V $^1\Sigma^+$ - X $^1\Sigma$ System (2670-2000Å)

This is the principal electronic band system ascribed to HF. The spectrum consists of a large number of lines, without any apparent regularity and there are no distinct band heads. The rotational structure is, however, strongly degraded to the red. The lines have been classified into distinct P and R branches. However, since the centrifugal distortion is so large in the lower state, the second differences between different members of the two branches are not constant. In all, about 1600 lines have been measured of which more than 1300 have been accounted for. Most of the remaining ones are too weak to be analysed satisfactorily. In the case of DF as many as 1900

248

lines were measured of which about 1150 have been assigned to 34 bands (Johns and Barrow, 1959). Table (9-XLIV) gives band origins (cm^{-1}) for the various observed bands in the system. Figure (9-76) presents the potential energy curves for the two states involved in the transition.

TABLE (9-XLIV). CONSTANTS FOR HF VALUES OF BAND-ORIGINS, $\nu_0(cm^{-1})$

ν',ν''	ν_0	ν',ν''	ν_0
1, 9	54619.4*	1, 15	41903.4
1, 10	52110.5*	1, 16	40415.3
1, 11	49741.1*	1, 17	39154.3
1, 12	47525.0	1, 18	38151.6
1, 13	45473.0	1, 19	37452.2
1, 14	43595.2		

* Bands with ν = 9, 10 and 11 have been observed at K > 27, K > 16, K > 11, respectively. The determination of these values of ν_0 therefore involves some extrapolation of the rotational constants.
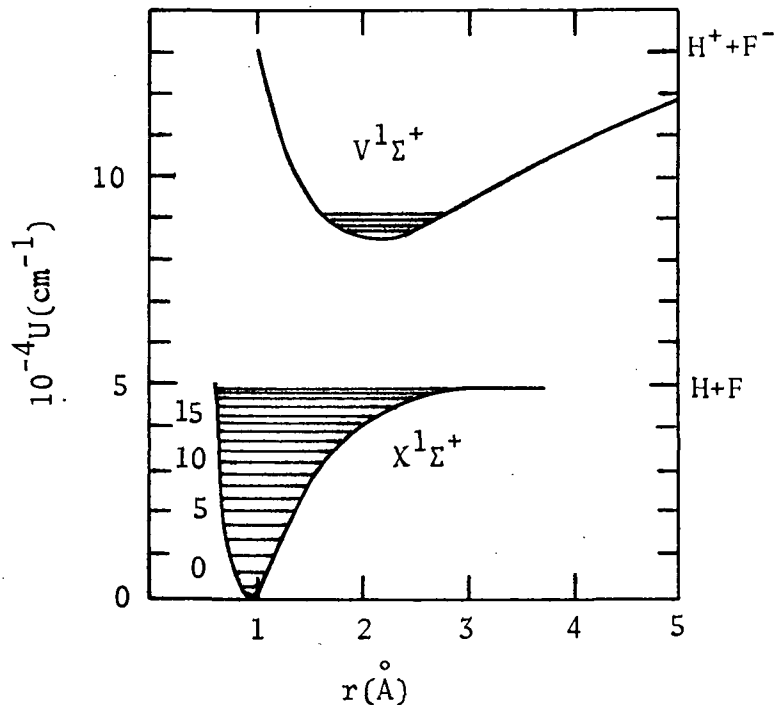
Figure (9-76). Schematic showing the two important electronic states of HF.

(2) Absorption Continuum ($\lambda_{max} \sim 1612\overset{\circ}{A}$)

An absorption continuum with $\lambda_{max} \sim 1612\overset{\circ}{A}$ has been reported by Safary, Romand and Vodar (1951) in the vacuum ultraviolet. They obtained the profiles of the absorption at different temperatures. Figure (9-77) depicts these results. No satisfactory information as regards true nature of the electronic transition involved in this absorption is yet available.
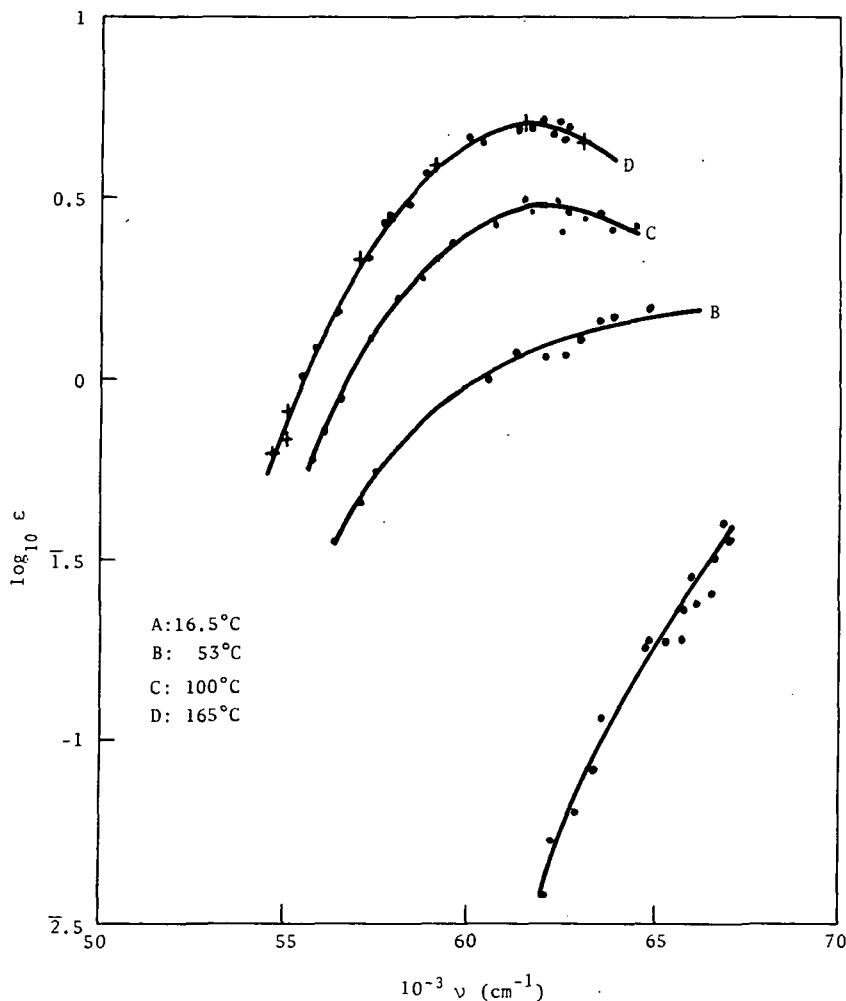
Figure (9-77). Absorption coefficient profile of HF at different temperatures.

The electronic states of hydrogen fluoride have been extensively discussed by Pauling, 1932; Mulliken, 1936, 1937; and recently by Bender and Davidson, 1968 and Bondybey, Pearson and Schaefer, 1972. While the ground electronic state $X \, {}^1\Sigma^+$ correlates at infinite internuclear separation with the ground state

atoms H+F, the upper state V $^1\Sigma^+$ is highly ionic. The state V $^1\Sigma^+$ was first predicted by Pauling (1932) to lie about 36000 cm^{-1} above X $^1\Sigma^+$ and to have a stable minimum with the same mean internuclear distance as in the ground state. Mulliken (1936, 1937) postulated a state 130,000 cm^{-1} with a slightly larger r_e. The actual situation does not correspond to either, since the minimum of the V curve is near 90,000 cm^{-1}. Also the minimum lies at a much larger value of r_e. Bender and Davidson (1968) established that both the X and V states could be assigned the ionic character at their respective minima. Configuration A $^1\Sigma^+$ ($1\sigma^2\ 2\sigma^2\ 3\sigma^2\ 1\pi^2\ 1\pi^2$) is ionic for all values of r. The configuration B $^1\Sigma^+$ ($1\sigma^2\ 2\sigma^2\ 3\sigma^1\ 4\sigma^1\ 1\pi^2\ 1\pi^2$) is covalent at larger r; but because of the orthogonality of 3σ and 4σ, it is more like a piece of the valence bound function orthogonal to the ionic configuration. At smaller values of r, it represents a repulsive state rather than a bonding state. The minimum in the V $^1\Sigma^+$ state at r = 3.75 results from a crossing of the repulsive B configuration with the strongly bonding ionic configuration. At this minimum, the state V is nearly an equal mixture of A and B. At smaller r, the ground state X $^1\Sigma^+$ corresponds to the ionic configuration A and at larger r, the excited V $^1\Sigma^+$ state corresponds to this configuration.

Vibration-Rotation Spectrum. - The earliest reported work on the vibration-rotation spectrum of HF is, most probably, of Imes (1919) who studied the fundamental band of HF in the infrared absorption spectrum. These spectral features were later investigated in greater detail by various workers (Schaeffer and Thomas, 1923; Kirkpatrick and Salant, 1935; Naude' and Verleger, 1950; Talley-Kayler and Nielsen, 1950; Kuipers, Smith and Nielson, 1956; Fishburne and Rao, 1966; Webb and Rao, 1968).

Kuiper et al. (1956) made extensive studies of the (1-0) and (2-0) bands (fundamental and the first overtone) and examined the rotational structures through J = 11 for the fundamental and through J = 8 for the first overtone. Later, Fishburne et al., and Webb et al. studied a number of other bands (3-0, 4-0, 5-0) in addition to the fundamental (1-0) and the first overtone (2-0) and presented precise data using a high dispersion 10-meter focal length Ebert-type grating spectrograph.

Vibration-rotation bands of the isotopic molecules DF and TF were studied by Spanbauer and Rao, 1965; and Jones and Goldblatt, 1957, respectively.

Benedict, Bullock, Silverman and Gross (1953) observed the vibration-rotation bands of HF in emission from a hydrogen-fluorine flame. Later, Mann, Thrust, Lide, Ball and Acquista (1961) investigated these features using a hydrogen-fluorine diffusion flame. They studied as many as 23 bands from 3200 cm^{-1} in the infrared through 5500Å in the visible and obtained extensive data on their rotational structure. Table (9-XLV) presents the band-center data of the various bands.

TABLE (9-XLV).   OBSERVED AND CALCULATED BAND CENTERS (cm^{-1}).

v"	v" = 0	1	2	3	4	5
1	3961.60					
	(3961.59)[a]					
2	7750.98	3789.42				
	(7751.01)	(3789.42)				
3	11372.92	7411.45	3622.02			
	(11373.02)	(7411.43)	(3622.01)			
4	14831.75	10870.37	7080.85			
	(14831.87)	(10870.28)	(7080.86)			
5	18131.10	14169.64	10380.29	6758.22		
	(18131.20)	(14169.61)	(10380.19)	(6758.18)		
6		17312.42	13523.02		6442.10	
		(17312.42)	(13523.00)	(9900.99)	(6442.14)	
7			16511.60	12889.53		
			(16511.56)	(12889.55)		
8				15725.33	12266.46	
				(15725.31)	(12266.46)	
9					14944.94	11650.72
					(14950.01)	(11650.68)

[a] Calculated values in parentheses.

High resolution interferometric spectra of the Venusian atmosphere have shown numerous weak, narrow absorption lines of the (1-0) and (2-0) vibration-rotation bands of HF. The strength of the identified HF lines is consistent with about 0.02mm Amagat of gaseous HF in the optical path at temperatures around 240°K and pressure 0.1 atmosphere (Connes, Connes, Benedict and Kaplan, 1967). Table (9-XLVI) gives a summary of the HF lines identified in the Venusian spectra.

Molecular laser action has been observed in quite a good number of vibration-rotation transitions mostly involving the low lying vibrational levels (v = 6). Table (9-XLVII) presents data on various HF laser transitions observed in flash photolysis of H_2 and F_2 (Suchard, 1973). The HF lasing molecules were produced by the reaction of a 50-torr mixture of mole ratio $H_2/F_2/H_e$ = 0.5/1/40 initiated by the flash photolysis of the F_2. Strong lasing action was found from all P-branch vibration-rotation bands from v = 6→5 to 1→0. Laser action in HF vibration-rotation transitions has also been observed in a number of other chemiluminescent reactions (Deutsch, 1967; and Mayer, Taylor and Kwok, 1973).

TABLE (9-XLVI)   HF LINES IN THE VENUSIAN SPECTRUM

(1   0) Fundamental

R(1)	R(4)	R(5)	R(6)
(4038.96)	(4142.84)	(4173.98)	(4203.30)

(2   0)

P(2)	P(1)	R(0)	R(1)	R(2)
(7665.59)	(7709.71)	(7788.87)	(7823.83)	(7855.65)

Numbers in parenthesis are in cm^{-1} units and represent laboratory data according to Rao and Webb.

Rotational Spectrum. - Czerny (1927) was most probably the first to study pure rotational transitions in HF. Later, many workers studied them both in absorption as well as in emission (Smith and Nielsen, 1955; Kuiper, Smith and Nielsen, 1956; Mason and Nielson, 1962, 1963; Rothschild, 1964; Revich and Stankevich, 1966).

The spectral data in respect to these transitions are now available for quite an extensive wavelength region, from 22μ to 250μ, and the rotational constants have been determined fairly accurately. The data presented here are due to Rothschild for lines with J = 0 to 8 and Revich et al. for lines with J = 9 to 40 (Tables 9-XLVIII and 9-XLIX).

The following values were obtained for the rotational molecular constants (in cm^{-1}) for HF by Revich et al. according to the following equation:

$$\nu = 2B_v(J + 1) - 4D_v(J + 1)^3 + 6H_v(J + 1)^5 - 8L_v(J + 1)^7 + - - -$$

where B_v, D_v, H_v and L_v are the rotational constant for the vibrational level with quantum number v.

$$B_0 = 20.559 \pm 0.005; \quad D_0 = (2.11 \pm 0.01) \cdot 10^{-3}$$

$$H_0 = (1.5 \pm 0.2) \cdot 10^{-7}; \quad L_0 = (0.7 \pm 0.5) \cdot 10^{-11}$$

TABLE (9-XLVII).   PHOTOLYSIS OF H_2 AND F_2.

Measured Wavelength (μm)	Identification		Calculated Wavelength (μm)	Peak Power (relative units)
	Vibrational Band	Transition (J)		
2.6727	1-0	3	2.6726	1
2.7076		6	2.7074	2190
2.7439		7	2.7440	6910
2.7822		8	2.7826	4390
2.8230		9	2.8231	781
2.8657		10	2.8656	89
2.6961	2-1	2	2.6963	872
2.7273		3	2.7275	1405
2.7605		4	2.7604	2985
2.7952		5	2.7952	3850
2.8320		6	2.8319	6100
2.8703		7	2.8705	4340
2.9107		8	2.9112	536
2.9536		9	2.9539	449
2.8538	3-2	3	2.8542	622
2.8888		4	2.8890	1195
2.9256		5	2.9257	1650
2.9642		6	2.9644	496
3.0051		7	3.0052	1785
3.0480		8	3.0482	3750
3.0933		9	3.0935	573
2.9223	4-3	1	2.9221	2920
2.9549		2	2.9549	3710
3.9897		3	2.9896	5980
3.0264		4	3.0263	3125
3.0651		5	3.0652	2225
3.1060		6	3.1062	684
3.1490		7	3.1494	1024
3.2424		9	3.2429	295

TABLE (9-XLVIII) OBSERVED AND CALCULATED VACUUM WAVENUMBERS OF PURE ROTATIONAL TRANSITIONS OF HF BETWEEN J = 0 AND 10

Transition J → J	Vacuum Wavenumbers Observed	(cm^{-1}) calc. - obs.	Apparent Half-Width (cm^{-1})	Spectral Slit-Width (cm^{-1})
0 → 1	41.30 ± 0.71	- 0.17	1.3	0.8
1 → 2	82.35 ± 0.25	- 0.18	2.2	1.6
2 → 3	122.83 ± 0.28	+ 0.30	3.5	2.1
3 → 4	163.92 ± 0.13	+ 0.01	2.9	1.7
4 → 5	204.50 ± 0.12	+ 0.03	2.6	1.1
5 → 6	244.97 ± 0.16	- 0.09	2.1	1.5
6 → 7	284.98 ± 0.13	- 0.05	1.9	1.5
7 → 8	324.52 ± 0.22	+ 0.10	2.0	1.5
8 → 9	363.89 ± 0.18	- 0.02	1.2	0.7
9 → 10	402.77 ± 0.18	- 0.03	1.6	1.4
10 → 11	441.05 ± 0.29	+ 0.01	0.8	----

255

TABLE (9-XLIX)   WAVE NUMBERS OF THE LINES IN THE ROTATIONAL SPECTRUM OF HF
(ν, cm^{-1})

J	$\nu = 0$	$\nu = 1$	$\nu = 2$	$\nu = 3$	$\nu = 4$	$\nu = 5$
9	403.1					
10	441.4	424.6	408.4			
11	479.1	460.8	443.4			
12	516.0	497.0	511.0			
13	552.6	532.3	544.4	522.7		
14	588.8	566.2	578.8			
15	625.0	600.4	609.2		561.1	538.6
16	658.6	634.4	641.0	615.2		
17	692.4	665.8	670.2			592.3
18	725.5	697.5	699.8			
19	757.6	723.4	728.4	698.8		
20	788.7	757.6	757.6			
21	819.4	787.2	783.2	751.5	721.8	
22	848.8	815.7	809.3	776.4		
23	877.2	843.3	835.0	801.0	767.2	
24	904.1	869.1	858.7	823.5		
25	931.2	894.4	882.0			
26	956.3	918.3				
27	980.3	942.3	924.4			
28	1003.3	963.6				
29	1025.6	984.5				
30	1047.2	1003.3				
31	1067.4	1025.6				
32	1086.0	1042.1				
33	1103.6	1058.8				
34	1120.2	1074.6				
35	1135.8					
36	1149.9					
37	1163.6					
38	1175.8					
39	1186.0					
40	1196.0					

The values of B_0 and D_0 as reported by Rothschild on the basis of his analysis for rotational lines with J = 0 to 10 are as follows:

$$B_0 = 20.559 \pm 0.006 \text{ cm}^{-1}$$

$$D_0 = 0.00211 \pm 0.0004 \text{ cm}^{-1}$$

These values agree nicely with those obtained by Revich et al.

Laser action has been reported in respect of a large number of pure rotational transitions in HF. The wavelengths lying between 10.2 and 21.8μ are listed and identifications given in Table (9-L).

TABLE (9-L). HF LASER PURE ROTATIONAL TRANSITIONS

		$\nu = 0$
10.1978	980.60	R(27)
10.4578	956.23	R(26)
10.7439	930.76	R(25)
11.0573	904.38	R(24)
11.4033	876.94	R(23)
11.7854	848.50	R(22)
12.2082	819.12	R(21)
12.6781	788.76	R(20)
13.2009	757.52	R(19)
13.7841	725.47	R(18)
14.4406	692.49	R(17)
16.0215	624.16	R(15)
16.975	589.10	R(14)
18.085	552.94	R(13)
		$\nu = 1$
12.2619	815.53	R(22)
12.7006	787.37	R(21)
13.1877	758.28	R(20)
13.7277	728.45	R(19)
15.0163	665.94	R(17)

16.655	600.42	R(16)
17.645	566.73	R(15)
18.8010	531.89	R(13)
20.1337	496.68	R(12)
21.6986	460.86	R(11)
	.	$\nu = 2$
10.5819	945.01	R(29)
10.8117	924.93	R(28)
13.2211	756.37	R(21)
14.2881	699.88	R(19)
16.444	608.12	R(16)
17.327	577.13	R(15)
20.9393	477.57	R(12)
		$\nu = 3$
11.5408	866.49	R(27)
17.095	584.97	R(16)
19.1129	523.21	R(14)
20.3513	491.37	R(13)
21.7885	458.96	R(12)

Page Intentionally Left Blank

Page Intentionally Left Blank

REFERENCES

SECTION I

Adel, A.; and Slipher, V.M.: The Methane Content of the Giant Planet Atmospheres. Phys. Rev., Vol. 47, 1935, pp. 787-788.

Beckman, J.E.: The Measurement of Abundances in Planetary Atmospheres Using an Image Intensifier and a Solar Spectrograph. Plan. Space Sci., Vol. 15, 1967, pp. 1211-1218.

Belton, M.J.S.; and Hunten, D.M.: A Search for O_2 on Mars and Venus: A Possible Detection of Oxygen in the Atmosphere of Mars. Astrophys. J., Vol. 153, 1968, pp. 963-974.

Bergstralh, J.T.; Gray, L.D.; and Smith, H.J.: An Upper Limit for Atmospheric Carbon Dioxide on Mercury. Astrophys. J., Vol. 149, 1967, pp. L137-L139.

Belton, M.J.S.; Hunten, D.M.; and McElroy, M.B.: A Search for an Atmosphere on Mercury. Astrophys. J., Vol. 150, 1967, pp. 1111-1124.

Bottema, M.; Plummer, W.; and Strong, J.: A Quantitative Measurement of Water Vapor in the Atmosphere of Venus. Ann. Astrophys. (suppl.), Vol. 28, 1964, pp. 225-228.

Broadfoot, A.L.; Kumar, S.; Belton, M.J.S.; and McElroy, M.B.: Mercury's Atmosphere From Mariner-10: Preliminary Results. Science, Vol. 185, 1974, pp. 166-169.

Brown, H.: Rare Gases and the Formation of Earth's Atmosphere in G.P. Kuiper's. The Atmosphere of the Earth and Planets, Univ. of Chicago Press, 1949, pp. 258-266.

Carleton, N.P.; and Traub, W.A.: Detection of Molecular Oxygen on Mars. Science, Vol. 178, 1972, pp. 988-992.

Carleton, N.P.; and Traub, W.A.: Observations of Spatial and Temporal Variations of the Jovian H_2 Quadrupole Lines. Exploration of the Planetary System, 1974, pp. 345-349.

Connes, P.; Connes, J.; and Maillard, J.P.: Atlas of the Infrared Spectra of Venus, Mars, Jupiter, and Saturn., CNRS, ed., (Paris-France), 1969.

Connes, P.; Connes, J.; and Benedict, W.S.: Traces of HCl and HF in the Atmosphere of Venus. Astrophys. J., Vol. 147, 1967, pp. 1230-1237.

Danielson, R.E.: The Infrared Spectrum of Jupiter. Astrophys. J., Vol. 143, 1966, pp. 949-960.

Danielson, R.E.; Gaustad, J.E.; Schwarzchild, J.; Weaver, H.F.; and Woolf, N.J.: Mars Observations from Stratoscope II. Astron. J., Vol. 69, 1964, pp. 344-352.

De Vaucouleurs, G.: The Climatology of Mars, Part II in Physics of the Planet Mars. Faber and Faber (London), 1954, pp. 139-189.

Denisov, V.P.; and Alimov, V.I.: The Moon and the Planets. Znaniye Press (Moscow), 1971, NASA TT F-767.

Dollfus, A.: Mesure de la quantite de Vapeur d'Eau Contenue dans l' atmosphere de la Planete Mars. (Measurement of the Quantity of Water Vapor in the Atmosphere of the Planet Mars.) C.R. Acad. Sci. (Paris), Vol. 256, 1963, pp. 3009-3011.

Emerson, J.P.; Eddy, J.A.; and Dulk, G.A.: Hydrogen Abundance in Jupiter's Atmosphere. ICARUS Vol. 11, 1969, pp. 413-416.

Fink, U.; Larson, H.P.; and Poppen, R.F.: A New Upper Limit for an Atmosphere of CO_2, CO, on Mercury. Astrophys. J., Vol. 187, 1974, pp. 407-415.

Fink, U.; Belton, M.J.S.: Collision-narrowed Curves of Growth for H_2 Applied to New Photoelectric Observations of Jupiter. J. Atmospher. Sci., Vol. 26, 1969, pp. 952-962.

Fox, K.: Infrared Spectra of Planetary Atmospheres. K.N. Rao, and C.W. Mathews, eds., Molecular Spectroscopy: Modern Research, Acad. Press, 1972.

Glasstone, S.: The Book of Mars. NASA-SP-179, 1969.

Goettel, K.A.; and Lewis, J.S.: Ammonia in the Atmosphere of Venus. J. Atmospher. Sci., Vol. 31, 1974, pp. 828-830.

Hanel, R.A.; and Kunde, V.G.: Fourier Spectroscopy in Planetary Research, Space Sci. Rev., Vol. 18, 1975, pp. 201-256.

Hansen, J.E., ed.: The Atmosphere of Venus. NASA-SP-382, 1975.

Herzberg, G.: Spectroscopic Evidence of Molecular Hydrogen in the Atmospheres of Uranus and Neptune. Astrophys. J., Vol. 115, pp. 337-340.

Hess, S.L.: Mars as an Astronautical Objective. Advances in Space Science and Technology. Vol. 3, F.I. Ordway, ed., Acad. Press, 1961, pp. 151-193.

Hodges, R.F., Jr.: Model Atmospheres for Mercury Based on a Lunar Analogy. J. Geophys. Res., Vol. 79, 1974, pp. 2881-2885.

Howard, H.T.; and Tyler, G.L.: Mercury Results on Mass, Radius, Ionosphere and Atmosphere From Mariner-10 Dual-frequency Radio Signals. Science, Vol. 185, 1974, pp. 179-180.

Hunten, D.M.; and Goody, R.M.: Venus: The Next Phase of Planetary Exploration. Science, Vol. 165, 1969, pp. 1317-1323.

Kaplan, L.D.; Connes, J.; and Connes, P.: Carbon Monoxide in the Martian Atmosphere. Astrophys. J., Vol. 157, 1969, pp. L187-L192.

Kaplan, L.D.; Münch, G.; and Spinrad, H.: An Analysis of the Spectrum of Mars. Astrophys. J., Vol. 139, 1964, pp. 1-15.

Kiess, C.C.; Corliss, C.H.; and Kiess, H.K.: High Dispersion Spectra of Jupiter. Astrophys. J., Vol. 132, 1960, pp. 221-231.

Kiess, C.C.; Corliss, C.H.; Kiess, H.K.; and Corliss, E.L.: High Dispersion Spectra of Mars. Astrophys. J., Vol. 126, 1957, pp. 579-584.

Kozyrev, N.A.: The Atmosphere of Mercury. Sky and Telescope, Vol. 27, 1964, pp. 339-341.

Kuiper, G.P.: Infrared Spectra of Stars and Planets: IV The Spectrum of Mars, 1-2.5 Microns, and the Structure of its Atmosphere. Lunar and Planetary Laboratory Communications, No. 31, Univ. of Arizona Press, 1964.

Kuiper, G.P.: New Absorptions in the Uranus Atmosphere. Astrophys. J., Vol. 109, 1949, pp. 540-541.

Kuiper, G.P.: Planetary Atmospheres and Their Origin. The Atmospheres of the Earth and Planets. Chicago Univ. Press, 1969, pp. 308-405.

Marmo, F.F.; and Warneck, P.: Laboratory and Theoretical Studies in the VUV for the Investigation of the Chemical Physics of Planetary Atmospheres. Geophys. Corp of America Quart. Prog. Rep., NAS-W-124, 1960.

McCormack, B.M., ed.: Physics and Chemistry of Upper Atmospheres. D. Reidel Publ. Co., 1973.

Michaux, C.M.: Handbook of the Physical Properties of the Planet Mars. NASA-SP-3030, 1967.

Mills, S.A.: Models of Mar's Atmosphere. NASA-SP-8010, 1974.

Moroz, V.I.: Physics of Planets. NASA-TT-F-515, 1968.

Moroz, V.I.: The Spectra of Jupiter and Saturn in the 1-25μ Region. Astro. Zh. (USSR), Vol. 43, 1966, pp. 579-592.

Newburn, R.L.; and Gulkis, S.: A Survey of the Outer Planets: Jupiter, Saturn, Uranus, Neptune, Pluto, and Their Satellites. Space Sci. Rev., Vol. 3, 1973, pp. 179-271.

Owen, T.: The Atmosphere of Jupiter. Science, Vol. 167, 1970, pp. 1675-1681.

Owen, T.: Water Vapor on Venus: A Dissent and a Clarification. Astrophys. J., Vol. 150, 1967, pp. L121-L123.

Owen, T.; and Mason, H.P.: The Abundance of Hydrogen in the Atmosphere of Jupiter. Astrophys. J., Vol. 154, 1968, pp. 317-326.

Planetary Atmospheres: A Continuing Bibliography with Indexes. NASA-SP-7017, 1965.

Planetary Atmospheres: A Continuing Bibliography with Indexes. NASA-SP-7017(01), 1966.

Planetary Atmospheres: A Continuing Bibliography with Indexes. NASA-SP-7017(02), 1968.

Planetary Atmospheres Staff, Office of Space Science & Applications, NASA, Significant Achievements in Planetary Atmospheres, 1958-1964. NASA-SP-98, 1966.

Potter, A.E.: Near Infrared Spectra of Jupiter, Saturn, and Uranus. NASA-SP-3086, 1974.

Richardson, R.S.: Preliminary Report on Observations of Mars Made at Mount Wilson in 1956. Astron. Soc. Pacific, Vol. 69, 1957, pp. 23-30.

Rottman, G.J.; and Moss, H.W.: The Ultraviolet (1200-1900)Å Spectrum of Venus. J. Geophys. Res., Vol. 78, 1973, pp. 8033-8048.

Sagan, C.; Owen, T.C.; and Smith, H.J., eds.: Planetary Atmospheres. D. Reidel Publ. Co., 1971.

Schadee, A.: The Formation of Molecular Lines in the Solar Spectrum. Bull. Astron. Inst. (Netherlands), Vol. 17, 1964, pp. 311-348.

Shorn, R.A.; Spinrad, H.; Moore, R.C.; Smith, H.J.; and Giver, L.P.: High Dispersion Spectroscopic Observations of Mars II - The Water Vapor Variations. Astrophys. J., Vol. 147, 1967, pp. 743-752.

Spinrad, H. and Shawl, S.J.: Water Vapor on Venus - A Confirmation. Astrophys. J., Vol. 146, 1966, pp. 238-239.

Spinrad, H.; Münch, G.; and Kaplan, L.D.: The Detection of Water Vapor on Mars. Astrophys. J., Vol. 137, 1963, pp. 1319-1321.

Spinrad, H.: Pressure-induced Dipole Lines of Molecular Hydrogen in the Spectra of Uranus and Neptune. Astrophys. J., Vol. 138, pp. 1241-1245.

Spinrad, H.; and Hodge, P.W.: An Explanation of Kozyrev's Hydrogen Emission Lines in the Spectrum of Mercury. ICARUS, Vol. 4, 1965, pp. 105-108.

Spinrad, H.; and Trafton, L.M.: High Dispersion Spectra of the Outer Planets I. Jupiter in the Visual and Red. ICARUS, Vol. 2, 1963, pp. 19-28.

Suess, H.E.: On the Radioactivity of K^{40}. Phys. Rev., Vol. 73, 1948, p. 1209.

Urey, H.C.: The Atmospheres of the Planets, Handbuch der Physik (Encyclopedia of Physics) S. Flügge, ed., Springer-Verlag (Berlin), Vol. 52, 1959, pp. 363-418.

Vinogradov, A.P.; Surkov, Y.A.; Andreichikov, B.M.; Kalinkina, O.M.; and Grechischeva, I.M.: Planetary Atmospheres. C. Sagan; T.C. Owen; and H.J. Smith, eds., Springer-Verlag, 1971.

Wildt, R.: Methan in den atmospharen des Grossen Planeten. (Methane in the Atmospheres of Giant Planets.) Naturwissenschaften, Vol. 20, 1932, p. 851.

Zabriskie, F.R.: Hydrogen Content of Jupiter's Atmosphere. Astron. J., Vol. 67, 1962, pp. 168-170.

BOOKS

SECTION II

Allen, H.C., Jr.; and Cross, P.C.: Molecular Vib-Rotors. John Wiley & Sons, Inc., 1963.

Avram, M.; and Mateescu, G. D. (L. Birladeanu, transl.): Infrared Spectroscopy. Wiley Interscience, 1972.

Bak, B.: Elementary Introduction to Molecular Spectra. John Wiley & Sons, Inc., 1954.

Banwell, C.N.: Fundamental of Molecular Spectroscopy. McGraw-Hill Book Co., Inc., 1966.

Baranger, M.: Atomic and Molecular Processes. Academic Press, 1962.

Barrett, J.: Introduction to Atomic and Molecular Structure. John Wiley & Sons, Inc., 1970.

Barrow, G.M.: Introduction to Molecular Spectroscopy. McGraw-Hill Book Co., Inc., 1962.

Barrow, R.F.; Long, D. A.; and Millen, D.J. (Senior Reporters): A Specialist Periodical Report: Molecular Spectroscopy. Vol. I. The Chemical Society (London), 1973.

Bauman, R.P.: Absorption Spectroscopy. John Wiley & Sons, Inc., 1962.

Boumans, P.W.J.M.: Theory of Spectrochemical Excitation. Hilger and Watts (London), 1966.

Breene, R.G.: The Shift and Shape of Spectral Lines. Pergamon Press (London), 1961.

Brittain, E.F.H.; George, W.O.; and Wells, C.H.J.: Introduction to Molecular Spectroscopy. Academic Press, 1970.

Brode, W.R.: Chemical Spectroscopy. John Wiley & Sons, Inc., 1943.

Browning, D.R., ed.: Spectroscopy. McGraw-Hill Publishing Co., Inc., 1969.

Calvert, J.G.; and Pitts, J.N., Jr.: Photochemistry. John Wiley & Sons, Inc., 1967.

Carson, T.R.; and Roberts, M.J., eds.: Atoms and Molecules in Astrophysics. Academic Press, 1972.

Chamberlain, J.W.: Physics of the Aurora and Airglow. Academic Press., 1961.

Chandrasekhar, S.: Radiative Transfer. Dover Co., 1960.

Chang, R.: Basic Principles of Spectroscopy. McGraw-Hill Book Co., Inc., 1971.

Clark, G.L., ed.: The Encyclopedia of Spectroscopy. Reinhold Publishing Co., 1961.

Coleman, C.D.W.; Bozeman, W.R.; and Meggers, W.F.: Tables of Wavenumbers. Vol. I (2000-7000Å). Vol. II (7000-100μ). N.B.S.-monograph no. 3. U.S. Government Printing Office, 1960.

Colthup, N.B.; Daly, L.H.; and Wiberley, S.E.: Introduction to Infrared and Raman Spectroscopy. Academic Press, 1964.

Condon, E.U.; and Shortley, G.H.: The Theory of Atomic Spectra. Cambridge University Press, 1963.

Cottrell, T.L.: Dynamic Aspects of Molecular Energy States. John Wiley & Sons, Inc., 1965.

Craig, R.A.: The Upper Atmosphere. Academic Press, 1965.

Cutting, T.A.: Manual of Spectroscopy. Chemical Publishing Co., 1949.

Daemaison, J.: Molecular Constants from Microwave Molecular Beam and ESR Spectroscopy. Vol. 6, Group 2 Bornstein Series, Springer-Verlag, 1974.

Damany, N.; Vodar, B.; and Romand, J.: Some Aspects of Vacuum Ultraviolet Radiation Physics. Pergamon Press, 1974.

Dickerman, P.J., ed.: Optical Spectrometric Measurements of High Temperatures. The University of Chicago Press, 1961.

Dixon, R.N.: Spectroscopy and Structure. Methuen (London), 1965.

Duncan, A.B.F.: Rydberg Series in Atoms and Molecules. Academic Press, 1971.

Dunford, H.B.: Elements of Diatomic Molecular Spectra. Addison-Wesley, 1968.

Dwig, J.R., ed.: Vibrational Spectra and Structure. Vol. I and II. Marcel Dekker, Inc., 1972.

Eyring, H.; Walter, J.; and Kimball, G.E.: Quantum Chemistry. John Wiley & Sons, Inc., 1944.

Flügge, S., ed.: Encyclopedia of Physics. Vol. LII-Astrophysics III. Springer-Verlag, 1959.

Flügge, S., ed.: Encyclopedia of Physics. Vol. XXVII-Spectroscopy I. Springer-Verlag, 1964.

Gatterer, A.: Grating Spectrum of Iron. Specola Vaticana (Rome), 1951.

Gaydon, A.G.: Dissociation Energies and Spectra of Diatomic Molecules. Chapman & Hall Ltd., 1968.

Gaydon, A.G.: The Spectroscopy of Flames. Chapman & Hall (London), 1957.

Gaydon, A.G.; and Hurle, I.R.: The Shock Tube in High Temperature Chemical Physics. Reinhold Publishing, Inc., 1963.

Goodman, L.; and Hollas, J.M.: Electronic Structure of Atoms and Molecules. Vol. III, D. Henderson, ed., Academic Press, 1969.

Goody, R.M.: Atmospheric Radiation I. Theoretical Basis. Clarendon Press, 1964.

Green, A.E.S.; and Wyatt, P.J.: Atomic and Space Physics. Addison-Wesley, 1965.

Griem, H.R.: Plasma Spectroscopy. McGraw-Hill Book Co., Inc., 1964.

Harmony, M.D.: Introduction to Molecular Energies and Spectra. Holt, Rinehart & Winston, 1972.

Henderson, D., ed.: Physical Chemistry--An Advanced Treatise. Vol. III Electronic Structure of Atoms and Molecules. Academic Press, 1969.

Herbig, G.H., ed.: Spectroscopic Astrophysics. University of California Press, 1970.

Herzberg, G.: Atomic Spectra and Atomic Structure. Dover, 1944.

Herzberg, G.: Molecular Spectra and Molecular Structure Vol. I, Spectra of Diatomic Molecules. Van Nostrand Reinhold Co., 1950.

Herzberg, G.: Molecular Spectra and Molecular Structure. Vol. II, Infrared and Raman Spectra of Polyatomic Molecules. Van Nostrand Reinhold Co., 1945.

Herzberg, G.: Molecular Spectra and Molecular Structure. Vol. III, Electronic Spectra and Electronic Structure of Polyatomic Molecules. Van Nostrand Reinhold Co., 1966.

Herzberg, G.: The Spectra and Structures of Simple Free Radicals: An Introduction to Molecular Spectroscopy. Cornell University Press, 1971.

Hottel, H.D.; and Sarofim, A.F.: Radiative Transfer. McGraw-Hill Book Co., Inc., 1967.

Hougen, J.T.: The Calculation of Rotational Energy Levels and Rotational Line Intensities in Diatomic Molecules. N.B.S.-monograph no. 115. U.S. Govt. Printing Office, 1970.

Howarth, O.: Theory of Spectroscopy. John Wiley & Son, Inc., 1973.

Itterbeek, A.V., ed.: Physics of High Pressures and the Condensed Phase. North-Holland Publ., Co., 1965.

Jevons, W.: Report on Band Spectra of Diatomic Molecules. The Physical Society (London), 1932.

King, G.W.: Spectroscopy and Molecular Structure. Holt, Rinehart & Winston, 1964.

Kovacs, I.: Rotational Structure in the Spectra of Diatomic Molecules. Elsevier Publishing Co., 1969.

Kronig, R. de L.: Band Spectra and Molecular Structure. Cambridge University Press, 1930.

Kuhn, H.G.: Atomic Spectra. Academic Press, 1969.

Kuiper, G.P., ed.: The Atmospheres of the Earth and Planets. The University of Chicago Press, 1952.

Laidlaw, W.G.: Introduction to Quantum Concepts in Spectroscopy. McGraw-Hill Book Co., Inc., 1970.

Lide, D.R.; and Martin, P.A., ed.: Critical Evaluation of Chemical and Physical Structural Information. National Academy of Sciences, 1974.

Linnett, J.W.: The Electronic Structure of Molecules. John Wiley & Sons, Inc., 1964.

Loudon, R.: The Quantum Theory of Light. Clarendon Press (London), 1973.

Margrave, J.L.: The Characterization of High Temperature Vapors. John Wiley & Sons, Inc., 1967.

Marr, G.V.: Photoionization Processes in Gases. Academic Press, 1967.

Martin, D.H.: Spectroscopic Techniques. North-Holland Publ. Co., 1967.

McCormac, B.M., ed.: Physics and Chemistry of Upper Atmospheres. D. Reidel Publ. Co., 1973.

Miegham, J.V., ed.: The Upper Atmosphere Meteorology and Physics. International Geophysics. Academic Press, 1965.

Mitchell, A.C.G.; and Zemansky, M.W.: Resonance Radiation and Excited Atoms. Cambridge University Press, 1971.

Möller, K.D.; and Rothschild, W.G.: Far Infrared Spectroscopy. Wiley Interscience, 1971.

Moroz, V.I.: Physics of Planets. NASA-TT-F-515, 1968.

Nawrocki, P.J.; and Papa, R.: Atmospheric Processes. Geophysical Corporation of America, 1961.

Non-Radiative Transitions in Molecules. Societe' de Chimie Physique (Paris), 1969.

Olfe, D.B.; and Zakkay, V., ed.: Supersonic Flow Chemical Processes and Radiative Transfer. Pergamon Press, 1964.

Parr, R.G.: The Quantum Theory of Molecular Electronic Structure. W.A. Benjamin, Inc., 1972.

Pearse, R.W.B.; and Gaydon, A.G.: The Identification of Molecular Spectra. Chapman & Hall Ltd. (London), 1965.

Penner, S.S.: Quantitative Molecular Spectroscopy and Gas Emissivities. Addison-Wesley, 1959.

Penner, S.S.; and Olfe, D.B.: Radiation and Reentry. Academic Press, 1968.

Phillips, J.G.; and Davis, S.P.: Analysis of Molecular Spectra. News Letter Publ. by University of California.

Phillips, L.F.: Basic Quantum Chemistry. John Wiley & Sons, Inc., 1965.

Rao, C.N.R.: Ultraviolet and Visible Spectroscopy. Plenum Press, 1967.

Rao, K.N.; and Mathews, C.W., ed.: Molecular Spectroscopy. Modern Research. Academic Press, 1972.

Robinson, J.W., ed.: CRC Handbook of Spectroscopy. CRC Press, Inc., 1974.

Samson, J.A.R.: Techniques of Vacuum Ultraviolet Spectroscopy. John Wiley & Sons, Inc., 1967.

Sandorfy, C.: Electronic Spectra and Quantum Chemistry. Prentice-Hall, Inc., 1964.

Shore, B.W.; and Menzel, D.H.: Principles of Atomic Spectra. John Wiley & Sons, Inc., 1967.

Simons, J.P.: Photochemistry and Spectroscopy. John Wiley & Sons, Inc., 1971.

Steinfield, J.I.: Molecules and Radiation. Harper & Row, Inc., 1974.

Thackeray, A.D.: Astronomical Spectroscopy. MacMillan Co., 1961.

Thompson, H.W., ed.: Advances in Spectroscopy. Vol. I and II. Interscience Publ., Inc., 1959.

Thorne, A.P.: Spectrophysics. Chapman & Hall (London), 1974.

Townes, C.H.; and Schawlow, A.L.: Microwave Spectroscopy. McGraw-Hill Book Co., Inc., 1955.

Tyte, D.C.; Hebert, G.R.; Innanen, S.H.; and Nicholls, R.W.: Identification Atlas of Molecular Spectra. Vol. I-IX. Molecular Excitation Group, Dept. of Physics, University of Western Ontario Press (London), 1964-1972.

Unger, H.G.: Introduction to Quantum Electronics. Pergamon Press, 1970.

Walker, S.; and Straw, H.: Spectroscopy. Vol. I and II. Chapman & Hall, 1966, 1967.

Wayne, R.P.: Photochemistry. Elsevier Publ. Co., Inc., 1970.

Whiffen, D.H.: Spectroscopy. John Wiley & Son's, Inc., 1972.

Wilson, E.B., Jr.; Decius, J.C.; and Cross, P.C.: Molecular Vibrations. McGraw-Hill Book Co., Inc., 1954.

Whitten, R.C.; and Poppoff, I.G.: Fundamentals of Aeronomy. John Wiley & Son's, Inc., 1971.

Wolfe, W.L., ed.: Handbook of Military Infrared Technology. Office of Naval Research, Dept. of the Navy, 1965.

Wu, T.Y.: Vibrational Spectra and Structure of Polyatomic Molecules. J.W. Edwards, Inc., 1946.

Zuev, V.E.: Propagation of Visible and Infrared Radiation in the Atmosphere. (English Translation), John Wiley & Son's, Inc., 1974.

REFERENCES

SECTION II

Anderson, P.W.: Pressure Broadening in the Microwave and Infrared Regions. Phys. Rev., Vol. 76, 1949, pp. 647-661.

Bates, D.R.: The Intensity Distribution in the Nitrogen Band Systems Emitted From the Earth's Upper Atmosphere. Proc. Roy. Soc. (London), Vol. A196, 1949, pp. 217-250.

Belton, M.J.S.: Theory of the Curve of Growth and Phase Effects in a Cloudy Atmosphere: Applications to Venus. J. Atmosph. Sci., Vol. 25, 1968, pp. 596-609.

Bennett, R.G.; and Dalby, F.W.: Experimental Determination of the Oscillator Strength of the First Negative Bands of N_2^+. J. Chem. Phys., Vol. 31, 1959, pp. 434-441.

Breene, R.G.: Line Shape. Rev. Mod. Phys., Vol. 29, 1957, pp. 94-143.

Budo, A.: Triplet b and Term Formula for the General Intermediary Case and Application on the $B^3\Pi$ and $C^3\Pi$ Terms of the N_2 Molecule. Z. Phys., Vol. 96, 1935, pp. 219-229.

Budo, A.: The Rotational Constants B, D, and Y of the $^3\Pi$ Terms of TiO, C_2, CO, PH, NH, and AlH. Z. Phys., Vol. 98, 1936, pp. 437-444.

Cashion, J.K.: Testing of Diatomic Potential Energy Functions by Numerical Methods. J. Chem. Phys., Vol. 39, 1963, pp. 1872-1877.

Chen, S.; and Takeo, M.: Broadening and Shift of Spectral Lines Due to the Presence of Foreign Gases. Rev. Mod. Phys., Vol. 29, 1957, pp. 20-73.

Churchill, D.R.; and Meyerott, R.E.: Spectral Absorption in Heated Air. J. Quant. Spectros. Rad. Tran., Vol. 5, 1965, pp. 69-86.

Condon, E.U.: A Theory of Intensity Distribution in Band Systems. Phys. Rev., Vol. 28, 1926, pp. 1182-1201.

Condon, E.U.: Nuclear Motions Associated with Electron Transitions in Diatomic Molecules. Phys. Rev., Vol. 32, 1928, pp. 858-872.

Condon, E.U.: The Frank-Condon Principle and Related Topics. American J. Phys., Vol. 15, 1947, pp. 365-374.

Coster, D.; and Brons, F.: Predissociation in the Angstrom Bands of CO. Physica, Vol. 1, 1934, pp. 155-160.

Dunham, J.L.: The Wentzel Brillouin Kramer Method of Solving the Wave Equations. Phys. Rev., Vol. 41, 1932, pp. 713-720.

Earls, L.T.: Intensities in $^2\Pi$-^2S Transitions in Diatomic Molecules. Phys. Rev., Vol. 48, 1935, pp. 423-424.

Farkas, L.: Absorption Spectrum of Aluminium Hydride. Z. Phys., Vol. 70, 1931., pp. 733-749.

Franck, J.: Elementary Processes of Photochemical Reactions. Transactions of Faraday Soc. (London), Vol. 21, 1925, pp. 536-542.

Fraser, P.A.: A Method for Determining the Electronic Transition Moment for Diatomic Molecules. Canadian J. Phys., Vol. 32, 1954, pp. 515-521.

Fraser, P.A.: Research Notes - Vibrational Transition Probabilities of Diatomic Molecules: III. Proc. Phys. Soc. (London), Vol. 67, 1954, pp. 939-941.

Froslie, H.M.; and Winans, J.G.: The Absorption Spectrum of InCl. Phys. Rev., Vol. 72, 1947, pp. 481-491.

Henri, V.: Molecular Structure and Absorption Spectra in Vapours. C. R. Acad. Sci. (Paris), Vol. 177, 1923, pp. 1037-1040.

Henri, V.; and Teves, M.C.: Absorption Spectrum and Constitution of Sulphur Vapour. Predissociation of Molecules. Nature (London), Vol. 114, 1924, pp. 894-895.

Herzberg, G.; and Mundie, L.G.: On the Predissociation of Several Diatomic Molecules. J. Chem. Phys., Vol. 8, 1940, pp. 263-273.

Hesser, J.E.; and Dressler, K.: Radiative Lifetimes of Ultraviolet Molecular Transitions. J. Chem. Phys., Vol. 45, 1966, pp. 3149-3150.

Hill, E.L.; and Van Vleck, J.H.: On the Quantum Mechanics of the Rotational Distortion of Multiplets in Molecular Spectra. Phys. Rev., Vol. 32, 1928, pp. 250-272.

Hönl, H.; and London, F.: The Intensities of Band Lines. Z. Phys., Vol. 23, 1925, pp. 803-809.

Hulburt, H.M.; and Hirschfelder, J.O.: Potential Energy Functions for Diatomic Molecules. J. Chem. Phys., Vol. 9, 1941, pp. 61-68.

Jarmain, W.R.: Franck-Condon Factors from Klein-Dunham Potentials for Bands of the Schumann-Runge System of O_2. Canadian J. Phys., Vol. 41, 1963, pp. 414-432.

Jarmain, W.R.: Simplified Analytical Representations of Klein-Dunham Potential Energy Functions. J. Chem. Phys., Vol. 31, 1959, pp. 1137-1138.

Jarmain, W.R.; and Nicholls, R.W.: A Theoretical Study of the O_2 $X^3\Sigma_g^-$-$B^3\Sigma_u^-$ Photodissociation Continuum. Proc. Phys. Soc. (London), Vol. 84, 1964, pp. 417-424.

Jarmain, W.R.; and Nicholls, R. W.: A Theoretical Study of the v" = 0, 1, 2, Progressions of Bands and Adjoining Photodissociation Continua of the O_2 Herzberg I System. Proc. Phys. Soc. (London), Vol. 90, 1967, pp. 545-553.

Jarmain, W.R.; and Nicholls, R.W.: Vibrational Transition Probabilities to High Quantum Numbers for the N_2 First and Second Positive Band Systems. Canadian J. Phys., Vol. 32, 1954, pp. 201-204.

Jen, C.K.: Rotational Magnetic Moments in Polyatomic Molecules. Phys. Rev., Vol. 81, 1951, pp. 197-203.

Kaplan, J.: Forced Predissociation in Nitrogen. Phys. Rev., Vol. 38, 1931, pp. 373-374.

Klein, O.: The Measurement of Potential Curves for Diatomic Molecules with Help From Spectral Analysis. Z. Phys., Vol. 76, 1932, pp. 226-235.

Kondrat'ev, V.; and Olson, E.: The Induced Predissociation in the Absorption Spectrum of Sulphur. Z. Phys., Vol. 99, 1936, pp. 671-676.

Kovacs, I.; and Budó, A.: On the Theory of Accidental Predissociation. J. Chem. Phys., Vol. 15, 1947, pp. 166-173.

Kronig, R.; and Rabi, I.I.: The Symmetrical Top in the Undulatory Mechanics. Phys. Rev., Vol. 29, 1927, pp. 262-269.

Kuhn, H.: Pressure Shift and Broadening of Spectral Lines. Phil. Mag., Vol. 18, 1934, pp. 987-1003.

Kuhn, H.; and London, F.: Limitation of the Potential Theory of the Broadening of Spectral Lines. Phil. Mag., Vol. 18, 1934, pp. 983-987.

Margenau, H.; and Lewis, M.: Structure of Spectral Lines From Plasmas. Rev. Mod. Phys., Vol. 31, 1959, pp. 569-615.

Morse, P.M.: Diatomic Molecules According to the Wave Mechanics, II. Vibrational Levels. Phys. Rev., Vol. 34, 1929, pp. 57-64.

Mulliken, R.S.: Electronic Structures and Spectra of Triatomic Oxide Molecules. Rev. Mod. Phys., Vol. 14, 1942, pp. 204-215.

Mulliken, R.S.: Electronic Structures of Molecules, XIV. Linear Triatomic Molecules Especially Carbon Dioxide. J. Chem. Phys., Vol. 3, 1935, pp. 720-739.

Mulliken, R.S.: Electronic Structures of Polyatomic Molecules and Valence. Phys. Rev., Vol. 40, 1932, pp. 55-62.

Murty, M.; and Nicholls, R.W.: Geometry of Condon Loci of Molecular Spectra. Nature, Vol. 213, 1967, pp. 1009-1010.

Nicholls, R.W.: Condon Parabolae in Molecular Spectra. Nature, Vol. 193, 1962, pp. 966-967.

Nicholls, R.W.: Franck-Condon Factors for Ionizing Transitions of O_2, CO, NO, and H_2 and for the NO^+ ($A^1\Sigma$ - $X^1\Sigma$) Band System. J. Phys., Vol. 1, 1968, pp. 1192-1211.

Nicholls, R.W.: Franck-Condon Factors to High Vibrational Quantum Numbers III:CN. (NBS), Vol. 68A, 1964, pp. 75-78.

Nicholls, R.W.: Franck-Condon Factors to High Vibrational Quantum Numbers IV NO Band Systems. (NBS), Vol. 68A, 1964, pp. 635-640.

Nicholls, R.W.: Interpolation of Franck-Condon Factors. Nature, Vol. 204, 1964, p. 373.

Nicholls, R.W.: Laboratory Astrophysics. J. Quant. Spectros. Rad. Tran., Vol. 2, 1962, pp. 433-449.

Nicholls, R.W.: On the Electronic Transition Moment and the $\bar{r}$ Centroid Approximation in Interpretation of Spectral Intensities of Diatomic Molecules. J. Quant. Spectros. Rad. Tran., Vol. 14, 1974, pp. 233-237.

Nicholls, R.W.: On the Relationship Between $\bar{r}$-centroid and Band Frequency. Proc. Phys. Soc. (London), Vol. 85, 1965, pp. 159-162.

Nicholls, R.W.: Transition Probabilities of Aeronomically Important Spectra. Ann. Geophys. (France), Vol. 20, 1964, pp. 144-181.

Nicholls, R.W.; Fraser, P.A.; Jarmain, W.R.; and McEachran, R.P.: Vibrational Transition Probabilities of Diatomic Molecules: Collected Results. IV BeO, BO, CH^+, CO, NO, SH, O_2, O_2^+. Astrophys. J., Vol. 131, 1960, pp. 399-406.

Nicholls, R.W.; and Jarmain, W.R.: r̄-centroids: Average Internuclear Separations Associated with Molecular Bands. Proc. Phys. Soc. (London), Vol. 69, 1956, pp. 253-264.

Nicholls, R.W.; and Jarmain, W.R.: r̄-centroids for Diatomic Molecules. J. Chem. Phys., Vol. 40, 1955, p. 1561.

Nicholls, R.W.; and Jarmain, W.R.: On r̄-centroids of Molecular Transitions Equilibrium Internuclear Separations and Oscillator Turning Points. Proc. Phys. Soc. (London), Vol. 74, 1959, pp. 133-136.

Nicholls, R.W.; Jarmain, W.R.; and Fraser, P.A.: Transition and Probability Parameters of Molecular Spectrum Arising from Combustion Processes. Combustion and Flame, Vol. 3, 1959, pp. 18-38.

Nicholls, R.W.; Robinson, D.; Parkinson, W.; and Jarmain, W.R.: r-centroids for the O_2^+ Second Negative, N_2 Lyman-Birge-Hopfield, and N_2 V-K Band Systems. Proc. Phys. Soc. (London), Vol. 69, 1956, pp. 713-715.

Nicholls, R.W.; and Stewart, A.L.: Chapter II. Atomic and Molecular Processes. (D. R. Bates, ed.). Acad. Press, 1962.

Patch, R.W.; Shackleford and Penner, S.S.: Approximate Spectral Absorption Coefficient Calculations for Electronic Band Systems Belonging to Diatomic Molecules. J. Quant. Spectros. Rad. Trans., Vol. 2, 1961, pp. 263-271.

Phillips, G.M.; Hunter, J.S.; and Sutton, L.E.: An Investigation of the Occurrence of the Coordinate or Dative Link by Electric Dipole Moment Measurements. J. Chem. Soc., 1945, pp. 146-162.

Plass, G.N.: Models for Spectral Band Absorption. J. Opt. Soc. America, Vol. 48, 1958, pp. 690-703.

Rees, A.L.G.: The Calculation of Potential Energy Curves from Band Spectroscopic Data. Proc. Phys. Soc. (London), Vol. 60, 1947, pp. 998-1008.

Reiche, F.; and Rademacher, H.: The Measurement of Symmetrical Rotations by Schrödinger's Vibrational Technique. Z. Phys., Vol. 41, 1927, pp. 453-492.

Rice, O.K.: A Contribution to the Quantum Mechanical Theory of Radioactivity and the Dissociation by Rotation of Diatomic Molecules. Phys. Rev., Vol. 35, 1930, pp. 1538-1551.

Rosen, B.: Study on the Predissociation Induced in the Molecules S_2, Se_2, and Te_2. Acta. Phys. Polonica, Vol. 5, 1936, pp. 193-205.

Rydberg, R.: Graphical Solution of Some Band Spectroscopic Products. Z. Phys., Vol. 73, 1932, pp. 376-385.

Rydberg, R.: On Some Potential Curves of Mercuric Hybrids. Z. Phys., Vol. 80, 1933, pp. 514-524.

Schwenker, R.P.: Experimental Oscillator Strengths of CO and CO^+. J. Chem. Phys., Vol. 42, 1965, pp. 1895-1897.

Shulman, R.G.; Dailey, B.P.; and Townes, C.H.: Molecular Dipole Moments and Stark Effects. III Dipole Moment Determinations. Phys. Rev., Vol. 78, 1950, pp. 145-148.

Spindler, R.J.: Franck-Condon Factors Based on RKR Potentials with Applications to Radiative Absorption Coefficients. J. Quant. Spectros. Rad. Trans., Vol. 5, 1965, pp. 165-204.

Steele, D.; Lippincott, E.R.; and Vanderslice, J.T.: Comparative Study of Empirical Internuclear Potential Functions. Rev. Mod. Phys., Vol. 34, 1962, pp. 239-251.

Tatum, J.B.: Hönl-London Factors for $^3\Sigma^\pm - {}^3\Sigma^\pm$ Transitions. Canadian J. Phys., Vol. 44, 1966, pp. 2944-2946.

Tatum, J.B.: The Interpretation of Intensities in Diatomic Molecular Spectra. Astrophys. J. (Suppl.), Vol. 14, 1967, pp. 21-56.

Turner, L.A.: Magnetic Quenching of Iodine Fluorescence and its Relation to Predissociation Phenomena. Z. Phys., Vol. 65, 1930, pp. 464-479.

Van IddeKinge, H.H.: Band Spectrum of Sulphur. Nature, Vol. 125, 1930, p. 858.

Van Kranendonk, J.: Induced Infrared Absorption in Gases. Calculation of the Binary Absorption Coefficients of Symmetrical Diatomic Molecules. Physica, Vol. 24, 1958, pp. 347-362.

Van Regemorter, H.: Spectral Line Broadening in 'Atoms and Molecules in Astrophysics'. T. R. Carson and M. J. Roberts, ed., Acad. Press, 1972.

Van Vleck, J.H.: Theory of Magnetic Quenching of Iodine Fluorescence and of Λ Doubling in $^3\Pi_0$ States. Phys. Rev., Vol. 40, 1932, pp. 544-568.

Varshni, Y.P.: Comparative Study of Potential Energy Functions for Diatomic Molecules. Rev. Mod. Phys., Vol. 29, 1957, pp. 646-682.

Walsh, A.D.: Types of Electronic Transitions in Polyatomics. Quart. Rev., Vol. 2, 1948, pp. 73-91.

Weisskopf, V.: Width of Spectral Lines in Gases. Z. Phys., Vol. 34, 1933, pp. 1-24.

Whiting, E.E.; and Nicholls, R.W.: Reinvestigation of Rotational Line Intensity Factors in Diatomic Spectra. Astrophys. J. (Suppl.), Vol. 27, 1974, pp. 1-19.

Williams, D.; Wenstrand, D.C.; Brockmann, R.J.; and Curnutte, B.: Collisional Broadening of Infrared Absorption Lines. Molec. Phys., Vol. 20, 1971, pp. 769-785.

Zare, R.N.; Larson, R.A.; and Berg, R.A.: Franck-Condon Factors for Electronic Band Systems of Molecular Nitrogen. J. Molec. Spectros., Vol. 15, 1965, pp. 117-139.

Zener, C.: Dissociation of Excited Diatomic Molecules by External Perturbations. Proc. Roy. Soc. (London), Vol. 140, 1933, pp. 660-668.

Page Intentionally Left Blank

REFERENCES
SECTION III

Abu-Romia, M.M.; and Tien, C.L.: Measurements and Correlations of Infrared Radiation of Carbon Monoxide at Elevated Temperatures. J. Quant. Spectros. Rad. Trans., vol. 6, 1966, pp. 143-168.

Adel, A.; and Dennison, D.M.: Infrared Spectrum of Carbon Dioxide: Part I. Phys. Rev., vol. 43, 1933, pp. 716-723.

Adel, A.; and Dennison, D.M.: Infrared Spectrum of Carbon Dioxide: Part II. Phys. Rev., vol. 44, 1933, pp. 99-104.

Adel. A.; and Dennison, D.M.: Notes on the Infrared Spectrum and Molecular Structure of Ozone. J. Chem. Phys., vol. 14, 1946, pp. 379-382.

Adel, A.; and Slipher, V.M.: The Identification of the Methane Bands in the Solar Spectra of the Major Planets. Phys. Rev., vol. 46, 1934, pp. 240-241.

Allen, H.C.; and Plyler, E.K.: ν_3 Band of Methane. J. Chem. Phys., vol. 26, 1957, pp. 972-973.

Amiot, C.; and Guelachvili, G.: Vibration-Rotation Bands of $^{14}N_2^{16}O$: 1.2μ - 3.3μ Region. J. Mol. Spectrosc., vol. 51, 1974, pp. 475-491.

Armstrong, R.L.; and Welch, H.L.: The Infrared Spectrum of Carbon Monoxide in CO-He Mixtures at High Pressures. Canadian J. Phys., vol. 43, 1965, pp. 547-556.

Astoin, N.: On the Absorption Spectrum of the Vapour of Water and Heavy Water in the Extreme Ultraviolet. Compt. Rend., (Paris), vol. 242, 1956, pp. 2327-2329.

Astoin, N.: Spectrography in the Extreme Ultraviolet. Absorption of NO, N_2O, H_2O, and D_2O (Gaseous). J. Rech. (CNRS), 1957, pp. 1-22.

Astoin, N.; and Granier, J.: On the Absorption Spectrum of N_2O in the Extreme Ultraviolet C.R. Acad. Sci. (Paris), vol. 241, 1955, pp. 1736-1738.

Astoin, N.; Johnnan-Gilles, A.; Granier-Mayenne, J.; and Romand, J.: Some Data on the

Absorption Spectra of Gaseous N_2O, NO, and H_2O in the Extreme Ultraviolet. Phys. in Space. pp. 136-142.

Barbe, A.; Secroun, C.; and Jouve, P.: Infrared Spectra of $^{16}O_3$ and $^{18}O_3$: Darling and Dennison Resonance and Anharmonic Potential Function of Ozone. J. Mol. Spectrosc., vol. 49, 1974, pp. 171-182.

Barbier, D.; and Chalonge, D.: On the Absorption Coefficients of Ozone in the Region of Huggins Bands. Ann de Phys., vol. 17, 1942, pp. 272-302.

Barchawitz, P.; Dorlec, L.; Farrenq, R.; Truffert, A.; and Vautier, P.: Infrared Emission of CO and CO_2 and Continous Laser Emission with CO_2 by Direct Action of High Frequency Excitation. C.R. Acad. Sci., (Paris), vol. 260, 1965, pp. 3581-3582.

Barker, E.F.; and Adel, A.: Resolution of Two Difference Bands of CO_2 Near 10μ. Phys. Rev., vol. 44, 1933, pp. 185-187.

Barker, E.F.; and Slater, W.W.: Infrared Spectrum of Heavy Water. J. Chem. Phys., vol. 3, 1935, pp. 660-663.

Barker, E.F.; and Wu, T.Y.: Harmonic and Combination Bands in CO_2. Phys. Rev., vol. 45, 1934, pp. 1-3.

Barnes, W.L.; Susskind, J.; Hunt, R.H.; and Plyler, E.K.: Measurement and Analysis of the ν_3 Band of Methane. J. Chem. Phys., vol. 56, 1972, pp. 5160-5172.

Barney, C.V.; and Eggars, D.V.: Infrared Spectrum of Carbon Dioxide Enriched in O^{18}. J. Chem. Phys., vol. 40, 1964, pp. 990-1000.

Barrett, J.J.; and Harvey, A.B.: Vibrational and Rotational Translational Temperatures in N_2 by Interferometric Measurement of the Pure Rotational Raman Effect. J. Opt. Soc. America, vol. 65, 1975, pp. 392-398.

Bates, R.D., Jr.; Flynn, G.W.; and Ronn, A.M.: Laser-Induced Vibrational Fluorescence in Nitrous Oxide. J. Chem. Phys., vol. 49, 1968, pp. 1432-1433.

Begun, G.M.; and Fletcher, W.H.: Infrared Spectra of the Isotopic Nitrous Oxides. J. Chem. Phys., vol. 28, 1958, pp. 414-418.

Bell, S.: The Spectra of H_2O and D_2O in the Vacuum Ultraviolet. J. Mol. Spectrosc., vol. 16, 1965, pp. 205-213.

Belozerova, V.P.: Absorption Spectra of Several Atmospheric Gases in the Vacuum Ultraviolet Region. Review: UDC-551.510.4:535.34-31, 1967, pp. 184-192.

Bender, C.F.; and Davidson, E.R.: Theoretical Study of Several Electronic States of the HF Molecule. J. Chem. Phys., vol. 49, 1968, pp. 4989-4995.

Benedict, W.S.: New Bands in the Vibration-Rotation Spectrum of Water Vapor. Phys. Rev., vol. 74, 1948, p. 1246.

Benedict, W.S.; Bullock, B.W.; Silverman, S.; and Grosse, A.E.: Infrared Emission of Hydrogen-Fluorine (H_2-F_2) Flame. J. Opt. Soc. America, vol. 43, 1953, pp. 1106-1113.

Benedict, W.S.; Gailar, N.; and Plyler, E.K.: Rotation-Vibration Spectra of Deuterated Water Vapour. J. Chem. Phys., vol. 24, 1956, pp. 1139-1165.

Benedict, W.S.; and Herman, R.: The Calculation of Self-Broadened Line Widths in Linear Molecules. J. Quant. Spectrosc. Rad. Trans., vol. 3, 1963, pp. 265-278.

Benedict, W.S.; Herman, R.; Morre, G.E.; and Silverman, S.: The Strengths, Width and Shapes of Lines in the Vibration-Rotation Bands of CO. Astrophys. J., vol. 135, 1962, pp. 277-297.

Benedict, W.S.; and Plyler, E.K.: Absorption Spectra of Water Vapor and Carbon Dioxide in the Region 2.7μ. J. Res. (NBS), vol. 46, 1951 pp. 246-265.

Benedict, W.S.; and Plyler, E.K.: Interaction of Stretching Vibration and Inversion in Ammonia. J. Chem. Phys., vol. 24, 1956, p. 904.

Benedict, W.S.; Plyler, E.K.; and Tidwell, E.D.: Vibration-Rotation Bands of Ammonia, II. The Molecular Dimensions and Harmonic Frequencies of Ammonia and Deuterated Ammonia. Canadian J. Phys., vol. 35, 1957, pp. 1235-1241.

Benedict, W.S.; Plyler, E.K.; and Tidwell, E.D.: Vibration Rotation Bands of Ammonia, III. The Region 3.2 - 4.3μ. J. Chem. Phys., vol. 29, 1958, pp. 829-845.

Benedict, W.S.; Plyler, E.K.; and Tidwell, E.D.: Vibration-Rotation Bands of Ammonia, I.

The Combination Bands $\nu_2 - (\nu_1, \nu_2)$. J. Res. (NBS), vol. 61, 1958, pp. 123-147.

Benedict, W.S.; Plyler, E.K.; and Tidwell, E.D.: Vibration-Rotation Bands of Ammonia, IV. The Stretching Fundamentals and Associated Bands Near 3μ. J. Chem. Phys., vol. 32, 1960, pp. 32-44.

Berkowitz, J.; Chupka, W.A.; Guyon, P.M.; Holloway, J.H.; and Spohr, R.: Photoionization Mass Spectrometric Study of F_2, HF, and DF. J. Chem. Phys., vol. 54, 1971, pp. 5165-5180.

Bernas, A.; and Truong, T.B.: On the Low-Lying Triplet of the Water Molecule and its Luminescent Decay. Chem. Phys. Letters, vol. 29, 1974, pp. 585-588.

Beutler, H.; Deubner, A.; and Jünger, H.O.: Absorption Spectrum of Hydrogen. Z. Phys., vol. 98, 1935, pp. 181-197.

Beutler, H.; and Jünger, H.O.: Absorption Spectrum of Hydrogen. Part III, Autoionization in the $3p\pi - \Pi u$ Term of H_2 and its Selection Rules. Z.Phys., vol. 100, 1936, pp. 80-94.

Birge, R.T.: The Band Spectra of Carbon Monoxide. Phys. Rev., vol. 28, 1926, pp. 1157-1181.

Bondybey, V.; Pearson, P.K.; and Schaefer, H.F.: Theoretical Potential Energy Curves of OH, HF^+, HF, HF^-, NeH^+, and NeH. J. Chem. Phys., vol. 57, 1972, pp. 1123-1128.

Boness, M.J.W.; and Schulz, G.J.: Vibrational Excitation in CO_2 Via the 3.8eV Resonance. Phys. Rev. A., vol. 9, 1974, pp. 1969-1979.

Bosomworth, D.R.; and Gush, H.P.: Collision-Induced Absorption of Compressed Gases in the Far Infrared I & II. Canadian J. Phys., vol. 43, 1965, pp. 729-750.

Botineau, J.: Infrared Absorption of Methane at High Resolution Between 1225 and 1440 cm^{-1}. J. Mol. Spectrosc., vol. 41, 1972, pp. 182-194.

Bott, J.F.: Vibrational Energy Exchange of the DF (v=2) State with DF(v=0). Chem. Phys. Letter, vol. 23, 1973, pp. 335-338.

Bouanich, J.P.; Larvor, M.: and Haeusler, C.: Study of the Vibration-Rotation Lines of the v0-3 Band of Carbon Monoxide Compressed with Argon, With N_2 and HCl. C.R. Acad. Sci., (Paris), vol. B269, 1970, pp. 1220-1223.

Boursey, E.: Electronic Excitation of HCl Trapped in Inert Matrices. J. Chem. Phys., vol. 62, 1975, pp. 3353-3354.

Boyd, D.R.J.; Thompson, H.W.; and Williams, R.L.: Vibration-Rotation Bands of Methane. Proc. Roy. Soc., (London), vol. 213, 1952, pp. 42-54.

Breeze, J.C.; and Ferriss, C.C.: Integrated Intensity Measurements on the Fundamental and First Overtone Band System of CO Between 2500 and $5000^{\circ}K$. J. Chem. Phys., vol. 3, 1965, pp. 3253-3258.

Bregman, J.D.; Lester, D.F.; and Rank, D.M.: Observation of the ν_2 Band of PH_3 in the Atmosphere of Saturn. Astrophys. J., vol. 202, 1975, pp. 55-56.

Britt, C.O.; Tolbert, C.W.; and Straiton, A.W.: Radio Wave Absorption of Several Gases. J. Res. (NBS), vol. 65, 1961, pp. 15-18.

Brundle, C.R.: Ionization and Dissociation Energies of HF and DF and Their Bearing on D_0^0 (F_2). Chem. Phys. Letters, vol. 7, 1970, pp. 317-322.

Buenker, R.J.; and Peyerimhoff, S.W.: Calculations on the Electronic Spectrum of Water. Chem. Phys. Letter, vol. 29, 1974, pp. 253-259.

Bunch, S.M.; Cook, G.R.; Ogawa, M.; and Ehler, A.W.: Absorption Coefficients of C_6H_6 and H_2 in the Vacuum Ultraviolet. J. Chem. Phys., vol. 28, 1958, pp. 740-741.

Burch, D.E.; and Gryvnak, D.A.: Strengths, Widths and Shapes of the Lines of the ν_3 CO Band. J. Chem. Phys., vol. 47, 1967, pp. 4930-4940.

Burch, D.E.; and Gryvnak, D.A.: Absorption of Infrared Radiant Energy by CO_2 and H_2O. Absorption of CO_2 Between 1100 and 1835 cm^{-1} (9.1 - 5.5µ). J. Opt. Soc. America, vol. 61, 1971, pp. 499-503.

Burch, D.E.; and Gryvnak, D.A.; and Patty, R.R.: Absorption of Infrared Radiation by CO_2 and H_2O. Absorption by CO_2 Between 8000 and 10,000 cm^{-1} (1 - 1.25µ). J. Opt. Soc. America, vol. 58, 1968, pp. 335-341.

Burch, D.E.; Gryvnak, D.A.; and Pembrook, J.D.: Infrared Absorption Bands of Nitrous Oxide. Tech. Rept. AFCRL-72-0387, 1972.

Burch, D.E.; Singleton, E.B.; France, W.L.; and Williams, D.: Infrared Absorption by Minor Atmospheric Constituents. RF Project Report-778, Ohio State Univ. Res. Foundation.

Burch, D.E.; and Williams, D.: Total Absorptance of Carbon Monoxide and Methane in the Infrared. Appl. Opt., vol. 1, 1962, pp. 587-594.

Burgess, J.S.: The Frequency of ν_2 in the Infrared Spectrum of CH_4. Phys. Rev., vol. 76, 1949, p. 302.

Burgess, J.S.; Bell, E.E.; and Nielsen, H.H.: The Forbidden Transition ν_2 in the Infrared Spectrum of Methane. J. Opt. Soc. America, vol. 43, 1953, pp. 1958-1060.

Burrus, C.A.: Stark Effect From 1.1 to 216 mm Wavelengths: PH_3, PD_3, DI and CO. J. Chem. Phys., vol. 28, 1958, pp. 427-429.

Burrus, C.A.; and Gordy, W.: Millimeter and Submillimeter Wave Spectroscopy. Phys. Rev., vol. 101, 1956, pp. 599-602.

Burrus, C.A.; Gordy, W.; Benjamin, B.; and Livingston, R.: One-to-Two Millimeter Wave Spectra of TCl and TBr. Phys. Rev., vol. 97, 1955, pp. 1661-1664.

Cairns, R.B.; and Samson, J.A.R.: Absorption and Photoionization Crossections of CO_2, CO, Ar and He at Intense Solar Lines. J. Geophys. Res., vol. 70, 1965, pp. 99-104.

Cairns, R.B.; and Samson, J.A.R.: Total Absorption Cross Section of CO and CO_2 in the Region 550-200Å. J. Opt. Soc. America, vol. 56, 1966, p. 526.

Callendar, G.S.: Infrared Absorption of Carbon Dioxide with Special Reference To Atmospheric Radiation. Quart. J. Roy. Meteorol. Soc., vol. 67, 1941, pp. 263-274.

Chackerian, C., Jr.: Calculation of High Temperature Steradiancy for Vibration-Rotation Bands of Carbon Monoxide. J. Quant Spectros. Rad. Trans., vol. 10, 1970, pp. 271-282.

Chang, T.Y.: Accurate Frequencies and Wavelengths of CO_2 Laser Lines. Opt. Com., vol. 2, 1970, pp. 77-80.

Chappuis, J.: On The Absorption Spectrum of Ozone. C. R. Acad. Sci., (Paris), vol. 91, 1880, pp. 985-986.

Chei, A.T.; and Williams, D.: Comparison of Collision Cross Sections for Line Broadening in the CO Fundamentals. J. Opt. Soc. America, vol. 58, 1968, pp. 1395-1399.

Chen, H.L.; and Morre, C.B.: Vibration-Rotation Energy Transfer in Hydrogen Chloride. J. Chem. Phys., vol. 54, 1971, pp. 4072-4084.

Clough, S.A.; and Kneizys, F.X.: Coriolis Interaction in the ν_1 and ν_3 Fundamentals of Ozone. J. Chem. Phys., vol. 44, 1966, pp. 1855- 1861.

Clough, S.A.; McCarthy, D.E.; and Howard, J.N.: $4\nu_2$ Band of Nitrous Oxide. J. Chem. Phys., vol. 30, 1959, pp. 1359-1360.

Codling, K.: Structure in the Photoionization Continuum of N_2 Near 500Å. Canadian J. Phys., vol. 143, 1966, pp. 552-558.

Cohen, N.: A Brief Review of Rate Coefficients for Reactions in the D_2 - F_2 Chemical System. Aerosp. Rept., No. TR-0074, 1974.

Coles, D.K.; Ebyash, E.S.; and Gorman, J.G.: Microwave Absorption Spectra of N_2O. Phys. Rev., vol. 72, 1947, p. 973.

Coles, D.K.; and Hughes, R.H.: Microwave Spectra of Nitrous Oxide. Phys. Rev., vol. 76, 1949, p. 178.

Cook, G.R.; and Ching, B.K.: Absorption, Photoionization and Fluorescence of Some Gases of Importance in the Study of the Upper Atmosphere. Aerosp. Corpt. Rept., No. TDR-469, 1965.

Cook, G.R.; Metzger, P.H.; and Ogawa, M.: Absorption,Photoionization, and Fluorescence of CO_2. J. Chem. Phys., vol. 44, 1966, pp. 2935-2942.

Cook, G.R.; Metzger, P.H.; and Ogawa, M.: Photoionization and Absorption Coefficients of N_2O. Aerosp. Corp. Rept., No. TR-0158, 1967.

Cook, G.R.; Metzger, P.H.; and Ogawa, M.: Photoionization and Absorption Coefficients of N_2O. J. Opt. Soc. America, vol. 58, 1968, pp. 129-136.

Connes, P.; Connes, J.; Benedict, W.S.; and Kaplan, L.D.: Traces of HCl and HF in the Atmosphere of Venus. Astrophys. J., vol. 147, 1967, pp. 1230-1237.

287

Corneil, P.H.; and Pimental, G.C.: Hydrogen Chloride Explosion Laser II DCl. J. Chem. Phys., vol. 49, 1968, pp. 1379-1386.

Costern, D.; Brons, F.; and Van Der Zeil, A.: Second Positive Group of Nitrogen. Z. Phys., vol. 86, 1933, pp. 411-412.

Courtoy, C.P.: Infrared Spectrum at High Dispersion and Molecular Constants. Ann. Soc. Sci., (Bruxelles), vol. 73, 1959, pp. 5-230.

Courtoy, C.P.: Vibrational-Rotational Spectra of Simple Diatomic or Polyatomic Molecules with a Long Absorption Path. Canadian J. Phys., vol. 35, 1957, pp. 608-648.

Cowen, M.; and Gordy, W.: Precision Measurements of Millimeter and Sub-millimeter Wave Spectra: DCl, DBr, and DI. Phys. Rev., vol. 111, 1958, pp. 209-211.

Crane-Robinson, C.; and Thompson, H.W.: Pressure Broadening Studies in Vibration-Rotation Bands. III, Experimental Methods for Determining Line Widths, IV, Optical Collision Diameters for Foreign Gas Broadening of CO and DCl Bands. Proc. Roy. Soc., (London), vol. 272, 1962, pp. 441-466.

Crawford, M.F.; Welsh, H.L.; and Locke, J.L.: Infrared Absorption of Oxygen and Nitrogen Induced by Intermolecular Forces. Phys. Rev., vol. 75, 1949, p. 1607.

Csavinszky, P.: Comments on the F-Factor Approximation for HF ($^1\Sigma$). Molec. Phys., vol. 28, 1974, pp. 487-852.

Czerny, M.: The Rotation Spectra of the Hydrogen Halides. Z. Phys., vol. 44, 1927, pp. 235-255.

Dalby, F.W.; and Nielson, H.H.: Infrared Spectrum of Water Vapour. Part I, The 6.26µ Region. J. Chem. Phys., vol. 25, 1956, pp. 934-940.

Damany-Astoin, N.; Sanson, L.; and Bonnelle, M.C.: On the Absorption Spectrum of Carbonic Anhydride in the Extreme Ultraviolet. C. R. Acad. Sci. (Paris), vol. 250, 1960, pp. 1824-1826.

De Leluw, F.H.; and Dymanus, A.: Magnetic Properties and Molecular Quadrupole Moment of HF and HCl by Molecular Beam Electric Resonance Spectroscopy. J. Molec. Spectros., vol. 48, 1973, pp. 427-445.

Debeler, V.H.; Walker, J.A.; and Rosenstock, H.M.: Mass Spectrometric Study of Photoion-ization. $\underline{V}$ Water and Ammonia. J. Res. (NBS), vol. 70, 1966, pp. 459-463.

De Lucia, F.C.; Helminger, P.; and Kirchhoff, W.H.: Microwave Spectra of Molecules of Astrophysical Interest, $\underline{V}$ Water Vapor, J. Phy. Chem. Ref. Data, vol. 3, 1974, pp. 211-219.

De Lucia, F.C.; Helminger, P.; Gordy, W.; Morgan, H.W.; and Staats, P.A.: Millimeter and Submillimeter Wavelength Spectrum and Molecular Constants of T_2O. Phys. Rev., vol. 8, 1973, pp. 2785-2791.

De More, W.B.; and Raper, O.: Hartley Band Extinction Coefficients of Ozone in the Gas Phase and in Liquid Nitrogen, Carbon Monoxide, and Argon. J. Chem. Phys., vol. 68, 1964, pp. 412-414.

Dennison, D.M.: Rotation of Molecules. Phys. Rev., vol. 28, 1926, pp. 318-333.

Dennison, D.M.: The Molecular Structure and Infrared Spectrum of Methane. Astrophys. J., vol. 62, 1925, pp. 84-103.

Dennison, D.M.: Vibrational Levels of Linear Symmetrical Triatomic Molecules. Phys. Rev., vol. 41, 1932, pp. 306-312.

Deutsch, T.F.: Laser Emission From HF Rotational Transitions. Appl. Phys. Letters, vol. 11 11, 1967, pp. 18-20.

Deutsch, T.F.: Molecular Laser Action in Hydrogen and Deuterium Halides. Appl. Phys. Letters, vol. 10, 1967, pp. 236-246.

Deutsch, T.F.: New Infrared Laser Transitions in HCl, HBr, DCl and DBr. IEEE. J. Quant. Electronics, vol. 3, 1967, pp. 419-421.

Dianov-Klokov, V.I.: Absorption Spectrum of Oxygen at Pressures From 2 to 35 atm. in the Region From 12600 to 3600Å. Opt. and Spectro., vol. 16, 1964, pp. 224-227.

Dianov-Klokov, V.I.: On the Bands of the $(O_2)_2$ Complex in the Near Infrared Absorption Spectrum of the Atmosphere. Opt. and Spectro., vol. 17, 1964, pp. 67-76.

Dianov-Klokov, V.I.: Shape of the Absorption Bands in Condensed Oxygen (6300-4773Å). Opt. and Spectro., vol. 13, 1962, pp. 109-112.

Dickenson, R.G.; Dillon, R.T.; and Rasetti, F.: Raman Spectra of Polyatomic Gases. Phys. Rev., vol. 34, 1929, pp. 582-589.

Dieke, G.H.; and Hopfield, J.J.: The Structure of the Ultraviolet Spectrum of the Hydrogen Molecule. Phys. Rev., vol. 30, 1927, pp. 400-417.

Ditchburn, R.W.: Absorption Cross Sections in the Vacuum Ultraviolet, III Methane. Proc. Roy. Soc. (London), vol. 229, 1955, pp. 44-62.

Dixon, J.K.: Ultraviolet Absorption Bands of Ammonia. Phys. Rev., vol. 43, 1933, pp. 711-715.

Dixon, R.N.: The Flame Bands of Carbon Monoxide. Proc. Roy. Soc., (London), vol. 275, 1963, pp. 431-446.

Douglas, A.E.: Electronically Excited States of Ammonia. Discuss. Faraday Soc., 1963, pp. 158-174.

Douglas, A.E.; and Hollas, J.M.: The 1600Å Band System of Ammonia. Canadian J. Phys., vol. 39, 1961, pp. 479-501.

Douglas, A.E.; and Moller, C.K.: The Near Infrared Spectrum and the Internuclear Distances of Nitrous Oxide. J. Chem. Phys., vol. 22, 1954, pp. 275-279.

Dowling, A.J.; Silverman, S.; Benedict, W.S.; and Quinn, J.W.: A Study of Line Shape of CO Infrared Emission Lines. J. Res. (NBS), vol. 75, 1971, pp. 469-479.

Dowling, J.M.: Comparison of Near and Far Infrared Spectral Data for the Water Molecule. J. Molec. Spectrosc., vol. 37, 1971, pp. 272-279.

Draegert, D.A.; and Williams, D.: Collisional Broadening of CO Absorption Lines by Foreign Gases. J. Opt. Soc. America, vol. 58, 1968, pp. 1399-1403.

Duchesne, J.; and Rosen, B.: Contribution to the Study of Electronic Spectra of Bent Triatomic Molecules. J. Chem Phys., vol. 15, 1947, pp. 631-644.

Duncan, A.B.F.: The Ultraviolet Absorption Spectrum of Ammonia. Phys. Rev., vol. 47, 1935, pp. 822-827.

Duncan, A.B.F.: The Ultraviolet Absorption Spectrum of Ammonia. Phys. Rev., vol. 50, 1936, pp. 700-704.

Duncan, A.B.F.: The Far Ultraviolet Absorption Spectrum of N_2O. J. Chem. Phys., vol. 4, 1936, pp. 638-641.

Duncan, A.B.F.; and Harrison, G.R.: The Ultraviolet Spectrum of Ammonia II, The Rotational Structure of Some Bands in the Schumann Region. Phys. Rev., vol. 49, 1936, pp. 211-214.

Duncan, A.B.F.; and Howe, J.P.: The Ultraviolet Absorption of Methane. J. Chem. Phys., vol. 2, 1934, pp. 851-852.

Dutta, A.K.: Absorption Spectrum of Nitrous Oxide and Heat of Dissociation of Nitrogen. Proc. Roy. Soc., (London), vol. 138, 1932, pp. 84-91.

Dyke, T.R.; and Muenter, J.S.: Microwave Spectrum and Structure of Hydrogen Bonded Water Dimer. J. Chem. Phys., vol. 60, 1974, pp. 2929-2930.

Eaton, D.R.: Infrared Temperature and Line Strength Measurements of Carbon Monoxide Excited in a Radio-Frequency Discharge. Canadian J. Phys., vol. 38, 1960, pp. 390-398.

Eaton, D.R.; and Thompson, H.W.: Pressure Broadening Studies in Vibration-Rotation Bands. 1. The Determination of Linewidths. 2. The Effective Collision Diameters. Proc. Roy. Soc., (London), vol. 251, 1959, pp. 458-485.

Eberhardt, W.H.: On the Structure of Ozone. J. Chem. Phys., vol. 14, 1946, p. 641.

Eberhardt, W.H.; and Shand, W.Jr.: On the Ultraviolet Absorption Spectrum of Ozone. J. Chem. Phys., vol. 14, 1946, pp. 525-530.

Edwards, D.K.: Absorption by Infrared Bands of Carbon Dioxide Gas at Elevated Pressures and Temperatures. J. Opt. Soc. America, vol. 50, 1960, pp. 617-632.

Edwards, D.K.: Absorption of Radiation by Carbon Monoxide Gas According to the Exponential Wide-Band Model. Appl. Opt., vol. 4, 1964, pp. 1352-1353.

Eldridge, R.G.: Water Vapor Absorption of Visible and Near IR Radiation. Appl. Opt., vol. 6, 1967, pp. 709-713.

Ernst, K.; Osgood, R.M.; and Javan, A.: Measurement of the Vibration-Vibrational Exchange Time (v=2) For DF Gas. Chem. Phys. Letters, vol. 23, 1973, pp. 553-556.

Farreng, R.; and Dupre-Maquaire, J.: Vibrational Luminescence of N_2O Excited by DC Discharge. J. Molec. Spectrosc., vol. 49, 1974, pp. 268-279.

Farreng, R.; Gaultier, D.; and Rossetti, C.: Vibrational Luminescence of N_2O Excited by DC Discharge. J. Molec. Spectrosc., vol. 49, 1974, pp. 280-288.

Fink, U.; Wiggins, T.A.; and Rank, D.H.: Frequency and Intensity Measurements on the Quadrupole Spectrum of Molecular Hydrogen. J. Molec. Spectros., vol. 18, 1965, pp. 384-395.

Fischer-Hjalmars, I.: The Electronic Structure of the Ozone Molecule. Arkiv for Fysik., vol. 11, 1957, pp. 529-565.

Fishburne, E.S.; and Rao, K.N.: Vibration Rotation Bands of HF. J. Molec. Spectrosc., vol. 19, 1966, pp. 290-293.

Flaud, J.M.; and Camy-Peyret, C.: The Interacting States (020), (100), and (001) of H_2O. J. Molec. Spectrosc., vol. 51, 1974, pp. 142-150.

Foltz, J.V.; and Rank, D.H.: Intensity of the 4-0 Quadrupole Band of Molecular Hydrogen. Astrophys. J., vol. 138, 1963, pp. 1319-1321.

Fowler, A.; and Strutt, R.J.: Absorption Bands of Atmospheric Ozone in Spectra of Sun and Stars. Proc. Roy. Soc., (London), vol. 93, 1917, pp. 577-586.

Fraley, P.E.; Brim, W.W.; and Rao, K.N.: Vibration-Rotation Bands of $N_2^{14}O^{16}$ at 4.5μ. J. Molec. Spectrosc., vol. 9, 1962, pp. 487-493.

Fraley, P.E.; Rao, K.N.; and Jones, L.H.: High Resolution Infrared Spectra of Water Vapor, ν_1 and ν_3 Bands of $H_2^{18}O$ and $H_2^{16}O$. J. Molec. Spectrosc., vol. 29, 1969, pp. 312-364.

France, W.L.; and Dickey, F.P.: Fine Structure of the 2.7μ CO_2 Rotation-Vibration Band. J. Chem. Phys., vol. 23, 1955, pp. 471-474.

Freed, C.; and Ross, A.H.M.: Determination of Laser Line Frequencies and Vibrational-Rotational Constants of the $^{12}C^{18}O_2$, $^{13}C^{16}O_2$, and $^{13}C^{18}O_2$, etc., J. Molec. Spectrosc. vol. 19, 1974, pp. 439-453.

292

Gaultier, D.: Infrared Emission of CO and OCS in $CS_2 + O_2$ Flames. C.R. Acad. Sci. (Paris) vol. 274, 1972, pp. 485-487.

Gilmore, F.R.: Potential Energy Curves for N_2, NO, O_2, and Corresponding Ions. J. Quant. Spectrosc. Rad. Trans., vol. 5, 1965, pp. 369-389.

Gilmore, F. R.: The Equilibrium Thermodynamical Properties of High Temperature Air. DASA Rept. 1971-1, Lockheed Research Labs., Palo Alto, CA, vol. I, 1967.

Gordon, H.R.; and McCubbin, T.K.: The 2.8 Micron Bands of CO_2. J. Molec. Spectrosc., vol. 19, 1966, pp. 137-154.

Gordon, H.R.; and McCubbin, T.K.: The 15-Micron Bands of $C^{12}O_2^{16}$. J. Molec. Spectrosc., vol. 18, 1965, pp. 73-82.

Gordon, H.R.; and McCubbin, T.K.: The $02^20 - 01^10$ Band of $^{14}N_2^{16}O$. J. Opt. Soc. America, vol. 54, 1964, p. 956.

Gott, J.R., III; and Potter, A.E., Jr.: Lunar Atomic Hydrogen and its Possible Detection by Scattered Lyman-α Radiation. ICARUS, vol. 13, 1970, pp. 202-206.

Gray, C.G.: Calculation of the Pressure Broadening of HCl and DCl Infrared and Raman Lines. J. Chem. Phys., vol. 61, 1974, pp. 418-421.

Gray, L.D.; and Schorn, R.A.: High Dispersion Spectroscopic Studies of Venus I. The Carbon Dioxide Bands Near 1 Micron. ICARUS, vol. 8, 1968, pp. 409-422.

Griggs, J.L.; Rao. K.N.; Jones, L.H.; and Potter, R.M.: Vibration-Rotation Bands of the $15N_2^{18}O$. Determination of Precise Values fo Internuclear Distances. J. Molec. Spectrosc., vol. 25, 1968, pp. 34-61.

Griggs, M.: Absorption Coefficients of Ozone in the Ultraviolet and Visible Regions. J. Chem. Phys., vol. 49, 1968, pp. 857-859.

Grosso, R.P.; and McCubbin, T.K., Jr.: The $(\nu_1 - 2\nu_2)$ Fermi Diads of $N_2^{14}O^{16}$, $N^{15}n^{14}O^{16}$, and $N_2^{15}O^{16}$. J. Molec. Spectrosc., vol. 13, 1964, pp. 240-255.

Gryvnak, D.A.; and Shaw, J.H.: Study of the Total Absorption Near 4.7 Microns by Two Samples of CO as Their Total Pressure and CO Concentrations Were Independently Varied.

J. Opt. Soc. America, vol. 52, 1962, pp. 539-542.

Garing, J.S.; Nielsen, H.H.; and Rao, K.N.: The Low Frequency Vibration Rotation Bands of the Ammonia Molecule. J. Molec. Spectrosc., vol. 3, 1959, pp. 496-527.

Haddad, G.N.; Lokan, K.H.; Farmer, A.J.D.; and Carver, J.H.: An Experimental Determination of the Oscillator Strengths for Some Transitions in the Lyman Bands of Molecular Hydrogen. Tech. Rept. AF-AFOSR-1131-66.

Hale, G.M.; and Querry, M.R.: Optical Constants of Water in the 200-nm to 200µm Wavelength Region. Appl. Optics. Vol. 12, 1973, pp. 555-563.

Hall, R.T.; and Dowling, J.M.: Pure Rotational Spectrum of Water Vapor. J. Chem. Phys., vol. 47, 1967, pp. 2454-2461.

Hall, R.T.; and Dowling, J.M.: Pure Rotational Spectrum of Water Vapor From 108 to 40µm. J. Chem. Phys., vol. 52, 1970, pp. 1161-1165.

Halmann, M.; and Laulicht, I.: Isotope Effects on Vibrational Transition Probabilities. The Schumann-Runge Absorption Bands f $^{16}O_2$ and $^{18}O_2$. J. Chem. Phys., vol. 42, 1965, pp. 137-139.

Hancock, J.K.; and Green, W.H.: Vibrational Deactivation Rates of HF(v=1) By CH_4, C_2H_6, C_3H_8, C_4H_{10}, and ClF_3. J. Chem. Phys., vol. 59, 1973, pp. 6350-6357.

Hansler, R.L.; and Oetjen, R.A.: The Infrared Spectra of HCl, DCl HBr and NH_3 in the Region From 40 to 140µ. J. Chem. Phys., vol. 21, 1953, pp. 1340-1343.

Hearn, A.G.: The Absorption of Ozone in the Ultraviolet and Visible Regions of the Spectrum. Proc. Phys. Soc., (London), vol. 78, 1961, pp. 932-940.

Helminger, P.; DeLucia, F.C.; and Gordy, W.: Extension of Microwave Absorption Spectroscopy to .37 mm Wavelengths. Phys. Rev. Letters, vol. 25, 1970, pp. 1397-1399.

Helminger, P.; DeLucia, F.C.; Gordy, W.; Staats, P.A.; and Morgan, H.W.: Millimeter and Submillimeter Wavelengths Spectra and Molecular Constants of HTO and DTO. Phys. Rev., vol. 10, 1974, pp. 1072-1081.

Henning, H.J.: Absorption Spectra in the Region 600-900Å. Ann. Phys., vol. 13, 1932,

pp. 599-620.

Henry, L.; Husson, N.; Andin, R.; and Valentin, V.: Infrared Spectrum of Methane From 2884 to 3141 cm^{-1}. J. Molec. Spectrosc., vol. 36, 1970, pp. 511-520.

Herbelin, J.M.; and Emanuel, G.: Einstein Coefficients for Diatomic Molecules. J. Chem. Phys., vol. 60, 1974, pp. 689-696.

Herget, W.F.; Deeds, W.E.; Gailar, N.M.; Lovell, R.J.; and Nielsen, A.H.: Infrared Spectrum of Hydrogen Fluoride: Line Positions and Line Shapes. Part II Treatment of Data and Results. J. Opt. Soc. America, vol. 52, 1962, pp. 1113-1119.

Herget, W.F.; and Muirhead, J.S.: Infrared Spectral Absorption Coefficients for Water Vapor. J. Opt. Soc. America, vol. 60,,1970, pp. 180-183.

Herzberg, G.: On the High Pressure Bands of Carbon and the Formation of C_2 Molecules. Phys. Rev., vol. 70, 1946, pp. 762-764.

Herzberg, G.; and Herzberg, L.: Rotation-Vibration Spectra of Diatomic and Simple Polyatomic Molecules with Long Absorbing Paths VI - The Spectrum of Nitrous Oxide (N_2O) below 1.2μ. J. Chem. Phys., vol. 18, 1950, pp. 155-161.

Herzberg, G.; and Herzberg, L.: Rotation-Vibration Spectra of Diatomic and Simple Polyatomic Molecules with Long Absorbing Paths. XI - The Spectrum of Carbon Dioxide below 1.25μ. J. Opt. Soc. America, vol. 43, 1953, pp. 1037-1044.

Herzberg, G.; and Howe, L.L.: The Lyman Bands of Molecular Hydrogen. Canadian J. Phys., vol. 37, 1959, pp. 636-659.

Herzberg, G.; Hugo, T.J.; Tilford, S.G.; and Simmons, J.D.: Rotational Analysis of the Forbidden d $^3\Delta_1 \leftarrow X^1\Sigma^+$ Absorption Band of Carbon Monoxide. Canadian J. Phys., vol. 48, 1970, pp. 3004-3015.

Herzberg, G.; and Spinks, J.W.T.: Photography with Large Dispersion of the Second Harmonic Vibration Band of HCl at 1.19μ. Z. Phys., vol. 89, 1934, pp. 474-479.

Herzberg, G.; and Verleger, H.: Two New Bands of CO_2 in the Photographic Infrared. Phys. Rev., vol. 48, 1935, p. 706.

Hese, H; and Rose, A.; Grafin zu Dohna, R. Research in the Schumann-Runge Region. Z. Physik, vol. 81, 1933, pp. 745-763.

Ho, Shau-Yau: Infrared Absorption and Emissions of Superheated Steam. Infrared Phys., vol. 14, 1974, pp. 37-56.

Hochard-Demolliere, L.: Dispersion Measurement in the Fundamental Band of Carbon Monoxide. J. Phys., (France), vol. 27, 1966, pp. 341-344.

Hoover, G.M.; and Williams, D.: Infrared Absorptance of Carbon Monoxide at Low Temperature. J. Opt. Soc. America, vol. 59, 1969, pp. 28-33.

Hopfield, J.J.: New Spectrum of the Hydrogen Molecule. Nature, vol. 125, 1930, p. 927.

Horne, B.H.V.; and Hause, C.D.: Near Infrared Spectrum of DCl. J. Chem Phys., vol. 25, 1956, pp. 56-59.

Howard, J.N.; Burch, D.E.; and Williams, D.: Infrared Transmission of Synthetic Atmospheres. J. Opt. Soc. America, vol. 40, 1956, pp. 183-190.

Howard, J.N.; Burch, D.E.; and Williams, D.: Instrumentation. J. Opt. Soc. America, vol. 46, 1956, pp. 237-241.

Howard, J.N., Burch, D.E.; and Williams, D.; Absorption by Carbon Dioxide. J. Opt. Soc. America, vol. 46, 1956, pp. 334-338.

Howard, J.N.; Burch, D.E.; and Williams, D.: Absorption by Water Vapor. J. Opt. Soc. America, vol. 46, 1956, pp. 334-338.

Howard, J.N.; Burch, D.E.; and Williams, D.: Application of Theoretical Band Models. J. Opt. Soc. America, vol. 46, pp. 334-338.

Hudson, R.D.: Critical Review of Ultraviolet Photoabsorption Cross Sections for Molecules of Astrophysical and Aeronomic Interest. NASA CR-122098, NSRDS-NBS(US)-38, 1971.

Huggins, W.: On a New Group of Lines in the Photographic Spectrum of Sirus. Proc. Roy. Soc., (London), vol. 48, 1890, pp. 216-217.

Hughes, R.H.: The Microwave Spectrum and Structure of Ozone. J. Chem Phys., vol. 21, 1953, pp. 959-960.

Humphrey, G.L.; and Badger, R.M.: The Absorption Spectrum of Ozone in the Visible.
I Examination for Fine Structure. II The Effect of Temperature. J. Chem. Phys., vol. 15,
1947, pp. 794-798.

Hunt, R.H., Toth, R.A., and Plyler, E.K.: High-Resolution Determination of the Widths
of Self-Broadened Lines of Carbon Monoxide. J. Chem. Phys., vol. 49, 1968, pp. 3909-
3912.

Imes, E.S.: Absorption of Some Diatomic Gases in the Near Infrared. Astrophys. J.,
vol. -0, 1919, pp. 251-276.

Inn, E.C.Y.; and Tanaka, Y.: Absorption Coefficients of Ozone in the Ultraviolet and
Visible Regions, J. Opt. Soc. Am., vol. 43, 1953, pp. 870-873.

Inn, E.C.Y.; and Tanaka, Y.: Ozone Absorption Coefficients in the Visible and
Ultraviolet Regions. Ozone Chemistry and Technology, Advances in Chem. series No. 21,
March, 1959, pp. 263-268.

Inn, E.C.Y.; Watanabe, K.; and Zelikoff, M.: Absorption Coefficients of Gases in the
Vacuum Ultraviolet Part III- CO_2. J. Chem. Phys. vol. 21, No. 10, 1953, pp. 1648-1650.

Ittmann, G.P.: Spectrum of Carbon Dioxide. Phys., vol. 13, 1933, pp. 177-188.

Jackson, W.M.; Brackmann, R.T.; and Fite, W.L.: Temperature Dependence of the Dissocia-
tive Ionization of CO_2. Int. J. Mass. Spect. and Ion. Phys. vol. 13, 1974,
pp. 237-250.

Jacques, J.K.; and Barrow, R.F.; The Transition $V^1 \Sigma^+ - X^1 \Sigma^+$ in Hydrogen Chloride.
Proc. Phys. Soc. A. (London) vol. 73, 1959, pp. 538-539.

Jaffe, J.H.; Rosenbery, A.; and Hirchfeld, M.A.; Pressure Induced Shifts of Hydrogen
Fluoride Lines Due to Noble Gases. Tech. Rept. No. L, AFCRL - 65 - 782, June, 1965.

Jen, C.K.: The Paschen-Back Effect in NH_3 and N_2O Microwave Spectra. Phys. Rev., vol. 75
1949, pp. 1319A-B.

Jen, C.K.: The Paschen-Back Effect in NH_3 and N_2O Microwave Spectra. Phys. Rev. vol. 76,
1949, pp. 1494-1501.

Jones, L.H.: Potential Constants of Nitrous Oxide. J. Molec. Spectros., Vol. 34, April, 1970, pp. 108-112.

Jones, L.H.; Brim, W.W.; and Rao, K.N.: ν_3 and ν_1 of the NH_3 Molecule. J. Molec. Spectros., Vol. 11, 1963, pp. 389-410.

Jones, L.H.; and Goldblatt, M.: Infrared Spectrum and Molecular Constants of Gaseous Tritium Flouride. J. Molec. Spectros, Vol. 1, 1957, pp. 43-48.

Jones, L.H.; and Robinson, E.S.: Infrared Spectra and Molecular Constants of Gaseous Tritium Bromide and Tritium Chloride. J. Chem Phys., Vol. 24, No. 6, 1956, pp. 1246-1249.

Jones, R.; and Bell, E.E.; The 2.7μ Bands of Carbon Dioxide. Phys. Rev., Vol. 79, 1950, p. 1004.

Johns, J.W.C.; and Barrow, R.F.: The Ultraviolet Spectra of HF and DF. Proc. Roy. Soc. A. (London) Vol. 251, 1959, pp. 504-518.

Johns, J.W.C.: On the Absorption Spectrum of H_2O and D_2O in the Vacuum Ultra violet. Canad. J. Phys., vol. 41, No. 2, 1963, pp. 209-219.

Johnson, C.M.; Trambarulo, R.; and Gordy, W.: Microwave Spectroscopy in the Region From Two to Three Millimeters Part II. Phys. Rev., vol. 84, 1951, pp. 1178-1180.

Jokowlewa, A.; and Kondratjew, V.: The Structure of the Ultraviolet Absorption Spectrum of Ozone. Soviet Phys., vol. 10, 1936, pp. 106-108.

Jokowlewa, A.; and Kondratjew, V.: Ultraviolet Absorption Spectrum of Ozone and the Structure of O_3 - Molecule. Phys. Z. D. Soviet Union, vol. 1, 1932, pp. 471-486.

Jones, G.; and Gordy, W.: Sub-millimeter-Wave Spectra of HCl and HBr. Phys. Rev., vol. 136, No. 5-A, 1964, pp. A-1229-A1232.

Jones, G.; and Gordy, W.: Extension of Submillimeter Wave Spectroscopy Below a Half Millimeter Wavelength. Phys. Rev.-A., vol. 135, No. 2A, 1964 pp. A 295-A 296.

Jones, J.W.C.; McKellar, A.R.W.; and Weitz, D.: Wavelength Measurements of 13_C 16_O Laser Transitions. J. Molec. Spectros., vol. 51, 1974, pp. 539-545.

Jungen, M.: Rydberg Character and Dissociative Behavior of the $\pi^3\pi*$ Configuration: Carbon Dioxide and Acetylene. Chem. Phys. Letters, Vol. 27, No. 2, 1974, pp. 256-259.

Kaplan, L.D.: The Absorption Spectrum of Carbon Dioxide from 14 to 16 Microns. J. Chem. Phys., vol. 15, 1947, pp. 809-815.

Kaplan, L.D.: Line Intensities and Absorptions for the 15μ Carbon Dioxide Band. J. Chem. Phys., vol. 18, 1950, pp. 186-189.

Kaplan, L.D.; and Eggers, D.F.: Intensity and Line Width of the 15μ CO_2 Band Determined by a Curve-of-Growth Method. J. Chem. Phys., vol. 25, 1956, pp. 876-883.

Kaplan, L.D.; Migeotte, M.V.; and Neven, L.: 9.6 Micron Band of Telluric Ozone and its Rotational Analysis. J. Chem. Phys., vol. 24, 1956, pp. 1183-1186.

Karl, G.; and Poll, J.D.: On the Quadrupole Moment of the Hydrogen Molecule. J. Chem. Phys., vol. 46, 1967, pp. 2944-2950.

Kasper, J.V.V.; and Pimentel, G.C.: HCl Chemical Laser. Phys. Rev. Letters, vol. 14, no. 10, 1965, pp. 352-354.

Katayama, D.H.; Huffman, R.E.; and O'Bryan, C.L.: Absorption and Photoionization Cross Sections for H_2O and D_2O in the Vacuum Ultraviolet. J. Chem. Phys., vol. 59, no. 8, 1973, pp. 4309-4319.

Kirkpatrick, D.E.; and Salant, E.O.: Overtone Absorption Bands of Gaseous HF. Phys. Rev., vol. 48, 1935, pp. 945-948.

Klessinger, M.: Chemical Bond in Hydrogen Fluoride. Chem. Phys. Letters, vol. 2, no. 8, 1968, pp. 562-564.

Knauss, H.P.; and Ballard, S.S.: Rotational Structure of the Schumann-Runge Bands of Oxygen in the Vacuum Region. Phys. Rev., vol. 58, 1935, pp. 796-799.

Korb, C.L.; Hunt, R.H.; and Plyler, E.K.: Measurement of Line Strengths at Low Pressure, Application to the 2-0 Band of CO. J. Chem. Phys., vol. 48, 1968, pp. 4252-4260.

Kostkowski, H.J.; and Base, A.M.: Direct Measurement of Line Intensities and Widths in the First Overtone Band of CO. J. Quant. Spectrosc. Radiat. Trans., vol. 1, 1961, pp. 177-184.

Kostkowski, J.H.; and Kaplan, L.D.: Absolute Intensities of the 721 and 742 cm^{-1} Bands of CO_2. J. Chem. Phys., vol. 26, 1957, pp. 1252-1253.

Krauss, M.; and Neumann, D.: Multi-Configuration Self-Consistent-Field Calculation of the Dissociation Energy and Electronic Structure of Hydrogen Fluoride. Molec. Phys., vol. 27, no. 4, 1974, pp. 917-921.

Krell, J.M.; and Sams, R.L.: Vibration-Rotation Bands of N_2O (4.1 μ region). J. Molec. Spectros. (USA), vol. 51, 1974, pp. 492-507.

Krupenie, P.H.: The Band Spectrum of Carbon Monoxide. NSRDS-NBS-5, July 8, 1966.

Krupenie, P.H.: The Band Spectrum of Carbon Monoxide. Nat. Bur. Stand. Ref. Data Ser., vol. 5, 1966, pp. 87.

Kuipers, G.A.: The Spectrum of Monomeric Hydrogen Fluoride: Line Shapes, Intensities, and Breadths. J. Molec. Spectros. (USA), vol. 2, 1958, pp. 75-98.

Kuipers, G.A.; Smith, D.F.; and Nielsen, A.H.: Infrared Spectrum of Hydrogen Fluoride. J. Chem. Phys., vol. 25, no. 2, 1956, pp. 275-279.

Lagermann, R.T.; Nielsen, A.H.; and Dickey, F.P.: The Infrared Spectrum and Molecular Constants of $C^{12}O^{16}$ and $C^{13}O^{16}$. Phys. Rev., vol. 72, 1947, pp. 284-289.

Lakshmi, K.; Rao, K.N.; and Nielsen, H.H.: Molecular Constants of Nitrous Oxide from Measurements of ν_2 at 17μ. J. Chem. Phys., vol. 24, 1956, pp. 811-813.

Lakshmi, K.; and Shaw, J.H.: Absorption Bands of N_2O Near 4.5μ J. Chem. Phys. vol. 23 1955, pp. 1886-1888.

Laufer, A.H.; and McNesby, J.R.: Deuterium Isotope Effect in V.U.V. Absorption Co-efficient of H_2O and CH_4. Canad. J. Phys., vol. 43, 1965, p. 3487.

Lawrence, G.M.: Lifetimes and Transition Probabilities in CO^+, J. Quant. Spectros. Radiat. Trans. vol. 5, 1965, pp. 359-367.

Lee, P.; and Weissler, G.L.: Absolute Absorption of the H_2 Continuum. Astrophys, J. Vol. 115, 1952, pp. 570-571.

Lefebvre, L.: The Absorption Spectrum of Ozone in the Photographic Infrared Region. Acad. Sci., (Paris) vol. 200, 1935, pp. 1743-1744.

Lefebvre, L.: Supression of Ozone Bands at Low Temperatures. Compt. Rendus., vol. 199, 1934, pp. 456-457.

Leifson, S.W.: Absorption Spectra of Some Gases and Vapors in the Schumann Region. Astrophys. J., vol. 63, 1926, pp. 73-89.

Lempka, H.J.; and Price, W.C.: Ionization Energies of HF and DF. J. Chem. Phys. vol. 48, 1968, pp. 1875-1876.

Lie, G.C.: Study of the Theoretical Dipole Moment Function and Infrared Transition Matrix for the $X^1\Sigma^+$ State of the HF Molecule. J. Chem. Phys., vol. 60, No. 8, 1974, pp. 2991-2996.

Lindholm, E.: Uber das Spectrum von HCl im Photographischen Ultrarot: Ark. Mat. Astro Fys. vol. 29B, No. 15, 1943, pp. 1-3.

Lowder, J.E.: Self-broadened Half-width Measurements in the CO Fundamental. J. Quant. Spectrosc. Radiat. Transfer, vol. 11, 1971, pp. 1647-1657.

Lukirskii, A.P.; Brylov, I.A.; and Zimkina, T.M.: Photoionization Absorption of He, Dr, Xe, and CH_4 and Methylal in the 23.6-250 A Region. Opt. and Spectrosc. Vol. 17, 1964, pp. 234-237.

Lyman, T.: The Absorption of Some Gases for Light of Very Short Wavelengths. Astrophys. J. vol. 27, 1908, pp. 87-105.

MacTaggart, J.W.; and Hunt, J.L.: An Analysis of the Profile of the Pressure-Induced Pure Rotational Spectrum of Hydrogen Gas. Canad. J. Phys., vol. 47, 1969, pp. 65-70.

Madden, R.F.: Study of CO_2 Absorption Spectra Between 15 and 18 Microns. Technical Report, Nonr. 248(01), 1957, John Hopkins University.

Madden, R.P.: A High Resolution Study of Carbon Dioxide Absorption Spectra Between 15-18 Microns. J. Chem. Phys., vol. 35, 1961, pp. 2083-2097.

Maki, A.G.; Plyler, E.K.; and Thibault, R.J.: Absorption Bands of CO_2 From 5.3 to 4.6μ. J. Research (N.B.S.), vol. A67, no. 3, 1963, pp. 219-213.

Mann, D.E.; Thrush, B.A.; Lide, D.R.; Ball, J.J.; and Acquista, N.: Spectroscopy of Flames I. Hydrogen Fluorine Flame and the Vibration-Rotation Emission Spectrum of HF. J. Chem. Phys., vol. 34, no. 2, 1961, pp. 420-431.

Mantz, A.W.; Nichols, E.R.; Alpert, B.D.; and Rao, K.N.: CO Laser Spectra Studied With a 10-Meter Vacuum Infrared Grating Spectrograph. J. Molec. Spectros., vol. 35, 1970, pp. 325-328.

Mantz, A.W.; Rao, K.N.; Jones, L.H.; and Potter, R.M.: Vibration-Rotation Bands of $^{15}N_2{}^{18}O$. Effects of Fermi Resonance and l-type Doubling. J. Molec. Spectros. vol. 30, 1969, pp. 513-530.

Mantz, A.W.; Watson, J.K.G.; Rao, N.K.; Albritton, D.L.; Scheltekopf, A.L.; and Zare, R.N.: Rydberg-Klein-Rees Potential for the $X^1\Sigma^+$ State of the CO Molecule. J. Mol. Spectrosc., vol. 39, 1971, pp. 180-184.

Margolis, J.S.; and Fox, K.: Infrared Absorption Spectrum of CH_4 at 9050 cm^{-1}. J. Chem. Phys., vol. 49, 1968, pp. 2451-2452.

Martin, P.E.; and Barker, E.F.: Infrared Absorption Spectrum of Carbon Dioxide. Phys. Rev., vol. 41, 1932, pp. 291-303.

Mason, A.A.; and Nielsen, A.H.: Spectrometer for the Far Infrared. Bull. Am. Phys. Soc., vol. 7, 1962, pp. 575-576.

Mason, A.A.; and Nielsen, A.H.: Pure Rotational Lines of Hydrogen Fluoride. Bull. Am. Phys. Soc., vol. 8, p. 555.

Mayer, S.W.; Taylor, D.; and Kwok, M.A.: HF Chemical Lasing at Higher Vibrational Levels. Appl. Phys. Letters, vol. 23, no. 8, 1973, pp. 434-436.

McBride, J.O.P.; and Nicholls, R.W.: The Vibration-Rotation Spectrum of Ammonia Gas I. J. Phys. B., vol. 5, 1972, pp. 408-417.

McCaa, D.J.; and Shaw, J.H.: The Infrared Spectrum of Ozone. J. Mol. Spectros., vol. 25, 1968, pp. 374-396.

McCubbin, T.K.: The Spectra of HCl, NH_3, H_2O from 100 to 700 Microns. J. Chem. Phys., vol. 20, no. 4, 1952, pp. 668-671.

McCubbin, T.K.; and Sinton, W.M.: Recent Investigations in the Far Infrared. J. Opt. Soc. Amer., vol. 40, 1950, pp. 537-539.

McCubbin, T.K., Jr.: The Spectra of HCl, NH_3, H_2O, and H_2S from 100 to 700 Microns. J. Chem. Phys., vol. 20, 1952, pp. 668-671.

McCubbin, T.K., Jr.; Pliva, J.; Pulfrey, R.; Telfair, W.; and Todd, T: The emission Spectrum of $^{12}C^{16}O_2$ From 4.2 to 4.7 Microns. J. Molec. Spectros., vol. 49, 1974, pp. 136-156.

McCulloh, K.E.: Photoionization of Carbon Dioxide. J. Chem. Phys., vol. 59, no. 8, 1973, pp. 4250-4259.

McDowell, R.S.: Determination of Carbon-13 by Infrared Spectrophotometry of Carbon Monoxide. Anal. Chem., vol. 42, 1970, pp. 1192-1193.

McNesby, J.R. and Okabe, H.: "Vacuum Ultraviolet Photochemistry." Advances in Photochemistry, vol. III ed. by W.A. Noyes, Jr., G.S. Hammond and J.N. PHS Wiley Interscience 1964.

Mecke, R.: Neue Absorptions bas den des Methans im nahen Ultra-roten Zeit-scrift fuer Astrophysile. Z.f. Astrophys., vol. 6, 1933, pp. 144-149.

Melcher, D.: Contribution on the Structure of Ozone-Huggins Band. Helv. Phys. Acta., vol. 18, 1945, pp. 72-78.

Mentall, J.E.; Coplan, M.A.; and Kushlis, R.J.: Excitation of CO_2^+ by Electron Impact on CO_2. J. Chem.Phys., vol. 59, no. 7, 1973, pp. 3867-3868.

Meredith, R.E.; and Smith, F.G.: Computation of Electric Dipole Matrix Elements for Hydrogen Fluoride. J. Quant. Spect. Rad. Transf., vol. 13, 1973, pp. 89-114.

Metzger, P.H.; and Cook, G.R.: On the Continuous Absorption, Photoionization and Fluorescence of H_2O, MH_3, CH_4, C_2H_4, C_2H_4 and C_2H_6 in the 600-1000 Å Region. J. Chem. Phys., vol. 44, no. 3, 1964, pp. 642-648.

Meyer, C.F.; and Levin, A.A.: On the Absorption Spectrum of Hydrogen Chloride. Phys. Rev., vol. 34, 1929, pp. 44-52.

Mills, I.M.; and Thompson, H.W.: The Fundamental Vibration Rotation Bands of $C^{13}O^{16}$ and $C^{12}O^{18}$. Trans. Farad. Soc., vol. 49, 1953, pp. 224-227.

Mills, I.M.; Thompson, H.W.; and Williams, R.L.: The Fundamental Vibration - Rotation Band of Hydrogen Chloride. Proc. Roy. Soc. A (London), vol. 218, 1953, pp. 29-43.

Moe, G.; and Duncan, A.B.F.: Intensities of Electronic Transitions of Acetylene in the Vacuum Ultraviolet. J. Amer. Chem. Soc., vol. 74, 1952, pp. 3136-3143.

Morgan, H.D.; and Mentall, J.E.: VUV Dissociative Excitation Cross Sections of H_2O, NH_3 and CH_4 by Electron Impact. J. Chem. Phys., vol. 60, no. 12, 1974, pp. 4734-4739.

Mould, H.M.; Price, W.C., and Wilkinson, G.R.; Infra-red emission from gases excited by a radio-frequency discharge. Spectrochem Acta (G.B.) vol. 16, 1960, pp. 479-492.

Mulliken, R.S.: Electronic Structures of Polyatomic Molecules. VII. Ammonia and Water Type Molecules and their Derivatives. J. Chem. Phys., vol. 3, 1935, pp. 506-514.

Mulliken, R.S.: Low Electronic States of Simple Heteropolar Diatomic Molecules III Hydrogen and Univalent Metal Halides. Phys. Rev., vol. 51, 1937, pp. 310-332.

Myer, J.A.; and Samson, J.A.R.: Vacuum Ultraviolet Absorption Cross Sections of CO, HCl, and ICN between 1050 and 2100Å. J. Chem. Phys., vol. 52, no. 1, 1970, pp. 226-271.

Naegeli, D.W.; and Ultee, C.J.: A cw HCl Chemical Laser. Chem Phys Letters, vol. 6, No. 2, 1970, pp. 121-122.

Nakata, R.S.; Watanabe, K.; and Matsunaga, F.M.: Absorption and Photoionization Coefficients of CO_2 in the Region 580-1670 Å. Science of Light, vol. 14, No. 1, 1965, pp. 54-71.

Namioka, T.: On the Absorption Spectrum in the $1s\sigma\, 3p\Lambda'\Pi cd \leftarrow (1s\sigma)^2\, {}^1\Sigma_g^+$ System of the Hydrogen Molecule. Sci. of Light, (Tokyo), vol. 2, 1953, pp. 73-86.

Naude, S.M.; and Verleger, H.: The Vibration-Rotation Bands of the Hydrogen Halides. HF, $H^{35}Cl$, $H^{37}Cl$, $H^{79}Br$, $H^{81}Br$, and $H^{127}I$. Proc. Phys. Soc. A. (London), vol. 63, 1950, pp. 470-477.

Nelson, R.C.; Benedict, W.S.: Absorption of Water Vapor Between 1.34μ and 1.97μ. Phys. Rev. vol. 74, 1948, pp. 703-704.

Newman, R.: Emission Spectrum of HCl in the Near Infrared. J. Chem. Phys. vol. 20, 1952, pp. 749-750.

Nielsen, A.H.; and Nielsen, H.H.: The Infrared Absorption Bands of Methane. Phys. Rev., vol. 48, 1935, 864-867.

Nielsen, A.H.; and Yao, Y.T.: The Analysis of the Vibration Rotation Band ω_3 for $C^{12}O_2^{16}$ and $C^{13}O_2^{16}$. Phys. Rev., vol. 68, 1945, pp. 173-180.

Nielsen, H.H.: The Near Infrared Spectrum of Water Vapor. Part I, The Perpendicular Bands ν_2 and $2\nu_2$. Phys. Rev. vol. 59, 1961, pp. 565-575.

Nugent, L.; and Duardo, J.: Study to Develop a Technique for Measurement of High Altitude Ozone Parameters. Progress Rept. No. 1, Contract NAS 12-137: (EOS Report 7087-Q-1) August 1, 1966.

Ny Tsi-Ze and Choong Shin-Piaw: Absorption Band of Ozone Between $3050\overset{o}{A}$ and $2150\overset{o}{A}$. Compt. Rend. Vol. 196, 1933, pp. 916-918.

Oberly, R.; Rao, K.N.; Hahn, Y.H.; and McCubbin, T.K. Jr.: Bands of Carbon Dioxide in the Region of 4.3μ. J. Molec. Spectros., vol. 25, 1968, pp. 138-165.

Ogawa, M.; and Cook, G.R.: Absorption Coefficients of O_3 in the Vacuum Ultraviolet Region. J. Chem. Phys, vol. 28, 1958, pp. 173-174.

Ogawa, M.; and Ogawa, S.; Absorption Spectrum of CO in the Hopfield Helium Continuum Region, $600 - 1020\,\overset{o}{A}$. J. Molec. Spectros., vol. 41, 1972, pp. 393-408.

Oppenheim, U.P.; and Goldring, H.: The Strengths of Absorption Lines in the 2-0 Bands of Carbon Monoxide. J. Quant. Spectros. Radiat. Transf., vol. 2, 1962, pp. 293-296.

Palik, E.D.; and Rao, K.N.: Pure Rotational Spectra of CO, NO and N_2O Between 100 and 600 Microns. J. Chem. Phys., vol. 25, 1956, pp. 1174-1176.

Parker, J.V.; and Stephens, R.R.; Pulsed HF Chemical Laser With High Electrical Efficiency. Appl. Phys. Letters, vol. 22, no. 9, 1963, pp. 450-452.

Patch, R.W.; Absorption Coefficients for Hydrogen. J. Quant. Spectros. Rad. Transf., vol. 9, 1969, pp. 63-87.

Patel, C.K.N.: Continuous-Wave Laser Action on Vibrational Rotational Transitions of CO_2. Phys. Rev., vol. 136, no. 5A, 1964, pp A1187 - A1193.

Patty, R.R.; Manring, E.R.; and Gardner, J.A.: Determination of Self-Broadening Coefficients of CO, using CO_2 Laser Radiation at 10.6u. Appl. Opt., vol. 7, 1968, pp. 2246-2251.

Pearson, R.; Sullivan, T.; and Frenkel, L.: Microwave Spectrum and Molecular Parameters for $^{14}N_2$ ^{16}O. J. Molec. Spectros. (USA), vol. 34, 1970, pp. 440-449.

Penner, S.S.; and Varanasi, P.: Spectral Absorption Coefficients in Pure Rotation Spectrum of Water Vapor. J. Quant. Spectros Rad. Transf. vol. 7, 1967, pp. 687-690.

Penner, S.S.; and Weber, D.: Quantitative Infrared Intensity Measurements. I Carbon Monoxide Pressurized with Infrared Inactive Gases. J. Chem. Phys., vol. 19, 1951, pp. 807-816.

Penner, S.S.; and Weber, D.: Quantitative Line-Width Measurements in the Infrared. II Unpressurized Carbon Monoxide. J. Chem. Phys., vol. 19, 1951, pp. 1361-1363.

Pickworth, J.; and Thompson, H.W.: The Fundamental Vibration-Rotation Band of Deuterium Chloride. Proc. Roy. Soc. (London), 1953, pp. 37-43.

Pierce, L.: Note on the Use of Ground-State Rotational Constants in the Determination of Molecular Structures. J. Molec. Spectros, vol. 30, 1959, pp. 575-580.

Pierre, Anthony G. St.: Highly Precise Measurements of the 2-0, 3-1, and 4-2 Bands of Carbon Monoxide. M.S. Thesis: Penn. State University, 1964.

Pliva, J.: Infrared Spectra of Isotopic Nitrous Oxides. J. Molec. Spectros. vol. 12, 1964, pp. 360-386.

Pliva, J.: Some Near Infrared Bands of Nitrous Oxides. J. Molec. Spectros. vol. 25, 1968, pp. 62-76.

Pliva, J.: Molecular Constants of Nitrous Oxide, $^{14}N_2O^{16}$. J. Molec. Spectros, vol. 27, 1968, pp. 461-488.

Plyler, E.K.; Benedict, W.S.; and Silverman, S.: Precise Measurements on the Infrared Spectrum of CO. J. Chem. Phys., vol. 20, 1962, pp. 175-184.

Plyler, E.K.; Blaine, L.R.; and Tidwell, E.D.: Infrared Absorption and Emission Spectra of Carbon Monoxide in the Region from 4 to 6 Microns. J. Res. (N.B.S.), vol. 55, 1955, pp. 183-189.

Plyler, E.K.; Tidwell, E.D.: The Precise Measurement of the Infrared Spectra of Molecules of the Atmosphere. Soc. Roy. Sci. (Liege), vol. 18, pp. 426-449, 1957.

Plyler, E.K. and Thibault, R.J.: Self-Broadening of Carbon Monoxide in the 2ν and 3ν Bands. J. Res. (N.B.S.), vol. 67A, 1963, pp. 229-231.

Pollack, J.B.; and Morrison, D.: Venus: Determination of Atmospheric Parameters From the Microwave Spectrum. ICARUS, vol. 12, 1970, pp. 376-390.

Preston, W.M.: The Origin of Radio Fade-Outs and the Absorption Coefficients of Gases for Light of Wavelength 1215.7Å. Phys. Rev., vol. 57, 1940, pp. 887-894.

Price, W.C.: The Far Ultraviolet Absorption Spectra and Ionization Potentials of H_2O and H_2S. J. Chem. Phys., vol. 4, no. 3, 1936, pp. 147-153.

Price, W.C.: The Absorption Spectra of the Halogen Acids in the Vacuum Ultraviolet. Proc. Phys. Soc. A. (London.), vol. 167, 1938, pp. 216-227.

Price, W.C.; and Simpson, D.M.: The Absorption Spectra of Nitrogen Dioxide, Ozone and Nitrosyl Chloride in the Vacuum Ultraviolet. Trans. Farad. Soc. (England), vol. 37, 1941, pp. 106-113.

Price, W.C.; and Simpson, D.M.: The Absorption Spectra of Carbon Dioxide and Carbon Oxysulphide in the Vacuum Ultraviolet. Proc. Roy. Soc. A (London), vol. 163, 1938, pp. 501-512.

Randall, H.M.; and Imes, E.S.: The Fine Structure of the Near Infrared Absorption Bands of the Gases HCl and HF. Phys. Rev., vol. 15, 1920, pp. 152-155.

Rank, D.H.; Eastman, D.P.; Rao, B.S.; and Wiggins, T.A.: Precise Measurements of Some Infrared Bands of HCl. J. Opt. Soc. Amer., vol. 50, no. 12, 1960, pp. 1275-1279.

Rank, D.H.; Eastman, D.P.; Rao, B.S.; and Wiggins, T.A.: Highly Precise Wavelengths in the Infrared. II. HCN, N_2O, and CO. J. Opt. Soc. Am., vol. 51, 1951, pp. 929-936.

Rank, D.H.; Eastman, D.P.; Rao, B.S.; and Wiggins, T.A.: Rotational and Vibrational Constants of the HCl^{35} and DCl^{35} Molecules. J. Opt. Soc. Amer., vol. 52, no. 1, 1962, pp. 1-7.

Rank, D.H.; Eastman, D.P.; Rao, B.S.; Wiggins, T.A.: Breadths and Shifts of Molecular Band Lines Due to Perturbation by Foreign Gases. J. Mol. Spectrosc., vol. 10, 1963, pp. 34-50.

Rank, D.H.; Guenther, A.H.; Saksena, G.D.; Shearer, J.N.; Wiggens, T.A.: Tertiary Interferometric Wavelength Standards From Measurements on Lines of the 2-0 Band of Carbon Monoxide and Derived Wavelength Standards for Some Lines of the 1-0 Band of Carbon Monoxide. The Velocity of Light Derived From a Band Spectrum Method. IV. J. Opt. Soc. Am., vol. 47, 1957, pp. 686-689.

Rank, D.H.; Rao, B.S.; Slomba, A.F.; Sitaram, P.; and Wiggins, T.A.: Fundamental Band of the Quadrupole Spectrum of the Hydrogen Molecule. Vol. 194, 1962, pp. 1267-1268.

Rank, D.H.; Rao, B.S.; and Wiggins, T.A.: Molecular Constants of HCl. J. Molec. Spectros. Vol. 17, 1965, pp. 122-130.

Rank, D.H.; Skorinko, G.; Eastman, D.P.; and Wiggens, T.A.: Highly Precise Wavelengths in the Infrared. J. Mol. Spectrosc., vol. 4, 1960, pp. 518-533.

Rank, D.H.; St. Pierce, A.G.; and Wiggens, T.A.: Rotational and Vibration Constants of CO. J. Mol. Spectrosc., Vol. 18, 1965, pp. 418-427.

Rank, D.H.; and Wiggins, T.A.: Collision Narrowing of Spectral Lines. H_2 quadrupole Spectrum. J. Chem. Phys., vol. 39, 1963, pp. 1348-1349.

Rao, K.N.: High Resolution Infrared Spectra of Small Polyatomic Molecules. Mem. Soc. Roy. Sci. Liege, (Belgium), 5th Series, Vol. 9, 1964, pp. 39-41.

Rao, K.N.; Brim, W.W.; Hoffman, J.M.; Jones, L.H.; and Mellowell, R.S.: ν_2 and ν_4 Bands of the NT_3 Molecule. J. Molec. Spectros., Vol. 7, 1961, pp. 362-383.

Rathenau, G.: Absorption Spectra of Water Vapor and of Carbon Dioxide Below 2000Å. Zeitschift fur Physik. Vol. 87, 1-2, 1933, pp. 32-56.

Revich, V.E.; and Stankevich, S.A.: The Rotational Spectra of HF and DF Molecules Report No: UDC-535-338-42. Translated from Doklady Akademii Nauk, USSR, Vol. 170, No. 6, 1966, pp. 1376-1379.

Rimpel, G.: Line Strengths in the 4-0 and 5-0 Rotation-Vibration Bands of Hydrogen Fluoride. Z. Naturforsch, (Germany), Vol. 29A, 1974, pp. 588-592.

Roberts, B.: The HCR Vibrational-Rotational Spectrum. J. Chem. Educ., vol. 43, No. 7, 1966, p. 357.

Roh, W.B.; and Rao, K.N.: CO Laser Spectra. J. Molec, Spectros. Vol. 49, 1974, pp. 317-321.

Romand, L.; and Mayence, J.: Spectroscopic Spectre b'absorption de l'oxde azoteaux gazeux dans la region de Schumann. C.R.Acad Sci. (Paris), vol. 228, 1949, pp. 998-1000.

Romand, J.; and Vodar, B.: Absorption Spectrum of Gaseous Hydrochloric Acid in the Schumann Region. Comp. Rend. (Paris) vol. 226, 1948, pp. 238-240.

Rosen, B. et al. Tables internationales de Constantes Selechonees (International Tables of Selected Constants) vol. 17 - Donnees spectroscopignes relatives aux molecules dia-tomiques (Spectroscopic data relative to diatomic molecules. Pergamon Press (Oxford).

Rosenblum, B.; and Nethercot, A.H.: Quadrupole Coupling Constants and Molecular Structure of CO^{17}. J. Chem.Phys., vol. 27, 1957, pp. 828-829.

Rosenblum, B.; Nethercot, A.H.; and Townes, C.H.: Isotopic Mass Ratios, Magnetic Moments and the Sign of Electric Dipole moment in Carbon Monoxide. Phys. Rev., vol. 109, 1958, pp. 400-412.

Rossmann, K.; France, W.L.; Rao, K.N.; and Nielsen, H.H.: Infrared Spectrum and Molecular Constants of Carbon Dioxide. Part II, Levels 10°0 and 02°0, 10°1 and 02°1 Coupled by Fermi Resonance. J. Chem. Phys., vol. 24, 1956, pp. 1007-1008.

Rossmann, K.; Rao, K.N.; Nielsen, H.H.; Infrared Spectrum and Molecular Constants of CO_2. Part I.ν_2 of $C^{12}O_2^{16}$ at 15μ. J. Chem. Phys., vol. 24, No. 1, 1956, pp. 103-105.

Rothschild, W.G.: Pure Rotational Absorption Spectrum of HF Vapor Between 22 and 250μ. J. Opt. Soc. Amer., vol. 54, No. 1, 1964, pp. 20-22.

Rosenthal, J.E.: Vibrations of Tetrahedral Pentatomic Molecules- Part I. Potential Energy, Part II. Kinetic Energy and Normal Frequencies of Vibration. Phys. Rev., vol. 45, 1934, -p. 538-544.

Rosenthal, J.E.: Vibration Frequencies of Symmetrical Pentatomic Molecules. Phys. Rev., vol. 45, 1934, p. 766.

Rao, K.N.: The Infrared CO Bands and Wave-number Standards in the Infrared Region. J. Chem. Phys., vol. 18, 1950, p. 213.

Roux, F.; Effantin, C.; and D'Incan, J.: Absolute Oscillator Strengths of Rotation in 2-0, 3-1, 4-2, 5-3, Transitions of the Vibration-Rotation Spectra of the CO Molecules Deduced From Measurement of Emission Intensities. J. Quant. Spectros. Radiat. Transf., (French), vol. 12, 1972, pp. 97-106.

Rustgi, O.P.: Absorption Cross Sections of Argon and Methane Between 600 and 170Å, J. Opt. Soc. Amer., vol. 54, 1964, pp. 464-466.

Safary, E.; Romand, J.; and Vodar, B.: Ultraviolet Absorption Spectrum of Gaseous Hydrogen Fluoride, J. Chem. Phys., vol. 19, 1951, pp. 379-380.

Sambe, H.; and Felton, R.H.: Calculation of the ionization Potentials of the Ozone and Ammonia by a LCAO-Xα Method. J. Chem. Phys. vo-. 61, 1976, pp. 3862-3863.

Schaeffer, C.; and Thomas, M.: Upper Harmonics in Infrared Absorption Spectra. Zeits f.Physik., vol. 12, 1923, pp. 330-341.

Schoen, R.I.: Absorption, Ionization and Ion Fragmentation Cross Sections of Hydrocarbon Vapors Under V.U.V. Radiation. J. Chem. Phys., vol. 37, 1962, pp. 2032-2040.

Schurin, B.; and Ellis, R.E.: Direct Determination of the Overtone Intensities for CO. Soc. Roy. Sci. (liege.), vol. 9, 1964, p. 53.

Schurin, B.; and Ellis, R.E.: First and Second overtone Intensity Measurements for CO and NO. J. Chem. Phys., vol. 45, 1966, pp. 2528-2532.

Schwartz, E.S.; and Thrush, B.A.: Energies of Vibrational Levels 22 to 33 Carbon Monoxide $X'\Sigma_g^+$. J. Mol. Spectrosc., vol. 32, 1969, pp. 343-346.

Sen Gupta, P.K.: Predissociation of Nitrous Oxide. Nature., vol. 136, 1935, pp. 513-514.

Shau-Yau, H.: Long-path Infrared Spectra of CO_2, NO_2, NO, SO_2, and N_2O observed in a Simulated Atmosphere in Trace Amounts. Infrared Physics., vol. 13, 1963, pp. 83-89.

Shaw, B.M.; and Lovell, R.J.: Foreign-gas Broadening of HF by CO_2. J. Opt. Soc. Amer., vol. 59, No. 12, 1969, pp. 1598-1601.

Shaw, J.H.; and Houghton, J.T.: Total Band Absorptance of CO Near 4.7μ. Appl. Opt., vol. 3, 1964, pp. 773-779.

Shimizu, F.O.; and Shimizu, T.: Infrared Spectrum of the 10μ band of $^{15}NH_3$. J. Molec. Spectros., vol. 36, 1970, pp. 94-109.

Shin, H.K.: Temperature Dependence of the Probability of Vibration-Vibration-Rotation Energy Transfer in HCl (v=2) + HCl (v=o) $\rightleftarrows$ HCl (v=1) + HCl (v=1). J. Chem. Phys., vol. 60, No. 6, 1974, pp. 2305-2309.

Shin, H.K.; and Young, A.W.: Vibrational De-excitation of HF (v=1) in HF + Ar: Importance of Rotational Transitions, J. Chem. Phys., vol. 60, No. 1, 1974, pp. 103-104.

Smith, A.G.; Ring, H.; Smith, W.V.; and Gordy, W.: Nuclear Quadrupole Coupling of Nitrogen in ICN and N_2O. Phys. Rev., vol. 73, 1948, p. 633.

Smith, D.F.: The Overlapping Hydrogen Flouride Monomer-dimer Spectra. J. Molec. Spectros., vol. 3, 1959, pp. 473-485.

Smith, W.D.; Chen, T.T.; and Simons, J.: Theoretical Studies of molecular ions. Vertical ionization potentials of Hydrogen Flouride. J. Chem. Phys., vol. 61, No. 7, 1974, pp. 2670-2674.

Smyth, H.D.; and Mueller, D.W.: The Ionization of Water Vapor by Electron Impact. Phys. Rev., vol. 43, 1933, pp. 116-120.

Snider, D.C.; and Shaw, J.H.: Upper State Rotational Constants for the $(\nu_1 + \nu_2 + \nu_3)$ Combination Band of Ozone. J. Molec. Spectrosc., vol. 44, 1972, pp. 400-402.

Spanbauer, R.M.; Rao, K.M.; and Jones, L.H.: Vibration Rotation Bands of the DF Molecule. J. Molec. Spectros., vol. 16, 1965, pp. 100-102.

Spencer, D.J.: Atmospheric Gas Absorption at DF Laser Wavelengths. Aerospace Corp. Rept. No. TR-0074 (4240-10) -7, January, 1974.

Sponer, H.; and Bonner, L.G.: Continuous Absorptions of N_2O. J. Chem Phys., vol. 8, 1940, pp. 33-37.

Stafford, F.E.; Holt, C.W.; and Paulson, G.L.: Vibration Rotation Spectrum of HCl, a Physical Chemistry Experiment. J. Chem. Educ., vol. 40, 1963, pp. 245-249.

Stamper, J.G.: The Vacuum Ultraviolet Spectrum of DCl. Canad. J. Phys., vol. 40, 1962, pp. 1274-1275.

Strilchuk, A.R.; and Offenberger, A.A.: High Temperature Absorption in CO_2 at 10.6 µm. Appl. Opt., vol. 13, No. 11, 1974, pp. 2643-2646.

Strong, J.: Pure Rotation Spectrum of the HCl Flame. Phys. Rev., vol. 45, 1934, pp. 877-882.

Suchard, S.N.: Lasing From the Upper Vibrational Levels of a Flash-initiated H_2-F_2 Laser. Aerospace Rept. TR-0074 (4531)-1 September, 1973.

312

Suchard, S.N.: Spectroscopic Constants for selected heteronuclear diatomic molecules, vols. I, II, and III. Aerospace Corporation. El Segundo, California. - March 1974.

Sullivan, J.O.; and Holland, A.C.: A Congeries of Absorption Cross sections for Wavelengths Less Than 3000Å. NASA - CR - 371, January 1966.

Sun, H.; and Weissler, G.L.: Absorption Cross Sections of Methane and Ammonia in the Vacuum Ultraviolet. J. Chem. Phys., vol. 23, 1955, pp. 1160-1164.

Sun, H. and Weissler, G.L.: Absorption Cross Sections of CO_2 and CO in the Vacuum Ultraviolet. J. Chem. Phys., vol. 23, 1955, pp. 1625-1628.

Sverdlov, B.A.; and Furashov, N.I.: Study of Some Absorption Lines of the Water Vapor Rotational Spectrum in the 100-600μm region. Optics and Spectrosc., vol. 36, No. 5, 1974, pp. 503-506.

Talley, R.M.; Kaylor, H.M.; and Nielson, A.H.: The Infrared Spectrum and Molecular Constants of HF and DF. Phys. Rev., vol. 77, No. 4, 1950, pp. 529-534.

Tanaka, Y.; Inn, E.C.Y.; and Watanabe, K.: Absorption Coefficients of Gases in the Vacuum Ultraviolet. Part IV. J. Chem. Phys., Vol. 21, 1953, pp. 1651-1653.

Tanaka, Y.; Jursa, A.S.; and Le Blanc, E.J.: Higher Ionization Potentials of Linear Triatomic Molecules I. CO_2. J. Chem. Phys., vol. 32, No. 4, 1960, pp. 1199-1205.

Tanaka, Y.; Jursa, A.S.; and LeBlanc, F.J.: Higher ionization Potentials of linear Triatomic Molecules II CS_2, COS, and N_2O, J. Chem. Phys., vol. 32, No. 4, 1960, pp. 1205-1214.

Tanaka, Y.; Jursa, A.S.; and LeBlanc, F.J.: Higher ionization Potentials of Linear Triatomic Molecules CO_2, CS_2, COS, N_2O. J. Chem. Phys., vol. 28, 1958, pp. 350-351.

Tanaka, T.; and Morino, Y.: Band Origin of the ν_2 Fundamental of Ozone. J. Molec. Spectros., vol. 33, 1970, pp. 552-553.

Tanaka, Y.; and Ogawa, M.: Rydberg Absorption Series of CO_2 Converging to the $^2\pi_u$ State of CO_2^+. Canada. J. Phys., vol. 40, 1962, pp. 879-886.

Tannenbaum, E.; Coffin, E.M.; and Harrison, A.J.: The Far Ultraviolet Absorption Spectra of Simple Alkyl Amines. J. Chem. Phys. vol. 21, 1953, pp. 311-318.

Tejwani, G.D.T.: Half-width Computations for Air Broadened CO Lines. J. Quant. Spectros. Radiat. Transf., Vol. 12, 1971, pp. 123-128.

Tetenbaum, S.J.: Six-millimeter Spectra of OCS and N_2O. Phys. Rev., vol. 88, 1952, pp. 772-774.

Thompson, B.A.; Harteck, P.; and Reeves, R.R. Jr.: Ultraviolet Absorption Coefficients of CO_2, CO, O_2, H_2O, N_2O, NH_3, NO, SO_2, and CH_4 Between 1850 and 4000Å. J. Geophys. Res., vol. 68, 1963, pp. 6431-6436.

Thompson, H.W.; and Williams, R.L.: Vibration Bands and Molecular Rotational Constants of Nitrous Oxides. Proc. Roy. Soc. A, (London), vol. 220, 1953, pp. 435-445.

Thompson, H.W.; and Williams, R.L.: Vibration - Rotation Bands of Nitrous Oxide. Proc. Roy. Soc. A, (London), vol. 208, 1951, pp. 326-331.

Thorndike, A.M.: The Experimental Determination of the Intensities of Infrared Absorption Bands. III CO_2, CH_4, and C_2H_6. J. Chem. Phys., vol. 15, 1947, pp. 868-874.

Tidwell, E.D.; Plyler, E.K.; and Benedict, W.S.: Vibration - Rotation Bands of N_2O. J. Opt. Soc. Amer., vol. 50, No. 12, 1960, pp. 1243-1263.

Tilford, S.G., Ginter, M.L.; and Vanderslice, J.T.: Electronic Spectra and Structure of the Hydrogen Halides: The $b^3\Pi_c$ and $c^1\Pi$ States of HCl and DCl. J. Molec. Spectros., vol. 33, 1970, pp. 505-519.

Tilford, S.G.; and Simmons, J.D.: Atlas of the Observed Absorption Spectrum of Carbon Monoxide Between 1060Å and 1900Å. J. Phys. Chem. Ref. Data., vol. 1, No. 1, 1972, pp. 147-188.

Toth, R.A.: Line Strengths of N_2O in the 2.9 Micron Region. J. Molec. Spectros., vol. 40, 1971, pp. 588-604.

Toth, R.A.: Wavenumbers, Strengths and Self-broadened Widths of CO_2 at 3μm. J. Molec. Spectros., vol. 53, 1974, pp. 1-14.

Toth, R.A.; Hunt, R.H.; and Plyler, E.K.: Line Intensities in the 3-0 Band of CO and Dipole Moment Matrix Elements for the CO Molecule. J. Molec. Spectros., vol. 32, 1969 pp. 85-96.

Townes, C.H.; Shulman, R.G.; and Dailey, B.P.: Dipole Moments From Microwave Spectra. Phys. Rev., vol. 76, 1949, p. 472.

Trajmer, S.; and McCaa, D.J.: The $(\nu_1+\nu_3)$ Combination Band of Ozone. J. Molec. Spectros., vol. 14, 1964, pp. 244-249.

Trambarulo, R.; Ghosh, S.N.; Burrus, C.A.; and Gordy, W.: Electric Dipole Moments of Several Molecules From the Stark Effect. Phys. Rev., vol. 21, 1953, pp. 308-310.

Trambarulo, R.; Ghosh, S.N.; Burrus, C.A.Jr.; and Gordy, W.: The Molecular Structure Dipole Moment and g-factor of Ozone From its Microwave Spectrum. J. Chem. Phys., Vol. 21, 1953, pp. 851-855.

Val, J.L.: Rotational Constants of CO_2 derived From Infrared Luminescence Spectra. J. Molec. Spectros, vol. 40, 1971, pp. 367-371.

Varanasi, P.: Linewidths Measurements on CO in an Atmosphere of CO_2. J. Quant. Spectros. Radiat. Transf., vol. 11, 1971, pp. 249-253.

Varanasi, P.; and Tejwani, G.D.T.: Half-width Calculations for CO Lines Broadened by CO_2. J. Quant. Spectros. Radiat. Transf., vol. 11, 1971, pp. 255-261.

Varanasi, P.; Sarangi, S.K.; and Tejwani, G.D.T.: Line Shape Parameters for HCl and HF in a CO_2 Atmosphere. J. Quant. Spectros. Radiat. Transf., vol. 12, 1972, pp. 857-872.

Vanderwerf, D.P.; and Shaw, J.H.: Temperature Dependence of the Total Absorptance of Bands of CO and CH_4. Appl. Opt., vol. 4, 1965, pp. 209-214

Vassy, E.: On Certain Properties of the Ozone and Their Geophysical Consequences. Ann. de Phys., vol. 8, 1937, pp. 679-775.

Vigroux, E.: Contribution to the Experimental Study of the Absorption of Ozone. Ann. de Phys., vol. 8, 1953, pp. 709-762.

Vigroux, E.; Migeotte, M.; Neven, L.; and Swensson, J.: An Atlas of Nitrous Oxide, Methane and Ozone Infrared Absorption Bands. Part II Measures and Identifications. Tech. Final Rept. AF 61 (514) -432, Inst. of Astrophys., University of Leige.

Vincent-Geisse, J.: Intensity Measurements and the Width of Absorption Lines in the Infrared. Application to Carbon Monoxide. J. Phys. Radium, vol. 15, 1954, pp. 539-540.

Wainfan, N.; Walker, W.C.; and Weissler, G.L.: Photoionization Efficiencies and Cross Sections in O_2, N_2, CO_2, A, H_2O, H_2, and CH_4. Phys. Rev., vol. 99, 1955, pp. 542-549.

Walker, W.C.; and Weissler, G.L.: Photoionization Efficiencies and Cross Sections in NH_3. J. Chem. Phys., vol. 23, No. 8, 1955, pp. 1540-1541.

Walsh, A.D.; and Warsop, P.A.: The Ultraviolet Absorption Spectrum of Ammonia. Trans Farad. Soc., (England), vol. 57, 1961, pp. 345-358.

Walsh, T.E.: Infrared Absorptance of Ammonia - 20 to 35 microns. J. Opt. Soc. Am., vol. 59, 1969, pp. 261-267.

Walshaw, C.D.; Dobson, G.M.B.; and MacGarry, B.M.F.: Absorption Coefficients of Ozone for Use in the Determination of Atmospheric Ozone. Quart. J. Royal Met. Soc., vol. 97, 1971, pp. 75-82.

Wang, V.K.; and Overend, J.: The Anderson Intramolecular Potential - Energy Function - I Application to SO_2, NO_2, and O_3. Spectrochimica Acta., vol. 30A, 1974, pp. 237-247.

Watanabe, K.: Photoionization and Total Absorption Cross Section of Gases (NH_3 and NO). J. Chem. Phys., vol. 22, No. 9, 1954, pp. 1564-1570.

Watanabe, K.; and Jursa, A.S.: Absorption and Photoionization Cross Sections of H_2O and H_2S. J. Chem. Phys., vol. 41, No. 6, 1964, pp. 1650-1653.

Watanabe, K.; and Mottl, J.R.: Ionization Potentials of Ammonia and Some Amines. J. Chem. Phys., vol. 26, 1957, pp. 1773-1774.

Watanabe, K.; and Sood, S.P.: Absorption and Photoionization Coefficients of NH_3 in the 580-1650A Region. Science of Light, vol. 14, No. 1, 1965, pp. 36-53.

Watanabe, K; and Zelikoff, M.: Absorption Coefficients of Water Vapor in the Vacuum Ultraviolet. J. Opt. Soc. Amer. Vol. 43, No. 9, 1953, pp. 753-755.

Watanabe, K.; Zelikoff, M. and Inn, E.C.Y.: Absorption Coefficients of Several Atmospheric Gases. Geophysical Research Papers, No. 21, AFCRC Technical Report No. 53-23, June 1953.

Webb, D.U.; and Rao, K.N.: Vibration - Rotation Bands of Heated Hydrogen Halides. J. Molec. Spectros., vol. 28, 1968, pp. 121-124.

Weber, D.; and Penner, S.S.: Integrated Absorption of the Fundamental of CO From Measurements using Self-broadening of Rotational lines. J. Chem. Phys., vol. 19, 1951, pp. 974-975.

Weinberg, J.M.; Fishburne, E.S.; and Rao, K.N.: Hot Bands of CO at 4.7 microns measured to High J Values. J. Molec. Spectrosc., vol. 18, 1965, pp. 428-442.

Weissler, G.L.; Samson, J.A.R.; Ogawa, M.; and Cook, G.R.: Photoionization Analysis by Mass Spectroscopy. J. Opt. Soc. Amer., vol. 49, 1959, pp. 338-349.

Wiggins, T.A.; Griffin, N.C.; Arlin, E.M.; and Kerstetter, D.L.: Broadening and Shifting of HF Lines Due to Noble Gases. J. Molec. Spectros., vol. 36, 1970, pp. 77-83.

Wilkinson, P.G.; Johnston, H.L.: The Absorption Spectra of CH_4, CO_2, H_2O and Ethylene. J. Chem. Phys., vol. 18, 1950, pp. 190-193.

Wilkinson, P.G.: Molecular Spectra in the Vacuum Ultraviolet. J. Molec. Spectros., vol. 6, 1961, pp. 1-57.

Williamson, J.G.; Rao, K.N.; and Jones, L.H.: High Resolution Infrared Spectra of Water Vapor v_2 Bands of H_2O. J. Molec. Spectros., Vol. 40, 1971, pp. 372-387.

Wilson, M.K.; and Badger, R.M.: A Reinvestigation of the Vibration Spectrum of Ozone. J. Chem. Phys., vol. 16, 1-48, pp. 741-742.

Wright, N; and Randall, H.M.: Far Infrared Absorption Spectra of Ammonia and Phosphine Gases Under High Resolving Power. Phys. Rev., vol. 44, 1933, pp. 391-398.

Wulf, O.R.; and Melvin, E.H.: The Effect of Temperature Upon the Ultraviolet Band Spectrum of Ozone and the Structure of its Spectrum. Phys. Rev., Vol. 38, 1931, pp. 330-337.

Wulf, O.R.: The Band Spectrum of Ozone in the Visible and Photographic Infrared. Proc. Nat. Acad. Sci. (USA) Vol. 16, 1930, pp. 507-511.

Vigroux, E.: Contribution to the Experimental Study of the Absorption of Ozone. Ann. de Phys., vol. 8, 1953, pp. 709-762.

Vigroux, E.; Migeotte, M.; Neven, L.; and Swensson, J.: An Atlas of Nitrous Oxide, Methane and Ozone Infrared Absorption Bands. Part II Measures and Identifications. Tech. Final Rept (AF 61 (514) - 432 Inst. of Astrophys. University of Leige.

Vincent-Geisse, J.: Intensity Measurements and the Width of Absorption Lines in the Infrared. Application to Carbon Monoxide. J. Phys. Radium, vol. 15, 1954, pp. 539-540.

Yamamoto, G.; and Sasamori, T.: Calculation of the Absorption of the 15μ Carbon Dioxide Band. Sci. Rept. Tohoku University (Japan), vol. 10, No. 2, 1958, p. 37.

Yeager, D.; McKoy, V.; and Segal, G.A.: Assignments in the Electronic Spectrum of Water. J. Chem. Phys., vol. 61, No. 3, 1974, pp. 755-758.

Young, I.A.: CO Infrared Spectra. J. Quant. Spectros. Radiat. Transf., vol. 8, 1968, pp. 693-716.

Young, L.A.; and Bachus, W.J.: Dipole Moment Function and Vibration - Rotation Matrix Elements for CO. J. Chem. Phys., vol. 44, 1966, pp. 4195-4206.

Young, R.A.; Black, G.; and Slanger, T.G.: $400-8000\overset{\circ}{A}$ Emission From far Ultraviolet Photolysis of the N_2O, NO, NO_2, CO, CO_2 and O_2. J. Chem. Phys., vol. 48, 1968, pp. 2067-2070.

Zelikoff, M.; Watanabe, K.; and Inn, E.C.Y.: Absorption Coefficients of Gases in the Vacuum Ultraviolet. Part II, N_2O. J. Chem. Phys., vol. 21, No. 10, 1953, pp. 1643-1647.

Zuev, V.E.; Ippolitov, I.I.; Makashkin, Yu.S.; Orlov, A.A.; and Formin, V.V.: The Fine Structure of the Vibration-Rotation Structure of Water Vapor. Sov. Phys. Dokl., Vol. 13, 1968, pp. 205-207.

1. Report No. NASA RP-1030	2. Government Accession No.	3. Recipient's Catalog No.
4. Title and Subtitle Molecules of Significance in Planetary Aeronomy		5. Report Date January 1979
		6. Performing Organization Code
7. Author(s) Dr. Hari Mohan		8. Performing Organization Report No.
		10. Work Unit No.
9. Performing Organization Name and Address National Aeronautics and Space Administration Wallops Flight Center Wallops Island, Virginia 23337		11. Contract or Grant No.
12. Sponsoring Agency Name and Address National Aeronautics and Space Administration Washington, DC 20546		13. Type of Report and Period Covered Reference Publication
		14. Sponsoring Agency Code

15. Supplementary Notes

16. Abstract

   This monograph is basically devoted to spectroscopic information of the molecules of planetary interest. Only those molecules have been dealt with which have been confirmed spectroscopically to be present in the atmosphere of major planets of our solar system and play an important role in the aeronomy of the respective planets. An introduction giving the general conditions of planets and their atmospheres including the gaseous molecules is given. Some typical planetary spectra is presented and supported with a discussion on some basic concepts of optical absorption and molecular parameters that are important to the study of planetary atmospheres. Quantities like dipole moments, transition probabilities, Einstein coefficients and line strengths, radiative life times, absorption cross sections, oscillator strengths, line widths and profiles, equivalent widths, growth curves, bond strengths, electronic transition moments, Franck-Condon factors and $\bar{r}$-centroids, etc., are discussed. Spectroscopic information and relevant data of 6 diatomic (HF, HCL, CO, H_2, O_2, N_2) and 6 polyatomic (CO_2, N_2O, O_3, H_2O, NH_3, CH_4) molecules are presented. Finally an exhaustive bibliography is given for reference details.

17. Key Words (Suggested by Author(s)) Aeronomy Planetary Atmospheres Molecular Spectra	18. Distribution Statement Unclassified - unlimited STAR Category 88		
19. Security Classif. (of this report) Unclassified	20. Security Classif. (of this page) Unclassified	21. No. of Pages 327	22. Price* $12.00

National Aeronautics and
Space Administration

Washington, D.C.
20546

SPECIAL FOURTH CLASS MAIL
BOOK

U.S.MAIL

NASA